ANNALS
OF THE
UNIVERSITY OF ORADEA

FASCICLE OF TEXTILES, LEATHERWORK

VOLUME 27

No. 1

EDITURA
UNIVERSITĂŢII
DIN ORADEA

2026

ISSN 1843 – 813X

ANNALS
OF THE
UNIVERSITY OF ORADEA

FASCICLE OF TEXTILES, LEATHERWORK

VOLUME 27
No. 1

EDITURA
UNIVERSITĂŢII
DIN ORADEA

2026

Contact and Editors' Address:
Liliana INDRIE
UNIVERSITATEA DIN ORADEA,
FACULTATEA DE INGINERIE ENERGETICĂ ŞI MANAGEMENT INDUSTRIAL
DEPARTAMENTUL: TEXTILE- PIELĂRIE ŞI MANAGEMENT INDUSTRIAL
Str. B.St.Delavrancea nr. 4,
Oradea, 410058, Romania,
Tel.: 00-40-259-408448
E-mail : lindrie@uoradea.ro

Published by
Editura Universităţii din Oradea
Universitatea din Oradea, Str. Universităţii Nr. 1, 410087, Oradea, Bihor, Romania
P- ISSN 1843 – 813X
E - ISSN 2457-4880
CD- ISSN 2068 – 1070

Indexed in:

EBSCO-Textile Technology Complete
Index Copernicus (ICV 2024: 100)
Directory of Open Access Journals (DOAJ)
Ulrich's Update - Periodicals Directory

ANNALS OF THE UNIVERSITY OF ORADEA
FASCICLE OF TEXTILES, LEATHERWORK

EVALUATION OF THE FUNCTIONAL FINISHING OF COTTON USING POKEWEED BERRY DYE MORDANTED WITH ALOE VERA

AKOLEBIRUNGI Bridget[1], SEREM Dorcas[2], MWASIAGI Josphat[3]

[1, 2] University of Eldoret, School of Agriculture and Biotechnology, Department of Family and Consumer Sciences, P.O. Box 1125-30100 Eldoret, Kenya, E-Mail: dorcas.serem@uoeld.ac.ke

[3] Moi University, School of Engineering, Department of Manufacturing, Industrial and Textile Engineering, P.O. Box 3900-30100, Eldoret, Kenya, E-Mail: igadwa@mu.ac.ke

Corresponding author: Akolebirungi, Bridget, E-mail: akolebirungibridget18@gmail.com

Abstract: *Cotton has a high reputation for being one of the most used fabrics in the world but because it is hydrophilic, has an extreme susceptibility to microbial damage, causing degradation of the fabric and skin irritations. Although synthetic antimicrobial finishes for cotton have shown effectiveness over time, they carry issues of environmental toxicity and the development of microbial resistance, therefore, the need for sustainable and plant-based alternatives must be fulfilled. This paper presents the use of a plant-derived functional finish using pokeweed (Phytolacca americana) berry dye and aloe vera (Aloe barbadensis) extract, together to cotton fabric. A two-step pre-treatment method was employed on the used cotton to increase the fabric's absorption potential. The procedure consisted of applying fresh aloe vera extract (varying concentrations 10% - 100% v/v) as the pre-mordant, then applying an aqueous pokeweed dye. To evaluate for antimicrobial activity of the finished samples before and after laundry (following AATCC LP2 procedure), Staphylococcus aureus and Escherichia coli were used as test organisms with AATCC 147 qualitative test procedure. Results indicated that aloe vera is a viable bio-mordant, the antimicrobial activity of the fabrics increased with increasing concentration of aloe vera pre-mordant with the maximum zone of inhibition occurring at the 100% concentration of the aloe vera extract. However, the after-laundry test showed a dramatic loss of activity, emphasising the need for non-toxic cross-linking agents for practical applications. This paper provides a foundational framework for the use of indigenous bio-resources in green fashion for hygiene-sensitive textile industries.*

Key words: *Antimicrobial textiles, sustainable cotton, bio-based finish, zone of inhibition, synergistic interactions*

1. INTRODUCTION

Cotton is one of the mainstays of the international textile market and is currently estimated to generate over $600 billion each year as an unprocessed good [1], with a unique cellulosic structure and desirable qualities contributing to its superior moisture management, allowing application for everyday garments, specialised textiles and home beddings [2], [3]. Additionally, due to cotton's natural ability to retain moisture, microorganisms can proliferate on the fiber leading to fabric deterioration, offensive odors, and skin irritation [4],[5], While there are synthetic antimicrobial compounds that can control the growth of bacteria and other microorganisms, their

environmental toxicity and tendency to cause microorganisms to develop resistance to them have created urgency for a need to develop safe, environmentally sound, naturally-derived alternatives [6], [7], [8].

This study examined an alternative natural-based finishing process through the use of pokeweed berries and aloe vera extract. Pokeweed provides a high concentration of anthocyanins, which provide color and some antimicrobial efficacy [9]. Aloe vera provides more than 75 components that can act against bacteria, including aloin and saponins, which are bactericidal by interrupting the bacterial cell membrane [10]. Although previous studies have documented the benefits of these individual plants, there is a limited amount of research that documents the synergistic effect of these two natural products. The presence of natural finishes on fabrics has been shown to decrease their effectiveness as a result of mechanical action caused during laundering and exposure to common detergents [11]. Therefore, the objective of this study is to identify how concentration of aloe vera added to pokeweed-dyed cotton will affect the antimicrobial characteristics and durability of the dye system as a means to create sustainable innovations in textiles.

2. EXPERIMENTAL MATERIALS AND METHODS

This study was conducted using a laboratory-based experimental design at Uganda Industrial Research Institute (UIRI). The cotton substrate obtained from UIRI was prepared through a two-stage treatment procedure to increase absorbance of the substrate, scouring with 2g/L of Na_2CO_3 at 90°-95°C and bleaching with 30% H_2O_2 (pH 10.5) at 70°-80°C. pH-neutralising of the scoured and bleached cotton with acetic acid was done, then performed mass per unit area (ASTM D3776), thickness (ASTM D1777) and pH characterisation to establish a baseline of the cotton's structural and chemical characteristics for use with bioactive agents.

The bioactive agents used in this study were extracted from onsite fences and farms in Kampala Uganda, and were used to ensure sustainability; specifically, aloe vera inner gel was extracted by hand and later centrifuged to generate concentrations of 10, 30, 50, and 100% v/v of the fresh extract; pokeweed dye was made by aqueous extraction method using 2:1 pokeweed berries: water ratio, and left to stand for atleast 12hours. Pre-mordanting of cotton in aloe vera solutions of varying concentrations for one hour, at 60°C, then dyeing with the pokeweed berry dye with a liquor ratio of 1:20 at the same conditions, at a pH of 4.5, to combine the cellulose and the anthocyanin pigments of the dye was done. Flat drying was done in the shade for at least 24 hours.

To evaluate the level of antimicrobial activity before and after laundry following the AATCC LP2 lab procedure against Escherichia coli and Staphylococcus aureus, the antimicrobial activity via the Zone of Inhibition (ZOI) was tested using the AATCC 147 qualitative test, where bacterial strains were revived and incubated overnight in a nutrient broth at 37 °C on Mueller-Hinton agar plates. The tests were done in triplicate per finish, and an average of the ZOI obtained from a 50x25mm cotton sample was recorded in the tables. An inoculum was prepared by transferring 1.0+_0.1mL of the 24hr broth culture into a 9.0+_0.1mL of sterile distilled water contained in a small flask followed by mixing well using agitation. The process was repeated 8 times for proper dilution, and the colony-forming units (CFU)were counted using a colony counter machine, and the CFU/mL was calculated.

3. RESULTS AND DISCUSSIONS

3.1 Pretreatment of cotton

Table 1: *Effect of pretreatment on cotton*

Cotton sample	GSM in (g/m2)	Thickness (mm)	pH
Before pre-treatment	133	0.42	7.92
After pre-treatment	145	0.47	7.65

GSM increased by 12 g/m² and thickness by 0.05 mm due to fabric shrinkage and increased thread density, as all individual fibres returned to their original curled form following the scouring process, there were additional threads per square foot [12]. The 0.42 pH change was minimal and was created by the neutralisation action that helps protect cellulose from alkaline hydrolysis and also improves the fabric's ability to receive naturally bioactive materials, resulting in alkaline soaps being converted into protonated acids, which are more easily rinsed from cellulose [13].

3.2 Dyeing performance and Biomordant synergy

Visual results indicated a strong correlation between aloe vera concentration and colour depth. Shades transitioned from bright fuchsia pink (100% aloe) to pale pink (0% aloe). This probably could have been due to aloe vera acting as an effective bio-mordant and fixative because its gummy polysaccharides and metallic ions (magnesium, calcium, sodium) create a "bridge" between the cellulose hydroxyl groups and the dye molecules [14]. Higher concentrations produced deeper shades due to the lightness value being a function of dilution of the aloe compounds [15].

In addition, the enzymatic properties of the aloe vera gel increase the wettability and absorbency of the fibers, allowing for exhaustion of the dye without the need for synthetic salts [16]. Conversely, the alum mordants resulted in a pale pink dyeing, confirming its ineffectiveness as a mordant for cellulose fibers because of the low number of reaction sites for the coordination of metal salts [17].

3.3 Antimicrobial efficacy and Optimal concentration

Table 2: *ZOI for the tested bacteria on the pretreated and finished control cotton samples*

Finished Control Cotton Sample	ZOI for the tested bacteria in (mm)	
	Staphylococcus aureus of Colony forming units (CFU/ml) $2.6x10^8$	Escherichia coli of forming units (CFU/ml) $8.8x10^8$
Known Antibiotic (GMYCIN)	9.5	5.5
Aloe Vera alone	2.5	1
Poke weed alone	0.5	0
Cotton only	0	0

Table 3: *ZOI for the tested bacteria on different cotton samples pre-wash*

Finished Cotton Sample	ZOI for the tested bacteria (mm)	
	Staphylococcus aureus of Colony forming units (CFU/ml) $2.6x10^8$	Escherichia coli of forming units (CFU/ml) $8.8x10^8$
100% Aloe vera and pokeweed dye	3	1.5
50% Aloe vera and pokeweed dye	1.5	0.5
30% Aloe vera and pokeweed dye	1	0
10% Aloe vera and pokeweed dye	0.5	0
Pokeweed Alum pre-mordant	0.5	0

Fabrics research confirmed a synergistic antimicrobial effect. Fabrics treated with both pokeweed and aloe vera indicated a larger inhibition zone than untreated and singly treated samples. This synergy could probably be due to a result of the combination of pokeweed's anthocyanins, which interfere with protein function, and aloe vera's anthraquinones and saponins, which disrupt bacterial cell walls and metabolic functions [18], [19].

Findings showed that the antibacterial effect was highly correlated positively with concentration. No evidence of saturation was found; the maximum ZOI occurred at 100% aloe vera concentration across *S. aureus* as well as in *E. coli* strains. These findings support the hypothesis that increasing the concentration of resulting active components like aloin and acemannan leads to greater disruption of bacterial cell functions [20].

3.4 Durability and Diffusion Challenges

Table 4: *ZOI for the tested bacteria on different cotton samples post-wash.*

Finished Cotton Sample	ZOI for tested bacteria in (mm)	
	Staphylococcus aureus of Colony forming units (CFU/ml) $2.6x10^8$	Escherichia coli of forming units (CFU/ml) $8.8x10^8$
100% Aloe vera and pokeweed dye	1.5	0.5
50% Aloe vera and pokeweed dye	0.5	0
30% Aloe vera and pokeweed dye	0	0
10% Aloe vera and pokeweed dye	0	0
Poke weed berry dye alone	0	0
Pokeweed Alum pre-mordant	0	0

Antimicrobial activity declined drastically after washing, as bioactive compounds are not wash-fast [21]. Measurable activity was only observed in samples treated with 100% aloe vera pre-mordant, and even then, at minimal levels. While aloe vera demonstrates partial durability due to

stronger binding at high concentrations, achieving industrial-grade durability will require crosslinking or binding agents to prevent removal during laundering and mechanical agitation [22].

A notable observation during testing was the diffusion of pink colour from the cotton fabric into the media, forming a dark, bloody, and seemingly roasted appearance inside the petri dishes. This could have resulted due to pokeweed dye being water-soluble and loosely adhering to the cotton fabric, moving from high concentrations on the cotton fabric to the lower concentrations through passive diffusion, altering the clarity of the media.

4. CONCLUSIONS

This research highlights an urgent requirement for the development of non-toxic biodegradable finishing chemicals for textiles in order to support innovation in the fabric industry. Higher concentrations of aloe vera demonstrated deeper pokeweed berry dye shades and higher antimicrobial effects on cotton fabrics. Washing significantly reduces antimicrobial activity; thus, the use of cross-linking agents and optimisation of application methods will be required to facilitate industrial transitioning.

REFERENCES

[1] M. A. Ali *et al.*, “Soil Management and Tillage Practices for Growing Cotton Crop,” in *Cotton Production and Uses*, Singapore: Springer Singapore, 2020, pp. 9–30. doi: 10.1007/978-981-15-1472-2_2.

[2] H. Khanzada, M. Q. Khan, and S. Kayani, *Cotton Science and Processing Technology*. Singapore: Springer Singapore, 2020. doi: 10.1007/978-981-15-9169-3.

[3] Md. Nuruzzaman, F. Ahmed, H. J. Kadri, and Md. I. H. Mondal, “Cotton and other cellulose fibres for comfort smart clothing,” in *Smart Textiles from Natural Resources*, Elsevier, 2024, pp. 65–108. doi: 10.1016/B978-0-443-15471-3.00014-5.

[4] J. Saha, *Modification of cotton fabric with Natural antimicrobial agents for Ecofriendly protective textiles.*

[5] M. Tausif, A. Jabbar, M. S. Naeem, A. Basit, F. Ahmad, and T. Cassidy, “Cotton in the new millennium: advances, economics, perceptions and problems,” *Textile Progress*, vol. 50, no. 1, pp. 1–66, Jan. 2018, doi: 10.1080/00405167.2018.1528095.

[6] M. T. Islam and S. Asaduzzaman, *Textiles and Clothing*. Wiley, 2019. doi: 10.1002/9781119526599.

[7] S. H. Mahmud and M. R. Repon, *Sustainable Finishing Techniques in Textiles*. Singapore: Springer Nature Singapore, 2025. doi: 10.1007/978-981-96-4860-3.

[8] A. Soroh, “Novel eco-friendly antimicrobial coatings for use in healthcare and sport textiles. ,” p. 240, Apr. 2019.

[9] A. K. Samanta and A. Konar, “Dyeing of textiles with natural dyes. ,” *Natural dyes*, vol. 3, no. 30–56, pp. 212-222., 2011.

[10] N. Khanam and G. K. Sharma, “ A critical review on antioxidant and antimicrobial properties of aloe vera ,” *Int. J. Pharm. Sci. Res.*, vol. 4, no. 9, p. 3304, 2013.

[11] K. Murugesh Babu and K. B. Ravindra, “Bioactive antimicrobial agents for finishing of textiles for health care products,” *The Journal of The Textile Institute*, vol. 106, no. 7, pp. 706–717, Jul. 2015, doi: 10.1080/00405000.2014.936670.

[12] Cotton Incorporated, “A Guide to Improved Shrinkage Performance of Cotton Fabrics,” Cary, North Carolina, 2004.

[13] Chemtradeasia, "Textile pH Control with Glacial Acetic Acid," Chemtradeasia Indonesia. Accessed: Jan. 29, 2026. [Online]. Available: https://www.chemtradeasia.co.id/market-insights/textile-ph-control-glacial-acetic-acid

[14] Abdouramane Nsangou, Doina Sibiescu, Dydimus Efeze Nkemaja, Pierre Marcel Anicet Noah, Fabien Ebanda Betene, and Valery Hambaté Gomdjé, "Aloe Vera Gel as a Biomordant in the Finishing of Vegetable Textiles: A Review," *Buletinul Institutului Politehnic din Iași, Secția Chimie și Inginerie Chimică (Bulletin of the Polytechnic Institute of Iași, Section: Chemistry and Chemical Engineering)*, vol. 68, no. 72, pp. 31–36, Jul. 2022.

[15] M. Odero, A. K. Kiprop, I. Owino, M. Arimi, and B. Maiyo, "Optimization of dyeing process parameters for dyeing of cotton fabric using extracts of aloe succotrina. .," *Annals Of The University Of Oradeafascicle Of Textiles, Leatherwork,* pp. 63–68, 2020.

[16] A. Rehman, M. Rehman, M. Naveed, K. Javed, and A. Khan, "Eco-friendly dyeing of cotton with natural colorants using natural mordants obtained from aloe vera," *Journal of the Indian Chemical Society*, vol. 101, no. 8, p. 101182, 2024.

[17] S. Haar, E. Schrader, and B. M. Gatewood, "Comparison of Aluminum Mordants on the Colorfastness of Natural Dyes on Cotton," *Clothing and Textiles Research Journal*, vol. 31, no. 2, pp. 97–108, Apr. 2013, doi: 10.1177/0887302X13480846.

[18] S. W. Ali, R. Purwar, M. Joshi, and S. Rajendran, "Antibacterial Properties of Aloe Vera Gel-Finished Cotton Fabric," *Cellulose*, vol. 21, no. 3, pp. 2063–2072, 2014.

[19] I. C. Marinas, "CHEMICAL COMPOSITION, ANTIMICROBIAL AND ANTIOXIDANT ACTIVITY OF PHYTOLACCA AMERICANA L. FRUITS AND LEAVES EXTRACTS," *Farmacia*, vol. 69, no. 5, pp. 883–889, Oct. 2021, doi: 10.31925/farmacia.2021.5.9.

[20] H. Mistry, S. Mundkur, and A. Tulshyan, "Antibacterial Treatment on Cotton Fabric from Aloe Vera," *SSRG International Journal of Polymer and Textile Engineering*, vol. 7, no. 1, pp. 54–58, 2020.

[21] Yuan Gao and R. Cranston, "Recent Advances in Antimicrobial Treatments of Textiles," *Textile Research Journal*, vol. 78, no. 1, pp. 60–72, Jan. 2008, doi: 10.1177/0040517507082332.

[22] A. Khan and Abdul Farhan, "Extraction, Stabilization and Application of Antimicrobial Agents from Aloe Vera," *PTJ Pakistan Textile Journal*, pp. 42–44, 2012.

ANNALS OF THE UNIVERSITY OF ORADEA
FASCICLE OF TEXTILES, LEATHERWORK

THE INFLUENCE OF COMPOSITE MATERIAL COMPONENTS ON MECHANICAL AND THERMOELECTRIC PROPERTIES

BACIU Valentin[1]

[1] The National Research & Development Institute for Textiles and Leather (INCDTP), Bucharest Str. Lucretiu Patrascanu nr. 16 sector 3, certex@certex.ro

Corresponding author: Baciu Valentin, valentin.baciu@incdtp.ro

Abstract: *This paper presents an overview of the properties of composite materials and their potential use in thermoelectric systems. Applications in which conventional materials did not fully meet structural requirements have made composite materials an alternative worth considering. This category of materials is often used because they allow control over the desired properties, which are influenced by the matrix and reinforcement elements. For applications where the objectives focus on certain mechanical properties, the polymer matrix is often used. Likewise, in order to achieve these same properties, various fibers are used to control the range of values of these properties. The field of composites has also influenced thermoelectric materials, with specialized studies demonstrating interest in converting a temperature gradient into electrical energy and vice versa.*

Key words: *polymer composites, fiber architecture, thermal gradient conversion, tensile strength, Seebeck coefficient.*

1. INTRODUCTION

Composite materials represent a class of materials that emerged from the desire to overcome the limitations of conventional materials. This type of material is characterized by the combination of at least two distinct types of materials whose structure provides superior properties compared to the elements used individually. In developments carried out over the years, a composite material consists of a continuous matrix and a reinforcement element dispersed or oriented in a certain manner [1]. The matrix has the role of holding the component elements together, transferring mechanical loads, and protecting the reinforcement against external factors, while the reinforcement material mainly contributes to increasing strength and stiffness [2].

Depending on the nature of the matrix, composite materials can be classified according to this element, resulting in composite materials with polymer matrix [3], metal matrix [4], or ceramic matrix [5]. As for reinforcement materials, these may consist of synthetic fibers, such as glass fibers, carbon fiber, or aramid fibers [6], natural fibers [7], fabrics [8], nanotubes [9], and nanofibers [10].

One of the main reasons why composite materials have attracted interest for the development of studies is related to their mechanical performance. Due to their strength-to-weight ratio, high stiffness, and the possibility of optimizing properties through the orientation and distribution of the reinforcement, these materials have become attractive for industrial applications [11].

In addition to their use in structural applications, composite materials have increasingly begun to be developed as multifunctional materials, capable of providing not only mechanical strength but also electrical responses under various external stimuli. In this context, composites with thermoelectric

properties represent a direction of interest, since they allow the conversion of a temperature gradient into an electrical signal through the Seebeck, Peltier, or Thomson effect [12], being used in sensing systems [13], wearable systems [14], or flexible devices [15].

This paper examines the influence of reinforcement materials on the mechanical or thermoelectric properties of composites integrated into various polymer matrices. The analysis comparing different types of matrices, reinforcement elements, and composite architectures makes it possible to highlight how these components control the final performance of the material. In this context, mechanical properties and thermoelectric behavior are correlated, since the structural parameters that influence mechanical strength can also affect heat and electrical transport within the material. The conversion of a temperature difference into electrical energy is based on the Seebeck effect, through which a thermal gradient generates an electrical potential difference. Mechanical properties do not directly determine the occurrence of this effect, however they are essential for evaluating the material's potential for use in practical applications. Thus, a flexible thermoelectric composite material can be integrated into wearable textile applications, where the analysis of thermoelectric and mechanical properties is essential.

2. INFLUENCE OF REINFORCEMENT MATERIALS ON THE PROPERTIES OF COMPOSITE MATERIALS

To summarize the influence of matrices and reinforcement elements on the resulting composite materials, Fig. 1 illustrates a simplification of the analyzed elements. The literature used in this paper was identified through searches on ScienceDirect and MDPI, using keywords such as polymer matrix, glass fiber, carbon fiber, thermoelectric composite, mechanical properties, and Seebeck coefficient. Sources were selected thematically in three stages: composite materials and their general classification, mechanical performance of fiber-reinforced composites, and thermoelectric composites combining mechanical and thermoelectric properties, with preference given to experimental works reporting quantitative data.

Composite materials	Influence on mechanical properties	Matrix	Epoxy resin Polyester resin
		Reinforcement material	Glass fibers Kevlar fibers Carbon fibers Flax fibers
	Influence on thermoelectric properties	Matrix	Epoxy resin PEDOT:PSS PVDF SEBS PVA
		Reinforcement material	Carbon Fibers Glass Fibers Tellurium nanofibres Bi_2S_3, Bi_2Te_3, Sb_2Te_3

Fig. 1 *– Matrix and reinforcement materials analysed for mechanical and thermoelectric properties*

2.1 Influence on mechanical properties

Rout et al. [16] produced various composite material samples using bidirectional woven fabrics based on Kevlar fibers (K), glass fibers (G), and carbon fibers (C), with an epoxy matrix.The authors produced five material samples in the form of [$G_2K_3G_2$], [KG_2CKG_2], [CKGCGKC], [CGKCKGC], [CK_2CK_2C], as well as three samples made from the base materials [G_7] [C_7], [K_7]. From the designation of the samples, the seven-component layered structure can be observed. These samples were tested by preparing specimens corresponding to each configuration, and the mechanical properties were evaluated using hardness, flexural, and impact tests.

The results showed that mechanical performance strongly depends on the laminate architecture. Among all the analysed variants, the [CGKCKGC] configuration showed the best overall results, reaching a flexural strength of approximately 380 MPa, a flexural modulus of about 36 GPa, a hardness of 59 BHN, and an impact strength of approximately 80 kJ/m^2. The authors attributed this behavior to the positive effect of combining rigid carbon fibers with Kevlar and glass fibers, as well as to a stacking sequence favorable to load distribution and energy dissipation. Moreover, for the previously mentioned configuration, the SEM analysis revealed active fiber involvement in the deformation and failure mechanism, indicating efficient load transfer at the matrix–reinforcement interface. Unlike the specimens in which fiber sliding or pull-outfrom the matrix predominated, in this case fiber fracture and the maintenance of local adhesion with the polymer phase were observed, confirming their direct contribution to the improvement in mechanical performance.

Cao et al. [17] focused strictly on the influence of glass fibers on the properties of the composite material under tensile loading, but it provides further insight by testing different matrices and different compounds added to them that improve the fiber–matrix interface. The research team created various samples based on E51 epoxy resin, together withother improvement agents such as a silane coupling agent, nano-TiO_2, or nano-SiO_2. For the different experiments, specimens were made from samples based on: EPA-650 (E51+PA650 at 1:1), EPA-650-Md (E51+PA650+modified SiO_2/TiO_2 at 50:50:1:1), EPAA (E51+ PAA–phenolic amine curing agent at 2:1), and EAA (E51+AA – alicyclic amine curing agent at 2:1).

In the tensile tests carried out by the authors, for the tensile test performed on the EPA650- Md specimen, a significant elongation exceeding 7.5% was observed, but it did not reach maximum stress values close to 40 MPa as in EPAA and EAA. For additional validation, tests were carried out with 2, 4, and 8 layers. Among all the analysed variants, the 4-layer EPAA system showed the best combination of strength, stiffness, and deformation, being highlighted by the authors as the optimal variant. The microstructural analysis supports these results, showing that improving adhesion at the interface limits fiber sliding and promotes their active participation in load bearing, which leads to anoverall increase in the tensile performance of the composite. It is worth noting that, with the increase in the number of layers to 8, all configurations showed inferior results compared to four layers.

The two studies show that mechanical performance depends on two distinct aspects: how the fiber layers are arranged and combined, as shown in [16], and how the matrix is formulated and how well it bonds to the fibers, as shown in [17]. This indicates that improving a composite for a given application requires attention to both aspects, since acting on only one of them may not lead to the expected results.

Islam et al. [18] presented a study on the influence of woven fabrics with carbon and flax fibers as warp and weft yarns, as well as a hybrid configuration. The composite materials had INF-114 epoxy resin and INF 211 curing agent as the matrix. Two architectures were produced, namely inter-ply, with layers [CF_2CF_2C], and intra-ply with 14 layers of that hybrid fabric. The experimental evaluation

included both static tensile tests and tensile fatigue tests, carried out at 70% of the ultimate tensile strength and at a frequency of 3 Hz. The results showed that the ultimate tensile strength of the two configurations is relatively close, with an average value of approximately 805.26 MPa for the inter-ply composite and 765.46 MPa for the intra-ply composite, which indicates small differences under static loading, however, the intra-ply configuration provided a linear behavior compared to the other configuration, which showed fluctuations after leaving the elastic domain. In contrast, the fatigue differences were very pronounced: the inter-ply composite recorded an average fatigue life of approximately 17,034 cycles, while the intra-ply composite reached approximately 365,939 cycles, which corresponds to an increase of over 2000% in fatigue life. Under cyclic loading, the material sample showed a scattered structure of failed fibers, this aspect being due to the failure of the first layer of carbon fibers, while the other configuration showed a more orderly behavior of the failed fibers.

The results of [18] show that the two architectures perform similarly under static loading, but differ significantly under cyclic loading, where the intra-ply configuration reached over 2000% more fatigue cycles. This suggests that the choice of fiber arrangement should take into account the type of loading expected in the application, since an architecture that appears comparable under static conditions may behave very differently under repeated loading.

2.2 Influence on thermoelectric properties

Rodrigues-Marinho et al. [19] investigated flexible thermoelectric composite materials based on two polymer matrices, poly(vinylidene fluoride) (PVDF) and styrene-ethylene/butylene-styrene (SEBS), loaded with thermoelectric ceramics (Bi_2S_3, Bi_2Te_3, Sb_2Te_3) and multiwalled carbon nanotubes (CNTs), comparing thermoelectric performance against mechanical flexibility. In the tensile tests, PVDF composites showed tensile strengths of approximately 20–35 MPa, while SEBS composites exhibited strains up to 750% in pure form and 470% for the SEBS/50Bi_2S_3 sample. The addition of 1 wt.% CNT led to a strong increase in conductivity, up to 32.9 (Ωm^{-1}) for PVDF/CNT/Bi_2S_3. With increasing Bi_2S_3 concentration, the Seebeck coefficient reached 36 μV/K for PVDF/80Bi_2S_3. For a device made from PVDF/50 Bi_2S_3 and PVDF/50 Bi_2Te_3, the generated voltage reached 3.5 mV for a single thermocouple and 5.1 V for two thermocouples at $\Delta T = 100$ °C.

Kong et al. [20] proposed a flexible TPP-type thermoelectric hydrogel composed of PEDOT:PSS and polyvinyl alcohol (PVA), into which tellurium nanowires (Te-NWs) were introduced to improve the thermoelectric properties. From a structural point of view, the system was based on a PEDOT:PSS/PVA matrix, with tellurium nanowires dispersed throughout the network that contributed to both charge-carrier transport and the optimization of thermoelectric performance. In terms of mechanical behavior, the TPP hydrogel showed the best results among the analyzed variants, reaching a tensile strength of approximately 0.905 MPa and a maximum strain of nearly 400%, which highlights high elasticity that can be exploited in wearable applications. From the thermoelectric point of view, the optimal composition was obtained at a content of 1.5 wt.% Te-NWs,for which the authors reported a maximum Seebeck coefficient of 787 μV/K. At a thermal gradient of 30 K, the hydrogel generated a voltage of approximately 23.8 mV, and a wearable module made up of 20 TPP units reached an output voltage of 138.5 mV when applied to the arm, demonstrating the potential of this material for low-temperature thermal energy harvesting in wearable applications.

Karalis et al. [21] proposed carbon-epoxy composite laminates capable of functioning as thermoelectric generators through the thickness direction, by integrating a functional layer based on glass fiber coated with a thermoelectric layer. The laminate matrix consisted of epoxy resin, and the reinforcement elements were represented by carbon fibers and glass fibers. The functional layer was obtained by depositing, on the glass fiber fabric, a thermoelectric paste formed from tellurium nanowires (Te NWs) dispersed in a PEDOT:PSS matrix, the optimal variant being the one with a 1:1

mass ratio, which showed an in-plane Seebeck coefficient of 189 μV/K. Based on this layer, unidirectional (UD) and cross-ply laminates with 10 layers were fabricated, and the UD configuration provided the best thermoelectric results, generating a voltage of 8.4 mV at ΔT = 100 K, while the cross-ply laminate reached approximately 7.9 mV. From the mechanical point of view, the integration of the thermoelectric function caused only a moderate reduction in flexural performance, of approximately 10%.

The three studies approach thermoelectric composites from different directions. In terms of generated voltage, [19] reached 5.1 V at ΔT = 100°C through thermocouple stacking, while [20] generated 23.8 mV at ΔT = 30 K for a single element, reaching 138.5 mV for a 20 unit module. Study [21] reports 8.4 mV at ΔT = 100 K, a lower value but obtained within a structural laminate. From a mechanical standpoint, the hydrogel in [20] offers the highest deformability with strains up to 400%, while [21] maintains flexural performance with only a 10% reduction compared to a standard carbon-epoxy laminate, and [19] sits between the two with tensile strengths of 20–35 MPa. This shows that the three systems target different application contexts, and the choice between them depends on whether the priority is thermoelectric output, mechanical flexibility, or structural integration.

3. CONCLUSIONS

The analyzed studies demonstrate that reinforcement materials influence the performance of composites, both mechanically and thermoelectrically. In laminated systems intended for integration into structures, optimizing the type of fiber, the stacking sequence, and the matrix–reinforcement interface leads to improved strength, stiffness, and fatigue resistance under static or cyclic loading.

The integration of thermoelectric phases into polymer matrices or functional laminates demonstrates the potential to extend the use of composites to applications where converting a temperature gradient into electrical energy is desired. Therefore, composite materials represent a feasible alternative for particular applications, and configurations can be developed to meet structural requirements.

ACKNOWLEDGEMENTS

This work was carried out through the Core Programme within the National Research Development and Innovation Plan 2022-2027, carried out with the support of MCID, project no. 6N/2023, PN 23 26 01 03, project title "Electroconductive materials based on multilayer metallization for thermoelectric systems, electromagnetic shielding and biomedical sensors integrated in IoT systems (3D-WearIoT)".

REFERENCES

[1] S. Sajan and D. Philip Selvaraj, “A review on polymer matrix composite materials and their applications”, Materials Today: Proceedings, vol. 47, pp. 5493-5498, 2021, doi: 10.1016/j.matpr.2021.08.034.

[2] M. R. M. Asyraf, et al., “Synthetic and Natural Fiber-Reinforced Polymer Matrix Composites for Advanced A*pplications”*, Materials, vol. 15, no. 17, art. 6030, 2022, doi: 10.3390/ma15176030.

[3] D. K. Rajak, D. D. Pagar, R. Kumar, and C. I. Pruncu, *“Recent progress of reinforcement materials: a comprehensive overview of composite materials”*, Journal of Materials Research and Technology, vol. 8, no. 6, pp. 6354-6374, 2019, doi: 10.1016/j.jmrt.2019.09.068.

[4] A. K. Sharma, R. Bhandari, A. Aherwar, and R. Rimašauskienė, *“Matrix materials used in composites: A comprehensive study”*, Materials Today: Proceedings, vol. 21, no. 3, pp. 1559-1562,2020,

doi: 10.1016/j.matpr.2019.11.086.

[5] L. Wietschel, F. Halter, A. Thorenz, D. Schüppel, and D. Koch, *"Literature review on the state of the art of the circular economy of Ceramic Matrix Composites"*, Open Ceramics, vol. 14, art. 100357, 2023, doi: 10.1016/j.oceram.2023.100357.

[6] D. K. Rajak, P. H. Wagh, and E. Linul, *"A Review on Synthetic Fibers for Polymer Matrix Composites: Performance, Failure Modes and Applications"*, Materials, vol. 15, no. 14, art. 4790, 2022, doi: 10.3390/ma15144790.

[7] A. R. Bhat, R. Kumar, and P. K. S. Mural, *"Natural Fiber Reinforced Polymer Composites: A Comprehensive Review of Tribo-Mechanical Properties"*, Tribology International, vol.189, art. 108978, 2023, doi: 10.1016/j.triboint.2023.108978.

[8] M.-P. Todor, I. Kiss, V. G. Cioată, and C. M. Cioată, *"Development of fabric-reinforced polymer matrix composites using bio-based components from post-consumer textile waste"*, Materials Today: Proceedings, vol. 45, pp. 4180-4184, 2021, doi: 10.1016/j.matpr.2020.11.927.

[9] X. Dong and S. Lv, *"Incremental analysis of thermal conductivity optimization model for polymer carbon nanotube composite materials considering branch heat conduction"*, Case Studies in Thermal Engineering, vol. 81, art. 107928, 2026, doi: 10.1016/j.csite.2026.107928.

[10] H. T. Tazwar, M. F. Antora, I. Nowroj, and A. B. Rashid, *"Conductive polymer composites in soft robotics, flexible sensors and energy storage: Fabrication, applications and challenges"*, Biosensors and Bioelectronics: X, vol. 24, art. 100597, 2025.

[11] H. Sharma, et al., *"Critical review on advancements on the fiber-reinforced composites: Role of fiber/matrix modification on the performance of the fibrous composites"*, Journal of Materials Research and Technology, vol. 26, pp. 2975-3002, 2023, doi: 10.1016/j.jmrt.2023.08.036.

[12] D. M. Rowe, *"Thermoelectrics Handbook: Macro to Nano"*, ch. 1, Taylor & Francis Group, 2006.

[13] H. Xie, Y. Zhang, P. Gao, J. Wang, Y. Su, and J. Zhu, *"Thermoelectric-Powered Sensorsfor Internet of Things"*, Micromachines, vol. 14, no. 1, art. 31, 2023, doi: 10.3390/mi14010031.

[14] S. Zhu et al., *"Review on Wearable Thermoelectric Generators: From Devices to Applications"*, Energies, vol. 15,no. 9, art. 3375, 2022, doi: 10.3390/en15093375.

[15] Y. Zhang and S.-J. Park, *"Flexible Organic Thermoelectric Materials and Devices for Wearable Green Energy Harvesting"*, Polymers, vol. 11, no. 5, art. 909, 2019.

[16] S. Rout, R. K. Nayak, S. C. Patnaik, and H. Yazdani Nezhad, *"Development of Improved Flexural and Impact Performance of Kevlar/Carbon/Glass Fibers Reinforced Polymer Hybrid Composites"*, J. Compos. Sci., vol. 6, art. 245, 2022, doi: 10.3390/jcs6090245.

[17] Y. Cao, G. Gao, P. Zhang, J. Bao, P. Feng, R. Li, and W. Wang, *"Improving tensile properties of glass fiber-reinforced epoxy resin composites based on enhanced multiphase structure:The modification of resin systems and glass fibers"*, Materials Today Communications, vol. 40, art. 110225, 2024, doi: 10.1016/j.mtcomm.2024.110225.

[18] M. Z. Islam, A. Amiri, and C. A. Ulven, *"Fatigue Behavior Comparison of Inter-Ply and Intra-Ply Hybrid Flax-Carbon Fiber Reinforced Polymer Matrix Composites"*, J. Compos. Sci., vol. 5, art. 184, 2021, doi: 10.3390/jcs5070184.

[19] T. Rodrigues-Marinho, V. Correia, C.-R. Tubio, A. Ares-Pernas, M.-J. Abad, S. Lanceros-Méndez, and P. Costa, *"Flexible thermoelectric energy harvesting system based on polymercomposites"*, Chemical Engineering Journal, vol. 473, art. 145297, 2023, doi: 10.1016/j.cej.2023.145297.

[20] S. Kong et al., *"Tellurium-nanowire-doped thermoelectric hydrogel with high stretchability andSeebeck coefficient for low-grade heat energy harvesting"*, Nano Energy, vol. 115, art. 108708, 2023, doi: 10.1016/j.nanoen.2023.108708.

[21] G. Karalis et al., *"Carbon fiber/epoxy composite laminates as through-thickness thermoelectric generators"*,Composites Science and Technology, vol. 220, art. 109291, 2022.

ANNALS OF THE UNIVERSITY OF ORADEA
FASCICLE OF TEXTILES, LEATHERWORK

RESULTS OBTAINED FROM THE APPLICATION OF TREATMENTS ON THE COMPONENT MATERIALS OF MATTRESS COVERS

BOHM Gabriella[1], ŞUTEU Marius Darius[1], DOBLE Liliana[1], GHERGHEL Sabina[1]

[1]University of Oradea, Faculty of Energy Engineering and Industrial Management, Department Textiles, Leather and Industrial Management, 410058, Oradea, România, E-Mail: suteu_marius@yahoo.com

Corresponding author: BOHM Gabriella, E-mail: bohmgaby@gmail.com

Abstract: *The chemical treatments applied to the materials used in the manufacture of mattress covers play an important role in improving the technical and functional characteristics of the final product. These treatments are intended to give materials special properties, such as wear resistance, protection against microorganisms, moisture or other degradation factors. In addition, they can help increase the durability and useful life of mattress covers, thus ensuring a higher level of performance and safety for users. The present paper demonstrates that these chemical treatments are not just simple additions, but essential components for adapting mattress covers to different environments and uses. In the case of home use, the treatments provide protection against dirt, dust or dust mites, helping to maintain a hygienic and healthy sleeping environment. In the palliative care sector or in the hospital environment, these treatments are becoming even more important, being essential for preventing the spread of infections and ensuring a safe environment for patients and healthcare staff. Also, the correct application of chemical treatments to the materials used in the manufacture of mattress covers can significantly influence their mechanical strength, reducing the risk of damage over time, such as tears or discolorations. Increased durability not only extends the life cycle of the product, but also helps to reduce the environmental impact by decreasing the frequency of replacement.*

Key words: *domestic use, chemical treatments, hospital regime.*

1. INTRODUCTION

The mattress cover plays an important role in ensuring comfort and hygiene in the use environment, being in direct and constant contact with the user's body [1]. Due to prolonged exposure, any chemical treatment applied to the materials used to make it must be carried out responsibly and in accordance with safety regulations, in order to prevent health risks. [2], [3], [4]. The use of irresponsible chemical treatments can have serious consequences for users' health [5]. For example, certain chemicals can cause allergic reactions, manifested by skin irritation, itching, redness, or rashes. In the case of people sensitive to certain substances, these reactions can be more severe and can even lead to respiratory problems, such as asthma or shortness of breath, especially if vapor or chemical particles are released into the air [6], [7]. In addition to the risk of allergic reactions, improper chemical treatments can also affect the quality of the air in the environment and lead to the accumulation of toxic substances in the human body, especially if they are inhaled or absorbed through the skin [8]. Additionally, certain substances can weaken the structure of the fibers, reducing the durability and strength of the cover, leading to faster wear and tear and the need

for frequent product replacement [4]. For this reason, it is very important that the chemical treatments applied to the textiles for mattress covers are effective, but also safe for health. In addition, it is important that these treatments are rigorously tested to avoid the release of harmful compounds into the environment or the air in the room [9].

2. GENERAL INFORMATION

In the present paper, a thorough analysis of the materials used to make two types of mattress covers was carried out: one intended for domestic use and the other oriented towards the medical care regime. This analysis aimed to evaluate the quality, durability and technical characteristics of the materials used according to the specific requirements of each type of case, as well as to identify any differences in composition, treatments applied and performance.

Fig. 1*: Equipment for the treatment of textile materials - Squeezing Pader Machine*

Thus, the aim was to adapt the materials to meet the comfort, hygiene and safety needs of the end users, depending on the environment of use.

Table 1: *Domestic cover (mattress) treatment*

Treatment	**LIKROLL**
Recipe	Citric Acid 0.2% Elastofin STO501 1.4%, Temp:160^{0}C
Request width	229-231 cm
Request weight	268-282 gr/m^2
Composition	18% Viscose + 82% Polyester
Color	Opera+Black+Basalt grey

Table 2: *Treatment cover (mattress) for hospital use*

Treatment	**PADDER**
Recipe	Active Biotic + AbioFlame 14% Temp:140^{0}C
Request width	239-241 cm
Request weight	345-360 gr/m^2
Composition	18% Viscose + 3,5% Elastane + 78,5% Polyester
Color	Natural, Nude

In this work, the materials used to make two types of mattress covers were approached and tested, using the Squeezing Pader Machine. The main aim was to obtain basic information on the

chemical treatment applied to the fibres in these covers, in order to assess the impact and effectiveness of these treatments on the final characteristics of the products.

The preparation and analysis of the samples were carried out using an internal standard operating procedure for the analysis of the fibrous content of the materials in the two mattress covers.

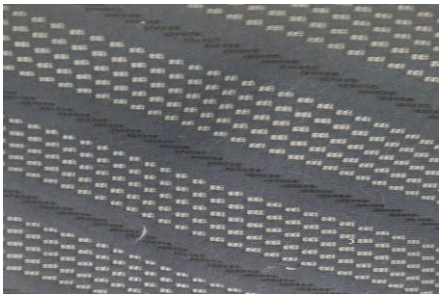

***Fig. 1**: Treated material for cover (mattress) for household use*

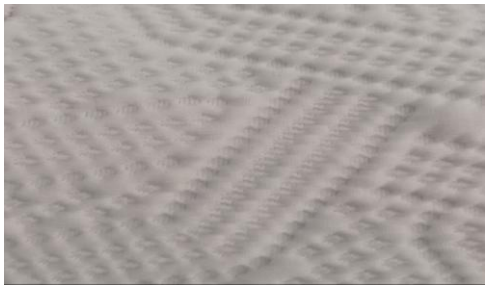

***Fig. 2**: Treated material for cover (mattress) for hospital use*

The main components of each mattress cover tested and their compositions observed are summarized in Tables 1 and 2. The different components of the mattress cover for domestic use were mixtures of Citric Acid 0.2% Elastofin STO501 1.4%, at a 100% control weight/weight control, Temp:160^{0}C, compared to the cover intended for hospital use, which consists of the Active Biotic treatment and AbioFlame JASMIN 14%, Temp:140^{0}C. It has a different treatment because it requires an immersion treatment, to get that 100% to 150% solution load. The destination of this material requires special treatment to ensure an antimicrobial effect. Being a knit made of a mixture of viscose fibers (18%) in a mixture with polyester (over 75%), an increased fireproofing treatment is required, and it will also be used in the medical environment.

The analysis carried out in this paper highlights the importance of chemical treatments in creating functional and durable mattress covers suitable for both home and hospital use. The results obtained demonstrate that, in most cases, chemically treated materials offer significant advantages, thus contributing to a better user experience.

It is very important to study how these treatments retain their effectiveness over time, as well as the possible risks or adverse effects on the health of users, especially in the case of frequent or long-term use. Thus, further studies could include monitoring the behaviour of materials under real conditions of use.

5. CONCLUSIONS

The present paper highlights the analysis of the differences between the finishing treatments applied to knitted materials, especially those intended for mattress covers made of yarns based on fibers of natural vegetable origin.

In conclusion, the continuation of these studies and innovations are essential steps to achieve safer, more sustainable and environmentally friendly products, in line with current trends in sustainable development and public health. These research directions can have a significant impact on the mattress cover materials industry, especially in the context of increasing awareness of environmental protection and user health.

REFERENCES

[1] Fiberglass and Other Flame-Resistant Fibers in Mattress Covers Jeff Wagner, Jefferson Fowles, Tracy Barreau Int J Environ Res Public Health. 2022 Feb; 19(3): 1695. Published online 2022 Feb 1. doi: 10.3390/ijerph19031695 PMCID: PMC8835476

[2] Bohm G., Șuteu, M.D., Doble, L., Fetea, L., Porav V. - ” Comparative analysis of the treatments attached to the materials in the composition of the mattress covers” Annals of the University of Oradea, Fascicle of Textiles, Leatherwork, ISSN 1843-813X, Oradea, Volume 24, 2023, No. 2, pp. 19-22.

[3] Șuteu, M.D, Bohm G., Doble, L. - ” Study on the treatment of textile materials for the manufacture of mattress covers” Annals of the University of Oradea, Fascicle of Textiles, Leatherwork, ISSN 1843-813X, Oradea, Volume 23, 2022, No. 2, pp. 71-74

[4] Bohm G., Șuteu, M.D., Doble, L., Fetea, L. - ” Analysis of different treatments of materials intended for mattress covers” Annals of the University of Oradea, Fascicle of Textiles, Leatherwork, ISSN 1843-813X, Oradea, Volume 25, 2024, No. 1, pp. 19-22.

[5] Șuteu, M.D, Bohm G., Doble, L. - ” Study on the treatment of textile materials for the manufacture of mattress covers” Annals of the University of Oradea, Fascicle of Textiles, Leatherwork, ISSN 1843-813X, Oradea, Volume 23, 2022, No. 2, pp. 71-74.

[6]https://ro.cncoverglass.com/info/chemical-poisoning-in-laboratories-prevention-17363631299830784.html[accessed on 05 aprilie 2026]

[7] OEKO-TEX® STANDARD 100, 3rd ed.; OEKO-TEX Service GmbH: Zurich, Switzerland, 2025

[8] Liu, Y., & Chen, J. (2021). "Environmental and health risks of chemical treatments in textile manufacturing." Environmental Science & Technology, 55(10), 6527-6536.

[9] Wang, S.-M.; Wu, J.-X.; Gunawan, H.; Tu, R.-Q. Highly Specialized Textiles with Antimicrobial Functionality—Advances and Challenges. Textiles 2023, 3, 219–245.

ANNALS OF THE UNIVERSITY OF ORADEA
FASCICLE OF TEXTILES, LEATHERWORK

SUSTAINABLE REDUCTION OF GRAPHENE OXIDE ON POLYESTER SPUNBOND NONWOVEN FABRIC USING RED ONION PEEL EXTRACT

DEMİREL GÜLTEKİN Nergis[1], SERT Zişangül[1], AKSOY Şevval[1]

[1] Marmara University, Faculty of Technology, Department of Textile Engineering, 34854, İstanbul, Türkiye,
E-Mail: ndemirel@marmara.edu.tr

Corresponding author: Demirel Gültekin, Nergis, E-mail: ndemirel@marmara.edu.tr

Abstract: *Graphene oxide (GO) coated conductive textiles have attracted significant attention due to their potential applications in smart textiles, sensors, and electromagnetic shielding materials. However, conventional chemical reduction methods for GO typically involve toxic reducing agents that pose harmful risks to both environmental and human health. Therefore, environmentally friendly reduction strategies have become increasingly important. In this study, graphene oxide was coated onto polyester spunbond nonwoven fabrics using dip-coating and blade coating methods. Subsequently, a green reduction approach was applied using the methanol extract of red onion peel as a natural reducing agent. The morphology, chemical structure, thermal stability, and electrical properties of the obtained samples were characterized by scanning electron microscopy (SEM), Raman spectroscopy, thermogravimetric analysis (TGA), and surface electrical resistance measurements. The results demonstrate that agricultural waste-derived natural extracts can serve as effective and sustainable reducing agents for the preparation of conductive graphene-based textile structures. This environmentally friendly approach offers a promising route for the development of conductive nonwoven materials for advanced functional textile applications.*

Key words: *graphene oxide, green reduction, waste management, nonwoven fabric, electrical conductivity.*

1. INTRODUCTION

One of the most significant global issues today is the valorization of waste. The rapid increase in population and imbalances in supply chains have led to a growing global concern regarding food waste. Cultivating plants requires intensive labor and significant economic resources. Therefore, using only the edible parts while discarding the rest leads not only to food waste but also to a loss of labor and resources. From a sustainability perspective, the utilization of waste materials has become increasingly important. About 20% of food waste occurs during production, 1% during processing, 19% during distribution, and 60% at the consumer and household level. Fruit and vegetable residues constitute a major portion of this waste, accounting for nearly 42% of the total. Although some food industry waste is currently composted or used as animal feed and fertilizer, recovering valuable bioactive compounds from these wastes and reusing them as sustainable resources offers a more effective waste management approach. Numerous studies have demonstrated that fruit and vegetable peels contain significant amounts of bioactive compounds. Furthermore, previous research has reported that the bioactive content of fruit and vegetable peels and seeds may be even higher than that of their edible tissues [1-3]. For the reduction of graphene oxide (GO), the chemical reduction method—an effective and relatively simple procedure—is commonly applied. Through this process, oxygen-containing functional groups are removed from the GO structure [4]. Conventional chemical reduction methods commonly use toxic reducing agents such as hydrazine hydrate, dimethylhydrazine, sodium borohydride, and hydroquinone, which are harmful to both human health and the environment [5]. Moreover, hazardous by-products formed during these reactions can attach to the reduced graphene oxide structure and limit its potential

applications. For this reason, environmentally friendly reduction methods have attracted increasing attention [6, 7]. In green reduction studies, natural extracts obtained from different plant parts, including leaves, fruits, roots, seeds, and whole plants, are widely used [8]. Studies have shown that red onions contain bioactive compounds such as antioxidants. Red onion peel is rich in phenolic compounds, mainly flavonoids, which are higher than those of the edible parts [9, 10]. Therefore, in this study, the potential of red onion peel extract on reducing oxygen-containing functional groups in GO, which is coated on a nonwoven textile substrate for applications in electro-conductive functional textiles.

2. MATERIALS AND METHOD

2.1 Materials

Graphite flakes were purchased from Sigma-Aldrich. Hydrogen peroxide (H_2O_2, 35%), sulfuric acid (H_2SO_4, 95%–98%), phosphoric acid (H_3PO_4), potassium permanganate (KMnO4), boric acid (H_3BO_3), and hydrochloric acid (HCl, 37%) were purchased from Merck. All chemicals were of analytical reagent grade and used without further purification. Distilled water was used throughout the experiments. Polyester spunbond nonwoven (NW) fabric with a mass per unit area of 25 g/m² was used as a substrate. Red onion peels (ROP) were obtained from the local market and used as a reducing agent to reduce the graphene oxide.

2.2 Synthesis of Graphene Oxide

Graphene oxide was synthesized using the improved Hummers' method using flake graphite. Briefly, 360:40 mL of a mixture of H_2SO_4 and H_3PO_4 was placed into a flask, to which 3g of graphite flakes were added. The flask was gradually filled with 18g of $KMnO_4$. Following the full dissolution of the $KMnO_4$, the reaction was placed in an oil bath, heated to 50°C, and stirred for 12 hours. The reaction was then poured onto 400 mL of ice after being cooled to room temperature. 6 mL of 35% H_2O_2 was added to terminate the reaction. The suspension was purified using ethanol (2×) and 1 M HCl by centrifugation. After washing, the centrifugation process was maintained until a pH of 4-5 was reached. The resulting sample was dried at 60°C to obtain solid GO nanosheets [11].

2.3 Ultrasonic Extraction

The red onion peels were removed, washed with distilled water, and dried in an oven at 70°C. The dried peels were ground into powder. 30 g of red onion peel powder was extracted with the mixture of 100 mL (1:1) methanol: distilled water by using the bath sonication at 50°C for 60 min. After the extraction, the mixture was filtered and then centrifuged for 10 min at 6000 rpm. The supernatant was stored at 4°C and used as a reducing medium.

2.4 GO Coating and Reduction Process of Polyester Spunbond Nonwoven Fabric

The polyester spunbond nonwoven fabric was first dip-coated with the 2 g/L aqueous dispersion of GO. The aqueous dispersion of GO was prepared by adding 2 g of GO into 1 L of distilled water, placing it into the ultrasonic bath for an hour at room temperature, and then transferring it to the magnetic stirrer to obtain a homogenous dispersion. The polyester nonwoven fabric was dip-coated with the as-prepared GO dispersion for about 10 min at ambient conditions (The sample coded as D-GO-NW). Secondly, the GO-coated polyester nonwoven fabric was blade-coated with 25 g/L of GO paste (The sample coded as B-GO-NW). The blade-coating paste was prepared with GO and distilled water without any auxiliary chemicals. The blade-coating parameters were fixed as given: blade-coating speed 1 and 2 m/min, blade-fabric distance 35 mm, curing temperature 190°C, curing duration 180 sec.

The GO-coated polyester nonwoven fabric samples were put into the methanolic extract of red onion peel, and the reaction was heated to 95°C and held for 24 h. The fabric samples were then rinsed with distilled water to remove the excess reducing agent and dried in an oven at 95°C. The samples after the reduction were coded as ROP-RGO-NW-1 and ROP-RGO-NW-2, indicating that the blade-coating speeds were 1 and 2 m/min, respectively.

2.5 Characterization

Scanning electron microscopy (SEM, Zeiss Evo MA10) was employed to observe the morphology of uncoated and coated samples. The surface of the samples was coated with Au/Pd (Quarum, SC7620) before analysis. Thermogravimetric analysis (Perkin ELMER TGA 8000) was applied to the nonwoven fabric samples at a rate of 10°C/min under nitrogen flow from 25 to 600°C. The Raman spectra were acquired using a WITec Alpha300 RA with a 532 nm laser (WITech, Germany). The electrical resistance of the nonwoven fabric samples was determined using a four-point probe technique. The configuration comprises a sourcemeter (Keithley 2450) and a four-point probe station (Everbeing International Corp.).

3. RESULTS AND DISCUSSIONS

3.1. Morphological Analysis

Scanning electron microscopy (SEM) images of the polyester spunbond nonwoven fabric, GO dip- and blade-coated, and red onion peel extract-reduced sample are presented in Figure 1. Figure 1a shows the surface of the polyester spunbond nonwoven fabric, where polyester filaments exhibited a smooth and uniform structure. After the GO dip-coating process, GO nanosheets were observed on the fabric surface and between the filaments (Figure 1b). Following the blade-coating application, the fabric surface became more densely covered with GO nanosheets. As shown in Figure 1c, no voids were observed between the polyester filaments, and the filament surfaces were completely coated with GO nanosheets exhibiting the characteristic wrinkled and crumpled morphology of GO. After the reduction process using the methanol extract of red onion peel, cracks appeared on the coated surface (Figure 1d). This observation indicated that the oxygen-containing functional groups in the GO structure were removed during the reduction reaction, leading to the formation of a more rigid and compact reduced GO structure.

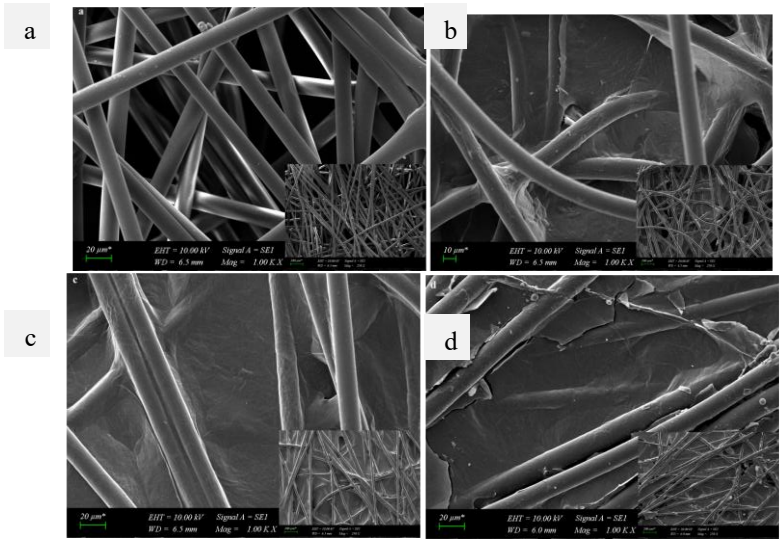

Fig.1. *SEM images at 1000× magnification of NW (a), D-GO-NW (b), B-GO-NW (c), and ROP-RGO-NW-1 (d)(inside images are at 250× magnification).*

3.2. Thermal Gravimetric Analysis (TGA)

The thermal behavior of the samples was analyzed using a thermogravimetric analysis (TGA) instrument. As observed from the TGA curves presented in Figure 2, all samples exhibited similar thermal degradation behavior. The thermal degradation process occurred in two stages. In the first stage, a slight mass loss was observed up to 100 °C, which was attributed to the removal of adsorbed water molecules from the samples [11]. In the second stage, a significant mass loss occurred within the temperature range of 380–480 °C. This could be explained by the chain scission of ester bonds and the

formation of vinyl ester and carboxylic acid groups. With increasing temperature, the ester bonds continued to break, leading to the formation of volatile low-molecular-weight segments. The release of these segments resulted in a substantial mass loss [12]. The TGA curve indicated that the thermal stability of the red onion peel extract-reduced sample showed a slight improvement. The residual mass percentages at 600 °C were determined as 9.50%, 9.70%, and 12.43% for samples coded NW, D-GO-NW, and ROP-RGO-NW-1, respectively. These results suggested that the reduction process with red onion peel extract enhanced the thermal stability of the sample.

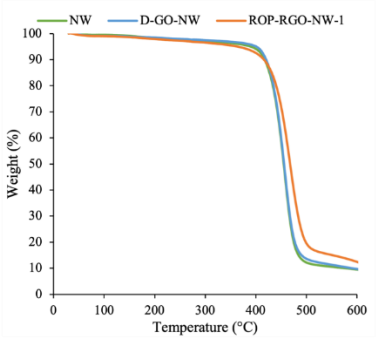

Fig.2. *TGA graph of NW, D-GO-NW, and ROP-RGO-NW-1.*

3.3. RAMAN Analysis

The Raman spectra of the polyester spunbond nonwoven fabric, GO dip-coated sample, and red onion peel extract reduced sample were presented in Figure 3. The polyester nonwoven fabric exhibited characteristic peaks at 1293 cm^{-1} (C–O), 1616 cm^{-1} (aromatic ring stretching), and 1728 cm^{-1} (C=O). No distinct new peak formation was observed in the polyester nonwoven fabric coated with GO via the dip-coating method. This could be attributed to the relatively low amount of GO present on the fabric surface. Following the reduction reaction using red onion peel extract, the Raman spectra of the samples revealed the characteristic D and G bands of carbon-based materials. The D band arises from the presence of defects and impurities in the basal plane of the graphitic structure [13]. The D band was observed at 1364 cm^{-1}. The G band is associated with the defects related to sp^2 hybridization in the ordered graphene structure [14]. The G band was observed at 1596 cm^{-1}. The I_D/I_G ratio was determined as 0.99. The I_D/I_G ratio indicated the reduction in the size of planar sp^2 domains during the reduction of GO and was considered an indicator of structural disorder [13, 15].

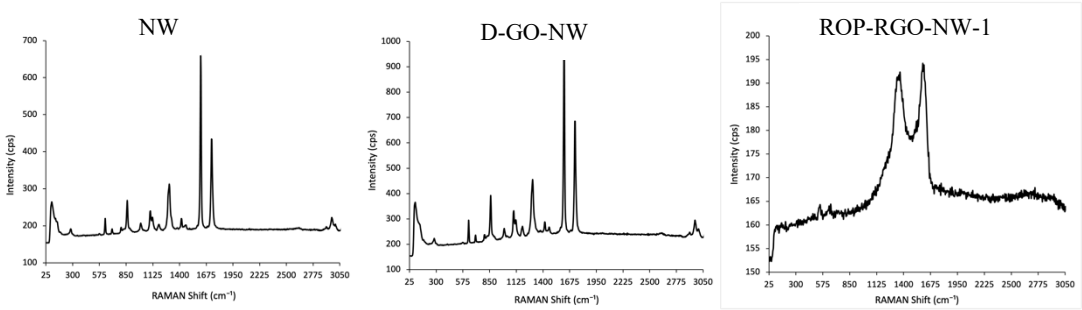

Fig.3. *RAMAN spectra of NW, D-GO-NW, and ROP-RGO-NW-1.*

3.4 Electrical Resistivity

The electrical surface resistance measurement results were presented in Table 1. Due to its inherently insulating nature, the polyester nonwoven fabric exhibited a very high electrical resistance value of 2.37×10^8 kΩ. The GO dip-coated nonwoven fabric sample also exhibited a high electrical resistance due to the insulating nature of GO nanosheets, which arises from the presence of oxygen-containing functional groups [11]. A significant decrease in electrical resistance value was observed after the reduction of GO. The lowest value was obtained in the ROP-RGO-NW-2 sample as 1.75×10^2

kΩ.

The electrical conductivity of the produced samples was also demonstrated by the illumination of an LED bulb in a simple circuit setup. The images presented in Figure 4 demonstrate that the sample reduced using red onion peel extract exhibited sufficient electrical conductivity to power an LED lamp.

Table 1: *The electrical resistivity of samples.*

Sample	*Electrical Resistivity (kΩ)*
NW	2.37E+08
D-GO-NW	3.94E+07
ROP-RGO-NW-1	3.08E+03
ROP-RGO-NW-2	1.75E+02

Fig.4. *The digital photographs showing the gloves (a, b), NW (c), D-GO-NW (d), and B-GO-NW (e) do not light the LED, while the ROP-RGO-NW-2 sample lights the LED.*

4. CONCLUSIONS

In this study, graphene oxide (GO) is successfully coated onto polyester spunbond nonwoven fabrics using dip-coating and blade coating methods, followed by a green reduction process using natural extract obtained from red onion peel. The study aims to develop an environmentally friendly approach for producing conductive textile structures while utilizing agricultural waste materials as sustainable reducing agents. SEM analysis confirms that GO nanosheets are successfully deposited on the polyester filament surfaces and within the inter-fiber spaces of the nonwoven structure. Raman spectroscopy results support the successful reduction of GO. Thermogravimetric analysis demonstrates that the reduced sample exhibited slightly improved thermal stability compared to the untreated and GO-coated fabrics. Electrical surface resistance measurements show that the reduction process significantly enhanced the electrical conductivity of the samples. The lowest electrical resistance value (174.75 kΩ) is obtained. Furthermore, the electrical conductivity of the obtained sample is visually demonstrated through the illumination of an LED lamp in a simple circuit setup.

Overall, the results indicate that plant-based waste extracts can be effectively used as green reducing agents for the preparation of conductive graphene-based textile materials. This sustainable approach not only contributes to the valorization of agricultural waste but also provides an environmentally friendly

alternative to conventional toxic reducing agents for the production of functional conductive nonwoven textiles.

ACKNOWLEDGEMENTS

The authors would like to thank TUBITAK (The Scientific and Technological Research Council of Türkiye) for supporting this work through the 2209-A programme.

REFERENCES

[1] M. Güzel and Ö. Akpınar, *"Meyve ve Sebze Kabuklarının Fitokimyasal ve Antioksidan Özelliklerinin İncelenmesi"*, Gümüşhane Üniversitesi Fen Bilimleri Enstitüsü Dergisi, 2019.

[2] K. S. Ganesh, A. Sridhar, and S. Vishali, *"Utilization of fruit and vegetable waste to produce value-added products: Conventional utilization and emerging opportunities-A review"*, Chemosphere, 287, (Pt 3), pp. 132221, 2022.

[3] K. Q. Lau, M. R. Sabran and S. R. Shafie, *"Utilization of Vegetable and Fruit By-products as Functional Ingredient and Food"*, Frontiers in Nutrition, 8, pp. 661693, 2021.

[4] V. B. Mohan, K. Jayaraman and D. Bhattacharyya, *"Fabrication of highly conductive graphene particle-coated fiber yarns using polymeric binders through efficient coating techniques"*, Advances in Polymer Technology, 37, (8), pp. 3438-3447, 2018.

[5] S. Pei and H. M. Cheng, *"The reduction of graphene oxide"*, Carbon, 50, (9), pp. 3210-3228, 2012.

[6] Z. Sui, et al., *"Easy and green synthesis of reduced graphite oxide-based hydrogels"*, Carbon, 49, (13), pp. 4314-4321, 2011.

[7] M. J. Fernandez-Merino, et al., *"Vitamin C Is an Ideal Substitute for Hydrazine in the Reduction of Graphene Oxide Suspensions"*, The Journal of Physical Chemistry C, 114, pp. 6426–6432, 2010.

[8] L. Mihaela-Cristina, et al., *"Antimicrobial Behavior of Green Silver Nanoparticles Deposited on Knitted Textile Support"*, Annals of the University of Oradea. Fascicle of Textiles, Leatherwork, 26, (1), 2025.

[9] N. T. N. Ha, N. L. A. Dao, and T. T. Truc, *"Assessing Red Onion (Allium cepa L.) Peel Extract as an Antioxidant and Antimicrobial Agent for Ice Storage of Tilapia (Oreochromis niloticus) Fillets"*, Journal of Food Processing and Preservation, 2025, (1), pp. 6642585, 2025.

[10] A. Bains, et al., *"Valorization of onion peel waste: From trash to treasure"*, Chemosphere, 343, pp. 140178, 2023.

[11] N. Demirel Gültekin, İ. Usta and B. Yalçin, *"Enhancing polyamide fabric performance through green reduction of graphene oxide for superior ultraviolet protection and electrical conductivity"*, Coloration Technology, 141, (1), pp. 26-43, 2025.

[12] A. Berendjchi, et al., *"Improved continuity of reduced graphene oxide on polyester fabric by use of polypyrrole to achieve a highly electro-conductive and flexible substrate"*, Applied Surface Science, 363, pp. 264-272, 2016.

[13] V. Babaahmadi, M. Montazer and W. Gao, *"Low temperature welding of graphene on PET with silver nanoparticles producing higher durable electro-conductive fabric"*, Carbon, 118, pp. 443-451, 2017.

[14] F. Shao, et al., *"Fabrication of Polyaniline/Graphene/Polyester Textile Electrode Materials for Flexible Supercapacitors with High Capacitance and Cycling Stability"*, Chemistry- An Asian Journal, 11, (13), pp. 1906-12, 2016.

[15] V. Babaahmadi, M. Montazer and W. Gao, *"Surface modification of PET fabric through in-situ reduction and cross-linking of graphene oxide: Towards developing durable conductive fabric coatings"*, Colloids and Surfaces A: Physicochemical and Engineering Aspects, 545, pp. 16-25, 2018.

ANNALS OF THE UNIVERSITY OF ORADEA
FASCICLE OF TEXTILES, LEATHERWORK

INVESTIGATION OF THE PHYSICAL AND MECHANICAL PROPERTIES OF COTTON FABRICS WITH DIFFERENT WEAVE STRUCTURES

DJORDJEVIC Suzana[1], STOJANOVIC Sandra[2], KODRIC Marija[3], DJORDJEVIC Dragan[4]

[1,2]Academy of Applied Studies Southern Serbia, Department of Technology and Art Studies Leskovac, Leskovac, Serbia, E-Mail: szn871@yahoo.com

[3,4]University of Nis, Faculty of Technology, Bulevar oslobodjenja 124, 16000 Leskovac, Serbia, E-Mail: drdrag64@yahoo.com

Corresponding author: Djordjevic, Dragan, E-mail: drdrag64@yahoo.com

Abstract: *Cotton fabrics represent one of the most commonly used groups of textile materials due to their favorable combination of mechanical, functional, and comfort-related properties. These properties largely depend on the structural parameters of the fabric, among which the weave structure plays a significant role. The interlacing pattern of warp and weft yarns determines the geometry of the fabric, the structural density, and the pore distribution, which directly affect its physical–mechanical and functional properties. The aim of this study is to investigate the influence of different weave structures on selected physical and mechanical properties of cotton fabrics. The research analyzed fabrics produced in three different weave structures: Panama, twill, and longitudinal rib. The following fabric properties were examined: thickness, breaking strength and elongation at break, dimensional stability, abrasion resistance, porosity, capillarity, and air permeability. Experimental testing was carried out using standardized methods for testing textile materials. The obtained results indicate that the weave structure significantly affects the mechanical behavior and functional characteristics of cotton fabrics. The results of this research contribute to a better understanding of the relationship between fabric structure and its properties and may serve as a basis for optimizing fabric construction according to their intended use and required functional characteristics.*

Key words: woven product, panama, twill, warp rib, physical and mechanical properties.

1. INTRODUCTION

Textile materials play an important role in modern society due to their wide range of applications in clothing, household products, technical textiles, and various industrial fields. Among the numerous natural fibers used in textile production, cotton occupies a prominent position because of its favorable properties, such as high moisture absorbency, comfort, softness, breathability, and relatively good mechanical performance. Owing to these characteristics, cotton fabrics are extensively used in the production of apparel and home textiles, which makes the investigation of their physical and mechanical properties particularly important for both textile engineering and practical applications [1, 2].

The properties of woven fabrics are largely determined by their structural characteristics, especially by the manner in which warp and weft yarns interlace. The type of weave significantly affects the arrangement of yarns within the fabric, the structural density, the contact area between fibers, and the distribution of stress when the material is subjected to mechanical loads. Consequently, different weave structures can substantially influence the physical and mechanical characteristics of fabrics, including strength, elongation, abrasion resistance, and functional properties such as air permeability, porosity, and dimensional stability. Among the commonly used weave structures in cotton fabrics are the Panama weave, twill weave, and rib weaves. The Panama weave is characterized by the grouping of warp and weft yarns, which creates a distinctive texture and usually results in a more open fabric structure with relatively larger pores. The 2/2 twill weave is recognizable by its diagonal lines on the fabric surface and provides a favorable distribution of mechanical stress within the structure, often leading to improved mechanical properties and higher resistance to abrasion. In contrast, the longitudinal rib weave forms pronounced longitudinal ribs, which can influence the fabric's thickness, stiffness, and structural stability [3, 4].

The physical and mechanical properties of fabrics represent important parameters that determine their functionality, durability, and overall quality. Fabric thickness affects thermal insulation, weight, and comfort of the material. Breaking strength and elongation at break indicate the ability of the fabric to withstand mechanical stresses during use. Dimensional stability reflects the ability of the fabric to maintain its original dimensions after exposure to moisture, heat, and mechanical forces. Abrasion resistance is another important parameter that determines the durability of textile materials under repeated friction during wear and use [5, 6].

In addition to mechanical characteristics, several functional properties significantly influence the comfort and performance of textile materials. Fabric porosity and air permeability determine the degree of air circulation through the material and play a crucial role in thermophysiological comfort. Capillarity describes the ability of a fabric to transport liquid through its structure, which is particularly important for clothing materials and technical textile applications. The tendency of fabrics to wrinkle affects their aesthetic appearance as well as the practicality of maintenance and use [7, 8].

Considering that the structural characteristics of woven fabrics have a significant influence on these properties, it is important to systematically investigate the effect of different weave structures on the performance of cotton fabrics.

In this study, cotton fabrics with three different weave structures are examined: Panama weave, 2/2 twill weave, and longitudinal rib weave. The analyzed properties include thickness, breaking strength and elongation, dimensional stability, abrasion resistance, porosity, capillarity, air permeability, and wrinkle behavior.

The aim of this research is to determine the influence of weave structure on the physical and mechanical properties of cotton fabrics and to provide results that contribute to a better understanding of the behavior of textile materials, as well as to support the optimization of fabric structure selection according to the intended application.

2. EXPERIMENTAL PART

The grey fabrics used in this investigation were produced from 100% cotton yarns with similar values of yarn fineness (linear densities of the yarns) and thread densities in both the warp and weft directions, but with different weave structures. The structural properties of the investigated fabrics are presented in Table 1.

Table 1: *Declared values of the main properties of grey cotton fabrics.*

Yarn linear density (tex)		Thread density (cm^{-1})		Fabric mass (g/m^2)	Weaves
Warp	Weft	Warp	Weft		
36	34	29	22	180	Panama
35	34	28	21	175	2/2 Twill
36	35	28	20	177	Warp rib

The weaving process was carried out on PICANOL looms with a maximum working width of 180 cm. The machine capacity is 240 picks per minute, depending on the fabric density being produced. The loom is equipped with a semi-automatic control unit with one operating speed, while the installed power is 1.4 kW.

Testing methods:

- Fabric thickness, according to the standard SRPS EN ISO 5084:2013.
- Dimensional change, according to the standard SRPS EN ISO 6330:2022.
- Breaking force and elongation of fabrics, according to the standards SRPS EN ISO 13934-1:2015 and SRPS EN ISO 13934-2:2012.
- Abrasion resistance, according to the standard SRPS EN ISO 12947-2:2017.
- Capillarity, according to the standard SRPS F.S2.042:1985.
- Air permeability, according to the standard SRPS EN ISO 9237:2010.
- Fabric porosity, determined using the cover factor, according to the standard SRPS EN ISO 7211-2:2024.

3. RESULTS AND DISCUSSION

The obtained experimental results indicate that the weave structure has a significant influence on the physical and mechanical properties of cotton fabrics. Overall, the results confirm that variations in weave structure lead to significant changes in fabric geometry and consequently influence the mechanical and functional performance of cotton fabrics. Namely, if the linear densities of the yarns (fineness) and the thread densities in both warp and weft are very similar for all three fabrics, then the tested properties are primarily influenced by the type of weave, i.e., by the manner in which the yarns interlace [9, 10].

The results of the thickness change of the cotton samples of the analyzed fabrics are presented in Table 2. Among other factors, fabric thickness is significantly influenced by the type of weave, since the weave determines the manner of yarn interlacing and bending within the fabric structure. In fabrics with approximately the same yarn fineness and similar thread densities, the panama weave usually results in greater thickness due to the grouped interlacing of yarns and a more pronounced volumetric structure. The 2/2 twill exhibits intermediate thickness values, whereas the warp rib structure, due to the greater compactness of yarns in the fabric structure, most often shows lower thickness values.

According to the results, depending on the weave structure, the mean fabric thickness varies between 0.25 and 0.28 mm, with a very small standard error ranging from 0.0058 to 0.0068 mm.

The standard error indicates the extent to which the mean values of fabric thickness may vary. Since the values of this statistical parameter are very low, it can be concluded that the mean value is highly reliable, the measurements are consistent, and the mean thickness adequately represents the entire series of samples.

Low values of the standard deviation in this case confirm that the measurements are very similar and consistent. This parameter indicates the homogeneity of the material and the stability of

the measurements. The coefficient of variation is a relative measure of variability and therefore enables comparison between different parameters. The numerical values of this statistical parameter for thickness indicate a moderate variation of the results and a moderate uniformity of the tested fabric samples.

The panama weave is characterized by grouped yarn interlacings, which create a more pronounced and fuller structure; therefore, the fabric is usually thicker and more voluminous. The twill weave has a diagonal structure and fewer interlacing points than the plain weave, resulting in a moderate fabric thickness. The warp rib weave exhibits pronounced rib lines in the warp direction, but a more compact structure; consequently, it is usually the thinnest when the other parameters are identical or similar.

The standard deviation (SD) for the examined parameter ranges from 0.018 to 0.022 mm, while the coefficient of variation (CV) reaches values between 7.0 and 7.8%.

Table 2: *Thickness results of grey fabrics with different weave structures*

Statistical parameters	**Thickness**		
	Panama	**Twill**	**Warp rib**
Mean value (mm)	0.28	0.26	0.25
Standard error (mm)	0.0068	0.0058	0.0061
Standard deviation (mm)	0.022	0.018	0.019
Coefficient of variation (%)	7.7	7.0	7.8

Dimensional stability of fibers, yarns, and textile products when brought into contact with hot water or hot solutions is an important indicator of their quality. The requirements regarding the dimensional stability of textile materials are that shrinkage should be as low as possible. In practice, however, it is usually difficult to ensure that a textile material does not change its dimensions to a certain extent [11].

According to Figure 1, it can be observed that after the dimensional change test, shrinkage of the fabric samples occurs for all weave structures, both in the warp direction and in the weft direction. Considering that the linear densities of the yarns and the thread densities of the fabrics are very similar, the dimensional changes (shrinkage) are mainly influenced by the type of weave, i.e., by the number of interlacing points and the yarn waviness (crimp) within the fabric structure.

Fabrics with a twill weave exhibit greater shrinkage due to the smaller number of binding points and the higher mobility of the yarns, whereas fabrics with a panama weave show moderate dimensional changes. The highest dimensional stability is observed in fabrics with a warp rib weave, owing to the greater binding and compactness of the structure.

It is noticeable that the fabric samples exhibit uniform and low values of statistical parameters in both directions. For all fabric weave structures and for the tested parameter of shrinkage, the standard error ranges from 0.073 to 0.098%, the standard deviation (SD) from 0.23 to 0.31%, while the coefficient of variation (CV) ranges from 7.4 to 11.1%.

The weft shrinkage in panama fabrics is slightly higher than in the warp direction because the weft has a higher crimp, experiences lower tension during weaving, and the panama weave structure is relatively looser. In addition, the relaxation of cotton fibers during washing increases the shortening of the yarns, etc.

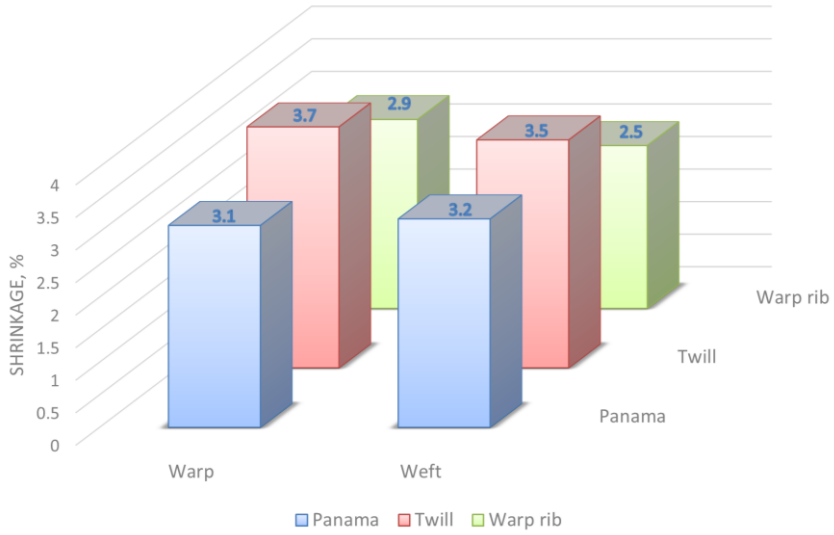

Fig. 1: *Dimensional changes of fabrics with different weave structures*

Mechanical properties of textile materials are highly significant, particularly breaking strength and elongation. These properties determine the quality and performance characteristics of the final textile product.

Figures 2 and 3 present the results of the breaking strength and elongation at break of the analyzed fabrics. The test results indicate that the type of weave structure has a significant influence on the breaking strength and elongation at break of the investigated cotton fabrics.

The twill weave exhibits the highest values of breaking strength in both the warp and weft directions, amounting to 485 N and 350 N, respectively. In contrast, the fabric with a rib weave shows the lowest breaking strength values, reaching 465 N in the warp direction and 333 N in the weft direction, respectively.

The highest measurement error for this parameter is observed in the rib weave fabric in the warp direction, amounting to 7.7 N, while the lowest error is recorded for the panama weave fabric, 6.0 N. The standard deviation (SD) of the same parameter ranges from 16.3 N (weft direction, panama weave) to 24.5 N (warp direction, rib weave). Regarding the coefficient of variation (CV), the values range from the highest value of 5.9% (weft direction, twill weave) to the lowest value of 4.0% (warp direction, panama weave).

Relatively low values of the standard error indicate that the mean value of the breaking strength has high reliability. The standard deviation, as a statistical parameter describing the dispersion of individual measurements around the mean, implies a certain variation of the results, which is common for textile materials due to the non-uniformity of fabric structure. The coefficient of variation, as a relative measure of variability and the best indicator of the uniformity of results, shows through its numerical values that the results are well balanced and that the fabric samples are relatively homogeneous.

The twill weave has fewer binding points and longer yarn floats, which allows the load to be distributed more uniformly, resulting in higher breaking strength. The panama weave is characterized by grouped yarn interlacings, which somewhat increases the structural rigidity, leading to intermediate strength values. The warp rib weave has a larger number of interlacings within one yarn system, which increases yarn bending and local stresses, and consequently results in the lowest breaking strength.

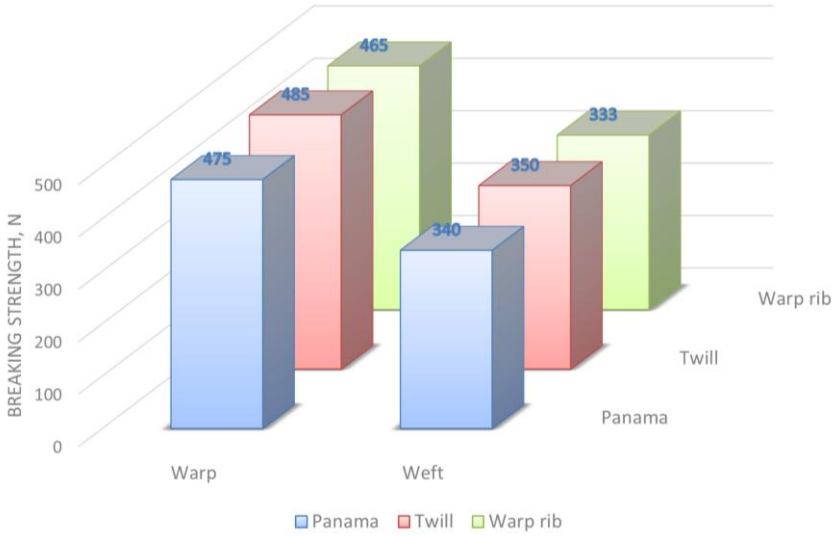

Fig. 2. *Changes in the breaking strength of fabrics with different weave structures*

According to Figure 3, the elongation at break of the fabrics in all weave structures varies from 10% (warp direction, rib weave) to 15% (weft direction, twill weave). The statistical data are appropriate and confirm the validity of the obtained measurement values for this tested parameter.

Namely, the standard error values are relatively uniform for fabrics of all weave structures, ranging from 0.56% (weft direction, rib weave) to 0.84% (weft direction, twill weave). The standard deviation (SD) varies from 1.49% (warp direction, twill weave) to 2.67% (weft direction, twill weave). The coefficient of variation (CV) ranges from the lowest value of 0.13% to 0.23%.

The twill weave has a longer wavy yarn path (higher crimp), allowing the fabric to elongate more before rupture. The panama weave exhibits moderate elongation due to the grouping of yarns. The warp rib weave has a greater number of interlacing points and limited yarn mobility, resulting in the lowest elongation at break.

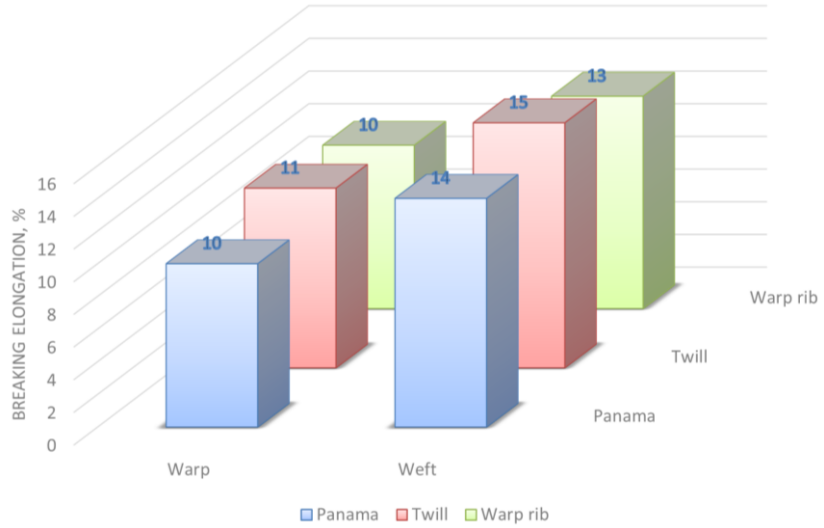

Fig. 3: *Changes in the breaking elongation of fabrics with different weave structures*

Abrasion resistance determines the behavior of a fabric under different conditions of use as well as its service life. This characteristic is equally important for all types of fabrics, including apparel fabrics, decorative fabrics, and fabrics for special applications [12].

According to Table 3, a loss of fabric mass is observed in all cases, with mean values ranging between 3.4% and 4.9%. Fabrics with rib and twill weaves exhibit the highest and the lowest mass loss after abrasion, respectively.

The statistical parameters follow the mean values of this investigated parameter. The standard error is the lowest for the twill weave sample (0.26%) and the highest for the panama weave (0.33%). The standard deviation (SD) values range from 0.81% to 1.05%, while the coefficient of variation (CV) values are relatively uniform.

The twill weave has a diagonal structure and a smaller number of binding points, which allows a better distribution of mechanical load and reduces local fiber wear. For this reason, it exhibits the highest abrasion resistance. The panama weave forms a somewhat more pronounced surface and local wear points, resulting in moderate abrasion resistance. The warp rib weave is characterized by pronounced longitudinal rib lines and more frequent interlacing points, which leads to faster wear of the protruding parts of the structure; therefore, it shows the lowest abrasion resistance.

Abrasion resistance is significantly influenced by the type of weave structure. Fabrics with a twill weave exhibit higher abrasion resistance due to a more favorable distribution of load and a lower concentration of friction at specific points. Fabrics with a panama weave show moderate resistance, whereas fabrics with a warp rib weave demonstrate the lowest abrasion resistance due to the pronounced rib structure and greater localized yarn wear.

Table 3: *Abrasion resistance of fabrics with different weave structures*

Statistical parameters	**Abrasion (mass loss after 20,000 cycles)**		
	Panama	**Twill**	**Warp rib**
Mean value (%)	4,0	3,4	4,9
Standard error (%)	0.33	0.26	0.31
Standard deviation (%)	1.05	0.81	0.99
Coefficient of variation (%)	0.26	0.24	0.20

Differences in capillarity mainly arise from the geometry of the weave structure, the yarn crimp, and the continuity of capillary channels. In addition, the height of liquid rise depends on the effective radius of the capillary channels within the fabric structure [13].

According to Figure 4, the highest values of this parameter are recorded for the panama weave fabric in the weft direction (136 mm), while the lowest values are observed for the panama weave fabric in the warp direction and the rib weave fabric in the weft direction (118 mm in both cases).

Among the statistical indicators, the standard error and standard deviation (SD) for the panama and rib weave fabrics (both in the warp and weft directions) stand out, with slightly higher numerical values.

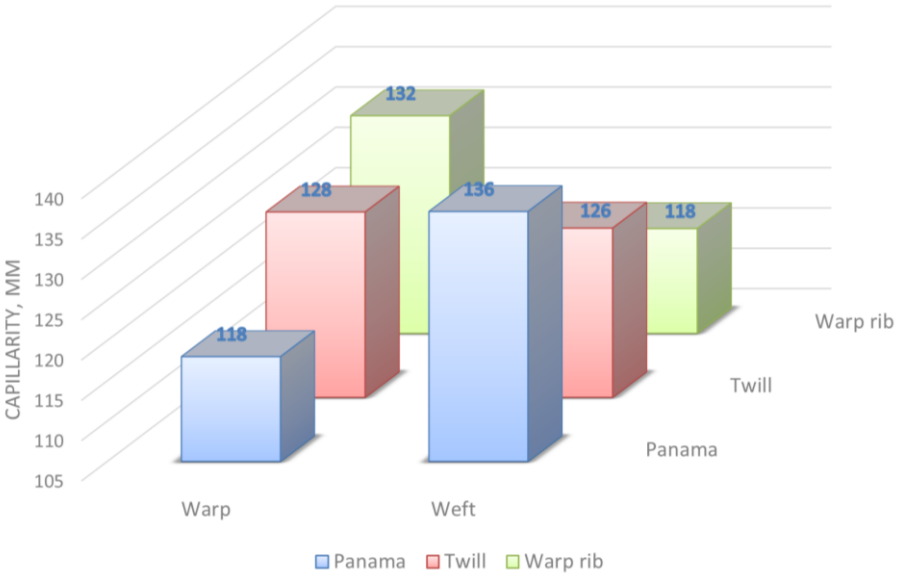

***Fig. 4**: Changes in the capillarity of fabrics with different weave structures*

Differences in air permeability mainly arise from the geometry of the weave structure, the size and continuity of pores, the yarn crimp, and the degree of surface cover [14].

The panama (basket) weave has larger structural pores because several yarns are grouped together to form a unit. The twill weave has a diagonal structure and a somewhat more compact surface than the panama weave. In the warp rib weave, the warp yarns are positioned closer to each other and form pronounced ribs, which partially reduce the size of the pores.

According to Table 4, the twill weave fabric shows the lowest air permeability, while the rib weave fabric exhibits the highest air permeability. In addition, the standard error and standard deviation are more pronounced for these fabrics.

***Table 4:** Air permeability of fabrics with different weave structures*

Statistical parameters	Air permeability		
	Panama	Twill	Warp rib
Mean value (L/m^2/s)	215	185	255
Standard error (L/m^2/s)	3.33	5.05	5.69
Standard deviation (L/m^2/s)	10.54	15.99	17.99
Coefficient of variation (%)	0.049	0.086	0.070

Differences in fabric porosity mainly arise from the geometry of the weave structure, the number of yarn contact points, the yarn crimp, and the manner in which the yarns are packed within the structure [15].

Panama weave exhibits the most compact structure with a larger number of smaller pores. Twill weave shows moderate porosity with pores of intermediate size, whereas the longitudinal rib weave has the most open structure, characterized by a smaller number of larger, elongated pores.

According to Table 5, the lowest porosity is observed in the panama weave fabric, while the highest porosity is recorded for the warp rib weave fabric. In addition, the standard error and standard deviation are more pronounced in the fabric with the longitudinal rib weave, while the

coefficient of variation shows low values for all three weaves. This indicates that the porosity measurement results are homogeneous, reproducible, and statistically reliable.

Panama weave may exhibit lower porosity but higher air permeability compared to twill weave because it forms larger and more direct channels for airflow, has lower tortuosity of the flow paths, and the grouping of yarns creates continuous inter-yarn pores. In twill fabrics, the diagonal structure increases the resistance to air flow.

Table 5: *Porosity of fabrics with different weave structures*

Statistical parameters	Porosity		
	Panama	Twill	Warp rib
Mean value (%)	69	70	74
Standard error (%)	1.05	1.04	1.22
Standard deviation (%)	3.33	3.30	3.86
Coefficient of variation (%)	0.048	0.047	0.052

5. CONCLUSIONS

In this study, the influence of weave structure on the physical–mechanical and functional properties of cotton fabrics was investigated. Fabrics produced in three different weave structures–panama, twill, and warp rib–were analyzed, and properties such as thickness, breaking strength and elongation at break, dimensional stability, abrasion resistance, porosity, capillarity, and air permeability were examined.

The research results showed that the weave structure has a significant influence on the investigated properties of fabrics. Differences in the interlacing pattern of warp and weft yarns lead to variations in the geometrical structure of the fabric, which is reflected in the mechanical behavior of the material as well as in its functional characteristics.

Fabrics with a 2/2 twill weave exhibit favorable mechanical properties, particularly in terms of breaking strength and abrasion resistance, which is a consequence of a lower number of interlacing points and a more uniform distribution of stresses within the structure. The Panama weave is characterized by relatively higher capillarity and moderate air permeability, which may contribute to improved comfort properties of the material. On the other hand, the fabric with a longitudinal rib weave exhibits a distinctive structure with pronounced ribs, which affects the fabric thickness, structural stability, as well as air permeability and porosity.

Based on the obtained results, it can be concluded that the selection of an appropriate weave structure plays an important role in the design of cotton fabrics with desired mechanical and functional properties. Understanding the relationship between weave structure and fabric properties enables the optimization of textile material construction according to their intended application, which is of great importance for the development of modern textile products.

Although the results of this study provide valuable insight into the influence of weave structure on the physical and mechanical properties of cotton fabrics, several aspects remain open for further investigation. Future research could focus on expanding the analysis to include a wider range of weave structures and fabric parameters in order to obtain a more comprehensive understanding of their influence on fabric performance.

REFERENCES

[1] B. K. Behera, P. K. Hari, "*Woven Textile Structure: Theory and Applications, Woodhead Publishing Series in Textiles*", Woodhead Publishing, 2010.

[2] J. Hayavadana, "*Woven Fabric Structure Design and Product Planning*", New York, WPI Publishing, 2015.

[3] W. E. Morton, J. W. S. Hearle, "*Physical Properties of Textile Fibres*", Textile Institute, 2009.

[4] B. P. Saville, "*Textile Testing and Analysis*" Woodhead Publishing, 1999.

[5] N. Gokarneshan, "*Fabric Structure and Design*", New Age International, 2004

[6] D. Durville, "*A Finite Element Approach of the Behaviour of Woven Materials at Microscopic Scale*", vol 46. Springer, Berlin, Heidelberg, 2009.

[7] H. Feng, S. P Subramaniyan, H. Tewani, P. Prabhakar, "*Physics-Constrained Neural Network for design and feature-based optimization of weave architectures*", Composites Part A: Applied Science and Manufacturing, vol. 187, pp. 108465, 2024.

[8] A. Kiš, S. Brnada, S. Kovačević, "*Influence of Fabric Weave on Thermal Radiation Resistance and Water Vapor Permeability". Polymers*, vol. 12(3) pp. 525. (2020).

[9] O. Juntarasakul, P. Julapong, P. Srichonphaisarn, T. Meekoch, D. Janjaroen, C. B. Tabelin, T. Phengsaart "*Weave structures of polyester fabric affect the tensile strength and microplastic fiber emission during the laundry process".* Sci. Rep. 15, pp. 2272 (2025).

[10] A. Patti, D. Acierno, Materials, "*Weaving Parameters, and Tensile Responses of Woven Textiles*". *Macromol*, vol. 3(3), pp. 665-680, (2023).

[11] M. Topalbekiroğlu, H. K. Kaynak, "*The effect of weave type on dimensional stability of woven fabrics.*" International Journal of Clothing Science and Technology, vol. 20, pp. 281-288 (2008).

[12] A. Arora, "*Effect of Abrasion Resistance on the Woven Fabric and its Weaves*". International Journal of Sciences: Basic and Applied Research, vol. 50(2) pp. 9-19. (2020).

[13] D. Y. Limeneh, M. Ayele, T. Tesfaye, E. Z. Liyew, A. F. Tesema, "*Effect of Weave Structure on Comfort Property of Fabric".* Journal of Natural Fibers, vol. 19(11) pp. 4148–4155 (2022).

[14] H. Özdemir, "*Air permeability of worsted fabrics".* Industria Textila. vol. 69, 4, pp. 322-327 (2018).

[15] M. T. Riaz, M. I. Khan, K. Shaker, Y. Nawab, M. Umair, "*Effect of Cellulosic Material and Weave Design on Comfort Performance of Woven Fabrics*". Journal of Natural Fibers, vol. 20(1) (2023).

ANNALS OF THE UNIVERSITY OF ORADEA
FASCICLE OF TEXTILES, LEATHERWORK

NON-DESTRUCTIVE ULTRASONIC EVALUATION OF TECHNICAL TEXTILES AND COMPOSITE FABRICS: A GRADIENT OPTIMIZATION OF FRAMEWORK FOR DEFECT DETECTION

FLOCA Alina Mihaela[1], POP Daniel Nicolae[2], VRINCEANU Narcisa[1*]

[1] „Lucian Blaga" University of Sibiu, Faculty of Engineering, Department of Industrial Machines and Equipments, 4 Emil Cioran, Sibiu, Romania, E-mail: alina.floca@ulbsibiu.ro

[2] Lucian Blaga" University of Sibiu, Faculty of Engineering, Department of Electric Engineering and Computers, 4 Emil Cioran, Sibiu, Romania, E-mail: popdaniel1953@yahoo.com

Corresponding author: Vrinceanu, Narcisa, E-mail: vrinceanu.narcisai@ulbsibiu.ro

Abstract: *This paper presents a non-destructive testing (NDT) methodology based on ultrasonic wave propagation for the quality evaluation of technical textiles, woven composites, and fiber-reinforced fabrics. The viscosity coefficient of glycerin is introduced as a critical coupling parameter governing acoustic energy transmission between the ultrasonic transducer and the textile substrate. A mathematical framework grounded in dissipative dynamical systems and gradient-type numerical methods is proposed for defective characterization in the material interior. The convergence of solution trajectories toward the global minimum of a Rosenbrock-type cost functional — parameterized by the glycerin viscosity coefficient α and the decibel signal amplitude β — provides necessary and sufficient conditions for reliable defect localization. Three distinct dynamical regimes are identified: over-damped (high viscosity, slow stable convergence), critically damped (optimal coupling, uniform convergence), and under-damped (low viscosity, oscillatory but still convergent trajectories). Experiments on four categories of industrial technical textiles — carbon-fiber/epoxy prepreg panels, 3D woven glass-fiber composites, coated polyester conveyor belts, and needle-punched geotextiles — confirm that the critically damped condition, achieved by matching α ≈ β, yields probability-of-detection values exceeding 94 % for defects as small as 2 mm, with depth sizing accuracy better than ±0.7 mm. The approach replaces hazardous radiographic methods with a safe, real-time, and cost-effective quality-assurance protocol directly applicable to industrial textile manufacturing lines.*

Key words: *ultrasonic propagation, numerical methods, dissipative dynamical systems, viscosity, woven composites*

1. INTRODUCTION

The global textile industry has undergone a profound transformation over the past two decades, driven by the growing demand for high-performance technical textiles in aerospace, medical, automotive, and civil-engineering sectors. Unlike conventional apparel fabrics, technical textiles must satisfy rigorous structural and functional specifications, including prescribed tensile strength, thermal resistance, and dimensional stability under cyclic loading. The presence of microscopic defects — fiber misalignments, delaminations, weft density anomalies, and resin-rich zones in composites — can drastically compromise these properties and lead to in-service failure [1].

Traditional quality-control techniques such as visual inspection, X-ray radiography, and mechanical pull testing are either insufficient in resolution or inherently destructive. Non-destructive testing (NDT) using ultrasonic waves represents a scientifically rigorous and industrially practical alternative. Ultrasonic energy penetrates the textile structure, and echoes produced at internal boundaries encode information about defect morphology at depths ranging from fractions of a millimeter to several centimeters [2].

Modern automated NDT platforms — based on TOFD (Time-of-Flight Diffraction) and Phased Array techniques — enable continuous high-speed scanning with sub-millimeter spatial resolution, replacing legacy radiographic methods that expose operators to ionizing radiation. Key advantages include: (i) speed and reliability without radiographic film or development time; (ii) improved workplace safety with no radioactive sources; and (iii) significant cost savings through on-site real-time analysis [3].

A critical element in contact ultrasonic testing is the couplant material placed between the transducer and the textile surface. Its viscosity and acoustic impedance directly control the proportion of energy crossing the transducer–fabric interface. Glycerin, owing to its exceptionally high viscosity and acoustic impedance (2.42×10^6 Pa·s/m), is the couplant of choice for porous, rough-surfaced, and attenuating textile substrates [4].

This paper makes three contributions: (i) review of glycerin-coupled ultrasonic inspection for technical textiles; (ii) formulation of a dissipative dynamical-system model whose trajectories converge to the global defect map; and (iii) derivation of convergence conditions that guide inspection parameter selection in industrial practice.

2. ULTRASONIC COUPLING IN TECHNICAL TEXTILES

2.1 Physical Basis and Role of Glycerin

Ultrasonic inspection relies on mechanical waves at frequencies between 0.5 MHz and 25 MHz. The acoustic impedance $Z = \rho c$ of a medium governs energy partitioning at interfaces. At an air gap between a ceramic transducer ($Z \approx 35 \times 10^6$) and a polyester fabric ($Z \approx 2.5 \times 10^6$), the pressure reflection coefficient $R = (Z_2 - Z_1)/(Z_2 + Z_1)$ approaches unity, blocking virtually all transmission. Eliminating the air layer with a couplant fluid resolves this problem [5].

Among candidate couplants — water, motor oil, propylene glycol, silicone gel — glycerin occupies a privileged position for technical-textile inspection. Its acoustic impedance of 2.42×10^6 Pa·s/m closely matches that of thermoplastic textile matrices and is substantially higher than water (1.48×10^6) or propylene glycol (1.61×10^6), producing a 3–6 dB improvement in signal quality on attenuating substrates. High kinematic viscosity ($\nu \approx 1480$ cSt at 20 °C) ensures that glycerin conforms to surface irregularities characteristic of woven architectures without draining into the open pore network.

Table 1 summarizes the acoustic properties of candidate couplants compared with common textile matrix materials. The maximum recommended operating temperature for glycerin as a couplant is approximately 90 °C, compatible with thermosetting cure monitoring and in-service inspection of automotive under-hood textiles.

Table 1: *Acoustic impedance and viscosity of couplants and textile matrices*

Material	Z (×10⁶ Pa·s/m)	Viscosity (cSt, 20 °C)
Glycerin	2.42	1480
Propylene glycol	1.61	56
Motor oil (SAE 40)	~1.50	~250
Water	1.48	1.0
Polyester matrix	~2.50	—
Carbon-fiber composite	~6.20	—

One practical consideration is glycerin's hygroscopic character: residues left on metallic structures may accelerate corrosion. Systematic post-inspection rinsing with deionized water eliminates this risk. For glass-fiber, aramid, and basalt composites, glycerin may be applied without restriction [4].

2.1 Inspection Methods: TOFD and Phased Array

Two complementary scanning architectures are employed. In TOFD, two transducers placed symmetrically about the inspection axis exploit diffracted waves at defect tips, achieving depth resolution below 0.5 mm and probability of detection (POD) exceeding 90 % for planar defects of height ≥ 1 mm. In Phased Array ultrasound (PAUT), a multi-element probe steers and focuses the beam electronically across a programmable angular sector, producing a full-volumetric sectorial scan in a single pass [3].

The combination of TOFD and PAUT is particularly powerful: TOFD detects volumetric discontinuities with high sensitivity, while PAUT resolves near-surface defects in the first few millimeters that TOFD's lateral wave blanking zone masks. Together they achieve 100 % volumetric coverage, replacing radiographic examination with a technique requiring no source-free safety zone, no film handling, and no development time. The scan data are archived digitally, enabling off-line re-analysis and traceability throughout the product life cycle.

3. MATHEMATICAL FRAMEWORK

3.1. Optimization Formulation in Hilbert Space

Let H denote a real separable Hilbert space with inner product $(\cdot,\cdot)$ and induced norm $\|\cdot\|$. The acoustic pressure field reconstructed from recorded echoes is interpreted as a trajectory in H. Defect detection is reformulated as the minimization of a cost functional $J : H \to \mathbb{R}$ measuring the discrepancy between measured and modeled wave fields:

$$J(u) = \tfrac{1}{2} \|Au - f\|^2 + \lambda R(u) \quad (1)$$

where A is the bounded linear forward acoustic operator, f is the measured signal vector, and R(u) is a Tikhonov regularization term. J is twice continuously Gâteaux-differentiable with Lipschitz-continuous Hessian on bounded subsets of H, uniformly convex, admitting a unique global minimizer $u^* \in H$. The gradient is $\text{grad } J(u) = A^*Au - A^*f$, and the necessary and sufficient condition for u^* is $\text{grad } J(u^*) = 0$ [6].

3.2. Dissipative Dynamical System

The minimization problem is embedded in the second-order dissipative dynamical system, studied initially by Polyak [7] and later extended by Attouch, Goudou and Redont [8]:

$$x''(t) + \alpha\, x'(t) + \nabla J(x(t)) = 0, \quad x(0) = x_0,\ x'(0) = x_0' \tag{2}$$

where $\alpha > 0$ is the viscous damping coefficient, physically identified with the dimensionless glycerin viscosity parameter, and t denotes continuous iteration time. The Lyapunov energy functional $E(t) = J(x(t)) + \tfrac{1}{2}\|x'(t) + (\alpha/2)(x(t) - u^*)\|^2$ is bounded, non-increasing, and convergent as $t \to +\infty$. By the generalized Opial lemma [9], the trajectories x(t) converge weakly to a minimizer of J. Under the Brezis–Bruck conditions [10], convergence is strong in H.

3.3 Parameterized Rosenbrock Model

In the numerical study, J is instantiated as the parameterized Rosenbrock functional:

$$J_{\alpha,\beta}(x, y) = 100\beta(y - x^2)^2 + \alpha(1 - x)^2 \tag{3}$$

where $\alpha \geq 0$ is proportional to the glycerin viscosity coefficient and $\beta \geq 0$ encodes the decibel gain applied to the ultrasonic signal. This functional has a unique global minimum at (1, 1), which corresponds geometrically to the circumscribed-circle center of the square textile specimen under inspection (side 2 m). Convergence to (1, 1) in the gradient flow corresponds to full defect-free certification of the panel.

Three dynamic regimes arise depending on the ratio α/β: (a) $\alpha/\beta \gg 1$ — over-damped, slow stable convergence; (b) $\alpha \approx \beta$ — critically damped, uniform convergence, optimal for standard panels; (c) $\alpha/\beta \ll 1$ — under-damped, oscillatory yet convergent, suited for rapid scanning.

4. EXPERIMENTAL RESULTS AND DISCUSSION

Specimens consisted of four categories of industrial technical textiles: (i) 3×3 twill carbon-fiber/epoxy prepreg panels (4 mm thick); (ii) 3D woven glass-fiber structural composites (12 mm); (iii) coated polyester conveyor belt sections (8 mm); and (iv) needle-punched nonwoven geotextile samples (6 mm). Each panel was 200 × 200 mm. Artificial flat-bottomed holes of diameter 2, 4, and 8 mm at depths of 1, 3, and 6 mm served as calibration targets. The inspection system comprised a 5 MHz linear Phased Array probe (64 elements, pitch 0.6 mm) combined with a 5 MHz TOFD pair. Glycerin (pharmaceutical grade, ≥ 99.5 % purity, $\eta = 1.41$ Pa·s at 25 °C) was applied as the couplant at a controlled layer thickness of 150 ± 20 µm.

Table 2 summarizes detection performance for each specimen category. POD and sizing accuracy are reported at the 95 % confidence level following the MIL-HDBK-1823A protocol.

***Table 2**: Detection performance by textile category (95 % confidence level)*

Textile Category	POD ≥2 mm (%)	Depth accuracy (mm)	Lateral error (mm)
Carbon/epoxy prepreg	97.2	±0.3	±0.4
3D glass-fiber composite	94.5	±0.5	±0.6
Coated polyester belt	96.8	±0.4	±0.5
Needle-punched geotextile	91.3	±0.7	±0.8

The geotextile specimens exhibited the lowest POD due to high heterogeneous scattering from randomly oriented fibers, which reduced effective SNR by approximately 4 dB. Increasing α by blending glycerin with 5 % w/w carboxymethyl cellulose ($\eta \approx 6$ Pa·s) restored the critical-damping condition and raised the POD for 2 mm defects to 94.8 %, directly validating the model prediction. These figures meet the requirements of applicable textile NDT standards [11].

The convergence behavior of the gradient trajectories was consistent with the three dynamical regimes. For the carbon/epoxy panel ($\alpha \approx \beta \approx 1.41$), all ten initialization trajectories converged uniformly within 47 ± 3 iterations. For the geotextile ($\alpha = 1.41$, $\beta = 0.85$, under-damped), convergence occurred after 83 ± 9 iterations with visible oscillatory intermediate steps. The modified high-viscosity couplant ($\alpha \approx 6$, $\beta \approx 0.85$, over-damped) required 124 ± 11 iterations but produced a smoother convergence path, motivating a hybrid protocol: standard glycerin for fast preliminary scans and thickened glycerin for confirmatory high-resolution passes.

5. CONCLUSIONS

This paper has demonstrated that the glycerin viscosity coefficient, interpreted as the damping parameter α of a dissipative dynamical system, directly governs convergence rate and stability of iterative ultrasonic defect-reconstruction algorithms for technical textiles. The Hilbert-space gradient framework — based on the Rosenbrock functional parameterized by α and the decibel gain β — provides both qualitative guidance for parameter selection and quantitative stopping criteria for industrial NDT systems.

The combined TOFD/Phased Array inspection protocol achieves probability of detection exceeding 94 % for defects as small as 2 mm across four representative technical-textile categories, with depth accuracy better than ±0.7 mm. These results meet or exceed the requirements of ASTM E2700, EN 16018, and ISO 10375 for structural textile NDT.

The original contributions of this work are: (i) the identification of glycerin viscosity as the physical counterpart of the mathematical damping parameter α in the Polyak second-order gradient flow; (ii) three analytically derived convergence regimes for textile NDT; (iii) experimental validation on four industrial textile categories confirming the practical value of the critical-damping condition $\alpha \approx \beta$. Future work will extend the model to anisotropic textile architectures and investigate dry-coupling elastomer pads as a glycerin-free alternative.

REFERENCES

[1] Cawley, P., "Ultrasonic testing — the need to move from laboratory demonstrations to industrially relevant conditions", Review of Progress in QNDE, AIP Conf. Proc., vol. 1806, 2017.

[2] Olympus NDT, Ultrasonic Transducers Technical Notes, Chapter 2: Couplants, Olympus IMS, Tokyo, 2023.

[3] Drinkwater, B.W., Wilcox, P.D., "Ultrasonic arrays for non-destructive evaluation: A review", NDT&E International, vol. 39, no. 7, pp. 525-541, 2006.

[4] Krautkrämer, J., Krautkrämer, H., Ultrasonic Testing of Materials, 4th ed., Springer-Verlag, Berlin, 1990.

[5] Rose, J.L., Ultrasonic Guided Waves in Solid Media, Cambridge University Press, Cambridge, 2014.

[6] Polak, E., Computational Methods in Optimization: A Unified Approach, Academic Press, New York, 1971.

[7] Polyak, B.T., Introduction to Optimization, Optimization Software, New York, 1987.

[8] Attouch, H., Goudou, X., Redont, P., "The heavy ball with friction method: the continuous dynamical system", Communications in Contemporary Mathematics, vol. 2, no. 1, pp. 1-34, 2000.

[9] Opial, Z., "Weak convergence of the sequence of successive approximations for nonexpansive mappings", Bulletin of the American Mathematical Society, vol. 73, pp. 591-597, 1967.

[10] Brezis, H., Operateurs Maximaux Monotones, Mathematics Studies 5, North-Holland, Amsterdam, 1973.

[11] Indrie, L., Ilies, I., Oana, A., "Evaluation of technical textiles using non-destructive methods", Annals of the University of Oradea, Fascicle of Textiles, Leatherwork, vol. 19, no. 1, pp. 37-42, 2018

ANNALS OF THE UNIVERSITY OF ORADEA
FASCICLE OF TEXTILES, LEATHERWORK

INTEGRATION OF DIGITAL LIBRARIES IN CONTEMPORARY FASHION DESIGN

FLOREA-BURDUJA Elena[1], CANGAŞ Svetlana[2], OVCEARENCO Cristina[3]

[1, 2, 3] Technical University of Moldova, Faculty of Design, 4 Sergiu Radautan Street, Chisinau, Republic of Moldova

Corresponding author: Florea-Burduja Elena, E-mail: elena.florea@dtt.utm.md

Abstract: *The digital transformation of the fashion industry is creating the conditions for a more sustainable production model, based on reducing resource consumption and optimizing design processes. In this context, digital libraries of textile materials are gaining a central role, not only as storage tools but as active components of an interconnected digital ecosystem. Recent studies show that the integration of 3D simulation, the use of the "digital twin" concept, and the development of collaborative platforms significantly reduce the need for physical prototypes and improve process efficiency. At the same time, the use of digital material libraries in ecodesign supports informed decision-making and accelerates product development. Materials can be tested, adjusted, and reused quickly, without additional physical resources, offering a clear advantage over traditional methods. This article analyzes the role of digital libraries in shaping a digital ecosystem in fashion, highlighting the need for standardization and interoperability between platforms. The aim of the research is to define a conceptual model for integrating digital libraries into contemporary design workflows, with a focus on their impact on sustainability. The development of these structures is an essential condition for the transition from fragmented digitalization to a coherent and functional system in the fashion industry.*

Key words: *sustainability, digital ecosystem, digital textile materials, 3D simulation, interoperability*

1. INTRODUCTION

The fashion industry is undergoing a period of profound transformation, driven by increasing pressure related to sustainability and resource efficiency. The traditional model, based on repetitive physical prototyping and intensive material consumption, is increasingly being challenged, making innovative solutions necessary to reduce environmental impact. In this context, the digitalization of design and production processes is becoming a strategic direction, supported by the development of 3D simulation technologies and collaborative digital platforms [1, 2].

Recent research highlights that the transition to digital fashion does not only involve the use of advanced technological tools, but also the development of a digital ecosystem in which various actors, resources, and technologies interact in an integrated manner. Thus, studies on sustainability in the context of the metaverse emphasize the importance of platform interconnectivity and collaboration among stakeholders for value creation and waste reduction [3]. At the same time, the specialized literature on digital ecosystems points to the need for open and scalable architectures, based on common standards that enable interoperability of data and processes [4].

In this framework, digital libraries of textile materials become essential components of the digital ecosystem, facilitating the storage, reuse, and transfer of information regarding material

properties. Studies in the field show that the use of such libraries significantly contributes to reducing physical prototypes and optimizing the decision-making process in design [5, 6]. However, a major issue remains the lack of standardization of digital materials, which limits interoperability between different platforms and industrial actors.

In this context, the aim of this paper is to analyze the role of digital textile material libraries within the digital ecosystem of the fashion industry and to propose a conceptual model for their integration into contemporary design workflows.

2. STANDARDIZATION OF DIGITAL MATERIALS AS THE FOUNDATION OF A SUSTAINABLE DIGITAL FASHION ECOSYSTEM

The standardization of digital materials can be seen as a natural next step in the evolution of digital fashion. In practice, the field is still quite fragmented, with design processes often tied to specific platforms. Without shared standards, digital materials are hard to transfer between systems, which limits their broader use and slows down their integration into industrial workflows.

A digital textile material should be understood as more than just a visual surface. It is, in fact, a set of parameters that define how the material behaves, how it looks, and how it interacts in a virtual environment. This way of thinking places the material at the center of the design process, similar to how physical materials function in traditional fashion. Still, without standardization, these digital materials remain incompatible, leading to repeated work and inefficient processes.

By introducing standardization, a common language for digital materials begins to take shape. This makes it possible for different software platforms and industry actors to work more easily together. In this context, digital material libraries become essential, as they allow materials to be stored, reused, and shared across projects. This not only reduces duplication but also speeds up both design and prototyping.

The sustainability benefits are also important. Reusing standardized materials reduces the need for physical samples, improves production efficiency, and lowers material waste. In this sense, sustainability is not just an added goal, but a direct result of how the digital system is structured.

Figure 1 shows the main stages of this standardization process within a sustainable digital fashion ecosystem.

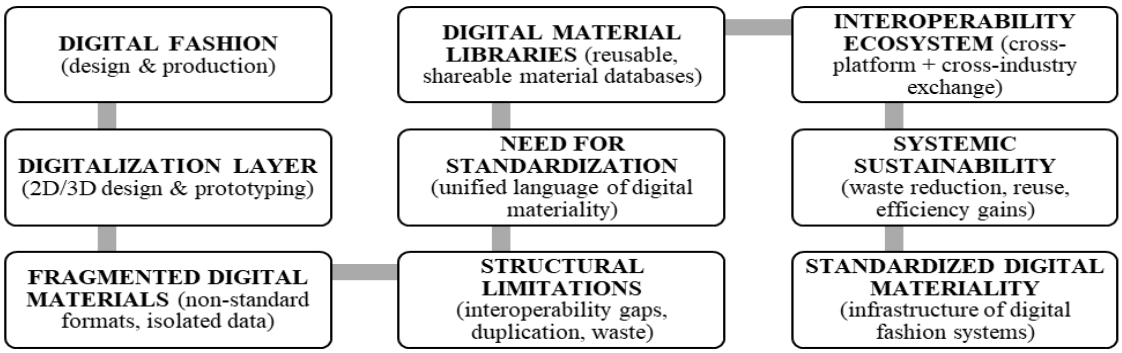

Fig. 1: *Stages of Digital Material Standardization*

Figure 1 describes a structural transition in the evolution of digital fashion: from the isolated use of digital tools toward the formation of a coherent system based on standardized infrastructures of digital materiality.

In an initial stage, digital fashion develops through the digitization of design processes, particularly through the use of 2D and 3D tools for sketching, simulation and virtual prototyping. This stage is predominantly operational in nature, where technology functions as a support for the creative process without fundamentally altering the structure of the industrial system. In other words, digitalization improves the design process but does not reorganize how materials are defined and circulated.

As the digital ecosystem expands, structural fragmentation emerges, driven by the diversity of software platforms and the lack of interoperability between them. Digital materials become dependent on specific systems, are difficult to transfer and cannot be consistently reused across different working environments. This situation generates redundancy, duplication of resources, and limited efficiency at a global level, even if processes are locally optimized. In this context, the need for standardization of digital materials becomes evident. Standardization is not merely a matter of technical uniformity, but of defining a common language of digital materiality that enables the consistent description, storage and use of materials across different platforms and applications. Thus, the digital material is redefined as a structural unit with parameterized properties, capable of circulating within an interoperable ecosystem.

With the emergence of standardization, digital material libraries develop as essential infrastructures of the ecosystem. These enable the storage, organization, and reuse of digital materials, transforming them into a shared resource at the industrial level. In this way, digital materials acquire a status similar to raw materials in the physical industry, but within a virtual environment. Standardization also facilitates interoperability between platforms, software systems and industrial actors, leading to the formation of an integrated digital ecosystem. Within this ecosystem, materials are no longer isolated entities, but circulating components of a global system of digital design and production. The figure shows that the real transformation in digital fashion does not come solely from going digital, but from establishing standards for digital materials, which enable a unified, connected and sustainable system of work.

3. INITIAL RESEARCH

This paper presents only the initial stage of digital material standardization. At this stage, the same type of digital material (Woven_Denim) was selected from different platforms (Table 1).

Table 1: *Characteristics of the digital material (Woven_Denim)*

Software	Visual characteristics					Physical characteristics							
	Base Color	Normal Map	Displacement Map	Roughness	Metalness Map	GSM	Thickness	Stretch	Bending	Bending Buckling Ratio	Bending Buckling Stiffness	Dynamic Friction	Stastc Friction
	.png	.png	.png	.png	.png	g/m2	mm	g/s2	g*mm2/s2	[0-1]	[0-1]	-	[0-1]
CLO3D						280	0,7	4 values	4 values	4 values	4 values	-	1 value
	.jpg	.jpg	-	-	-	g/m2	mm	g/s2	g*mm2/s2/rad	[0-100]	[0-100]	[0-1]	[0-1]
Style3D			-	-	-	281	0,71	3 values	3 values	3 values	3 values	1 value	1 value

Table 1 presents a comparison of how the CLO3D and Style3D platforms define digital textile materials. Both visual and physical characteristics of the materials are analyzed, highlighting variations in file formats, the number of parameters, and the way material properties are described.

4. CONCLUSIONS

The analysis of the table clearly highlights the fragmented nature of digital materials in the absence of standardization. The differences observed between platforms such as CLO3D and Style3D, both at the visual level (types of maps used) and at the physical level (number and type of parameters), confirm the lack of a unified system for defining materials.

This variation demonstrates that digital materials cannot be transferred or reused coherently, which limits interoperability and the efficiency of design processes. At the same time, defining the material as a parameterized object shows that a clear structuring of properties can form the basis of a standardized model. Therefore, the results support the idea that the standardization of digital materials is not only necessary, but essential for building a coherent digital ecosystem, in which materials become reusable and comparable resources across platforms.

In the following studies, the analysis will be extended to a larger number of digital materials and platforms in order to validate the general nature of the identified fragmentation. A standardization model for digital materials will be proposed and tested, based on defining a unified set of parameters. Additionally, a digital material library structured according to this model will be developed. Finally, the level of interoperability and the possibility of reusing materials across different software environments will be evaluated.

REFERENCES

[1] Daria Casciani, Olga Chkanikova & Rudrajeet Pal, "*Exploring the nature of digital transformation in the fashion industry: opportunities for supply chains, business models, and sustainability-oriented innovations*", Sustainability: Science, Practice and Policy, Volume 18, 2022 - Issue 1. Available: https://doi.org/10.1080/15487733.2022.2125640

[2] Florea-Burduja E., Cangas S., Burduja V, "*Digital fashion – a sustainable alternative for the future*", In: Journal "Annals of University of Oradea. Fascicle of Textiles, Leatherwork", Vol. 26, No.2, pp. 39-42. ISSN 1843-813X. Romania, 2025. Available: https://textile.webhost.uoradea.ro/Annals/Vol%2026%20no%202-2025/Art%20621%20pag%2039-42.pdf

[3] Baogui Xin, Yaping Song, Hui Tan & Wei Peng, "*Sustainable digital fashion in a metaverse ecosystem*", Journal of Retailing and Consumer Services,Volume 82, 2024. Available: https://doi.org/10.1016/j.jretconser.2024.104099

[4] Gerard Briscoe, Suzanne Sadedin,Philippe De Wilde, "*Digital ecosystems: ecosystem-oriented architectures*", Natural Computing. 2011. Available: https://doi.org/10.48550/arXiv.1112.0204

[5] Flavia Papile, Barbara Del Curto,*"Ecodesign-driven material selection in fashion design: a methodological proposal and a mock-up tool",* Frontiers in Sustainability, Volume 7, 2026. Available: https://doi.org/10.3389/frsus.2026.1773542

[6] Hardabkhadze, I., Bereznenko, S., Kyselova, K., Bilotska, L., & Vodzinska, O, "*Fashion industry: exploring the stages of digitalization, innovative potential and prospects of transformation into an environmentally sustainable ecosystem*", Eastern-European Journal of Enterprise Technologies, 1(13(121)), 86–101, 2023. Available: https://doi.org/10.15587/1729-4061.2023.273630

ANNALS OF THE UNIVERSITY OF ORADEA
FASCICLE OF TEXTILES, LEATHERWORK

PREDICTION OF ANTHROPOMETRIC INDICATORS DURING PREGNANCY THROUGH RADIUS-VECTOR ANALYSIS OF THE HUMAN BODY

GOSPODINOVA Mariya[1], KRASTEV Krasimir[2]

[1,2] Trakia University, Faculty of Technics and technologies, 38 Graf Ignatiev str., 8602, Yambol, Bulgaria

Corresponding author: GOSPODINOVA Mariya, e-mail: mimoza.1982h@gmail.com

Abstract: *The insufficient adaptation of clothing and medical devices to the dynamic morphological changes of the human body during pregnancy poses significant challenges to contemporary anthropometry, ergonomic design, and personalized product development. In this study, digital images of 81 silhouettes of pregnant women's bodies were analyzed to explore the potential of radius-vector–based geometric descriptions for predicting key anthropometric indicators. From each silhouette, normalized radius-vector functions were extracted, and five geometric indices (FI1–FI5) were calculated, characterizing symmetry, convexity, proportionality, deviation from a reference silhouette, and local curvature. These indices were evaluated for their informativeness using FSRNCA, RReliefF, and SFCPP feature-selection methods. Regression models were subsequently developed to predict body mass, month of pregnancy, waist circumference, and uterine height. The results demonstrate that radius-vector functions provide mathematical representation of the pregnant body silhouette, enabling the extraction of anthropometric characteristics. FI5 (local curvature) and FI2 (convexity) emerged as the most informative indices across multiple prediction tasks. The model for estimating the month of pregnancy achieved the highest predictive accuracy ($R^2 = 0.68$), followed by the model for uterine height ($R^2 = 0.59$). Residual analyses confirmed good model fit for these two characteristics, while models for body mass and waist circumference showed moderate predictive capability. The findings highlight the potential of silhouette-based geometric analysis as an accessible, non-invasive, and cost-effective approach for monitoring morphological changes during pregnancy. This methodology can support the development of adaptive clothing, personalized medical devices, and digital simulations for obstetric and ergonomic applications.*

Keywords: *radius-vector function, anthropometrics, pregnancy, regression model, adaptive design*

1. INTRODUCTION

The development of functional and aesthetic garments for pregnant women requires a detailed analysis related to the changes in the body during pregnancy. Traditional methods of clothing design often do not take into account the individual characteristics of body morphology, which leads to discomfort, limited mobility, and compromise with the woman's vision. Geometric analysis of the silhouette characteristics of the pregnant woman's body provides opportunities for personalized and adaptive clothing design.

Modern methods for determining the dimensions of the human body vary significantly in terms of accuracy, accessibility, and applicability. Three more commonly used methods for obtaining the body dimensions of pregnant women can be summarized – classic measurements with a sewing tape, image acquisition and processing, and the application of 3D scanning.

Traditional anthropometric methods, based on manual measurements [1] using instruments such as tape measures, anthropometers, and calipers, remain widely used due to their accessibility and standardization [2, 3]. They allow direct measurement of body dimensions and are well-established in clinical practice, garment design, and scientific research. The main limitations of this approach include

subjectivity, the possibility of human error, and the difficulty of self-measurement. Furthermore, the method does not provide spatial information about body geometry and volume.
Table 1 presents a comparative analysis of methods for determining anthropometric dimensions.

Photo-based techniques [4] offer a sufficiently high degree of convenience and the possibility of remote data collection, making them suitable for large population studies and application in online platforms. They require minimal equipment and allow the extraction of multiple anthropometric parameters from ordinary digital images. However, the accuracy of these methods depends on the quality of visualization, lighting, and body position, which limits their reliability for precise measurements.

The application of 3D scanners is a modern approach to anthropometric measurements, which provides sufficiently high accuracy, speed, and the ability to create detailed 3D models of the human body [5, 6]. They allow automated extraction of a sufficiently large number of anthropometric parameters and are suitable for designing personalized clothing, including for specific groups such as pregnant women. Despite its advantages, this method requires equipment with a higher cost compared to photographic images and classical measurement methods and specialized infrastructure, which limits its accessibility for wider use.

***Table 1**: Comparative analysis of methods for determining anthropometric dimensions*

Method	Accuracy	Applicability in pregnancy	Accessibility	Source
Classical anthropometric measurements	Average – depends on experience of the measurer	Limited – difficult to track dynamic changes	High – cheap measuring tools	[7]
Photo-based methods	Low to medium – depends on image quality	Partially applicable – difficult to capture volumetric changes	Very high – only camera and app	[8]
3D scanning	High – captures volumetric and spatial changes	Excellent – tracks non-linear changes throughout gestation	Low – expensive equipment and software	[9]

In the reviewed available scientific literature sources, the focus is mainly on linear and volumetric measurements applicable to the design of clothing for pregnant women, but there is a lack of in-depth analysis of the morphology and its dynamics through mathematical descriptions. Mathematical functions that describe the silhouettes of the body during the different stages of pregnancy in polar or parametric form have not been used, nor have geometric indices derived from them been defined – such as curvature, symmetry or local deformations. Such type of analyses will provide sufficient precision in the creation of adaptive structures and personalized clothing, especially in the dynamic transformation of the female body during the gestation period.

The photo-based method for determining human body dimensions offers a combination of accessibility, speed, and sufficient accuracy, which makes it particularly suitable for studies with large samples and dynamic changes in the human body, such as those that occur during pregnancy. Unlike classical measurements, which are laborious and subjective, and 3D scanning, which requires expensive equipment and a specialized environment, photo-based measurements allow data collection with minimal resources and without physical contact with the photographed object. According to García Flores et al. [10], the photo-based approach shows a lower average error and a shorter measurement time compared to 3D scanning, making it more effective in a practical environment. This feature makes it a suitable tool for analyzing the body silhouette of pregnant women and for creating adaptive clothing based on real and current characteristics of the human body.

The aim of this study is to propose a way to determine body changes using mathematical functions that describe the silhouettes of the pregnant woman's body. These descriptions of changes in the silhouette of the pregnant woman's body are suitable for creating adaptive, personalized clothing, building on existing approaches that do not take into account the dynamics and complexity of the female body silhouette during the gestational period.

2. MATERIAL AND METHODS

A total of 81 body silhouette images were used, representing changes in the body of women during pregnancy. The search for body silhouettes of pregnant women on the Internet was done using the keywords – "pregnancy period", "Pregnant woman silhouette", "Maternity silhouette", "Maternity 9 months". The body silhouettes are free to download and were used solely and exclusively for the purposes of this study. They were downloaded from the following Internet sources:

Source	Accessed on:
https://www.vecteezy.com	17.07.2025
https://www.123freevectors.com	11.07.2025
https://www.freepik.com	28.06.2025
https://www.freevector.com	25.06.2025
https://www.instagram.com	12.06.2025
https://de.pinterest.com	12.06.2025

After being downloaded, the silhouettes of the pregnant women's bodies were separated into separate objects from the original image. They were vectorized in Inkscape ver. 1.0.1 (https://inkscape.org, accessed 12.07.2025). After this procedure, the separate silhouettes of the pregnant women's bodies were exported to *.png file format for further processing. In Appendix A, Figure A1, the used silhouettes of the pregnant women's bodies are presented.

The description of the contours of the pregnant women's body silhouettes was made using a radius-vector function [11, 12]. In this work, the calculation of the radius-vector functions starts from the top point of the object. The obtained values are normalized to the height of the pregnant woman's body silhouette. The following notations are used when presenting the mathematical formulas:

$$C = (x_c, y_c) \in R^2 \quad \text{Center of gravity of the object} \quad \textbf{(1)}$$

$$\{P_i = (x_i, y_i)\}_{i=1}^{N} \quad \text{The points on the object's contour, which are N in number} \quad \textbf{(2)}$$

$$\theta \in [0, 2\pi] \quad \text{Polar angle relative to horizontal axis} \quad \textbf{(3)}$$

A total of 360 measurements (k) are made from the center of gravity to points on the object's contour, in the interval [0, 2π]:

$$\theta_k = \frac{2\pi(k-1)}{360}, \quad k = 1, 2, \dots, 360 \quad \textbf{(4)}$$

In order to standardize the starting point, each radius-vector function starts from the top point of the body silhouette, defined by:

$$j^* = \arg \min_{i \in \{1,\dots,N\}} y_i \quad \textbf{(5)}$$

The loop is then rearranged so that P_{j*} becomes the starting point and the others follow cyclically:

$$B' = \{P_{j*}, P_{j*+1}, \dots, P_N, P_1, \dots, P_{j*-1}\}, \qquad P_j = (x_j, y_j), \qquad j = 1, \dots, N \quad \textbf{(6)}$$

For each θ_k, the nearest point P_j is chosen whose angle with respect to the center of gravity C is closest to θ_k:

$$\mathrm{j} = \arg\min_j \left| atan2(y_j - y_c, x_j - x_c) - \theta_k \right| \quad \textbf{(7)}$$

The distance from the center to the selected point P_j determines the value of the radius at the corresponding angle:

$$r(\theta_k) = \sqrt{(x_j - x_c)^2 + (y_j - y_c)^2} \quad \textbf{(8)}$$

The radius-vector function is normalized to the height of the pregnant woman's body (H):

$$r_n(\theta_k) = \frac{r(\theta_k)}{H}, \quad H = \max_i y_i - \min_i y_i \quad \textbf{(9)}$$

The resulting generalized equation, by which the normalized radius-vector function is calculated, has the form:

$$r_n(\theta_k) = \frac{1}{H}\min_j \left\{ \sqrt{(x_j - x_c)^2 + (y_j - y_c)^2} \middle| \theta_j = atan2(y_j - y_c, x_j - x_c) \approx \theta_k \right\}, \quad \theta_k = \frac{2\pi(k-1)}{360} \quad \textbf{(10)}$$

Using the obtained radius-vector functions characterizing the silhouettes of the body of pregnant women, indices reflecting changes in the body were calculated. These indices were summarized based on available literature sources [13, 14, 15, 16, 17].

FI1 is an index of symmetry. It assesses the degree of symmetry of the silhouette of the pregnant woman's body relative to a vertical axis passing through the center of the body. During pregnancy, especially in advanced stages, asymmetries may occur, for example, due to posture, pressure from the fetus or unilateral displacement. FI2 is an index of convexity. It reflects the relative convexity of the abdomen in the anterior part of the silhouette of the pregnant woman's body, relative to the average body size. The index can be used as an indicator of pregnancy progress, as its value increases with advancing gestation. The index is sensitive to changes in the anterior projection of the abdominal region. FI3 is a body silhouette index that describes the overall proportion between the maximum radial length of the body (the most prominent point) and its average radius. The index indicates the extent to which the body silhouette changes from a uniform (circular) to a more irregular, convex structure characteristic of advanced pregnancy. FI4 is an index measuring the difference between the current body silhouette and a reference (initial) silhouette of the pregnant woman's body. It is used to quantify dynamic changes in the body silhouette between individual gestational weeks. The index is suitable for longitudinal monitoring of morphological development during pregnancy.

FI5 assesses the variation in the local curvature of the pregnant woman's body silhouette along its entire circumference. High values of this index reflect irregularities and abrupt changes in the pregnant woman's body silhouette such as sharp contours, local protrusions or uneven expansion. This index is sensitive to structural changes in the body, including changes in the breasts, abdomen and pelvis. The body silhouette indices of pregnant women have the following form:

$$FI1 = \frac{1}{\pi}\int_0^{\pi} \frac{|R(\theta) - R(\pi - \theta)|}{\bar{R}} d\theta \quad \textbf{(11)}$$

$$FI2 = \frac{R(\theta_{max})}{\bar{R}} \quad \textbf{(12)}$$

$$FI3 = \frac{R_{max}}{\bar{R}} \quad \textbf{(13)}$$

$$FI4 = \frac{1}{2\pi}\int_0^{2\pi} \frac{|R_t(\theta) - R_0(\theta)|}{\bar{R}_0} d\theta \quad \textbf{(14)}$$

$$FI5 = \sqrt{\frac{1}{2\pi}\int_0^{2\pi}(R'(\theta) - \bar{R}')^2 d\theta} \quad (15)$$

where R(θ) is a radius-vector function; $\bar{R}$ is the average value of R(θ); R_{max} is the largest radius, relative to the center of gravity of the object; the angle θ changes in the interval θε[0, 2π]; $R_t(\theta)$ is the current value of the radius; $R_0(\theta)$ is the initial radius; R'(θ) is the first derivative of the radius-vector function R(θ) with respect to the angle θ.

The informativeness of body silhouette indices in pregnant women was determined using the FSRNCA, RreliefF, and SFCPP selection methods. FSRNCA (Feature Selection for Classification and Regression by Neighboring Component Analysis). This method identifies the most appropriate body silhouette indices of expectant mothers, using their weights obtained in such a way as to minimize the prediction error [18]. RReliefF is used for feature selection in regression tasks. It evaluates the importance of features based on their ability to distinguish data that are close to each other [19]. This algorithm is suitable for assessing the significance of features for distance-based models. SFCPP (Feature Selection with Comparable Predictive Ability). A feature selection method in which the identification of those with similar predictive capabilities while reducing data redundancy [20]. Informative are those indices that have weight coefficients with a value above 0.6 [21].

Data on pregnant women's body mass, waist circumference and uterine height, measured during the implementation of previous scientific projects [22], were used. These data are presented in Table 2.

***Table 2**: Data from measurements of pregnant women*

Characteristic / Month	BW, kg	WC, cm	UH, cm
M1	55±5	75,44±5,17	15±3,08
M2	55±5	75,44±5,13	15±1,76
M3	55±5	75,44±5,17	15±3,08
M4	58±5	79,78±5,74	17,89±2,71
M5	60±5	84±6,06	21,22±2,28
M6	62±4	87,33±5,24	25±2,06
M7	65±4	91,11±5,3	27,22±1,48
M8	66±5	95,11±3,95	30,67±1,32
M9	68±5	98±3,04	33±1,12
BW-body weight; WC-waist circumference; UH-uterine height			

The ability to predict data from measurements of pregnant women was tested using a second-order polynomial regression model, which is more commonly used in practice [23]. The model describes the relationship between the independent and dependent variables and has the following form:

$$z = b_0 + b_1x + b_2y + b_3x^2 + b_4xy + b_5y^2 \quad (16)$$

where z is the dependent variable. The independent variables are x and y; the coefficients of the model are denoted as b.

The regression model was evaluated based on: Coefficient of determination (R^2); Values of the regression coefficients; Standard error (SE) of the regression coefficients; p-values of the coefficients and of the model; Value of the Fisher test (F) compared to the critical value Fcr. An analysis of the residuals of the regression model was performed.

The processing of the experimental data was carried out in the Matlab 2017b programming environment (The Mathworks Inc., Natick, MA, USA).

All statistical analyses were performed at a level of significance α=0,05.

3. RESULTS

The developed algorithm for determining a normalized radius-vector function along the contour of a pregnant woman's body silhouette is presented in Figure 1. The RGB image is converted to HSV color space and the saturation channel (S) is extracted to isolate the object (the silhouette of a pregnant woman's body) along a given saturation range. Then, a binary gradient mask is created, the object contours are found, and the center of gravity is calculated. The contour is rearranged so that it starts from the top point of the pregnant woman's body silhouette. In this way, each radius-vector function starts from the same point. For each point, an angle and radius are calculated relative to the center of gravity. Based on these values, a radius-vector function with 360 samples is built, which is normalized by the height of the figure and smoothed. Finally, the results are visualized graphically - both in the form of a function and by marking a contour, center, and starting point on the pregnant woman's body silhouette.

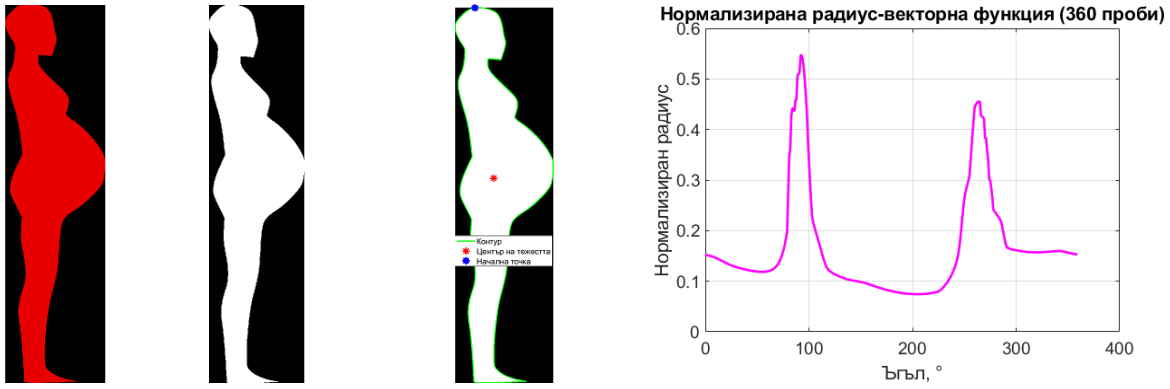

a) original RGB image | b) S(HSV) component of the image | c) object outline with characteristic points | d) normalized radius-vector function

***Fig. 1**: Algorithm for obtaining a normalized radius-vector function of a pregnant woman's body silhouette*

Figure 2 presents averaged normalized radius-vector functions for the stages of pregnancy (from M1 to M9). As pregnancy progresses (from M1 to M9), progressive changes in the radii are observed - most significantly around 75°, which reflects the abdominal area. There, the radii increase significantly, showing the typical increase in volume in the front of the body. This affects maternity clothes, which must follow these changes, ensuring comfort, freedom of movement and aesthetics.

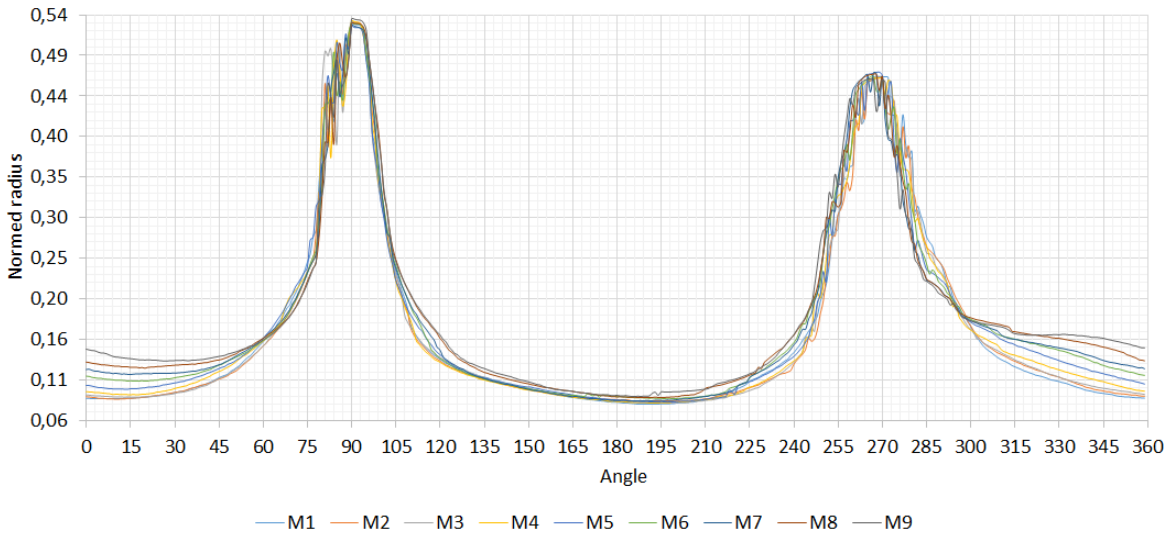

***Fig. 2**: Averaged normalized radius-vector functions representing stages of pregnancy in women*

Table 3 presents the calculated values of the body silhouette indices of women during pregnancy. Analysis of the results from the table shows a clear dynamics in the morphology of the body silhouette of pregnant women during the gestation period. FI1 (symmetry index) gradually increases from 0,19 to 0,29, which suggests a slight increase in asymmetry due to changes in posture and pressure from the fetus. FI2 (convexity index) has a tendency to increase from 1,11 to 1,63, reflecting the progressive enlargement of the abdominal area. FI3 (shape index) shows a tendency to decrease – from 3,36 to 3,02 – which indicates a transition from a more even to a more convex and uneven body silhouette, typical of advanced pregnancy. FI4 remains relatively constant (0,02), which is due to the use of a fixed reference body silhouette (in the first month of pregnancy), as well as the limited sensitivity of the index to monthly changes. FI5 (local curvature index) shows the most significant increase compared to the other indices – from 0 to 0,24 – which indicates increasing structural complexity and the appearance of local irregularities in the silhouette of the pregnant woman's body, especially in the abdomen, chest and pelvis.

***Table 3**: Values of body geometrical indices of pregnant women*

Index / Month	FI1	FI2	FI3	FI4	FI5
M1	0,19±0,07	1,11±0,24	3,36±0,66	0,02±0,01	0±0
M2	0,21±0,05	1,1±0,19	3,36±0,57	0,02±0,01	0,06±0,04
M3	0,23±0,05	1,13±0,2	3,33±0,6	0,02±0,01	0,08±0,03
M4	0,25±0,03	1,21±0,28	3,32±0,58	0,02±0,01	0,11±0,04
M5	0,25±0,05	1,26±0,22	3,24±0,56	0,02±0	0,13±0,04
M6	0,27±0,04	1,33±0,24	3,14±0,55	0,02±0	0,15±0,04
M7	0,28±0,07	1,45±0,25	3,15±0,47	0,02±0	0,17±0,06
M8	0,29±0,06	1,49±0,26	3,06±0,51	0,02±0	0,22±0,07
M9	0,28±0,06	1,63±0,28	3,02±0,46	0,02±0	0,24±0,09

Figure 3 shows the results of the selection of informative signs for predicting the month of pregnancy, human body mass, waist circumference and uterine height.

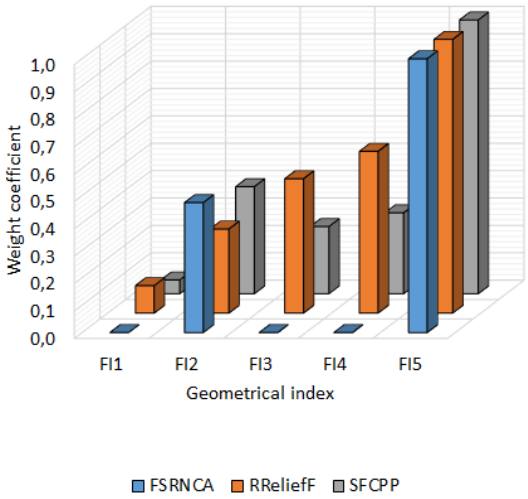

a) month of pregnancy (M)

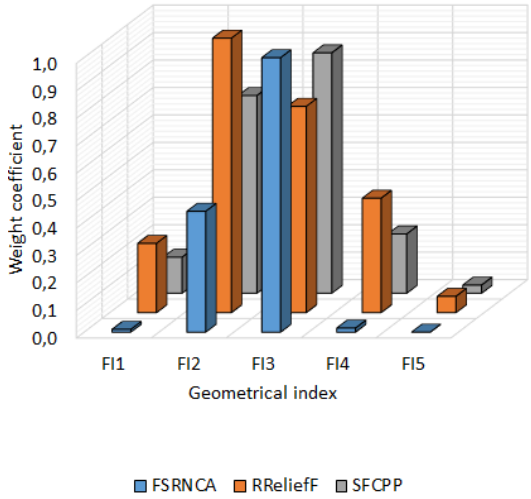

b) body weight (BW)

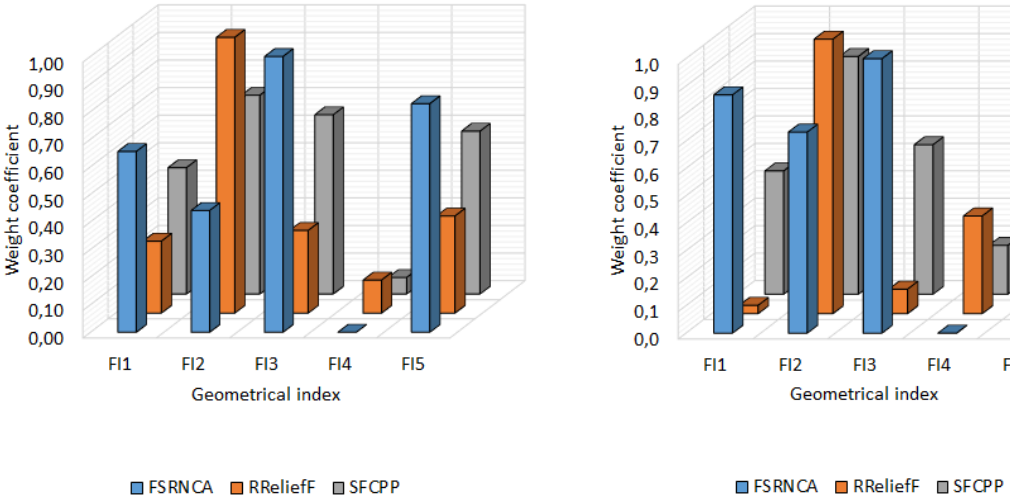

c) waist circumference (WC) d) uterine height (UH)

***Fig. 3**: Selection of informative features*

The appropriate pair of indices for predicting the month is FI5 and FI4. FI5 clearly meets the criterion of informativeness, since it has weighting coefficients above 0,6 by all methods and is appropriate for predicting several of the characteristics of the human body during pregnancy. For body mass (W), the most informative are the indices FI2 and FI3, which have high values by all methods (FI2 is 1,00 by RReliefF and 0,72 by SFCPP; FI3 is 1,00 by FSRNCA and 0,88 by SFCPP), which makes them a suitable pair for predicting body mass. For waist circumference (WC), the most relevant indices are FI3 and FI5, both of which have weighting coefficients above 0,6 by FSRNCA and SFCPP, and FI5 has the highest summary value among the other indices. Regarding uterine height (HM), the best predictors are FI2 and FI5, which show high significance by all methods (FI2 has a weighting coefficient of 0,73 by FSRNCA, 1,00 by RReliefF and 0,87 by SFCPP; FI5 is 0,83, 0,66 and 0,74 respectively).

Regression models were constructed to test the ability to predict month of pregnancy (M), body weight (BW), waist circumference (WC), and uterine height (UH) from geometric data obtained from body profile silhouettes of pregnant women. After removing the insignificant coefficients from the regression models with p>α, the models have the form:

$$M = 1{,}49 + 34{,}6FI5 - 165{,}1FI4^2 - 36{,}3FI5^2 \quad \textbf{(17)}$$

$$BW = 106{,}96 - 33{,}68FI3 + 3{,}95FI2^2 + 5{,}17FI3^2 \quad \textbf{(18)}$$

$$WC = 123{,}66 - 29{,}6FI3 + 4{,}38FI3^2 + 23{,}6FI3FI5 \quad \textbf{(19)}$$

$$UH = 12{,}1 + 48{,}44FI5 + 2{,}21FI2^2 \quad \textbf{(20)}$$

Table 4 presents the results of the regression model evaluation. The best predictive value among the analyzed models is shown by the one for M=f(FI4, FI5) with a coefficient of determination R^2=0,68, which means that 68% of the variation of the dependent variable is explained by the independent variables. This model also has the lowest standard error (SE=1,51), which further confirms its precision. The second most effective model is the model BM=f(FI2, FI5) with R^2=0,59 and a significantly high value of the F-criterion (F=54,94), exceeding the critical value Fcr=3,11. The models OT=f(FI3, FI5) and W=f(FI2, FI3) show lower values of R^2 – 0,43 and 0,26, respectively – which indicates their weaker explanatory power. However, all models are statistically significant, as the p values are below 0,00, confirming the presence of a significant relationship between the studied independent and dependent variables.

***Table 4**: Results of regression model estimation*

Model	R^2	F	Fcr	SE	p-value
M=f(FI4, FI5)	0,68	F(3, 77)=53,31	2,72	1,51	<0,00
BW=f(FI2, FI3)	0,26	F(3, 77)=8,23	2,72	5,89	<0,00
WC=f(FI3, FI5)	0,43	F(3, 77)=19,43	2,72	7,39	<0,00

UH=f(FI2, FI5)	0,59	F(2, 78)=54,94	3,11	4,59	<0,00
R^2-coefficient of determination; F-Fisher's test; Fcr-critical value of F; SE-standard error					

Figure 4 shows the obtained regression models in general. The presented models demonstrate diversity in the structure and degree of explanatory power in relation to the dependent variables. The shape of these surfaces varies - in models with higher values of the coefficient of determination R^2, such as M=f(FI4, FI5) and BM=f(FI2, FI5), a smoother and more clearly expressed surface is observed, which indicates a stable and predictable relationship between the variables. Conversely, the models W=f(FI2, FI3) and OT=f(FI3, FI5) show a more scattered and uneven regression shape, which corresponds to their lower explanatory power. However, all models are statistically significant, which is confirmed by the values of p<0,00. The model M=f(FI4, FI5) is most informative at medium to high values of FI4 and FI5, where the dependent variable M shows a stable and predictable change. Similarly, BM=f(FI2, FI5) is more informative at high values of FI5, which is reflected in the distinct shape of the regression surface.

Figure 5 shows normal probability plots of the residuals for the obtained regression models. The plots show slight deviations from the straight line, especially for the models W=f(FI2, FI3) and OT=f(FI3, FI5). These models exhibit more pronounced tails, which suggests the presence of extreme values and deviations from the normal distribution of the residuals. This is a sign of a weaker adaptation of the model to the real data. On the other hand, the models M=f(FI4, FI5) and BM=f(FI2, FI5) show a close location of the residuals to the straight line, which is an indicator of normality and more accurate regression estimates compared to the other two models considered.

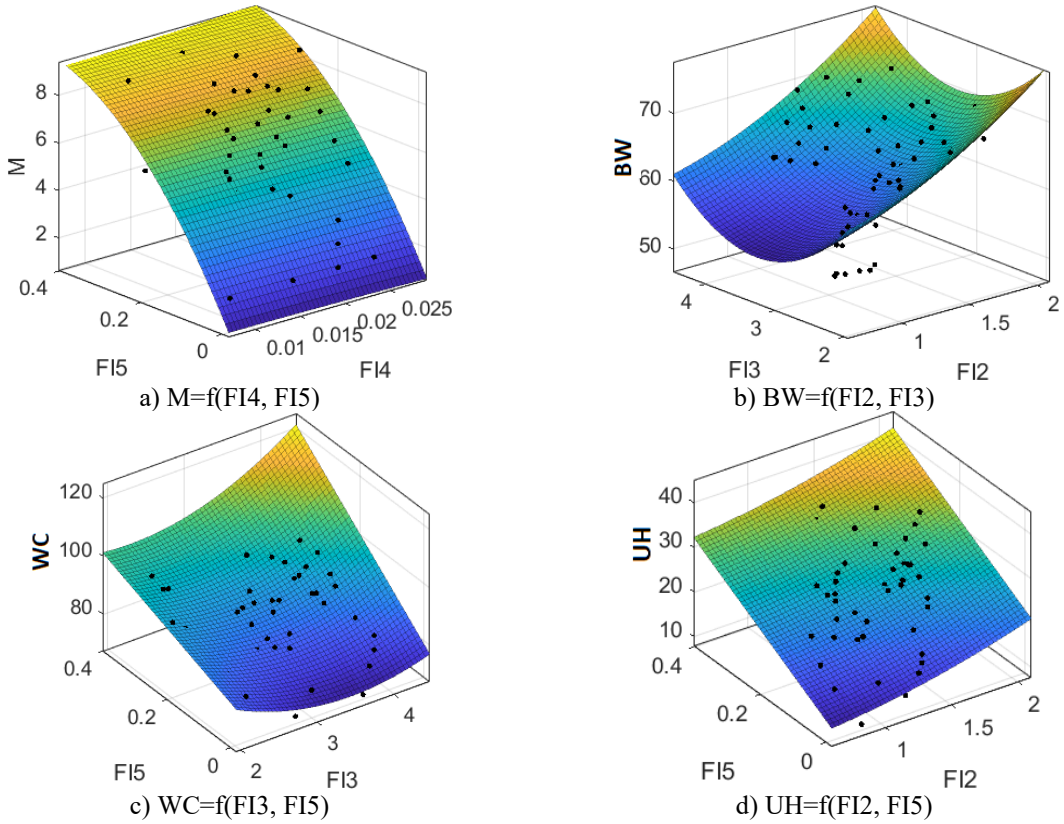

a) M=f(FI4, FI5) b) BW=f(FI2, FI3)

c) WC=f(FI3, FI5) d) UH=f(FI2, FI5)

***Fig. 4**: Regression models for predicting the body size of pregnant women – general view*

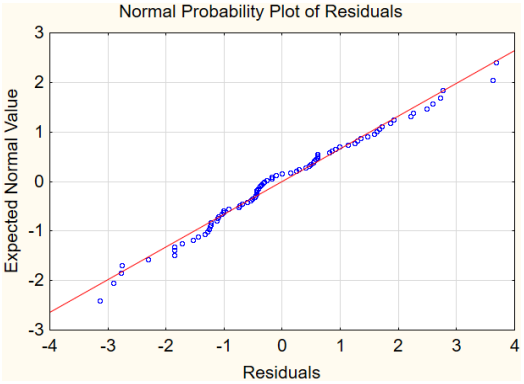

a) M=f(FI4, FI5)

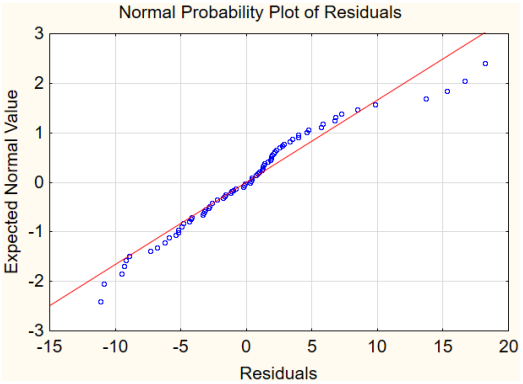

b) BW=f(FI2, FI3)

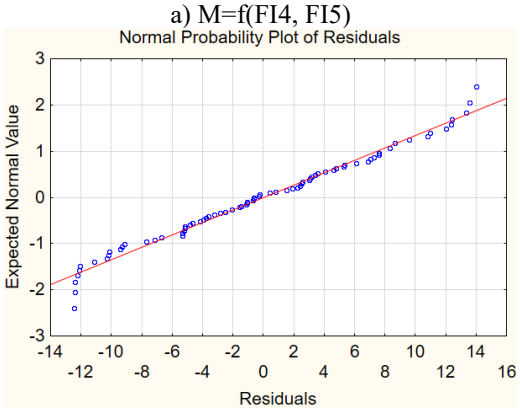

c) WC=f(FI3, FI5)

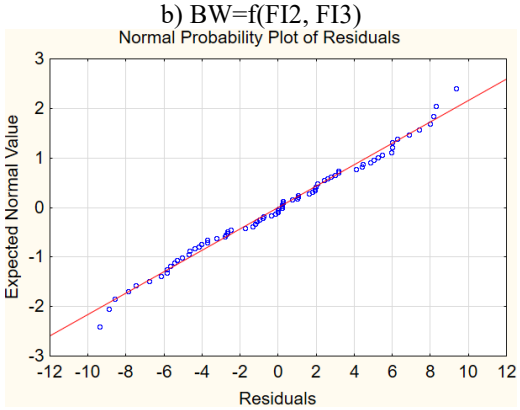

d) UH=f(FI2, FI5)

***Fig. 5**: Normal probability plots for the resulting regression models*

Figure 6 shows the distribution of the residuals for the obtained regression models. In the models M=f(FI4, FI5) and BM=f(FI2, FI5), the distribution of the residuals is closest to normal, which is evident from the symmetrical shape of the histograms and the good fit to the normal curve. This indicates that the models adapt to the data and that the assumption of normality of the errors is relatively fulfilled. In the models W=f(FI2, FI3) and OT=f(FI3, FI5), deviations from the normal distribution are observed - the residuals are more scattered and there is a presence of asymmetry, which is a sign of heteroscedasticity or the presence of unregistered factors that affect the accuracy of these regression models.

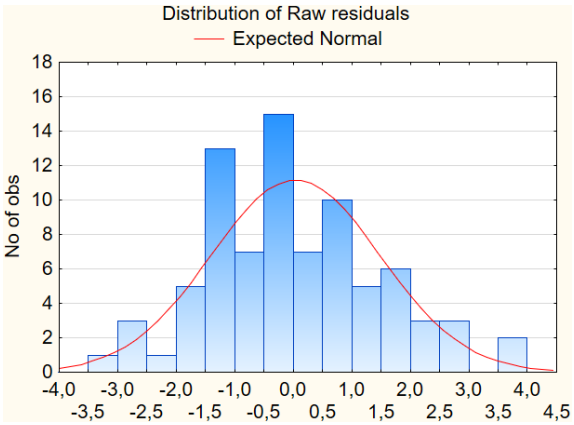

a) M=f(FI4, FI5)

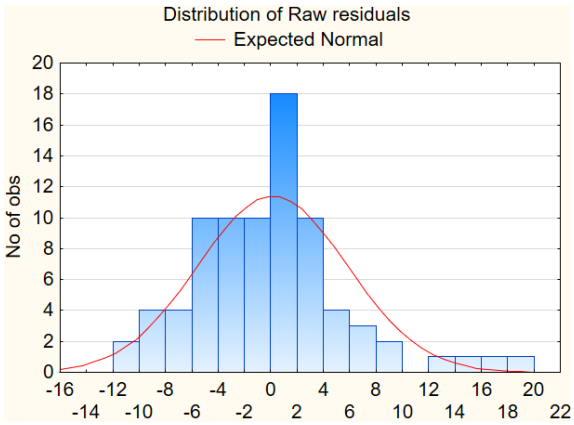

b) BW=f(FI2, FI3)

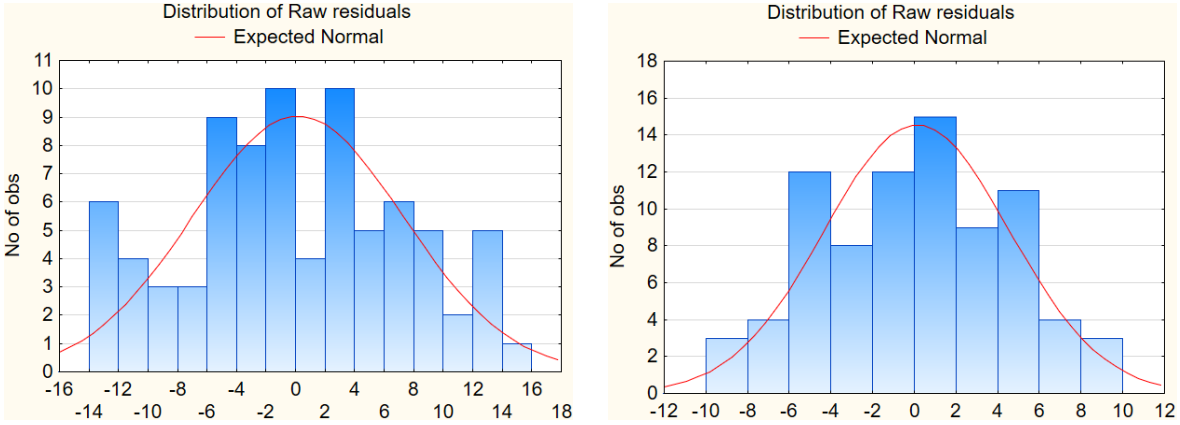

c) WC=f(FI3, FI5) d) UH=f(FI2, FI5)

***Fig. 6**: Distribution of residuals for the resulting regression models*

4. DISCUSSION

The results obtained in this study show that the FI1–FI5 indices are suitable for quantitative assessments of symmetry, convexity, and local deformations of the body silhouette, which builds on the traditional linear and volumetric measurements of pregnant women used in the available literature. Salzer et al. [24] point out that most existing tools for assessing the body silhouette of pregnant women focus on psycho-emotional aspects, but do not include geometric or mathematical descriptions of their body silhouette. This shortcoming is addressed in the present study. The regression models based on the indices proposed in this study show varying degrees of predictive power – the model M=f(FI4, FI5) with R^2=0,68 shows a sufficiently high accuracy, which complements the results of Bao et al. [25] that the use of complex regression structures (including hybrid models) significantly improves the predictive ability in human body measurements. On the other hand, the model W=f(FI2, FI3) with R^2=0,26 shows limited predictive ability, which complements the observations of Bicevskis et al. [26] that linear models often fail to capture nonlinear relationships between different characteristics of the human body. Residual analysis further confirms the reliability of the models for predicting month of gestation (M) and uterine height (BM), showing a normal distribution of errors, while the models for body mass (W) and body circumference (OT) have larger biases, which is typical of less well-adapted models. This complements the findings of Choutas et al. [27] that the accuracy of measuring human body dimensions and determining its silhouettes is important for applications such as virtual garment visualization and personalized designs, and that models that do not capture the real body silhouette lead to compromises in the final product and failure to meet customer requirements.

The results of this work can be useful in designing clothing for pregnant women by using radius-vector functions to model basic body proportions by month, which facilitates the creation of elastic adaptive or transformable clothing with the ability to predict changes in dimensions for future stages, supporting the production of clothing that "grows" with the body and detecting areas with the greatest changes, such as the abdomen and back, in which the design should provide additional volume of appropriate fabrics or structure, as well as creating digital avatars or 3D models of body silhouettes on which to simulate interaction with textile materials and clothing structures.

5. CONCLUSION

It has been proven that the use of radius-vector functions provides a sufficiently reliable tool for describing morphological changes in the silhouette of the pregnant woman's body. The derived body silhouette indices (FI1–FI5) describe with sufficient accuracy both global and local changes in body shape during the gestational period.

It has been established that the indices of symmetry, convexity, local curvature, and dynamics of the silhouette of the pregnant woman's body show a sufficiently high sensitivity to changes in the female body with the progress of pregnancy. They correlate significantly with basic anthropometric

parameters such as body mass (BM) and waist circumference (M), which is a suitable basis for creating regression models with prognostic value and statistical reliability.
The results of the available literature have been supplemented by introducing a formalized mathematical apparatus for geometric analysis of the human body silhouette using radius-vector functions. This builds on existing approaches that are based primarily on linear dimensions and do not sufficiently account for the complexity of the transformations of the human body during pregnancy.

The research should be continued with the integration of radius-vector analysis with 3D scanning technologies for more precise determination of changes in the silhouette of the human body during pregnancy and the application of body silhouette indices in algorithms for automated design of adaptive clothing for pregnant women, as well as the development of virtual avatars and simulation models for visualization and testing of interaction with clothing designs.

APPENDIX A

Figure A1 shows 81 silhouettes of women's bodies during the stages of pregnancy. "Mx" indicates the months of pregnancy. A nine-column grid is used in the illustration, labeled M1 to M9, to map out each month of pregnancy. In every column, red-dot silhouettes show how a pregnant woman's body changes as time goes on. At first, from M1 to M3, the changes are barely noticeable. Then, around the middle months (M4 to M6), the belly started to grow. By the last months, M7 to M9, the abdominal expansion is hard to miss. This month-by-month setup makes it easy to follow the gradual transformation and compare how the body shape shifts as pregnancy moves along.

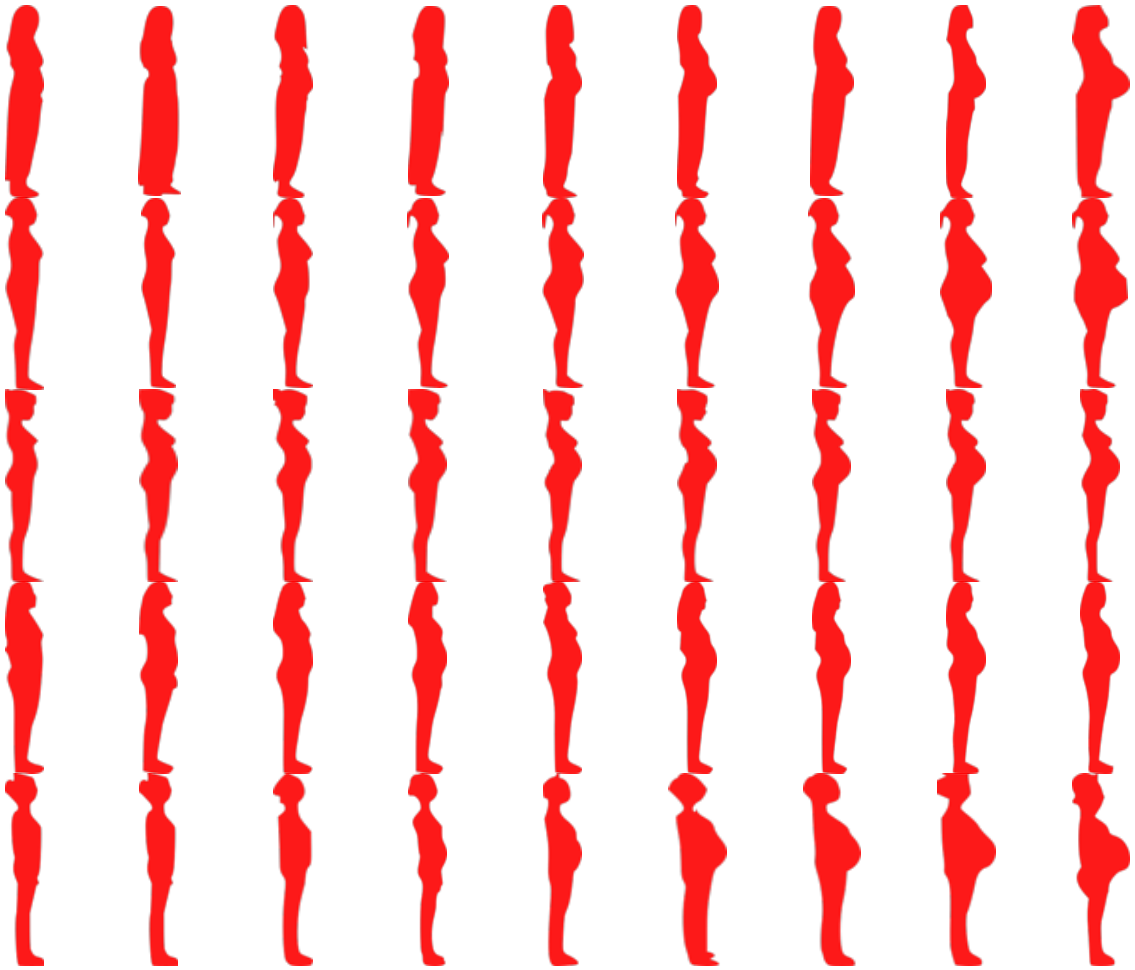

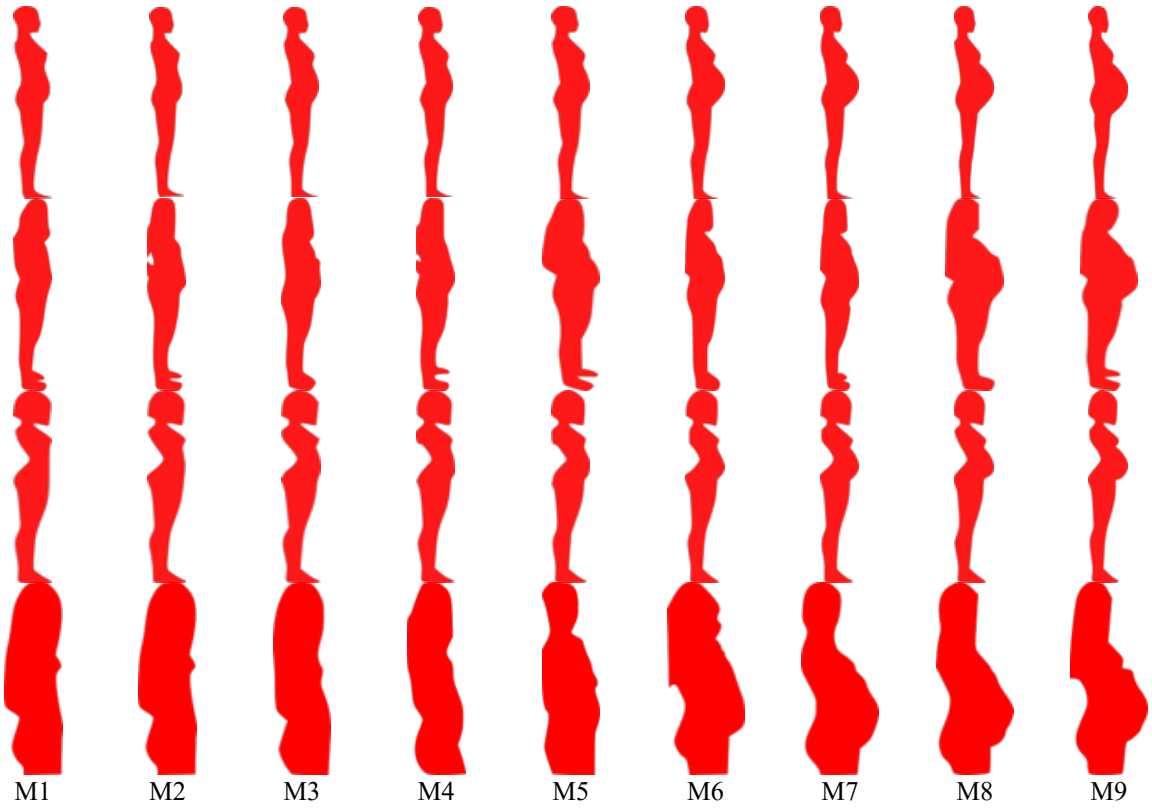

***Fig. A1**: Silhouettes of women's bodies during the stages of pregnancy*

REFERENCES

[1] Centers for Disease Control and Prevention, Anthropometry Procedures Manual. National Health and Nutrition Examination Survey (NHANES III), 1996. [Online]. Available: https://wwwn.cdc.gov/nchs/Data/Nhanes3/Manuals/anthro.pdf

[2] International Organization for Standardization, ISO 8559-1:2017 – Size designation of clothes – Anthropometric definitions and body measurement procedures. Geneva, Switzerland: ISO, 2017.

[3] International Organization for Standardization, ISO 20685-1:2018 – 3-D scanning methodologies for internationally compatible anthropometric databases. Geneva, Switzerland: ISO, 2018.

[4] Fytted, "How accurate are body measurements from photos?" 2025. [Online]. Available: https://www.fytted.com/blog/photo-measurement-accuracy-2025.

[5] O. Koval and M. Koval, "Quantitative comparison of manual and 3D body scanner measurements," in Proc. 3DBODY.TECH Conf., 2020. [Online]. Available: https://proc.3dbody.tech/papers/2020/2035koval.pdf

[6] J. Lee, S. Kim, and H. Park, "Comparison of body scanner and manual anthropometric measurements: A systematic review," Int. J. Environ. Res. Public Health, vol. 18, no. 12, p. 6213, 2021. doi: 10.3390/ijerph18126213.

[7] A. Jaiswal, "Smart motherhood wear: A solution to the problem of maternity wear," Int. J. Home Sci., vol. 8, no. 1, pp. 278–281, 2022.

[8] S. Tripathi, M. Sharma, and P. Sinha, "Innovative clothing design for maternity wear," Int. J. Home Sci., vol. 3, no. 3, pp. 151–154, 2017.

[9] M. Balasubramanian, A. Petrova, and K. Robinette, "Anthropometric dynamics of pregnant women and their implications on apparel sizing," in Proc. Int. Conf. 3D Body Scanning Technologies, Long Beach, CA, USA, Nov. 19–20, 2013, pp. 439–446.

[10] T. J. García Flores and P. M. Pascua Cantarero, "Evaluation of the impact of 3D scanning and photogrammetry methods on anthropometric university practices: A case study," J. Mach. Intell. Data Sci., vol. 5, pp. 82–93, 2024. doi: 10.11159/jmids.2024.010.

[11] M. Rani and N. Dahiya, "Comprehensive study on shape representation methods in image processing: A review," Sādhanā, vol. 48, no. 13, pp. 1–17, 2023. doi: 10.1007/s12046-023-02017-3.

[12] Y. H. Wong, M. A. Rahman, and M. Rizon, "A set of bilateral and radial symmetry shape descriptors for object classification," IET Comput. Vis., vol. 11, no. 4, pp. 303–311, 2017. doi: 10.1049/iet-cvi.2015.0413.

[13] K. Gościewska and D. Frejlichowski, "The analysis of shape features for the purpose of exercise types classification using silhouette sequences," Applied Sciences, vol. 10, no. 19, p. 6728, 2020. doi: 10.3390/app10196728.

[14] L. F. Costa and R. M. Cesar, Jr., Shape Analysis and Classification: Theory and Practice. Boca Raton, FL, USA: CRC Press, 2001.

[15] M. D. Klarqvist, Q. F. Wills, et al., "Prediction of fat depot volumes from silhouette images using deep learning," Commun. Med., vol. 2, p. 74, 2022. doi: 10.1038/s43856-022-00124-y.

[16] H. J. Miller, "A measurement theory for time geography," Geogr. Anal., vol. 33, no. 4, pp. 367–386, 2001. doi: 10.1111/j.1538-4632.2001.tb00456.x.

[17] F. J. A. Poirier and A. D. Wilson, "A visual saliency account of figure–ground perception," Front. Psychol., vol. 6, p. 1685, 2015. doi: 10.3389/fpsyg.2015.01685.

[18] FSRNCA, "Feature selection using neighborhood component analysis for regression," MathWorks, 2025. [Online]. Available: https://www.mathworks.com/help/stats/fsrnca.html. Accessed: Jul. 18, 2025.

[19] W. Wei, D. Wang, and J. Liang, "Accelerating ReliefF using information granulation," Int. J. Mach. Learn. Cybern., vol. 13, pp. 29–38, 2022.

[20] SFCPP, "Select subset of features with comparative predictive power," MathWorks, 2025. [Online]. Available: https://www.mathworks.com/help/stats/feature-selection.html. Accessed: Jul. 26, 2025.

[21] A. Farrell, G. Wan, S. Rush, J. Martin, J. Belant, A. Butler, and D. Godwin, "Machine learning of large-scale spatial distributions of wild turkeys with high-dimensional environmental data," Ecology and Evolution, pp. 1–12, 2019.

[22] TK-Yambol Project, Research into the change in some dimensional features of the female body during pregnancy, necessary for the design of maternity clothing (in Bulgarian), 2001.

[23] Ts. Georgieva, A. Mihaylova, and P. Daskalov, "Research of the possibilities for determination of some basic soil properties using image processing," in Proc. 7th Int. Conf. Energy Efficiency and Agricultural Engineering (EE&AE), 2020, pp. 1–4.

[24] E. B. Salzer, J. F. F. Meireles, A. F. Â. Toledo, M. R. de Siqueira, M. E. C. Ferreira, and C. M. Neves, "Body image assessment tools in pregnant women: A systematic review," Int. J. Environ. Res. Public Health, vol. 20, no. 3, p. 2258, 2023. doi: 10.3390/ijerph20032258.

[25] C. Bao, Y. Miao, J. Chen, and X. Zhang, "Developing a generalized regression forecasting network for the prediction of human body dimensions," Applied Sciences, vol. 13, no. 18, p. 10317, 2023. doi: 10.3390/app131810317.

[26] J. Bicevskis, Z. Bicevska, E. Diebelis, and L. Purina, "Quality control of body measurement data using linear regression methods," in Proc. 19th Conf. Computer Science and Intelligence Systems (FedCSIS), vol. 39, pp. 289–300, 2024. doi: 10.15439/2024F6463.

[27] V. Choutas, L. Müller, C.-H. P. Huang, S. Tang, D. Tzionas, and M. J. Black, "Accurate 3D body shape regression using metric and semantic attributes," in Proc. IEEE/CVF Conf. Computer Vision and Pattern Recognition (CVPR), 2022. doi: 10.48550/arXiv.2206.07036.

ANNALS OF THE UNIVERSITY OF ORADEA
FASCICLE OF TEXTILES, LEATHERWORK

ELECTRONIC CUTTING PLAN FOR GARMENT INDUSTRY

HORA Simina Teodora[1], FAUR Monica[1], BODEA Renata[2]

[1,] University of Oradea, Faculty of Energy Engineering and Industrial Management, Department of Textile-Leather and Industrial Management, 4 Universității Street, 410058, Oradea, Bihor, Romania,
E-Mail: horasimina@gmail.com, monifaur@gmail.com

[2,] University of Oradea, Faculty of Managerial and Technological Engineering, Department of Engineering and Management, 1 Universității Street, 410058, Oradea, Bihor, Romania, E-Mail: renata.bodea@gmail.com

Corresponding author: Hora Simina Teodora, E-mail: horasimina@gmail.com

Abstract: *Textile industry is widely spread worldwide, with important numbers in products volume and number of employees. It is, also, an important consumer in terms of energy, water and raw materials and an important generator of waste. Thus, this industry is not sustainable. A key element in making textile industry a sustainable one is adoption of Industry 4.0 components, among which digitization is a powerful tool. Digitization, which is far from being accomplished, means electronic documents, software implementation in design, manufacturing and distribution. There is a wide space for innovation in the creation of industry-specific databases and software applications. The paper proposes an electronic document, part of a more comprising library, created as order for the cutting department of a garment company. The purpose of the electronic document is to replace paper-based documents and to provide data resulted from automated calculus. The document is designed as a MS Excel spreadsheet, which displays data input by the user and results of different calculations, proving all information needed to cut the fabric in an accurate and efficient manner. The spreadsheet is designed as a template suited for most applications, (it takes into account the usual sizes 32…54) and contains calculation forms for six main markers and five supplementary markers.*

Key words: *electronic documents, textile industry, cutting plan, MS Excel application.*

1. INTRODUCTION

Textile industry is important worldwide, in terms of products volume and number of employees. In Europe, for instance, according to the 2023 European Commission report, based on data provided by EURATEX (The European Apparel and Textile Confederation), [1], the textile sector in the Union recorded a turnover of €147 billion in the previous year, with exports of €58 billion and imports of €106 billion. Production is carried out overwhelmingly in small and medium-sized enterprises (143,000 companies, representing 99.8% of producers), with approximately 1.3 million employees.

Despite the flourishing nature of this industry, especially after the implementation of the fast-fashion model in the 1980s, it is not a sustainable industry, due to the large amount of waste it generates and the high consumption of energy and water.

An important path to sustainability is to introduce Industry 4.0 components, as much as possible, into all stages of production. The most effective component is digitization.

Making a clothing product involves going through several stages, illustrated synthetically in Figure 1.

Digitization allows the replacement of paper-based documents and use of software tools in design of models and patterns. The key documents and software tools are:

- ❒ Synthetic product sheet (fabric type and auxiliary materials, manufacturing instructions, costs and sourcing)
- ❒ Digital design and arrangement of patterns
- ❒ 3D Prototypes and Digital twins
- ❒ Electronic Data Interchange (EDI) - used for automated information exchange between retail partners, suppliers, and manufacturers (electronic purchase orders, invoices, and shipping notices)
- ❒ Digital Product Passport [2, 3].

Fig. 1: *Stages in the process of clothing making*

Digitization has started to work especially in small companies [4], which use subcontractors for different digital tasks.

Digitization enables a sustainable and efficient transformation in the textile industry, improving production processes, minimizing environmental impact, and enhancing supply chain transparency [5], mainly through the adoption of Industry 4.0 technologies.

In Romania, the digital work is mostly represented by CAD generation of patterns [6, 7], performed by means of software applications such as Gemini CAD.

There is a wide space for innovation in the creation of industry-specific databases and software applications. The present paper describes a worksheet created to control the cutting of patterns.

2. CUTTING SHEET – MS EXCEL APPLICATION

At the end of stage 2 (Fig. 1), the fabric is purchased and the markers are generated. The product is going to start being manufactured. The first operation is the cutting of patterns. The order

for the cutting department is designed as a spreadsheet, containing all information needed to perform the operation in the most efficient way.

The spreadsheet is designed as a template suited for most applications, (i.e. it takes into account the usual sizes 32…54), contains calculation forms for six main markers and five supplementary markers. Figure 2 presents a general view of the application.

The user enters numerical values for the cells with green filling (the cells with green filling require input data): the number of pieces (a piece contains the patterns needed for a size in the model) per size, the width l and length L of the available fabric, the allocation of sizes to markers, the number of pieces of each size per markers and the number of markers. From the file resulting from the optimization in GeminiCAD, the lengths of the markers, the utilization coefficient per marker, UC marker (with blue filling) are extracted.

Company	
Model code	
Date	

l [m]	L total [m]
1.2	80

			Markers						Supplementary markers				
Sizes	Number of pieces		M1	M2	M3	M4	M5	M6	SM1	SM2	SM3	SM4	SM5
32	0	Sizes	38	40	42	0	0	0	46	40	0	0	0
34	0		46	44	0	0	0	0	0	0	0	0	0
36	0	No.pcs/size/	1	1	2	0	0	0	2	2	0	0	0
38	20	marker	1	1	0	0	0	0	0	0	0	0	0
40	22	No. pcs./ marker	2	2	2	0	0	0	2	2	0	0	0
42	24	Check total pcs.	108										
44	20	L marker [m]	1.21	1.24	1.22	0.00	0.00	0.00	1.26	1.21	0.00	0.00	0.00
46	22	n [markers]	20	20	12	0	0	0	1	1	0	0	0
48	0	Total markers	54										
50	0	Area marker [sm]	29.02	29.76	17.57	0.00	0.00	0.00	1.51	1.45	0.00	0.00	0.00
52	0	UC (marker)	0.83	0.81	0.82	0.00	0.00	0.00	0.82	0.83	0.00	0.00	0.00
54	0												
Total [pcs]	108	UC (total)	0.83										

L util [m]	66.09
Waste [sm]	16.69

***Fig. 2**: Cutting spreadsheet*

The yellow cells are calculated automatically. The application determines the useful length of the material Lutil, the total utilization coefficient UC total and the area of material that is lost, Waste.

For the example presented in Figure 2, three main markers were required, which ensure the cutting of 20 pieces for sizes 38 and 46, 20 pieces for sizes 40 and 44, 12 pieces for size 42 and two additional markers, which ensure the cutting of two pieces of size 46 and, respectively, 40.

The user can check whether all pieces in the batch have been included in the cutting plan. When the data is entered correctly, the value of the Check total pieces cell must match Total [pieces].

The utilization coefficient and waste are calculated as follows:

$$UC_{total} = \Sigma(L_{marker} \cdot n)/L_{total} \cdot 100\ [\%], \quad \textbf{(1)}$$

$$Waste = (L_{total} - L_{util}) \cdot l\ [sm]. \quad \textbf{(2)}$$

In the example shown, the material utilization coefficient has a high value of 83%. The chosen model has simple patterns, which fit relatively easily on the sheet, with a high degree of surface filling. The value of this coefficient can be very different if conditions are imposed regarding the thread orientation and/or the presence of a pattern on the fabric.

3. CONCLUSIONS

The spreadsheet replaces paper-based tables and manual calculus. It can be used as a template for any model, ensuring fast, accurate and complete calculus of data needed for the operation of cutting the patterns.

The application is part of an extended library of templates created by the authors for the use of small companies working in garment industry.

REFERENCES

[1] https://www.europarl.europa.eu/doceo/document/A-9-2023-0176_RO.html#_section2

[2] European Parliamentary Research Service, "*Digital product passport for the textile sector*", PE 757.808 – June 2024.

[3] J. Domskienė1, E. Gaidule, "*An Overview Of Technological Challenges In Implementing The Digital Product Passport In The Textile And Clothing Industry*," AUTEX Research Journal, Vol. 24, No. 1, pp. 1–9, 2024.

[4] D. Casciani, O. Chkanikova, R. Pal, "*Exploring the nature of digital transformation in the fashion industry: opportunities for supply chains, business models, and sustainability-oriented innovations*", Sustainability: Science, Practice and Policy, 18:1, pp. 773-795, 2022.

[5] M. Glogar, S. Petrak, M. Mahni´c Nagli´c, "*Digital Technologies in the Sustainable Design and Development of Textiles and Clothing—A Literature Review*", Sustainability, 17, 1371, pp. 1-26, 2025.

[6] M. Rosca, M. Avadanei, A.-D. Vatra, "*The digital transformation of garment product development*", Industria textilă, 74, 1, pp. 98-106, 2023.

[7] R. M. Aileni, R. I. Radulescu, C. A. Marin, "*Digital Transition For Romanian Textile Industry*", ANNALS OF THE UNIVERSITY OF ORADEA, FASCICLE OF TEXTILES, LEATHERWORK, p. 5-10, 2024.

[8] R. J. Vidmar. (1992, Aug.). On the use of atmospheric plasmas as electromagnetic reflectors. IEEE Trans. Plasma Sci. [Online]. 21(3), pp. 876–880. Available: http://www.halcyon.com/pub/journals/21ps03-vidmar

ANNALS OF THE UNIVERSITY OF ORADEA
FASCICLE OF TEXTILES, LEATHERWORK

THERMAL COMFORT STUDY OF ACRYLIC AND COTTON KNITTED FABRICS USING STATISTICAL ANALYSIS

IMRITH Manoj Kumar[1], ROSUNEE Satyadev[2], UNMAR Roshan[3]

[1, 2, 3] University of Mauritius, Faculty of Engineering, Department of Applied Sustainability & Enterprise Development, Réduit, Mauritius, 80837, Port-Louis, Mauritius

Corresponding author: Imrith, Manoj Kumar, manoj.imrith@gmail.com

Abstract: *Yarn made from natural cellulose and man-made polymer fibres is contemporarily used in virtually all ramifications of textiles. Ostensibly, different raw materials and fabric structures affect the characteristics of the finished textiles. This paper presents a comparative analysis of the thermal comfort, namely thermal conductivity, thermal diffusivity, thermal absorptivity, and thermal resistance, of knitted fabrics made from 100% acrylic and 100% cotton yarns with the same nominal linear density. Using a combination of miss, knit, and tuck stitches, 27 fabrics were designed and knitted for each yarn composition, each with a distinct surface configuration. The fabric's porosity was measured using image processing. Furthermore, the Alambeta instrument was used to determine the thermal comfort properties and fabric thickness. The results were statistically and graphically depicted. In parametric statistical testing, the R^2 was determined based on simple regression analysis. Because low correlations were observed between porosity-thickness and thermal comfort parameters, Parametric Plots (P-P) in conjunction with non-parametric test methods viz. Anderson-Darling, Cramér-von Mises, Kolmogorov-Smirnov, Mardia Combined, Shapiro-Wilk and Watson U^2 were conducted using hypothesis test of their p-values using Wolfram Mathematica software. All the test results exhibited failure to reject the null hypothesis.*

Key words: *Comfort, Textile, Knitting, Thermal insulation, Statistics*

1. INTRODUCTION

Thermal comfort is among the most salient characteristics of textiles for consumers (Das and Alagirusamy, 2010). Generally, heat transfer from the human body to a fabric layer occurs via radiation, conduction, and convection simultaneously (Starr *et al*., 2014). Fabrics play an adjustment role, and their thermal properties influence wearing comfort. As such, thermal insulation provided by clothing maintains a comfortable microenvironment between clothing and the human body in fluctuating atmospheric surroundings (Özdil *et al*., 2007). Cotton has been the most commonly used natural fibre for thousands of years. Attributable to their thermal comfort properties and easy laundering, knitwear accounts for the highest use of cotton. Acrylics are synthetic fibres made from the organic polymer, polyacrylonitrile. Acrylic knitted fabrics possess easy-care properties, good shape retention and durability. A plethora of textile products are manufactured and marketed using acrylic (Gries *et al*., 2015).

Weft knitting is the most common fabric manufacturing process and can be produced using tuck, knit and miss stitches (Spencer, 2001). Owing to its freedom of movement, soft feel and high elasticity, knitted fabrics are much desired for garments. Also, knitted fabrics are favoured for summer and winter as next-to-skin wear, in which comfort is essential.

Porosity is the physical characteristic indicating the difference between the total fabric area and the estimated area covered by the yarns (Burleigh *et al*., 1949). Knitted textile fabrics are considered to have an open porous structure. Hence, determining the porosity of knitted fabric is critical because it affects heat transfer from the body to the environment (Song, 2011). Digital image analysis has gained endorsement as a sensible approach to measure the porosity of knitted fabrics (Imrith *et al*., 2016).

Hes (1995) broached the notion of thermal absorption as an estimate of the warm-cool sensation of textiles. Thermal properties of textiles are the cornerstones underpinning comfort during hot and cold weather. The contact temperature between two materials depends on their thermal absorptivity. This warm-cool feeling property determines whether an individual feels cool or warm initially, as a fabric contacts the human skin. The particularity is that thermal absorptivity does not depend solely on the experimental conditions; it is linked to thermal properties such as thermal diffusivity and conductivity (Uttam *et al*., 2013). It is well known that thermal properties depend on several factors such as fabric porosity, thickness, fibre types and structure (Hes, 1987). The porosity of a fabric improves its breathability, and thickness improves its thermal insulation properties. In this purview, several investigations have examined the thermal comfort of knitted fabrics (Hes *et al*., 2002; Oğlakcioğlu and Marmarali, 2007). In the alluded references, the Alambeta device, manufactured by the Czech company Sensora (Hes and Dolezal, 1989), has been used to measure the thermal comfort properties of fabrics.

The review of literature reports that studies have been limited mainly to knitted structures such as single jersey, ribs or interlock. Conversely, few studies have been reported on the thermal comfort properties when the structures of knitted fabrics vary. Practically, it is presumed that during shopping, customers do not intend to buy a specific type of knitted fabric apparel structure (Jeong and Lee, 2014). Few researchers have examined cellulosic and synthetic knits across all types of thermal comfort conditions.

Drawing from these insights, the objective of this work is to design and produce assorted weft-knitted fabric structures using acrylic and cotton yarns and to compare their thermal comfort characteristics.

2. MATERIALS AND METHODS

The notations of the knitted fabrics were designed, Fig. 1, which were used to produce the fabrics on a 5-gauge V-flat bed manual knitting machine set with a stitch cam 15 mm. 100% cotton and 100% acrylic yarns were used for knitting, both bearing a linear density of 236.2 tex (2.5 Ne) to maintain consistency during the analysis. Weft knitted fabrics can be created by either: knit + miss loops; knit + tuck + miss loop; all knit loops, and or knit + tuck loops. Firstly, a plain fabric was produced consisting only of knit stitches. Combinations of knit, tuck, and miss stitches were incorporated during knitting to produce 27 different fabric structures, both with 100% acrylic yarns 100% cotton yarns, respectively. The aftermath of this operation yielded a total of 54 fabrics for both yarn compositions. The knitting notations are given in Fig. 1.

Conditioning of fabric samples was done at 21 ± 1°C (70 ± 2°F), and 65 ± 2% relative humidity for 48 hours, as per the ASTM D1776-04 standard. Images of fabrics were captured in a light box designed and constructed as reported by Imrith et al. (2019). The porosity was evaluated using digital image processing and an analysis routine in Wolfram Mathematica. The Alambeta apparatus was used to determine the thermal properties of the fabrics.

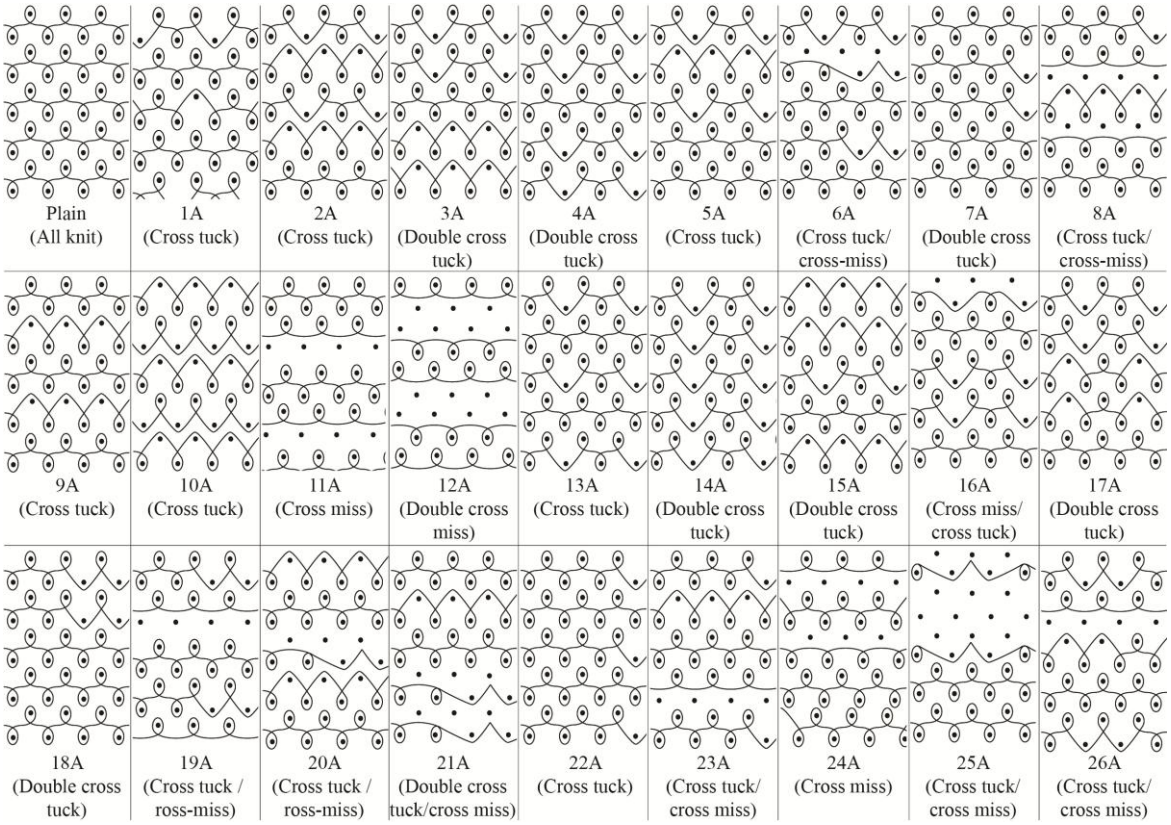

Fig. 1. *Knitting notations and fabric structures generated*

3. RESULTS AND DISCUSSIONS

3.1. Structural parameters of fabrics and thermophysiological comfort

The porosity *(p_o)* of acrylic fabrics is generally higher than that of cotton, ranging from 38.88% to 52.80%. Double cross tuck structures exhibit higher porosity and fabric thickness as the tuck stitches produce greater openness. On the other hand, the miss stitches resulted in thinner and tighter fabrics. In general, both acrylic and cotton followed similar trends in thickness and porosity.

Acrylic fabrics have lower thermal absorptivity and higher thermal resistance than cotton due to their smooth and regular fibrous structure, which creates tortuous paths that scatter and absorb heat. The increased porosity in acrylic fabrics inhibited heat transfer by entrapping air, consequently promoting insulation. Cotton, with its convoluted cross-section, yields a fabric with a low cover factor. Hence, the cotton fabrics have higher thermal absorptivity and conductivity, as heat passes more easily through their twisted ribbon-like fibre surfaces. Generally, the bulky fibrous assembly of acrylic fabrics confers higher thermal insulation than cotton, emphasising their suitability for applications where heat retention is required.

The smooth surface of cotton increases contact area, enhancing thermal absorptivity and producing a warmer sensation. Conversely, acrylic fabrics may have a lower contact area with the skin. Cotton and acrylic have substantially different thermal conductivities, with a mean of 57.02 W/mK for cotton and 110.29 W/mK for acrylic. Cotton, a cellulosic material, has polar groups in its molecular chains and has a higher moisture regain than acrylic (Dias and Delkumburewatte, 2007), hence, imparting the cotton fabrics with higher thermal conductivity. Although the linear density of

the cotton and acrylic yarns was the same, cotton fabrics have lower thermal insulation than acrylic fabrics. This is because the acrylic fabrics were thicker than the cottons.

3.2. Statistical methods to evaluate experimental results

Linear regression was used to estimate the relationship between the thermal comfort variables and fabric porosity and thickness. The correlation hypothesis put forward was that porosity and thickness would show good correlation with thermal comfort properties. Pearson's correlation *(ρ)* analysis was conducted to analyse the correlation between thermal comfort and fabric parameters.

3.3. Effect of Porosity: Acrylic and Cotton fabrics

Fig. 2(a) shows the inverse relationship between thermal conductivity and porosity. Fig. 2(e) shows a coefficient of variation of 0.036 when thermal absorptivity is plotted as a function of porosity. The decrease or increase in fabric porosity was inversely proportional to thermal absorptivity and thermal resistance, as evidenced by the respective negative and positive ρ values. Still, the % ratio of the coefficients of correlation for the regression equations relating thermal absorptivity to porosity and thermal resistance to porosity is 29:71. From these R^2 values, it may be deduced that the porosity of the 100% acrylic macrostructures has a low influence on the thermal properties.

The coefficients of the linear regression for thermal conductivity and resistance are higher than the equivalent coefficients for 100% acrylic. The R^2 between porosity and thermal absorptivity is 0.0145, that is, 29% compared to 71% for 100% acrylic. Between thermal diffusivity and porosity, the R^2 is 0.0047, implying only 7% of influence compared to only 93% for the 100% acrylic fabrics. The correlation coefficient ranges from 0.0037 to 0.1868 for the thermal comfort of 100% cotton. Thus, the low values indicate strong statistical linear reliance. For 100% acrylic, the influences of thermal comfort properties range from 0.0151 to 0.00473. These values support the hypothesis that thermal comfort properties of knitted macrostructures have low correlation with attributes such as fabric thickness and porosity.

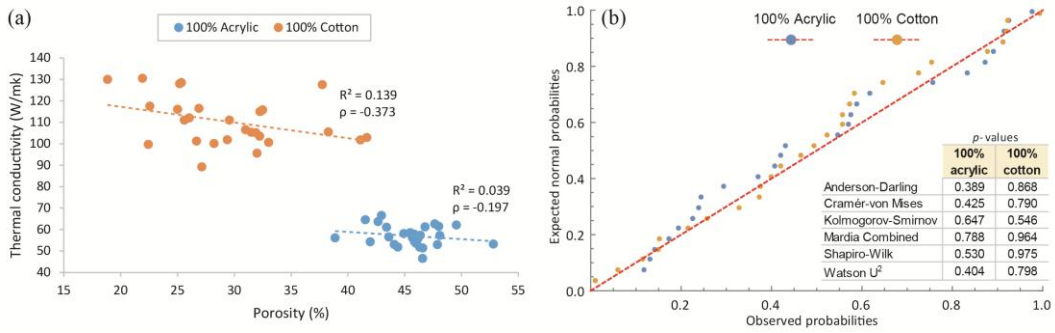

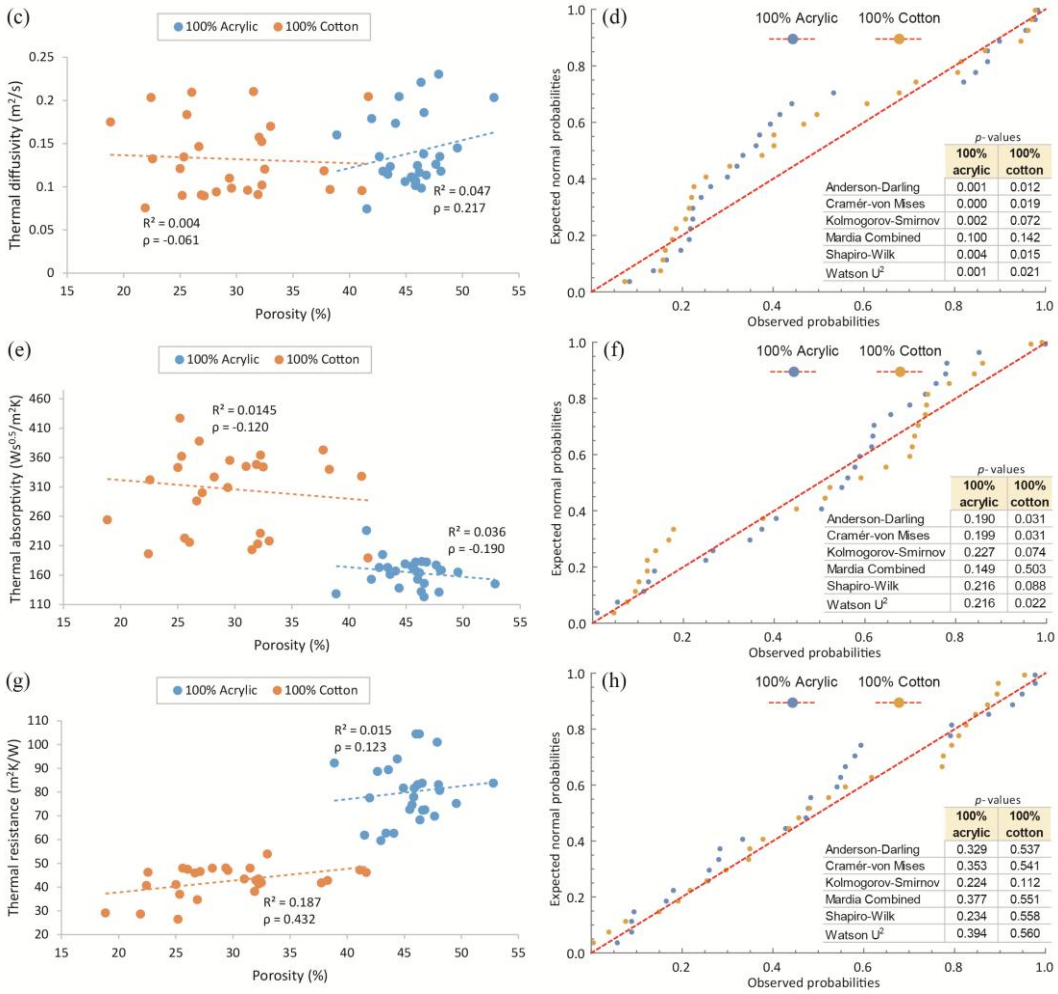

Fig. 2 (a - h). *Scatter plots with R^2, ρ and P-P with non-parametric results between porosity and thermal properties*

3.5. Effect of Thickness: Acrylic and Cotton fabrics

Fig. 3 (a - h) depicts scatter plots with R^2 and ρ and a probability plot with non-parametric test results between thickness and thermal comfort characteristics. Thickness is a key parameter of the structure, and strongly influences the thermal comfort properties of the fabrics.

Fig. 3 (a) shows a high linear correlation between thickness and thermal resistance, R^2 = 0.723. An increase in fabric thickness reduced thermal absorptivity, whereas the opposite trend was observed for the thermal resistance. The linear relationship between thermal resistance and thickness has a high correlation coefficient, R^2 = 0.495. Both fabric compositions show a high correlation between thermal resistance and fabric thickness. Conversely, thermal absorptivity and thickness show very low correlation, R^2 = 0.010, which is 6% compared to 94% for the acrylic structures. It demonstrates that as fabric thickness increases, the thermal insulation also increases.

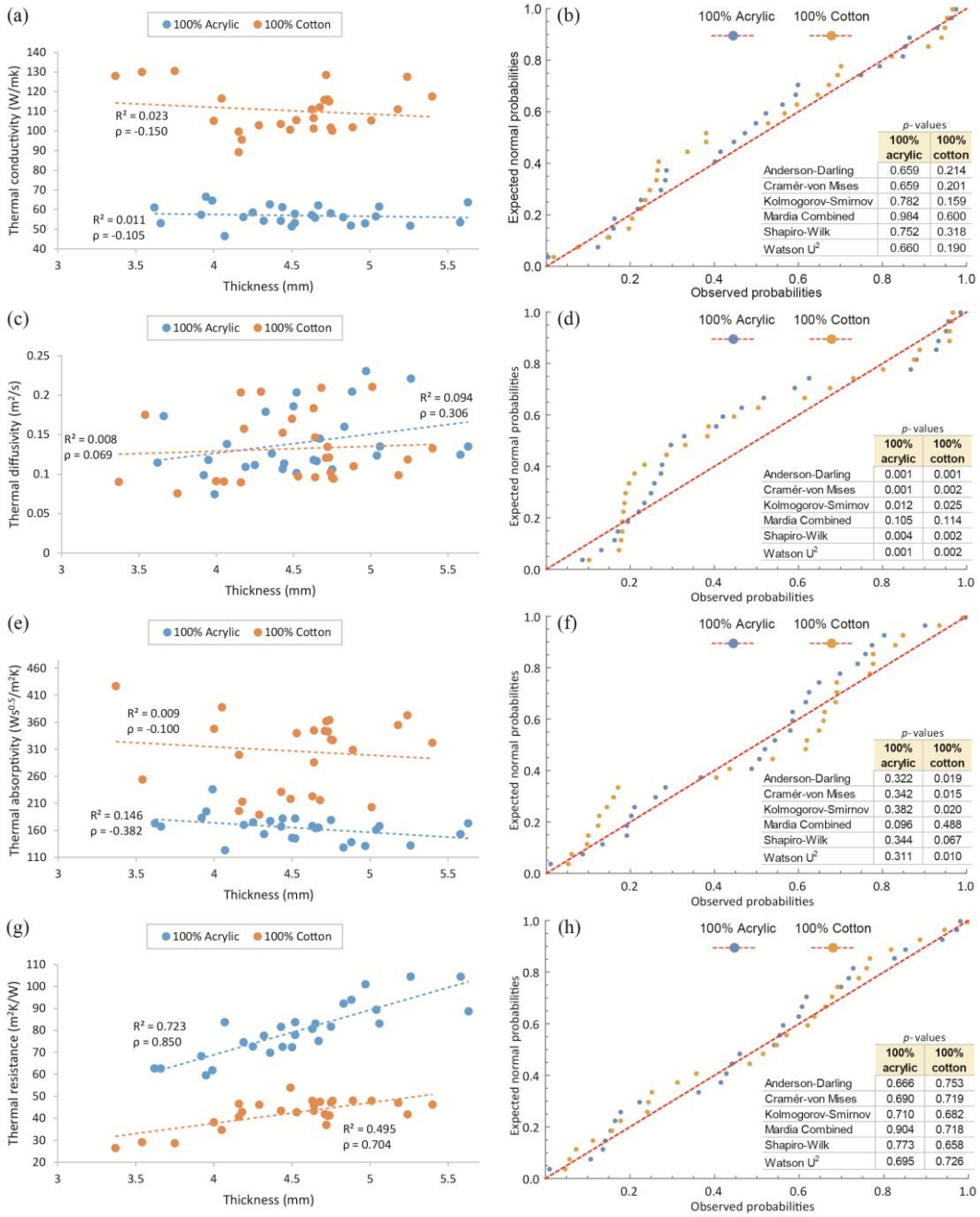

Fig. 3 (a - h). *Scatter plots with R^2, ρ and P-P with non-parametric results between porosity and porosity*

3.7. Analysing results using *p*-value

The normality of residuals was formally assessed based on hypothesis tests of *p*-values from non-parametric tests. The research question was as follows: whether fabric porosity and thickness influence the targeted thermal comfort characteristics to a significant degree. The null hypothesis *(H_0)* and alternative hypothesis *(H_a)* were defined:

$H_0 : p \geq 0.01$: Data are not statistically significant

H_a : $p < 0.01$: Data statistically significant

With a significance level of $\alpha = 0.01$, the null hypothesis states that the anticipated *p*-value is equal to or greater than 0.01. The computation of the significance level and *p*-value helped to decide whether or not to reject the null hypothesis. If the *p*-value is smaller than the significance level, it means that the null hypothesis is rejected; otherwise, the null hypothesis is true. On that score, to decrease the probability of type I error rate, the significance level was set to 0.01, akin to a confidence level of 99%. This is the non-rejection region in the normal distribution. This means that 1% would be expected to be either below or above the rejection region. For this reason, it was acceptable with the likelihood of committing a type I error 1% of the time. The test sample's *p*-value must be inside the critical region, 99% of the time. The current sampling distribution is a one-tailed test. Although it was shown that the majority of the correlation tests have low R^2 values, all non-parametric tests, Fig. 2 (b, d, f, h) and Fig. 3 (b, d, f, h), showed that the *p*-values are higher than the significance level, underlying the null hypothesis. Excepting thermal diffusivity against thickness and also against porosity, Anderson-Darling, Cramér-von Mises, Kolmogorov-Smirnov, Shapiro-Wilk and Watson U^2 resulted in $p < 0.01$. It is inferred that there is enough evidence to reject the null hypothesis. Accordingly, the smaller the *p*-value obtained from these five test methods, the more likely it is that H_0 can be true. It was seen that there was a significant difference between the means of all groups of the paired data using a critical value of 0.01. The non-parametric results concluded that the null hypothesis was rejected in favour of the alternative hypothesis (*p*-value < 0.01).

The smaller the *p*-value, the stronger the indication against H_0 provided by the data. Therefore, it indicated a type II error because the non-parametric test showed that porosity, thickness, and thermal diffusivity are statistically significant. Contrarily, the Mardia Combined test for both fabric compositions gives a *p*-value ≥ 0.01 for thermal diffusivity against porosity, and also against thickness. The null hypothesis is that the porosity-thickness against thermal diffusivity is normally distributed and is not rejected at the significance level 0.01, depending on the Mardia Combined test. Here, it indicated failure to reject the null hypothesis, meaning that the data are not statistically significant. The fabrics' areal porosity and thickness against the thermal comfort properties have $p \geq 0.01$ for both sets of fabrics. Non-parametric tests resulted in $p < 0.01$. In 100% cotton and 100% acrylic, thermal conductivity, thermal absorptivity and thermal resistance have $p \geq 0.01$ in all six statistical tests, substantiating the normality of the data.

4. CONCLUSION

Acrylic fabrics show maximum thermal resistance and porosity. The combination of cross-tuck/cross-miss for both fabric compositions gave the lowest thermal comfort properties compared to only double cross-tuck and cross-tuck fabrics. Double cross-tuck fabrics are characterised by higher values of porosity and thermal resistance as compared to the other structures. There is strong agreement of Pearson correlation for all thermal comfort between porosity and thickness, respectively. Moreover, to support the relationship among the variables statistically, this work applied a non-parametric test to evaluate the normality of the residuals. In a nutshell, low R^2 values were observed, and it can be concluded that if the parametric test failed to give satisfactory results, then non-parametric test methods can be employed. The points of all the models in the P-P plot are clustered along the 45° line, signifying that the normality assumption is practically satisfied. The spreads of thermal comfort characteristics residuals are moderately equal around the line. And so, the linearity of errors is not violated. Hence, the conclusions of this investigation can aid textile technologists and manufacturers to optimise thermo-physiological comfort, based on fibre composition and engineered fabric structures. Future works may investigate the effect of various

fibre compositions and structures, including warp-knitted, woven and non-woven fabric structures, and the application of mathematical optimisation tools for predicting the thermo-physiological comfort of textiles.

REFERENCES

[1] Das, A. and Alagirusamy, R. (2010), *Science in Clothing Comfort*, Woodhead Publishing Limited, India, pp. 79-105.

[2] Starr, C., Taggart, R., Evers, C. and Starr, L. (2014), *Biology: The Unity and Diversity of Life,* Cengage Learning, Boston, USA, pp. 468-481.

[3] Ozdil, N., Marmaralı, A. and Kretzschmar, S.D. (2007), "Effect of yarn properties on thermal comfort of knitted fabrics", *International Journal of Thermal Science*, Vol. 46 No. 12, pp. 1318-122.

[4] Gries, T., Veit, D., Wulfhorst, B. (2015), *Textile Technology: An Introduction.* Hanser Publications, Cincinnati, pp. 95-120.

[5] Spencer, D.J. (2001), *Knitting Technology: A Comprehensive Handbook and Practical Guide,* Woodhead Publishing Limited, United Kingdom.

[6] Burleigh, E.G., Wakeham, H., Harold, E. and Skau, E.L. (1949), "Pore size distribution in textiles", *Textile Research Journal,* Vol. 19 No. 9, pp. 547-555.

[7] Imrith, M.K., Rosunee, S., Unmar, R. (2016), "Investigating the relationship between knitted fabric porosity and light permeability", *Indian Journal of Materials Science,* Vol. 2016 No. 4, pp. 1-12.

[8] Hes L. (1995), "New achievements in the area of the objective evaluation of thermal insulation and thermal-contact properties of textiles", The 3rd Asian Textile Conference, Vol. II pp. 1201-1203.

[9] Uttam, D., Mukhopadhyay, A. and Ishtiaque, S. (2013), "Modelling to predict thermophysiological properties of hollow/ microporous yarn fabrics", *The Journal of the Textile Institute,* Vol. 104 No. 4, pp. 407-413.

[10] Hes. L. (1987), "Thermal properties of nonwovens", Proceedings of Congress Index 87, Geneva.

[11] Hes, L., Geraldes, M.J. and Araújo, M. (2002), "How to Improve the Thermal Comfort with High Performance PP Fibres", 2nd AUTEX Conference Proceeding, Bruges, Belgium, p. 428.

[12] Oğlakcioğlu, N. and Marmaralı, A. (2007), "Thermal comfort properties of some knitted structures", *Fibres and Textiles in Eastern Europe*, Vol. 5-6 No. 64-65, pp. 94-96.

[13] Hes, L. and I. Dolezal. (1989), "New method and equipment for measuring thermal properties of textiles", *Journal of Textile Machinery Society of Japan* Vol. 42 No. 8, pp. 71-75.

[14] Jeong, S.W. and Lee, K.H (2014), "Impact of evaluative criteria on satisfaction and dissatisfaction: identifying the role of knitwear involvement", *Fashion and Textiles,* Vol. 1 No. 9, pp. 1-15.

[15] Imrith, M.K., Rosunee, S., Unmar, R. (2019), "Bio-inspired knitted fabric development using 3D modelling and image processing", *The Journal of the Textile Institute,* Vol. 111 No. 8, pp. 1123-1139.

[16] Dias, T. and Delkumburewatte, G.B. (2007), "The influence of moisture content on the thermal conductivity of a knitted structure", *Measurement science and technology*, Vol. 18 No. 5, pp. 1304-1314.

ANNALS OF THE UNIVERSITY OF ORADEA
FASCICLE OF TEXTILES, LEATHERWORK

EFFECT OF STRUCTURAL ELEMENTS ON THE MECHANICAL PROPERTIES OF HYBRID LENO WOVEN FABRIC

KASTACI Bilge Berkhan[1], ÖZEK H.Ziya[2]

[1] Kahramanmaraş Istiklal University, Occupational Health and Safety Service, 46100, Kahramanmaraş, Turkiye
E-Mail: bilgeberkhan.kastaci@istiklal.edu.tr

[2] Namik Kemal University, Corlu Faculty of Engineering, Dept. of Textile Engineering, 59850,Corlu, Tekirdag, Turkiye
E-Mail: zozek@nku.edu.tr

Corresponding author: Ozek, H.Z., zozek@nku.edu.tr

Abstract: *Hybrid leno woven fabrics represent a unique class of textile structures combining the interlacement stability of conventional weaves with the locking mechanism of leno (gauze) constructions. This study investigates the influence of key structural parameters—namely leno weave ratio of hybridization with ground weave, leno warp yarn float number, leno interlacing and weft densities on the structural and mechanical properties of such fabrics. A series of hybrid leno fabrics were engineered with controlled structural variations and tested for tensile strength, tear resistance, bursting strength and bending rigidity. The experimental results revealed that leno weave tends to increase warp crimp but decrease the weft crimp. Eventually it affects the fabric width and unit mass. The nature of loose structure of leno weave appears to have a direct effect on the structural parameters of the hybrid fabric. The hybrid structures significantly influence, durability, flexibility and deformation behaviour of the construction. The findings of the study provide a design framework for optimizing hybrid leno fabrics in applications such as technical textiles, and composite reinforcements.*

Keywords: *Hybrid weave, leno weave, leno fabric, mechanical properties, textile structures.*

1. INTRODUCTION

Textile materials are converted into final products with different forms and functions thanks to multi-stage mechanical and partly chemical operations. The range of conversion starts from fibre stage up to a garment or a 3D preform as the finalized products. By means of the intersection of warp and weft yarns in a specific order of weave, a plenary layer of textile material is produced which is identified as woven fabric [1]. Any possible changes in the basic traits and order of yarns, or in the weave are directly imparted into the appearance and performance of woven fabric. That means any variation in the fabric construction affects the mechanical properties of the woven fabric. Previous studies have already confirmed that the construction parameters also have an effect on the mechanical properties of the fabric to a great extent.[2],[3].

The properties of fabric are essentially a function of fabric structure, which in turn depends on nature of fibres, the density of yarns in the fabric, weave, the characteristics of warp and weft threads like count and twist level and the factors established during weaving such as yarn crimp. As a matter of fact, the weave is the most influential elements of woven fabrics, enabling to design or develop almost limitless forms of fabric. Moreover, the application of 2D or 3D woven fabrics for composite

preforms [4], [5] has boosted the significance of weave, even further. Weave being the most important parameter of fabric structure plays a significant role in deciding the performance of composites.

Because of inherent characteristics of basic and derived weaves, it may often be necessary to combine two or more weaves in one single fabric structure. These structures are often called hybrid weave or hybrid fabric. Therefore, a hybrid fabric being a versatile technique enables to combine weave as well as various fibres within a single fabric to optimize performance, strength, and appearance [5]. The combination of various forms of leno weave with classic plain weave was selected as the object of this study to analyse possible effects on the fabrics structure and basic mechanical characteristics. Since such studies concerning leno weave or hybrid fabric are limited in the literature, this work is likely to raise an interest in leno structure especially for researchers in composite materials.

Leno weave is a specialized weaving technique in which warp threads are twisted together in pairs during the weaving process to securely lock the weft yarns in place. Those twisting warps, called as leno warp yarns cross the weft yarns from each side in successive weaving cycle. This weave structure imparts additional stability to fabric, which is important when using fine yarns loosely spaced. Eventually, an open, mesh-like fabric with relatively large openings maintaining dimensional stability is produced because the twisted warp threads prevent the crossing points from shifting [6],[7].

It is also called as gauze weave or cross-weave. The term *gauze* historically referred to lightweight, open fabrics described by their transparency and handle, with origins linked to early textile trade routes (e.g., Gaza) [8]. In contrast, *leno* emerged later (around 18th century) as a structural classification within textile engineering, denoting a specific warp-crossing mechanism that stabilizes open weaves. While modern usage often treats the two terms as synonymous, they are conceptually distinct: gauze is a functional descriptor, whereas leno is a precise weave structure. Concerning the origin of the word “Gauze”, it is claimed that it was derived from French “gaze,” or possibly from Spanish “gasa” which are attributed to the Arabic word “qazz” meaning “silk”. [9] These words come from their place of origine-the Gaza (gazza) city in the Palestinian territory on the eastern Mediterranean coast. It is believed that this light and loose fabric originally made of silk was launched in the city of Gaza and used for clothing.

The controlled combination of weaves and other components theoretically allow to the emergence of a very wide design range. It should be emphasized that the pattern in woven fabrics is not only a visual element but also an engineering organization that emerges from the controlled interaction of structural parameters [10]. The weaving design process is a holistic approach requiring a joint evaluation of yarn properties, weave structure, production parameters, and the pattern as a structural design element. Hybridization of weaves in the fabric structure by using forms of weaves may be beneficial in obtaining optimum mechanical performance and also minimizing the cost. There exists very limited literature on the mechanical performance of the hybrid leno woven fabric alone. In this article, the breaking strength, elongation, tearing strength and bursting strength of cotton hybrid fabric together with some structural parameters are studied.

2. LENO WEAVE STRUCTURE AND PREVIOUS STUDIES

Leno weave is different from conventional weave in its level of complexity both in terms of fabric formation and structure. It is categorized as compound weave structure and there needs an extra set of warp ends that are divided into leno groups. Among these leno yarns, certain warps termed crossing (or leno) warps are passed from side to side of what are termed standard (or stationary) warps, and are bound in by the weft in these positions. Therefore, the parallel arrangement of warp yarns in the fabric is no longer possible.

Depending on the frequency of leno motion, three leno structures are possible as seen in Fig.1. When the leno warp pair crosses every two picks it is called half leno (Fig 1.a), in the case of crossing at every pick, it is called full leno. The alternating leno (Fig 1.c) which is the combination of both is also possible. Half leno provides looser binding and larger pores in comparison with full leno.

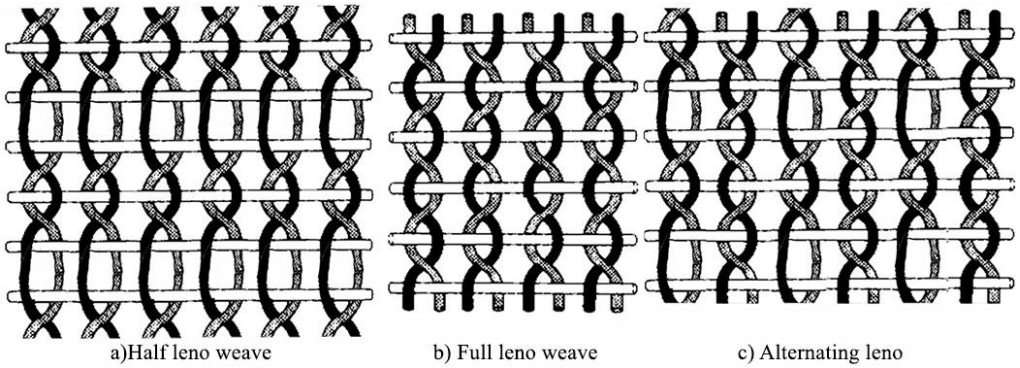

***Fig. 1**: The types of leno weaves in accordance with the sequence of leno crossing*

Different variants of leno weave is possible. Leno arrangement can be positioned all over the fabric width or at certain intervals. The leno and standard warp ends may be arranged with each other in various proportions, such as 1:1, 2:1, 1:2, 2:2 or 1:3 etc., but an essential condition is that each group of leno and standard ends (as well as ground warps) must be placed in one split of the reed [7]. The number of interlacing between leno warp and weft yarn can also be varied. The leno and standard warp ends may be arranged with each other in various proportions, such as 1:1, 2:1, 1:2, 2:2 or 1:3 etc., but an essential condition is that each group of leno and standard ends (as well as ground warps) must be placed in one split of the reed [11]. Among the typical leno fabrics, gauze characterized by a thin and translucent appearance is an all over leno structure and probably the oldest version of leno fabrics. Grenadine is a fine leno-weave with overall leno structure including stripes and merquisette a sheer, light and open meshed fabric used for curtains and mosquito nets. Fancy leno and tulle are other available leno fabric [11].

Production of leno woven fabric is more complicated than producing normal weave fabrics and special shedding equipment is required. The crossing motion of warps are achieved by special devices called doup heald. They should be used addition to the normal heald equipment for the fabric production. The crossing warp yarns are controlled by this leno attachment of the leno heald and by the side-to-side movement of the ground warp yarns. Two warp yarns in the same leno pair cross over each other and interlace with one or more weft threads. Initially twine leno healds were developed and used until the development of metallic leno healds. The twine leno heald is composed of a standard harness and a half heald. While, the metallic leno heald is composed of two standard harnesses and a half heald. An innovative solution against using inverted leno heddles was introduced as developed by Dornier. Dornier EasyLeno system is capable of producing all over leno fabric by using needle bars and a fluctuating reed across the warp yarns. It is claimed to be very high speed and efficient way of leno weaving [12]. Powerleno is also a similar approach for leno fabric production invented by Sulzer. A guide bar and eyeleted reed are introduced into the weaving system, replacing the traditional leno healds to produce all over leno cloth [11].

Leno weave is a novel method of weaving which result in a a specialized textile structure where adjacent warp yarns twist around each other, locking weft threads in place to create a strong, yet open mesh-like fabric. This construction prevents slippage, providing lightweight and breathable nature, often used for curtains, industrial bags, summer clothing, and insect screens. This interlacing produces

high in-plane stability relative to other open weaves while keeping porosity and low areal density. In apparel and home usage, leno fabrics are generally used for ornamental objective. In the case of technical textiles, functional uses come first, particularly the applications where high permeability and shape retention are required. Drying and conveyor belts and filter substrates are typical application fields where air and liquids need to pass through while the main substrate maintains stability under stress. In architectural use, they are used as decorative or functional elements [5].

In the literature there are various studies investigating the mechanical performance of different woven fabrics by varying the weave architecture [3],[4], [5]. They serve as useful guides for ensuring the required quality of fabric and appropriate design and in relation to certain usages. However, studies for leno structures or leno integrated hybrid structures are rather limited. There are many patent applications exploiting the leno structures for various end products such as bags in tubular form, medical bandage, sports shoes and refractor mesh-like fire protecting panel, according to a patent review by Kastacı [13]. The structural part of these materials are entirely leno based or hybrid structures combined with leno and other constructions. There are a number postgraduate thesis focusing on different aspects of leno weave, namely physical properties of leno fabrics [13], [14], possibility of tubular leno weaving [15], adaptation of leno healds into dobby loom [16], new design aspects for leno weaving [17], [18] and for smart textiles application [19].

Leno weave establishes a locked structure that prevents yarn displacement as a result of the crossing of adjacent warp yarns around the weft. This interlacement mechanism distinguishes leno from conventional weaves such as plain or twill where warp yarns remain parallel. The twisting action generates a stable, open structure with minimal yarn slippage, enabling both permeability and structural integrity. It is known that the mechanical behaviour of leno fabrics is governed not only by yarn properties and density, but also by the topological constraint introduced by warp crossing, which enhances frictional interaction and load transfer at yarn junctions. This unique mechanism underpins most of the mechanical advantages reported in the literature. Tensile properties are the most extensively studied mechanical characteristic of leno fabrics. Experimental investigations show that leno fabrics exhibit comparable or improved tensile strength relative to conventional woven fabrics, depending on structural configuration. A key study by Shaker et al. [14, 21] demonstrated that both pure leno and hybrid leno fabrics achieve similar tensile strength; however, tensile behaviour is strongly influenced by weft density and structural design. Increasing thread density improves tensile strength by enhancing inter-yarn friction and reducing yarn mobility.

More recent developments focus on advanced leno architectures. For example, multi-warp leno configurations (e.g., four-warp systems) have been shown to significantly enhance tensile performance due to improved load sharing among multiple crossing warp yarns [22]. These structures increase both breaking force and elongation at break, indicating improved energy absorption capacity. At the composite level, tensile behaviour is further influenced by matrix interaction. Textile-reinforced systems show that fabric geometry, fibre type, and matrix bonding determine tensile stiffness and ultimate strength, with woven structures providing superior load distribution and damage tolerance. Enhanced shear resistance and dimensional stability appear to be a distinctive mechanical advantages of leno fabrics. [23]. Unlike loosely woven plain fabrics, which exhibit yarn slippage under shear deformation, leno fabrics maintain structural integrity due to the interlocked warp system. The crossing of warp yarns creates a self-locking junction, which resists rotational movement and delays shear deformation resulting in reduced fabric distortion and improved resistance to skewing. This property is particularly important in applications involving open mesh structures, where conventional weaves suffer from instability. The enhanced junction stability of leno fabrics has been widely reported in technical textile applications, especially in reinforcement grids and open-mesh fabrics.

Leno fabrics exhibit superior resistance to localized mechanical damage, including puncture and yarn pull-out. This behaviour is primarily attributed to the high frictional locking at warp–weft junctions. Experimental results indicate that pure leno fabrics show significantly higher puncture resistance compared to hybrid leno structures. The twisting of warp yarns tightly secures the weft, preventing yarn displacement and increasing resistance to penetration forces [24]. Similarly, studies on yarn pull-out behaviour in woven fabrics highlight the importance of inter-yarn friction and structural configuration. Higher interlocking and frictional contact increase the peak pull-out force and energy absorption, which are critical parameters in impact and protective applications .

Recent studies confirm that leno weave's main mechanical advantage is junction stability under load. That stability improves resistance to yarn slippage, pull-out, shear distortion, and local damage. Newer architectures such as four-warp leno show that it is possible to increase both strength and extensibility while keeping the breathable, open nature of the fabric. However, the literature is still fragmented, and direct studies on dry-fabric bending, fatigue, cyclic damage, and standardized comparison between half, full, hybrid, and multi-warp leno remain relatively limited [26].

A significant portion of recent research on leno fabrics is embedded within the field of textile-reinforced composites, where leno structures are used as reinforcement grids. It is claimed that the mechanical performance of the composite in such systems depends on fabric geometry, fibre type, matrix properties and fibre–matrix interfacial bonding.

3. MATERIAL AND METHOD

The hybrid leno samples are woven on a Smit G6300 model rapier loom equipped with a total of 6 frames dobby. Metal heald doup are used for leno warps and classic heald wires for the standard warps. Pure cotton Ne 40/2 combed yarn was used as warp and weft. The actual yarn count was given as Ne 20,45 and the average strength and elasticity ratio were 16,68 cN/tex and 1,19% respectively.

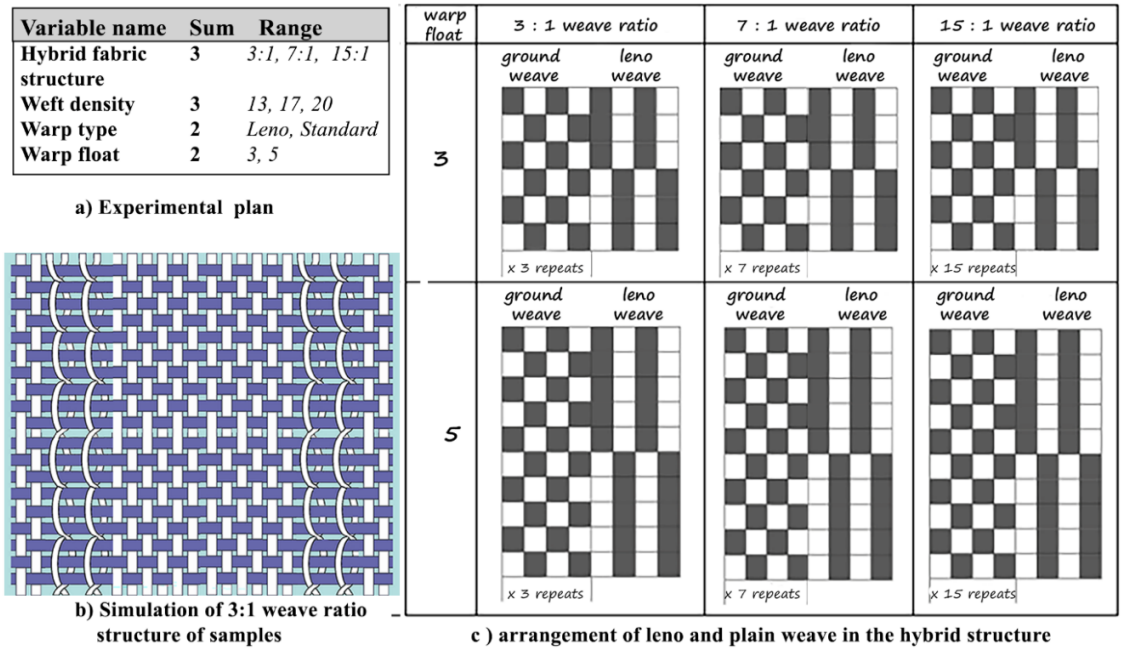

***Fig. 2**: The experimental plan, hybrid leno simulation and the arrangement of hybrid weave samples*

The experimental plan with variables and hybrid weave structures are given in Fig. 2. The total of amount of samples reached to 39 with three additional fabric samples of fully plain fabric at the 3 different weft density. The density of warp yarn was fixed at the value of 16,2 ends/cm. To achieve the same mechanical density in the warps, reed threading was performed, thus equalizing the warp densities of all fabrics The leno weave was integrated with plain weave at three different repeats. Each fabric structure has 2 pairs of leno weave, while the ground weave of plain consists of 3, 7 and 15 repeats. This configuration enables to change the proportion of leno weave against the basic plain weave. With the hope of more precise measurement of the effect of leno warp, the same structures were also woven with standard warp replacing leno warp ends.

The sample coding "A.3L17" comprising 4 variables are arranged as follows:

F. Structure	***Float No***	***Warp type***	***Weft Density***
A	3	L	17
A: Weave ratio 15:1	3 picks over	L:leno warp	17 *picks/cm*
B: Weave ratio 7:1	5 picks over	S: std. warp	20 *picks/cm*
C: Weave ratio 3:1			23 *picks/cm*

The list of the conducted tests and test methods are tabulated in Table 1. Since the three different weave ratio is used, the number of leno weave repeats are varied. Therefore, great attention was paid to keep the samples of the same group identical in order to prevent any possible bias in measurements. In other words A, B and C coded all samples were prepared to contain the same number of leno and non-leno standard warp section. On the other hand, three all plain weave samples are also produced at the three identical weft densities and named as; P17, P20 and P23.

Table 1: *The list of conducted tests and test standards*

No	THE TEST DEFINITION	STANDARD CODE	STANDARD NAME
1	Determination of yarn density	TS 250 EN 1049-2 :1996	*Textiles-Woven Fabrics-Construction-Methods of Analysis-Part 2 Determination of Number of Threads Per Unit Length*
2	Unit weight measurement	TS 251	*Textile Woven fabrics – Structural Analysis Determining the unit length and unit mass*
3	Measurement of fabric width	TS EN 1773	*Textile Woven fabrics – Structural Analysis Determining the width and the length*
4	Determination of yarn crimp	ASTM D 3883-04	*Standard Test Method for Yarn Crimp and Yarn Take-up in Woven Fabrics*
5	Measurement of resistance to tearing	TS EN ISO 13937-1 :2000	*Textiles — Tear properties of fabrics Part 1: Determination of tear force using ballistic pendulum method (Elmendorf)*
6	Measurement of breaking strength	TS EN ISO 13934-2 :2014	*Textiles — Tensile properties of fabrics Part 2: Determination of max force using the grab method*
7	Assessment of bursting strength	TS EN ISO 13938-2 :2019	*Textiles — Bursting properties of fabrics Part 2: Pneumatic method for determination of bursting strength and bursting distension*

4. EXPERIMENTAL FINDINGS AND DISCUSSION

A total of 39 samples were tested for some structural components and also for breaking, tearing and bursting strength. The close view of the three group of samples are shown in Fig. 3. The samples of Group A has the lowest leno warp repeats, while Group C has the highest. Warp and weft yarn

densities were accurately calculated and adjusted during the design of samples, and density **measurements were** taken after the fabrics were woven. The average warp density values obtained from the measurements are given with reference to nominal value, in Fig. 4. In the graphics, the first series of column displays the sample group A incorporating minimum leno weave, the middle column belongs to the sample group B and the third column at the back displays the sample group C incorporating maximum rate (3:1) of leno weave. Results for the three plain woven fabrics are given as a separate group at the right side of the graphic.

***Fig. 3**: The close view of the three main group of samples*

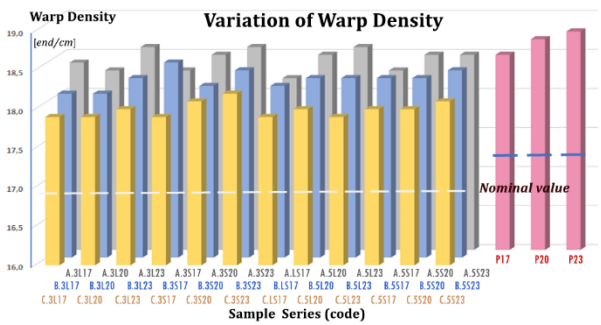

***Fig. 4**: Nominal and actual warp density variation for all the sample groups*

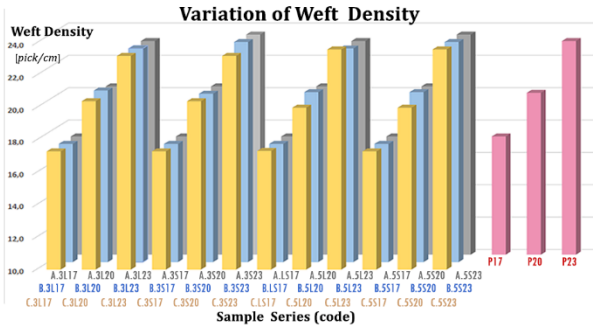

***Fig. 5.** Actual values of weft density variation for all the sample groups*

The warp density of the samples A.3L17, A.3S20, A.3L20, A.3S17, A.5L17, A.5L23 are measured as 17 which is the lowest figure. The highest warp density for the hybrid weaves is recorded as 18,6 for the group A samples and 18,8 for the plain P.23 sample. It is seen that an increase in the weft density rises the warp density, while a decrease in the leno weave content has the same affect. The presence of leno interlacing seems to have a negative affect on the warp density. The effect of floating number do not display a clear effect.

The average weft densities for all the samples are given in Fig.5. It may be easily noticed that variation in weft density is comparatively higher than warp because the samples were woven at three densities. However, the variation between the samples of the same weft density is too low. It is also noticed that weft density of all the samples were recorded slightly above or equal to the nominal setting on the loom. The effect of leno interlacing has not been apparent on these samples.

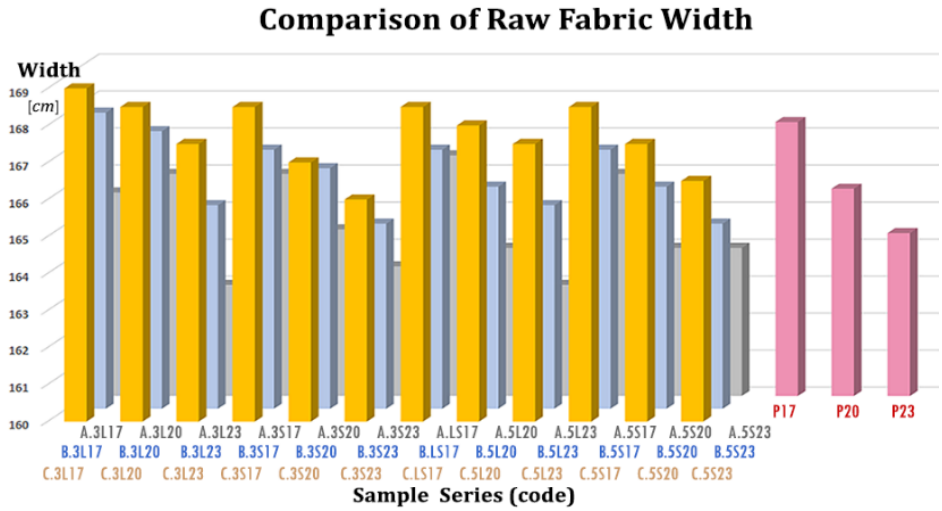

***Fig. 6**: Actual values of fabric width for all the sample groups*

The average values of the raw fabric width measurement are shown in Fig.6. The range of fabric width varied between 163 and 169 cm. As expected, an increase in the weft density results in lower fabric width for all the samples. The affect of the leno content also seems to be decisive, as the incorporation of leno weave slackens the structure leading to the wider cloth width. The samples of group C has the highest widths whereas the samples of the group A has the lowest ones. The effect of floating number and the difference between leno warp and standard warp are not evident. The widths of all plain samples are found lower than group C but higher than the other two groups.

The unit mass values of the samples varied between 109 and 130 g/sq.m. The results are shown in Fig.7. The positive effect of weft density on the fabric weight is clearly visible in the graphics. The effect of leno content is also apparent and it seems to have a tendency to increase the fabric mass. The higher values were obtained with the samples of group C (3:1 weave ratio). There is no clear effect of floating number and the difference between leno warp instead of standard. The widths of all plain samples are found lower than group C but higher than the other two groups. The variation between the samples of the same weft density are found low.

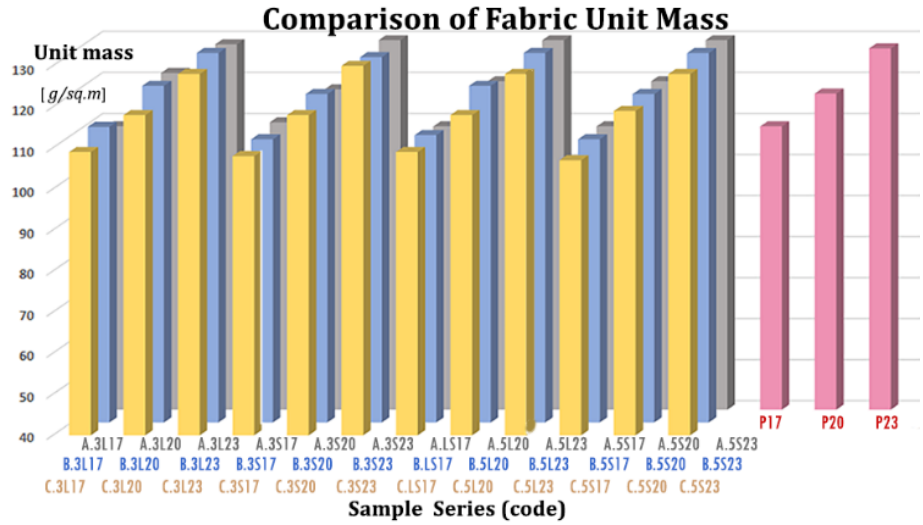

***Fig. 7**: Actual values of unit fabric mass for all the sample groups*

The warp and weft crimps for all the samples are displayed in Fig 8 and Fig.9 respectively. For the sake of measuring the direct affect of leno interlacing, the measurements in the hybrid fabrics were made on the basis of individual warp yarns. The average of a total of 10 measurements are presented. The warp crimp ratios for the all plain fabric were measured as 3,64%, 5,0% and 6,75% in succession for the increasing weft density. The range of crimp for leno and standard warp yarns only varied between 3,24% and 8,76 %. The highest values are measured with the 3 float leno warp construction for all the weft densities. The warp crimp rate of the 3 float leno warp was almost twice

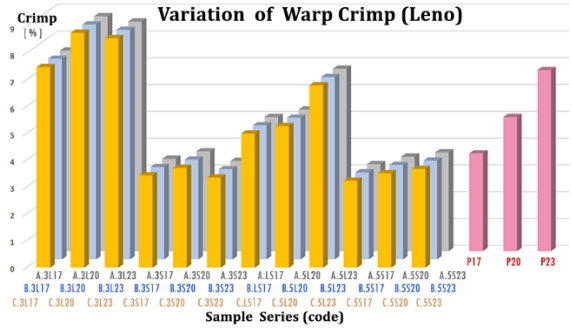

***Fig. 8**: Comparison of the warp crimp variation for leno and standard warps of all the samples*

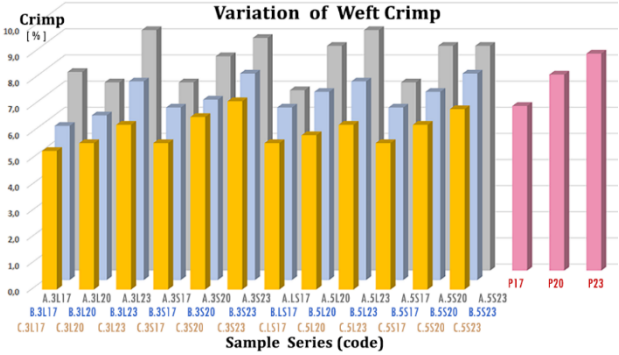

***Fig. 9**: Comparison of the weft crimp variation of all the fabric samples*

the crimp of the standard non-leno warp. The difference between 3 and 5 float is also apparent; the higher the float, the lower the warp crimp. In overall average, the group C fabric structure samples the crimp of the standard non-leno warp. The difference between 3 and 5 float is also apparent; the higher the float, the lower the warp crimp. In overall average, the group C fabric structure samples with the highest leno weave content provide the highest weft crimp for all the cases. The behaviour of the warp

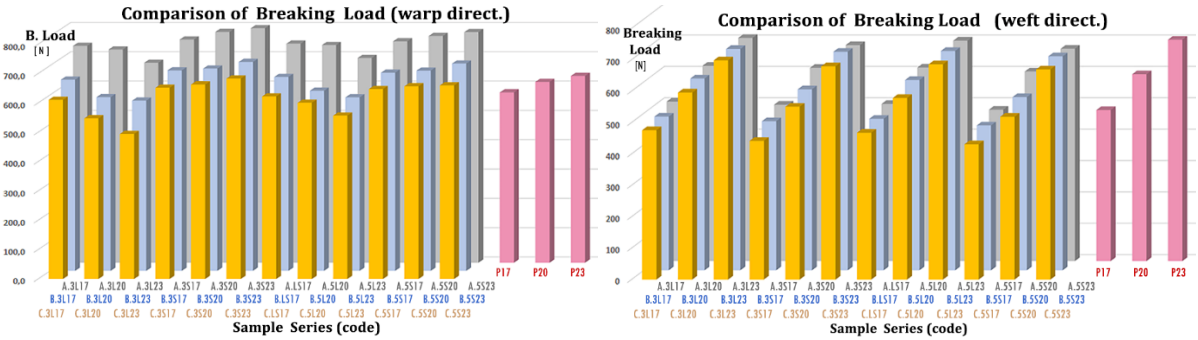

***Fig. 10**: Comparison of the breaking load of all the samples along the warp and weft directions*

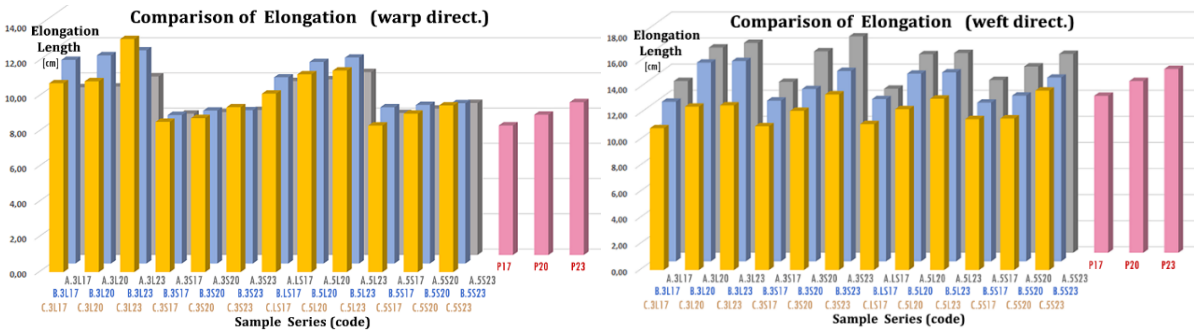

***Fig. 11**: Comparison of the breaking elongation of all the samples along the warp and weft directions*

The mechanical properties of the samples are also tested. The breaking load and breaking elongation of all the sample groups are graphically shown in Fig.10 and Fig.11 for the direction both warp and weft. The range of breaking load varied between 494,6 N and 799,35 N along the warp direction and between 430,9 N and 710,83 N along the weft direction. Despite higher densities of weft yarns, the breaking capacity along the warp yarn are found greater. That clearly shows the positive affect of leno weave integration in the fabric construction. Regarding the elongation, the min and max values are 7,34 cm and 13,23 cm along the warp direction and values are 10,9 cm and 16,58 cm along the weft yarns. The presence of leno warps tends to lower the warp crimp hence reduces the extension through this way. The affect of leno warp or the leno weave is much more apparent on the warp-way fabric strength than the weft way fabric strength. The increasing ratio of leno weave has a positive affect on the warp-way as seen in the first graphic of Fig.10. This affect is not clear for the weft-way strength unlike the positive effect of the weft density. One would expect that leno weave structure will show more rigidity along the warp-way than the weft-way as it was confirmed by these graphics.

The tearing resistance of the samples are also measured and the results recorded along the weft direction was given in Fig.12. Tearing tests along the warp direction was also carried out but failed to tear the fabric samples. The range of tearing force along the weft-way was measured between 10,2 N and 16,5 N. The effect of weft density on the resistance to tearing is very apparent as it increases with increasing weft density. This case is valid for all sample structure types. The effect of integration of the leno structure is not clear, but it seems that there is some inclination of increase in resistance to tearing with higher ratio of leno concentration. The presence of non-leno warp appears to impart a positive effect on the tearing resistance. In the case of floating number, it has a negative effect on the tearing strength since the interlacing and contact points are reduced by increasing float number. The effect of weft density on the tearing strength is also very apparent with reference to all plain samples of P17, P20 and P23.

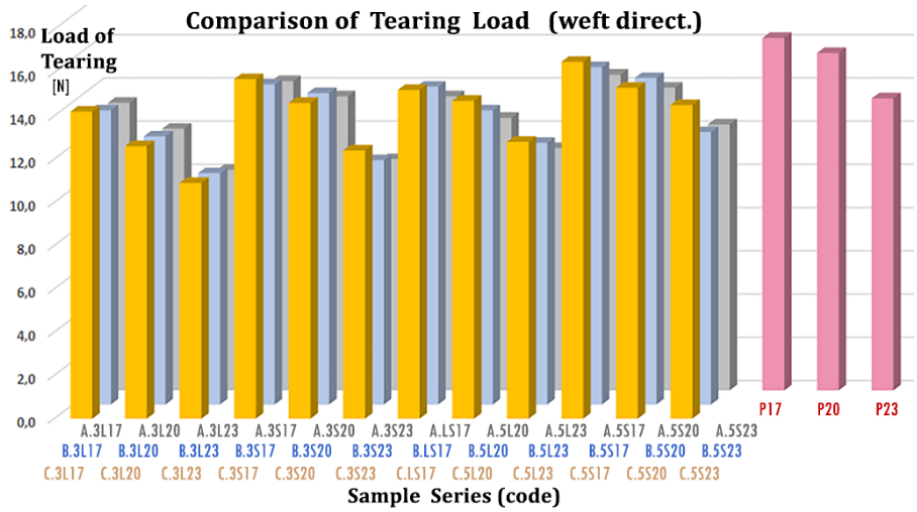

***Fig. 12**: Comparison of the tearing strength of all the samples along the weft direction*

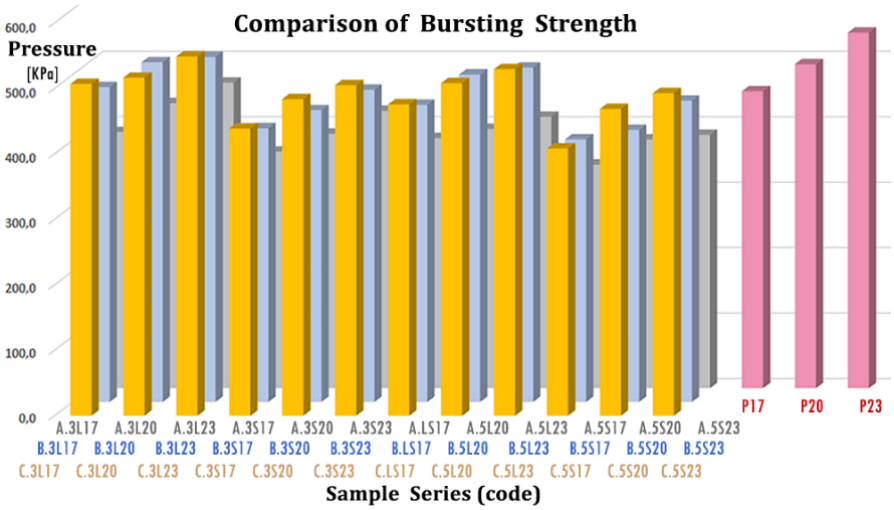

***Fig. 13**: Comparison of the bursting strength and pressure of all the samples*

The bursting measurements are for all the samples are shown in Fig.13. The range of bursting varied from 341,5 KPa to 548,8 Kpa. ailed to tear the fabric samples. The max. values are achieved by the samples with higher leno weave ratio. As expected, the presence of leno interlacing and extra contacts between yarns play an important role in improving the bursting pressure. Increases in the weft density also improves the toughness of the structure, unlike the float number which has a negative affect on the bursting reducing the interlacing and contact points.

5. CONCLUSION

The effect of leno weave in a hybrid fabric structure is analyzed with reference to the variables of weave arrangement, weft density, float number and leno warp connection. Among these variables, the effect of weft density appears the most decisive and also similar for both hybrid and the plain weave structures. The presence of leno weave is also visible on both structural and mechanical characteristics.

The difference between leno warp interlacing and standard non-leno interlacing are more apparent on the mechanical characteristics than the structural ones. In the determination of the breaking strength of the fabrics, it is observed that the breaking strength in the warp direction of the samples with 3 floats leno connections is lower than that of the samples with 5 leno float connections. In the case of non-leno interlacing, this situation was reverse. The breaking load of the 3 float standard non-leno construction is higher than that of the 5 float non leno. In other words, the presence of leno warps, increases the breaking strength with increasing float number, unlike the adoption of standard warp which reduces the strength as the number of float rises. It is observed that the integration of leno weave into the structure tends to improve the breaking resistance along the warp direction. As the weft density increases, the breaking strength in the weft way uniformly increases. In the case of bursting strength, the existence of leno interlacing in the construction tends to increase the bursting strength.

The current body of literature confirms that leno weave provides a unique combination of mechanical stability, permeability, and structural integrity. Its defining feature, the crossing of warp yarns, enhances inter-yarn friction and suppresses yarn slippage, leading to improved performance in tensile, puncture, and shear-related properties. Among all woven structures, only leno weave has this unique characteristic ensuring enhanced dimensional stability. It is known that the mechanical behaviour of woven fabrics is intrinsically governed by their structural architecture, where yarn interlacement, density, and material properties interact in complex ways.

In recent years, hybrid woven structures, combining leno with conventional weaves have gained attention for their ability to balance openness, stability, and mechanical performance. Recent advancements in multi-warp and hybrid leno structures demonstrate the potential for tailoring mechanical behaviour for specific applications [26], [27]. However, further systematic research is required to fully exploit the mechanical capabilities of leno fabrics, particularly in emerging areas such as hybrid structures, smart textiles, advanced composites. Typical technical applications are filtration systems, geotextiles, and composite reinforcements, where both structural integrity and permeability are required. It is believed that this study shall enable to quantify the effect of structural parameters on mechanical properties and provide design guidelines for hybrid leno fabrics.

ACKNOWLEDGEMENTS

We would like to acknowledge valuable contributions of Arsan Dokuma Boya San Tic A.Ş. for the preparation of samples and Denge Kimya AŞ from Çorlu for the conduction of tests.

REFERENCES

[1] I. Emery, ‘‘The primary structures of fabrics’’. Thames & Hudson. The Textile Museum Washington, D.C. 3rd Edition. 1994.

[2] J.E. Booth, ‘‘Principles of textile testing: An introduction to physical methods of testing textile fibres, yarns and fabrics’’. Heywood Books, London. 3rd Edition, 1968.

[3] P. Grosberg. “The Mechanical Properties of Woven Fabrics Part II: The Bending of Woven Fabrics”. *Text Res Journal*. 1966; 36: 205-211.

[4] I. R. Shekar et al., “Hybrid fabrics for structural composites,” J*ournal of Industrial Textiles*, vol. 41, no. 1, pp. 70–103, Jul. 2011, doi: 10.1177/1528083710396263.

[5] H. Iftekhar, M. Umair, S. T. A. Hamdani, S. M. Imran, M. S. Nazir, and Z. Ali, “Effect of Hybrid Weave Patterns on the Mechanical Performance of Woven Fabrics,” *Journal of Natural Fibers*, vol. 20, no. 1, pp. 1–14, 2023, doi: 10.1080/15440478.2022.2145411.

[6] I.C.S. Staff, *Leno Weaves*, 1st ed., vol. ICS 512. Scranton, Pennsylvania: International Textbook Co., 1905. [Online]. https://www2.cs.arizona.edu/patterns/weaving/monographs/ics512.pdf

[7] W. Watson, *Advanced Textile Design*. London: Longmans, Green and Co., 1913.

[8] D. Harper, "Origin and history of gauze," Online Etymology Dictionary. Accessed: Apr. 02, 2026. [Online]. Available: https://www.etymonline.com/word/gauze

[9] A.Roguin. "Gauze: Origin of the Word," *Journal of the American College of Surgeons* 233(3):pp. 494-495, September 2021. *DOI:* 10.1016/j.jamcollsurg.2021.05.026

[10] H.Z. Özek. "Tekstilde tasarım ve ürün geliştirme (LÜ-T.04)" *Postgrduate Course, Lecture Notes (unpublished)*. Namık Kemal University Garaduate School. 2017-18 Spring Term).

[11] Y. Chen, "Developments in leno-weave fabrics," in *Specialist Yarn and Fabric Structures*, R. H. Gong, Ed., Cambridge: Woodhead Publishing Lmt, 2011, ch. 6, pp. 118–140.

[12] Anonymous, "A touch of Dornier : DORNIER's EasyLeno Technology," Machine Leaflet, Lindauer DORNIER GmbH.

[13] B.B.Kastacı. "Leno Dokumaşların Yapısal Değişkenleri ile Fiziksel Özellikleri Arasındaki İlişkinin Araştırılması," MSc Thesis, Namık Kemal University, Graduate School of Natural and Applied Sciences 2016.

[14] A. Y. Ahmed, "Physical Properties of Leno Fabrics," Ph.D Thesis. University of Manchester Institute of Science and Tech. Manchester, 1972.

[15] A. Cetin and B. Guldemet, "Manufacturing Of Tubular Leno Fabrics By Modified Standard Sampling Loom," *Annals of the University of Oredea Fascicle of Textiles, Leatherwork*, vol. 19, no. 1, pp. 13–18, 2018.

[16] H. Doğu, "Leno Dokuma Sistemlerinin Analizi ve Tasarım Açısından Yeni Öneriler". MA Thesis, "570853" Mimar Sinan Fine Arts University, Textiles and fashion Dept. Istanbul. 2019.

[17] Y. Akelma ."Döner Gücü Sistemi ve Eğitim Amaçlı Armürlü Dokuma Tezgahlarına Uyarlanabilirliği"., Gazi Üniversitesi Eğitim Bilimleri Enstitüsü, Yüksek Lisans Tezi Ankara. 2007

[18] N.Redmore. "Embracing nature and the fragility of design. An investigation into outdoor seating materials through the practice of leno weaving. University of Huddersfield. Master thesis, Huddersfield, June 2014.

[19] L. Ge. "Novel Woven Structure Design for Polymeric Optical Fiber (POF) Textiles" The Hong Kong Polytechnic University Institute of Textiles and Clothing, Ph.D thesis, August 2020.

[20] Anonymous, "A touch of Dornier : DORNIER's EasyLeno Technology," Lindauer DORNIER GmbH. Accessed: Apr. 02, 2026. [Online]. Available: https://www.manich-ylla.com/Documentos/DORNIER_Telar%20de%20gasa%20de%20vuelta%20EasyLeno_E.pdf

[21] K. Shaker, Y. Nawab, M. Ayub Asghar, A. Nasreen, and M. Jabbar, "Tailoring the properties of leno woven fabrics by varying the structure," *Mechanics of Advanced Materials and Structures*, vol. 27, no. 22, pp. 1865–1872, Nov. 2020, doi: 10.1080/15376494.2018.1527964.

[22] X. Tian, M. Yao, Y. Li, and L. Li, "Design and fabrication of mesh-like four-warp leno cotton fabric based on self-locking effect: outstanding mechanical performance and breathability," *Cellulose*, vol. 32, no. 3, pp. 1979–1991, Feb. 2025, doi: 10.1007/s10570-024-06365-y.

[23] M. H. Kashani, A. Hosseini, F. Sassani, F. K. Ko & A. S. Milani. "The Role of Intra-Yarn Shear in Integrated Multi-Scale Deformation Analyses of Woven Fabrics: A Critical Review", Critical Reviews in Solid State and Materials Sciences, 43:3, 2018, pp.213-232.

[24] H. Pan, J. Liu, J. Xie, Z. Feng. "A review on the yarn pull-out behavior of high-performance woven fabrics for impact resistance," Composites Part C: Open Access, Volume 18, 2025, 100658. https://doi.org/10.1016/j.jcomc.2025.100658.

[25] Rampini, M.C.; Zani, G.; Schouler, L.; Colombo, M.; di Prisco, M. Effect of Textile Characteristics on the AR-Glass Fabric Efficiency. *Textiles* **2021**, *1*, 387-404.

[26] Xu, Z. Li, H. Zhu, and H. Shi, "Geometric modeling and simulation for leno fabrics," *J. of Engineered Fibers and Fabrics*, vol. 19, pp.1–19, Jan. 2024, doi: 10.1177/15589250241291198.

[27] P. Preinstorfer, P., M. El Kadi, G. Dittel, *et al.* "Article of RILEM TC 292-MCC: bond behaviour of textile-reinforced concrete—a review". *Mater Structure* **57**, 97. 2024.

ANNALS OF THE UNIVERSITY OF ORADEA
FASCICLE OF TEXTILES, LEATHERWORK

STUDY OF THE CONDUCTIVITY AND RESISTIVITY OF CONDUCTIVE YARN

LÓPEZ-RODRÍGUEZDaniel[1*], DÍAZ-GARCÍAPablo[2], BONET-ARACIL Marilés[2], BOU-BELDA Eva[2]

[1]Departamento de Matemática Aplicada, Universitat Politècnica de València, Plaza Ferrándiz y Carbonell s/n, Alcoi, Spain, Email: pdiazga@txp.upv.es, maboar@txp.upv.es, evboble@upvnet.upv.es

[2]Departamento de Ingeniería Textil y Papelera, Universitat Politècnica de València, Plaza Ferrándiz y Carbonell s/n, Alcoi, Spain

Corresponding author: Daniel López-Rodríguez, E-mail: dalorod@upv.es

Abstract: *The new epoch of the textile industry is very focused on the development of smart textiles, which provide added value to conventional textiles and break into the market with more impact. For this work, a characterization study has been carried out on several samples of textile yarns with conductive properties. The yarns studied are from the manufacturer Bekintex and the samples studied are referenced as Bekinox VN 14/1x90/100z, Bekinox VN 15/1x90 and Bekinox VN 8/1x275. Representative resistivity values in the order of* 10^{-6} *and* 10^{-7} *(for example,* $1.0239 \cdot 10^{-6}$ *and* $3.2569 \cdot 10^{-7}$*) have been obtained; these very small values confirm that the fibers are good electrical conductors, while the variation between samples indicates that yarn structure, filament diameter and test configuration influence electrical behavior. In order to carry out the appropriate measurements, an assembly was made with two multimeters and a power supply, in order to vary the voltage and record the intensity and resistance at the same time. Depending on the different conductive characteristics of each filament, we can use them for smart textiles that require little resistivity to be able to feed some element or more resistivity to be able to use them as thermal emitters. This electrical selection also defines the possible contribution of the yarn to textile thermal comfort, either as a low-loss conductive path or as a localized Joule-heating element. The Q of the Joule effect was also calculated to assess the thermal emission of the same yarns.*

Key words: *metallic yarn, conductive yarn, smart textile*

1. INTRODUCTION

The economic experts of the textile world present smart textiles as the next generation of fibers, fabrics and articles to be produced thanks to their enormous possibilities and functionalities. They can be described as textile materials that think for themselves, for example, through the incorporation of electronic devices or intelligent materials. Many smart fabrics are already used in advanced types of clothing, mainly for protective and safety garments, although concepts of fashion, comfort and innovation are being successfully embraced [1–4].

One of the main reasons for the rapid development of smart textiles is the significant

investment made by the military industry [5–8]. This is because they are used in various projects such as winter jackets for extreme temperature conditions or uniforms that change color to improve camouflage effects.

Smart textiles provide evidence of the potential and enormous opportunities that can still be realized in the textile industry, in fashion or design, as well as in the technical textiles sector. On the other hand, these advances are the result of active collaboration between people from different disciplines: engineering, science, design, process development, business and marketing. Our daily life, in the coming years, will be significantly regulated by smart devices and many of these devices will be integrated into garments or different textile substrates.

There are two ways to develop electrical and/or thermal conductive fabrics, just as there are two types of materials, metals and polymers, that provide these properties. The same materials could be used for both conductivities (thermal and electrical). Indeed, both processes are similar and result from electronic agitation/conduction [9].

The first way uses finishes (pigments and print pastes) with a high metallic content but still retaining the flexibility required for clothing. From the addition of layers of nickel, copper, silver or carbon of various thicknesses, these finishes provide a versatile combination of physical and electrical characteristics that cover a wide variety of use demands. The second way consists of the direct use of conductive threads. The thread can be made up of a traditional base (cotton, wool, PES, etc.) and a metal core such as silver, copper, etc. or conductive polymer such as polythiophene [10], polyaniline, polyacetylene [11] and its derivatives.

Although there are many different brand names that market these materials, they all have the same main characteristics. They are light, durable, flexible and competitive and can be pressed, welded and integrated into the textile process. Although, as has been described, the use of smart textiles can be very diverse and different, in this work the research focuses on initial studies and characterization of certain filaments to achieve textiles with thermoregulable properties [12].

On the planet, many people are living and working in extremely cold places, so they require accessories or elements that allow them to maintain or increase the temperature of their body and their outerwear. A clear example of this type of need is that of the military or the traffic police. But common textiles made of cotton, synthetic fibers try to provide warmth by reducing heat loss that occurs through convection and conduction. What these types of garments do is trap the air between the layers of the textile article and thanks to the heat emitted by the human body, that air heats up and by reducing the loss of that heat it keeps the body warmer. In this way the classic method to keep warm is to wear more clothes, it has been proposed as an idea of "personal thermal management" as an efficient way of saving based on the idea of keeping the human body warm [13]. Many researchers seek to develop a textile that has integrated systems capable of responding to the variation of the external temperature, achieving another method to the classic described, thus managing to develop an effective method to obtain thermoregulable intelligent textiles [14], [15].

2. MATERIALS AND METHODS

In the first place will be carry out measurements on the independent metallic filaments, before their manipulations with other more conventional yarns. For this will be used the setup described above. First evaluation of the electrical conductivity was made. From here will come the material or materials that we will manipulate in a winder, to obtain the composite yarns that we will use in the weaving of the final textile.

Metallic yarns: Several samples of metallic yarns are used, one of a copper/tin alloy and several samples of steel provided by a producer of this type of yarn (Bekintex), these were Bekinox

VN 14/1x90/100z, Bekinox VN 15 /1x90 and Bekinox VN 8/1x275.

This study focuses on the characterization of the filaments, specifically on the conductive characteristics, which are what will give the textile development these differentiating characteristics. There are some magnitudes that will give information about the behavior of the material, these are the intensity (I) measured in amperes (A), the voltage measured in volts (V), the electrical resistance, measured in ohms (Ω) and resistivity (ρ) [16]. To record these measurements, a power supply and two multimeters are mounted in series (Image 1), to simultaneously record the current and voltage measurements, subsequently calculating the resistance.

The electrical measurements were performed under controlled laboratory conditions, with the yarns conditioned for 24 h before testing at 20 ± 2 ºC and 65 ± 4% relative humidity. Each sample was tested in dry state on an insulating support, the effective length between clamps was kept constant for each test, and the same multimeter/power-supply arrangement and contact points were used to reduce variation due to contact resistance.

***Fig. 1**: Multimeter and power supply*

The thermal emission of heat that the yarns will give off by the Joule [17], [18] effect will also be quantified. This effect is defined as the amount of heat energy produced by an electric current, which depends directly on the square of the intensity (I) of the current, the time in mintus (t) that it circulates through the conductor and the resistance (R) that opposes it to the flow of current. Mathematically it is expressed with equation 1 shown below.

$$Q = I^2 \cdot \mathrm{R} \cdot \mathrm{t} \quad \textbf{(1)}$$

After the conductivity tests carried out, heat radiation tests are carried out by the joule effect. For this, different samples of filament are taken, and with the same assembly described above in which its resistivity is measured, a controlled electrical intensity is passed through, and the heat released is recorded. In order to measure this thermal emission, the filament is introduced into a container with ultra pure water (so that it does not interfere with conductivity) and the variation in water temperature is controlled in constant periods of time.

The Joule-effect tests were carried out in the same laboratory atmosphere. A 200 ml volume of ultrapure water was used for each test, with an initial temperature close to 24.6 ºC, and the

temperature increase was recorded at five-minute intervals to compare the heating behavior of the different yarns.

3. RESULTS AND DISCUSSSION

For each of the metallic yarns, several measurements of voltage and intensity were made and their resistivity was calculated (Tables 1-3), obtaining the corresponding formulas of said straight lines that can be extrapolated to other results that are desired to be calculated theoretically.

Values such as $1.0239 \cdot 10^{-6}$ and $3.2569 \cdot 10^{-7}$ represent very small resistivity values and therefore confirm that the tested fibers are good conductors of electricity. Nevertheless, the results are not identical for all samples: the observed variation is consistent with differences in filament diameter, yarn structure, sample length and contact conditions. Consequently, yarn selection must be linked to the final function of the smart textile, distinguishing between efficient electrical transmission and controlled resistive heating.

***Table 1**: Bekinox VN 14/1X90/100Z*

V	I	R	D (cm)	L (cm)	ρ
7.76	0.152	51.0526316	0.0014	66.4	$1.1835 \cdot 10^{-6}$
4.83	0.0986	48.9858012	0.0014	66.4	$1.1356 \cdot 10^{-6}$
9.89	0.1994	49.5987964	0.0014	66.4	$1.1498 \cdot 10^{-6}$
14.19	0.28	50.6785714	0.0014	66.4	$1.1749 \cdot 10^{-6}$
16.78	0.33	50.8484848	0.0014	66.4	$1.1788 \cdot 10^{-6}$
22.8	0.46	49.5652174	0.0014	66.4	$1.1490 \cdot 10^{-6}$
32.1	0.63	50.9523811	0.0014	66.4	$1.1812 \cdot 10^{-6}$

***Table 2**: Bekinox VN 15/1X90*

V	I	R	D (cm)	L (cm)	ρ
8.7	0.0818	106.356968	0.0014	159.9	$1.0239 \cdot 10^{-6}$
12.9	0.12	107.501145	0.0014	159.9	$1.0349 \cdot 10^{-6}$
16.9	0.1568	107.780612	0.0014	159.9	$1.0376 \cdot 10^{-6}$
20.8	0.1916	108.559499	0.0014	159.9	$1.0451 \cdot 10^{-6}$
24	0.21	114.285714	0.0014	159.9	$1.1002 \cdot 10^{-6}$
31.8	0.28	113.571429	0.0014	159.9	$1.0934 \cdot 10^{-6}$

***Table 3**: Bekinox VN 8/1X275*

V	I	R	D (cm)	L (cm)	ρ
2.73	0.0374	72.9946524	0.0008	116	$3.1630 \cdot 10^{-7}$
7.98	0.108	73.8888889	0.0008	116	$3.2018 \cdot 10^{-7}$
11.6	0.1576	73.6040609	0.0008	116	$3.1894 \cdot 10^{-7}$
14.33	0.1937	73.980382	0.0008	116	$3.2057 \cdot 10^{-7}$
18.06	0.24	75.2511056	0.0008	116	$3.2608 \cdot 10^{-7}$
23.3	0.31	75.1612903	0.0008	116	$3.2569 \cdot 10^{-7}$
30.5	0.42	72.6190476	0.0008	116	$3.1468 \cdot 10^{-7}$

On the one hand we see the values obtained for thermal emission for voltage values (V) of 30 v. and a time of 60 seconds, with which the values calculated and shown in table 4 are obtained.

***Table 4**: Thermal emission Joule Effect for each sample*

Sample	Voltage	Time (s.)	Q (Joule)
Bekinox VN 14/1X90/100Z	30	60	719.39
Bekinox VN 15/1X90	30	60	787.28
Bekinox VN 8/1X275	30	60	850.89

Finally, the thermal variation that occurs in the 200 ml of water in which each sample is immersed and the temperature variation that it experiences over time are shown. The results of each sample can be seen in table 5.

***Table 5**: Thermal variaton*

	Bekinox VN 14		Bekinox VN 15		Bekinox VN 8	
t (min.)	Water ºC	Increase ºC	Water ºC	t (min.)	Water ºC	Increase ºC
0	24.6	0	24.6	0	24.6	0
5	25.6	1	25.6	5	25.6	1
10	27.4	2.8	27.4	10	27.4	2.8
15	28.7	4.1	28.7	15	28.7	4.1
20	29.9	5.3	29.9	20	29.9	5.3
25	30.7	6.1	30.7	25	30.7	6.1
30	32	7.4	32	30	32	7.4
35	32.4	7.8	32.4	35	32.4	7.8
40	33	8.4	33	40	33	8.4
45	33.7	9.1	33.7	45	33.7	9.1

4. CONCLUSION

In view of the results, it can be concluded that the yarns studied are optimal to be used in the development of intelligent textiles, since they have a conductivity and resistivity that will allow them to provide possibilities to the fabrics. In cases where a yarn with higher resistivity and less conductivity is needed, the Bekinox VN 15/1X90 type could be used, which would be useful for using the Joule effect to increase the temperature of the fabric [19], [20]. If the objective is to conduct electricity to power an element, we should use one with a lower resistivity such as the Bekinox VN 8/1X275. Therefore, it is observed that in the market there are different possibilities of yarns depending on the needs to be satisfied. In view of the results of the Joule effect and that a sample of 200 ml of water can increase by up to 9 ºC, they are filaments that can be used to build fabrics that have thermal characteristics or that the increase in temperature can produce certain changes in the textile, as could be in the use of thermochromic dyes. From the perspective of thermal comfort, the higher-resistivity yarns can be deployed as distributed heating elements in selected areas of a garment, while the lower-resistivity yarns can be used as conductive tracks to supply power to sensors, controllers or heating zones. This combination would allow the textile to regulate the local microclimate close to the body, compensate for heat losses in cold environments and reduce the need for bulky insulating layers, improving comfort and wearer mobility.

5. REFERENCES

[1] S. Schneegass and O. Amft, *Smart textiles*. Springer, 2017.

[2] S. Mondal, "Phase change materials for smart textiles–An overview," *Appl. Therm. Eng.*, vol. 28, no. 11–12, pp. 1536–1550, 2008.

[3] G. Chen, Y. Li, M. Bick, and J. Chen, "Smart textiles for electricity generation," *Chem. Rev.*, vol. 120, no. 8, pp. 3668–3720, 2020.

[4] K. Cherenack and L. Van Pieterson, "Smart textiles: Challenges and opportunities," *J. Appl. Phys.*, vol. 112, no. 9, p. 91301, 2012.

[5] L. Affatato and C. Carfagna, "Smart Textiles: a strategic perspective of textile industry," in *Advances in Science and Technology*, 2013, vol. 80, pp. 1–6.

[6] H. Ramlow, K. L. Andrade, and A. P. S. Immich, "Smart textiles: An overview of recent progress on chromic textiles," *J. Text. Inst.*, vol. 112, no. 1, pp. 152–171, 2021.

[7] G. K. Stylios, "SMART textiles special issue," *Transactions of the Institute of Measurement and Control*, vol. 29, no. 3–4. Sage Publications Sage UK: London, England, pp. 213–214, 2007.

[8] M. D. Syduzzaman, S. U. Patwary, K. Farhana, and S. Ahmed, "Smart textiles and nano-technology: a general overview," *J. Text. Sci. Eng*, vol. 5, no. 1, 2015.

[9] H. Gómez, M. K. Ram, F. Alvi, P. Villalba, E. L. Stefanakos, and A. Kumar, "Graphene-conducting polymer nanocomposite as novel electrode for supercapacitors," *J. Power Sources*, vol. 196, no. 8, pp. 4102–4108, 2011.

[10] H. L. Wang, L. Toppare, and J. E. Fernandez, "Conducting polymer blends: polythiophene and polypyrrole blends with polystyrene and poly (bisphenol A carbonate)," *Macromolecules*, vol. 23, no. 4, pp. 1053–1059, 1990.

[11] S. Etemad and A. J. Heeger, "Polyacetylene,(CH) x: The prototype conducting polymer," *Annu. Rev. Phys. Chem.*, vol. 33, no. 1, pp. 443–469, 1982.

[12] Y. Fang, G. Chen, M. Bick, and J. Chen, "Smart textiles for personalized thermoregulation," *Chem. Soc. Rev.*, 2021.

[13] Y. Lu *et al.*, "Achieving multifunctional smart textile with long afterglow and thermo-regulation via coaxial electrospinning," *J. Alloys Compd.*, vol. 812, p. 152144, 2020.

[14] G. G. D. Han, H. Li, and J. C. Grossman, "Optically-controlled long-term storage and release of thermal energy in phase-change materials," *Nat. Commun.*, vol. 8, no. 1, pp. 1–10, 2017.

[15] Y. Cui, H. Gong, Y. Wang, D. Li, and H. Bai, "A thermally insulating textile inspired by polar bear hair," *Adv. Mater.*, vol. 30, no. 14, p. 1706807, 2018.

[16] A. A. Antonov, "Ohm's law is the general law of exact sciences," *PONTE Int. J. Sci. Res.*, vol. 72, no. 7, 2016.

[17] S. Castiñeira Ibáñez and D. Tarrazó Serrano, "Descarga de un condensador a través de una resistencia. Efecto Joule," 2020.

[18] M. Herrejón Escutia, "Modelación matemática de la evolución térmica y microestructural del calentamiento continuo por efecto Joule," 2019.

[19] J. Orellana, I. Moreno-Villoslada, R. K. Bose, F. Picchioni, M. E. Flores, and R. Araya-Hermosilla, "Self-healing polymer nanocomposite materials by Joule effect," *Polymers (Basel).*, vol. 13, no. 4, p. 649, 2021.

[20] A. Nicolaÿ *et al.*, "Influence of Joule Effect Heating on Recrystallization Phenomena in Inconel 718," *Metall. Mater. Trans. A*, vol. 52, no. 10, pp. 4572–4596, 2021.

ANNALS OF THE UNIVERSITY OF ORADEA
FASCICLE OF TEXTILES, LEATHERWORK

PSYCHOPHYSICAL RESPONSES TO TEXTILE MECHANICAL PROPERTIES: A NEURO-MECHANISTIC APPROACH TO FABRIC-HUMAN INTERACTION

PATZLAFF Airton Carlos[1], PATZLAFF Priscila Maria Gregolin[2]

[1, 2] Federal University of Technology, Paraná, Pato Branco, Brazil

Corresponding author: Patzlaff, Airton, E-mail: airtonpatz@gmail.com

Abstract: *This manuscript establishes a comprehensive and empirically grounded framework for the Psychophysics of Style, creating a transdisciplinary bridge between the material engineering of textiles and the neurobiology of human cognition. Situated within the contemporary crisis of the attention economy and the increasing dematerialization of the self into digital constructs, this research posits that the act of dressing is not merely a sociocultural signaling mechanism but a fundamental psychophysical interface that regulates emotional stability, cognitive processing, and ontological coherence. We argue that the materiality of clothing serves as critical ontological ballast, counteracting the fragmentation of the digital age through quantifiable mechanical inputs. By synthesizing Kansei Engineering and advanced tactile neurobiology, this approach moves from the metaphorical to the measurable. We incorporate verified empirical data, including the identification of a precise texture recognition threshold of 45.4μm that demarcates the transition from passive to active neural processing. Furthermore, the study demonstrates that fabric volume modulates Electroencephalography (EEG) Alpha bands, validating that textile substantivity impacts cognitive orientation. Such biological findings were corroborated with Life Cycle Assessments to prove the validity of natural fibers over synthetic materials in this case. Therefore, these results set out the basis of Sustainable Enclothed Cognition with a proposition that added mechanical strength and moral mass of natural textiles are a sufficient counterpoint in this way to sustain human awareness in such a fluid digital culture.*

Keywords: *Enclothed Cognition, Neuroaesthetics, Kansei Engineering, Tactile Neurobiology, KES-FB.*

1. INTRODUCTION

The sociocultural and psychological environment of the present era is marked by a deep paradox: the hyper-visibility of superficial aspects coexists with a fundamental emptiness of internal experience [1]. This era sees the unprecedented projection of the image of the individual, at the same time as the experience of subjectivity itself appears ever more precarious. By means of the mediations of digital social media, the subject of humanity is reproduced in digital form, creating a milieu in which the subject experiences itself reflected and offered as a minutely articulated digital projection.

We exist within an increasingly digitized society that has evolved into an assertive attention economy, a system in which human attention constitutes the primary commodity for which algorithmic entities contend [2].

In this context, described as surveillance capitalism, the management of self-presentation has emerged as the principal currency of social interaction, and identity is progressively transformed into an ongoing design endeavor, continuously optimized based on engagement metrics [3].

Such a marked transition into a digital reality leaves a sensory gap that a human nervous system is never designed to cope with. A study of human evolution shows how cognitive functions have a fundamentally embodied nature in which our conception of reality is constructed through our bodily experiences. With a newfound mode of self-expression in digital pixels that do not have any mass or resistance in space, our proprioceptive loops, which are meant to confirm our reality in space, therefore go out of function because our brains simply lack a sufficient level of ontological friction.

To properly apprehend the profound implications of this ontological dilemma, it is imperative to distinguish human volition from the results produced by algorithms. Indeed, recent scholarly inquiry contends that while Artificial Intelligence can replicate creative endeavors, it fundamentally lacks the authentic essence characteristic of human expression [4].

Furthermore, the disintegration of personal identity is a reflection of a deeper neurological reality rather than just a social phenomenon. In this context, tangible belongings, which were formerly essential pillars of one's identity, have gradually evolved into ephemeral digital data stored in interconnected networks.

As a result, the collaborative formation of selfhood is increasingly mediated by abstract computational processes rather than by tangible physical artifacts, leading to a precarious understanding of reality [5, 6]. As a result, there is a kind of existential unmooring; the individual psyche struggles to define its own boundaries because it is deprived of the physical world's tangible resistance and engagement.

Within this context of dematerialization and pervasive digital influence, textile artistry and the practice of adorning the physical body emerge as a crucial locus of ontological resistance. As Sturza [7] argues, the intersection between text and textile has historically shaped human individuality, serving as a palpable language of identity. Clothing is reconceptualized here not as a trivial endeavor, but as the foremost interface where the internal self navigates its manifestation in the external world.

From the vantage point of textile engineering and psychophysics, this interface constitutes the microclimate situated between the skin and the fabric, a region where physiological regulation converges with psychological perception. This paper proposes that the congruence between an individual's internal state and its visible material expression constitutes an essential requirement for psychological well-being.

The idea of Ontological Ballast is proposed to clarify the nature of resistance, texture, and mechanical hysteresis provided by fabric in order to allow the psyche to interact with and understand its surroundings. The idea proposes that in a digitalized society where the external environment is increasingly virtualized, the clothes worn on the body are an essential protection mechanism for ontological security. Therefore, the primary objective of this research is to validate a neuro-mechanistic framework for the 'Psychophysics of Style,' demonstrating how quantifiable textile mechanical properties directly regulate cognitive processing and emotional stability.

2. GENERAL INFORMATION

The establishment of a shared understanding of the Psychophysical aspects of Style demands that much existing scholarship in three totally different fields (affective engineering, or Kansei Engineering; neurobiology which underpins tactile impressions, and Enclothed Cognition, where psychological dynamism and clothing meet) has to be reviewed.

In the past, conventional textile engineering paid more attention to quantifiable indices like tensile strength and wear resistance. Although these indices are essential for the working life of a

garment or some other product, they often do not take into account the human experience. This is where Kansei Engineering comes in. Kansei engineering is an approach to technological innovation which focusses on the user, and aims at converting qualitative attributes marked out by consumers into objective, quantifiable physico-chemical features of materials [8].

This technique is nowadays successfully employed in parts of consumer electronics, motor vehicles and daily necessities. It has expanded from a primarily engineering-based means of qualitative differentiation to one which also takes account of neurophysiological data - specifically via Electroencephalography (EEG) - in order to avoid subjectively verbalized descriptions, and so establishes a direct relationship between physical stimulation and neurophysiological response.

Concurrently with the study of affective engineering is the neurobiological examination of the skin interface. The integumentary system serves as the primary interface between an organism and its external environment, featuring an elaborate system of sensory structures that transmit tactile information through both pathways for detailed perception and pathways for emotional response [9].

The discriminative pathway, facilitated by rapidly conducting nerve fibers, enables the identification of texture and spatial location of an object, utilizing Pacinian corpuscles to perceive high-frequency vibrations indicative of subtle textures [10].

Recent research has identified subtle points involving neural processing, moving beyond the mere reception of stimuli toward active interpretation [11]. In contrast, the affective pathway is mediated by slowly conducting C-tactile afferents, mainly in hairy skin, which respond to the velocity of gentle touch and transmit signals to brain regions associated with emotion, contributing significantly to interoceptive body awareness and to emotional regulation [12]. This system evolved to convey signals of social safety and bonding.

The third foundational element is the theory of Enclothed Cognition, which suggests that clothing's impact on an individual stems from the simultaneous presence of its symbolic significance and the tangible experience of wearing it [13].

While initial investigations encountered questions concerning reproducibility, more recent meta-analytic reviews, employing Z-curve analysis, have substantiated the robust and significant impact of attire on cognitive processes, contingent upon the congruence of symbolic and physical elements [14]. This corroboration permits the consideration of Enclothed Cognition as a dependable parameter for design. Moreover, the effectiveness of such psychophysical interventions relies on ethical consistency, herein termed Sustainable Enclothed Cognition [15].

An individual's awareness of a garment's ecological footprint can impose a cognitive burden; consequently, accurate environmental information, derived from refined Life Cycle Assessments, is vital to harmonize the wearer's tactile perception with their ethical principles [16].

Consequently, to operationalize this theoretical convergence, this research addresses four specific tasks: 1) The objective quantification of subjective tactile sensations using the KES-FB system; 2) The determination of specific neural thresholds for texture recognition using EEG; 3) The verification of fabric volume's impact on cognitive vigilance via Alpha wave modulation; and 4) The validation of environmental sustainability through corrected Life Cycle Assessments (LCA) to ensure ethical consistency in the proposed framework.

3. MATERIAL AND METHOD

To establish a robust theoretical framework for the Psychophysics of Style, this investigation employed a multidisciplinary theoretical approach synthesizing empirical data. This methodology linked measurable material attributes to neurological activity and established psychological constructs. A primary obstacle in the domain of affective engineering pertains to the objective

quantification of the intrinsically subjective tactile experience of textile materials. For this reason, data derived from an extensive and diverse assortment of fabrics from commercial sources (spanning lightweight silk to heavyweight tweeds) were analyzed using the Kawabata Evaluation System for Fabrics (KES-FB) to evaluate the physical properties of fabrics (via 10 mechanical properties) [17]. By breaking down the way people perceive the feel of fabrics into ten measurable physical properties (resistance to shear; flexure stiffness; compressive force; surface texture), through the process of the KES-FB system, researchers were able to define the physical characteristics of each of the fabrics analyzed as independent variables in their study.

To establish a link between these mechanical properties and neurological conditions, we analyzed data from neurophysiological studies, specifically those involving 40 healthy participants. The initial phase of the analyzed protocols investigated the perceptual threshold for texture recognition, employing electroencephalography (EEG) event-related potentials. Subjects were exposed to surfaces exhibiting incrementally increasing geometric irregularity while EEG data were acquired to observe the P300 component, an established indicator of cognitive resource allocation [11].

The next step was to see how the thickness of clothing affects how alert people are. This was done by looking at the brain waves of people wearing clothes of thickness and weight. The brain waves that were looked at were the Alpha waves. When these Alpha waves were not as strong it meant that the brain was working harder and people were more aware of what was going on around them [18].

Lastly, to substantiate the framework of Sustainable Enclothed Cognition, the ecological footprint of the selected fabrics was reassessed employing Life Cycle Assessment with expanded system boundaries (cradle-to-grave). This analysis drew upon the 2025 Ecoinvent database and specialized data pertaining to wool processing to mitigate historical prejudices against natural materials, thereby enabling a direct comparison of the true environmental cost of natural versus synthetic fibers, extending beyond the manufacturing stage [16].

The statistical credibility of the psychological premises was further strengthened through a Z-curve analysis of extant research on Enclothed Cognition, thereby confirming the solidity of the theoretical underpinnings.

4. EMPIRICAL RESULTS AND PHYSIOLOGICAL ANALYSIS

The studies discussed in this study demonstrate an integration of mechanical, neural, and meta-analysis evidence to significantly validate the psychophysical principles pursued in this research. This represents evidence that all of the material characteristics were consistently associated with correspondingly patterned brain activity. Another critical finding from neurophysiological studies is the exact sensory threshold for tactile recognition of textures, which has been identified at a level of 45.4 μM [11].

Surfaces with a tactile texture that measures less than the noted amount elicited very little change in the P300 event-related potential, which suggested that the neural mechanism which generates this potential, which is thought of as a passive mechanism, passes or screens out smooth tactile stimulation and treats it as background information, or ambient, and does not pay attention to it. Conversely, once surface roughness surpassed this 45.4-micrometer threshold, a statistically significant elevation in P300 amplitude was consistently observed [11].

This qualitative shift signifies a change from spatial to vibrational encoding of sensory data. At this point, friction produces complex signals that stimulate Pacinian corpuscles, thereby activating the somatosensory cortex and eliciting an orienting response.

Moreover, analysis of the EEG Alpha wave revealed a strong inverse relation between the overall volume of fabric and the power of Alpha waves [18, 19]. The presence of thick and compression-resistant fabrics resulted in a substantial decrease in Alpha wave activity. Since Alpha attenuation is a proxy for active cerebral processing, this suggests that heavy and massive fabrics produce a proprioceptive requirement, demanding continuous neuronal activation. Additionally, the employment of deep pressure stimulation, delivered via substantial clothing, was validated as a mechanism to reorient autonomic nervous system activity toward parasympathetic dominance, alleviating anxiety while preserving attentiveness [20].

Regarding the validity of the cognitive impact, meta-analytic validation employing Z-curve analysis confirmed the genuine and reproducible impact of clothing on cognitive processes, specifically when there is alignment between a garment's symbolic meaning and its physical experience. Finally, new data for Life Cycle Assessment (LCA) showed that natural fibers like wool often have a superior environmental performance compared with synthetic fibers when the use phase and biodegradability are taken into account [21].

4.1. Theoretical Implications: The Psychophysics of Style

Drawing upon the physiological data presented herein, we put forth a theoretical framework for elucidating these observed mechanisms. By engaging in physical contact with materials that exhibit a certain level of roughness (>45.4um) by using our sense of touch, we can derive a physiological basis for the personality construct known as a "Grounded Realist." Furthermore, it is hypothesized based on these results that the act of touching coarse textures provides a tangible/physical connection that mitigates the feelings associated with being digitally disengaged [22].

Similarly, we interpret the modulation of Alpha waves described in the results as evidence of "Ontological Ballast". We posit that the proprioceptive load of heavier fabrics achieves a sense of embodied alertness, whereas light, low-density fabrics - common in fast production - may contribute to a sense of disembodiment due to the lack of this neural feedback.

Therefore, the implication of the complex interaction amongst these mechanical factors is that cloth not only overlays the body, it also translates mechanical constraints into psychological affordances. The linkage between precise parameters of KES-FB, such as shear stiffness, mechanical hysteresis, and surface friction, and particular neurophysiological states enables a direct translation of the somatic topography of the cloth onto the cognitive demands of the wearer, thereby illustrating that particular patterns of weight, resistance, and rigidity do not work independently; instead, they constitute a unitary somatic language that is deciphered by the nervous system to communicate a particular way of existing within the world.

From a neuro-mechanistic point of view, these psychological phenotypes outlined within this text are more than arbitrary designations with aesthetical merit – rather, they represent a necessary cognitive architecture for this particular era. Each type remedies a particular inadequacy in the digital age: a hard edge for a boundless zone on the web, a comforting touch in a distant age, or a sudden sensual friction necessary for a drift toward the virtual. It is a corrective mechanism that enables a specific type or quality of physical friction that allows for allostatic regulation on a psyche.

For this relationship to be harnessed effectively in engineering and design, it is crucial to translate analysis into prescriptive action. It is through a synthesis of texture, alpha-wave attenuation, and a quantifiable link established between micro-mechanics and macroscopic behavior that this relationship can be traced, thereby allowing a reverse engineering of desired psychological states through calculated material selection and the translation of biological reality into engineered constructs.

These collective findings facilitated the construction of a Psychophysical Translation Matrix (Table 1), which correlates specific mechanical properties with distinct psychological profiles. For example, individuals categorized within the "Strategist" phenotype were observed to benefit from high bending rigidity, which appears to offer a proprioceptive scaffolding that bolsters self-perception and consumer confidence [19].

Table 1: *Psychophysical Translation Matrix*

Psychological Phenotype	Cognitive Goal	Key Mechanical Parameter (KES-FB)	Neurobiological Mechanism	Material Examples
The Strategist	Authority, Boundaries	High Bending Rigidity (B), High Shear Stiffness (G)	Proprioceptive scaffolding; Deep Pressure Stimulation (Parasympathetic activation)	Heavy Gabardine, Structured Leather, Canvas
The Grounded Realist	Alertness, Presence	Surface Roughness (SMD) > 45.4 μm; High Thickness (T_0)	Pacinian Activation (250Hz); P300 Amplitude Increase; Alpha Attenuation	Raw Denim, Tweed, Raw Linen, Hemp
The Nurturer	Safety, Connection	High Compressional Energy (WC); Low Roughness	C-Tactile Afferent Stimulation (Insular Cortex); Oxytocin Release	Cashmere, Velvet, Angora, Soft Knits
The Innovator	Flow, Divergence	Low Shear (G), Low Bending (B), Low Weight (W)	Minimal proprioceptive load; Reduced somatic attention	Silk Crepe, Fine Jersey, Tencel, Tech Silk

Moreover, the temporal element in these materials is a relevant factor in this bonding process. Natural materials such as wool and linen have a quality of aging in which they attain a patina that records in a physical sense the passage of time with the wearer. Such a quality in these materials can hardly be compared with synthetic materials, which decay without developing in any way. Our contention in this matter is that this "material narrative" informs, in our view, the Ontological Ballast by registering in a tangible manner a narrative of self through time [6].

Finally, the integration of LCA data supports the concept of "Sustainable Enclothed Cognition" [15]. This finding implies that the harmony between the physical grounding of the material and the user's ethical values is essential [16]. It eliminates the cognitive dissonance that may arise from donning a "grounding" material known to be ecologically destructive. Thus, we conclude that true psychological stability cannot be assumed when the environmental provenance of the garment is unstable.

5. CONCLUSIONS

This study confirms a direct relationship between textile mechanical properties and human neurophysiological responses. The role of texture in this respect has proved to be a powerful neural control factor, with dedicated attentional resource allocation by the brain being a function of fabric thickness and roughness. In particular, establishing the 45.4-micrometer threshold level as a gateway to active neural processing provides a vital design guideline in an increasingly distracting environment to foster presence.

The benefit of using Kansei Engineering will enable a direct conversion of emotional qualitative descriptions into a mechanical parameter to deliberately design a state of mind, such as authority, alertness, and control over emotions, among others.

Additionally, enclothed cognition validity confirms the strength and viability of these findings and implications, underscoring an understanding that people wear and live within clothes, as opposed to wearing them. The rigidity supplied by a custom-made suit or the texture offered by denim meets neurobiological functions regarding the establishment of self-boundaries and alerting.

Nevertheless, there are some inconsistencies that interventions on these concepts should address. The notion of Sustainable Enclothed Cognition specifies that mental stability requires an intact environment.

The utilization of corrected LCA data supports the preference for natural fibers, not only for their inherent tactile complexity, but also for their alignment with a sustainable future.

Most importantly, these findings enable a paradigm shift in design philosophy from aesthetic design towards “prescriptive psychophysics”. Through these findings that prove a particular set of mechanical stimulation, such as shear stiffness and surface roughness, will cause a predictable state of neurophysiology, designers can function as cognitive architects rather than simple aesthetes.

The applications are not limited to consumer-related fashion design studies alone. They include medical interface design studies, where the mechanics of textile could be defined to eliminate sensorimotor processing disorders or cognitive fatigue in the field of high performance. The industry will shift from the visual concept of obsolescence to the concept of cognitive support, whereby the usefulness of the garment will lie in its ability to maintain the cognitive concentration of the wearer.

Ultimately, in a digital age characterized by the dissolution of the self, it is the essence of true fabric - that is, its friction, weight, and moral pedigree - that serves as a constitutive anchor in a world of digital flux. The Significant Form of our clothing is thus used to ground our consciousness.

REFERENCES

[1] Giddens, A. (1991). *Modernity and self-identity: Self and society in the late modern age*. Stanford University Press.

[2] Simon, H. A. (1971). Designing organizations for an information-rich world. In M. Greenberger (Ed.), *Computers, Communications, and the Public Interest* (pp. 37-72). Johns Hopkins Press.

[3] Zuboff, S. (2019). *The age of surveillance capitalism: The fight for a human future at the new frontier of power*. PublicAffairs.

[4] Runco, M. A. (2025). The misleading definition of creativity suggested by AI must be kept out of the classroom. *Education Sciences*, 15(9), 1141. https://doi.org/10.3390/educsci15091141

[5] Belk, R. W. (2013). Extended self in a digital world. *Journal of Consumer Research*, 40(3), 477-500. https://doi.org/10.1086/671052

[6] Miller, D. (2010). *Stuff*. Polity Press.

[7] Sturza, A. (2017). The relationship between words, texts, clothes and textiles. *Annals of the University of Oradea. Fascicle of Textiles, Leatherwork*, 18(2), 95-98.

[8] Nagamachi, M. (1995). Kansei engineering: A new ergonomic consumer-oriented technology for product development. *International Journal of Industrial Ergonomics*, 15(1), 3-11. https://doi.org/10.1016/0169-8141(94)00052-5

[9] McGlone, F., Wessberg, J., & Olausson, H. (2014). Discriminative and affective touch: Sensing and feeling. *Neuron*, 82(4), 737-755. https://doi.org/10.1016/j.neuron.2014.05.001

[10] Bensmaïa, S. J., & Hollins, M. (2005). Pacinian representation of fine surface texture. *Perception & Psychophysics*, 67(5), 842-854. https://doi.org/10.3758/BF03193537

[11] Zeng, Y., Xia, Y., Zhang, M., Zhang, S., & Tang, W. (2025). Recognition of fine textures using friction and EEG methods. *Biosurface and Biotribology*, 11(1). https://doi.org/10.1049/bsb2.70006

[12] Löken, L. S., Wessberg, J., Morrison, I., McGlone, F., & Olausson, H. (2009). Coding of pleasant touch by unmyelinated afferents in humans. *Nature Neuroscience*, 12(5), 547-548. https://doi.org/10.1038/nn.2312

[13] Adam, H., & Galinsky, A. D. (2012). Enclothed cognition. *Journal of Experimental Social Psychology*, 48(4), 918-925. https://doi.org/10.1016/j.jesp.2012.02.008

[14] Horton, C. B., Adam, H., & Galinsky, A. D. (2023). Evaluating the evidence for enclothed cognition: Z-curve and meta-analyses. *Personality and Social Psychology Bulletin*, 51(2), 203-221. https://doi.org/10.1177/01461672231182478

[15] Cegarra-Navarro, J.-G., Martínez-Martínez, A., Cegarra-Sánchez, J., & Muñoz Faus, J. (2025). Using sustainable enclothed cognition and envisioning sustainable learning to enhance relational capital in the fashion industry. *Journal of Intellectual Capital*, 26(3), 716-737. https://doi.org/10.1108/JIC-10-2024-0300

[16] Nautiyal, M., Cleveland, D., Hunting, A., & Smith, A. (2025). Legacy datasets and their impacts: Analysing Ecoinvent's influence on wool and polyester LCA outcomes. *Sustainability*, 17(14), 6513. https://doi.org/10.3390/su17146513

[17] Kawabata, S. (1980). *The standardization and analysis of hand evaluation*. Textile Machinery Society of Japan.

[18] Balasubramanian, M., & Periyaswamy, T. (2023). Specific fabric properties elicit human neuro and electrophysiological responses. *bioRxiv*. https://doi.org/10.1101/2023.11.24.568599

[19] Liu, H. (2025). Clothes make the man: The effect of wearing types on consumer self-confidence. *Italian Journal of Marketing*, 2025(2), 131-154. https://doi.org/10.1007/s43039-025-00110-4

[20] Reynolds, S., Lane, S. J., & Mullen, B. (2015). Effects of deep pressure stimulation on physiological arousal. *American Journal of Occupational Therapy*, 69(3), 6903350010p1–6903350010p5. https://doi.org/10.5014/ajot.2015.015560

[21] Laitala, K., Klepp, I. G., & Henry, B. (2018). Does use matter? Comparison of environmental impacts of clothing based on fiber type. *Sustainability*, 10(7), 2524. https://doi.org/10.3390/su10072524

[22] Zeki, S. (2013). Clive Bell's "Significant Form" and the neurobiology of aesthetics. *Frontiers in Human Neuroscience*, 7, 730. https://doi.org/10.3389/fnhum.2013.0073

ANNALS OF THE UNIVERSITY OF ORADEA
FASCICLE OF TEXTILES, LEATHERWORK

STUDY ON THE IR SPECTRAL STABILITY OF CAMOUFLAGE FABRICS AFTER DURABILITY TESTS

PERDUM Elena[1], VISILEANU Emilia[1], DINCA Laurentiu[1], DONDEA Felicia[1]

[1]National Institute for Textile and Leather, Bucharest, Romania, Lucretiu Pastrascanu Street no 16

Corresponding author: Visileanu Emilia, E-mail: e.visileanu@incdtp.ro

Abstract: *The IR spectral stability of camouflage fabrics directly affects the survivability of personnel and assets in multispectral combat environments. While traditional camouflage focuses on disrupting the visual silhouette through pattern and colour, its effectiveness in the near-infrared (NIR) and short-wave infrared (SWIR) ranges is what determines its ability to bypass sophisticated night-vision devices (NVDs) and optoelectronic sensors. Military equipment designed for protection against infrared (IR) detection, such as uniforms and textile camouflage, must simultaneously meet requirements for tactical functionality, mechanical strength, and stability under various environmental conditions. Regarding the IR camouflage efficiency, the goal is to reduce the infrared signature; the materials must attenuate the wearer's thermal emission, making them difficult to detect with cameras and sensors. The purpose of this study is to evaluate the IR spectral stability after durability tests of camouflage fabrics, using spectrophotometric analysis. The reflectance index was quantitatively assessed for the five constituent colours of the camouflage pattern. For all five analysed colours, regarding the impact of abrasion, the results showed that the IR reflectance index increased compared to the initial state, due to the fact that the mechanical abrasion process induces surface gloss (sheen) on the material. Following the snagging test, which introduces structural irregularities and pulls threads, a decrease in the IR reflectance index was observed across all five colours compared to the initial samples.*

Keywords: *camouflage fabrics, infrared reflectance, durability test, military equipment*

1. INTRODUCTION

The IR spectral stability of camouflage fabrics is a critical factor in modern defence technology, determining the long-term effectiveness of multispectral concealment. While standard camouflage is designed to disrupt visual detection, its performance in the near-infrared and short-wave infrared spectrums is what prevents detection by night-vision devices and thermal sensors. This stability refers to the fabric's ability to maintain its specific reflectance properties despite exposure to environmental stressors such as UV radiation, mechanical wear, moisture, and repeated laundering [1]. The performance and durability of military equipment engineered for infrared counter-detection are defined by the following criteria: thermal signature mitigation: materials must significantly attenuate the wearer's thermal emissivity to minimize detectability by advanced IR imaging systems and sensors [2]; surface thermal homogeneity: optimized heat dissipation mechanisms are essential to minimize localized thermal gradients ("hot spots"), ensuring a uniform temperature distribution across the material surface [3]; multispectral coverage: high-performance

systems maintain camouflage efficacy across critical infrared bands, specifically the MWIR (3–5 μm) and LWIR (8–12 μm) atmospheric windows, which are the primary spectra utilized in tactical reconnaissance [4].

2. MATERIALS AND METHODS

2.1 Sample and Experimental Setup

Regarding the chemical composition of the textile structures, 100% Cotton (Bbc) and 100% Polyester (PES) yarns were utilised. The ripstop structure fabric was produced on the STB 2-212 weaving machine. Manufacturing of IR camouflage printing was made using Screen Printing technology and water-based inks with Cromatex HD-10 pigments.

Fig.1. *5-color camouflage*

The developed camouflage pattern is presented in Fig. 1 and comprises 5 colours. Infrared reflectance was determined using spectrophotometric analysis to evaluate the reflectance of a planar textile substrate as a function of the incident wavelength. Reflectance, an intrinsic optical property, is defined as the percentage ratio of the total radiation intensity reflected in all directions to the intensity of the radiation incident on the material's surface. The phenomenon of reflection occurs at the interface between two optical media (Medium 1: air; Medium 2: the test material), where electromagnetic radiation is redirected into the medium of origin.

2.2. Instrumentation

All measurements were conducted according to the INCDTP internal standardised method. The spectral data were acquired using a Perkin Elmer Lambda 950 UV-VIS-NIR Spectrophotometer (Serial No. 950N6050402), which operates within a broad spectral range of 185–3300 nm.

3. RESULTS AND DISCUSSION

3.1. IR reflectance evaluation - initial fabric

The reflectance index was quantitatively assessed for the five constituent colours of the camouflage pattern: beige-brown, bordeaux, black, dark green, and green. The analysis was

performed in the NIR spectrum between 800 and 1200 nm, utilising a scanning step of 10 nm (Table 1).

Table 1. *Reflectance index values for the initial sample*

No.	**Sample Description**	**Color**	**Wavelength Range (nm)**	**Measured Reflectance (%)**
1.	Initial Camouflage Material	Beige-Brown	860-1200	81,59
		Black		77.47
		Bordeaux		94,58
		Green		97,56
		Dark green		94,98

The reflectance index values for the initial sample, printed using Grafco inks and Cromatex HD-10 pigments, demonstrate high performance within the 680–1200 nm wavelength range, with values ranging from 77.47% (black) to 97.56% (green).

3.2. Abrasion and Snagging Resistance Test (10,000 and 20,000 cycles)

Colour fastness to abrasion was evaluated using the Martindale apparatus at 1,000 and 3,000 cycles, respectively, in accordance with the SR EN ISO 12947-1 standard. Additionally, the snagging resistance was assessed using the Orbitor Pilling & Snagging Tester, following the INCDTP internal methodology. The results are summarised in Table 2.

Table 2. *Results of the abrasion and snagging resistance tests*

No.	Performed Tests	Beige		Green	Dark green	Bordeaux	Black
1	Abrasion Resistance Determination	10000 cycles No broken threads		10000 cycles No broken threads	10000 cycles No broken threads	10000 cycles No broken threads	10000 cycles No broken threads
		20000 cycles No broken threads		20000 cycles No broken threads	20000 cycles No broken threads	20000 cycles No broken threads	20000 cycles No broken threads
2	Determination of Snagging Resistance	U	3600	4-5			
			7200	4			
			10800	4			
			14400	3-4			
			18000	3-4			
		B	3600	4-5			
			7200	4			
			10800	4			
			14400	3-4			
			18000	3-4			

The abrasion resistance of the printed textile structure is excellent, as no broken threads were identified on the material surface even after 20,000 cycles.

Following the snagging resistance testing of the printed textile substrate, grades of 3, 4, and 5 were obtained, corresponding to the different testing levels. These results indicate variable snagging behaviour, ranging from average to very good performance. A Grade 3 rating highlights a

moderate occurrence of snagging defects, suggesting that the material exhibits relative sensitivity under more severe stress conditions. Grade 4 indicates good snagging resistance with minimal defects, while Grade 5 demonstrates excellent performance with no visible alterations to the textile surface. Overall, the textile substrate exhibits good snagging resistance; however, performance may be influenced by the specific testing conditions applied.

3.3. Reflectance Index Following Abrasion and Snagging Tests

Table 3 presents the reflectance index values obtained for each colour (IR) following the mechanical stress tests: a) 10,000 abrasion cycles; b) 20,000 abrasion cycles, and snagging resistance testing.

Table 3. *Results of the abrasion and snagging resistance tests*

No.	Sample Description	Color	Wavelength Range (nm)	Measured Reflectance (%)		
				10000 cycles	20000 cycles	Snagging
1.	Camouflage material: abrasion and snagging	Beige-Brown	860-1200	121,5	92,93	82,22
		Black		106,47	89,35	95,9
		Bordeaux		89,62	116,17	80,96
		Green		88,65	86,53	116,48
		Dark green		105,51	142,57	92,32

Table 4 shows the overlapped reflection curves for the following colors: a) beige-brown, b) bordeaux, c) black, d) dark green, and e) green (initial state – black curve, abrasion resistance test at 10,000 cycles – red curve, and abrasion resistance test at 20,000 cycles – green curve); Table 5 shows the curves after the snagging test.

Table 4. *Overlapped reflection curves for each of five color*

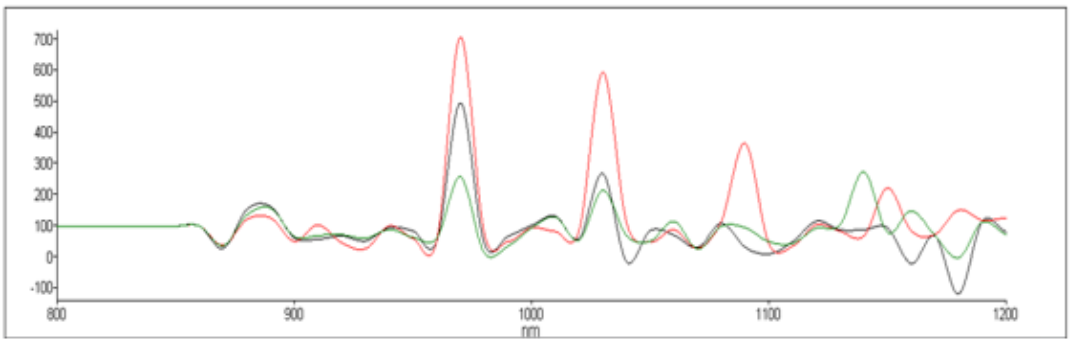

a)

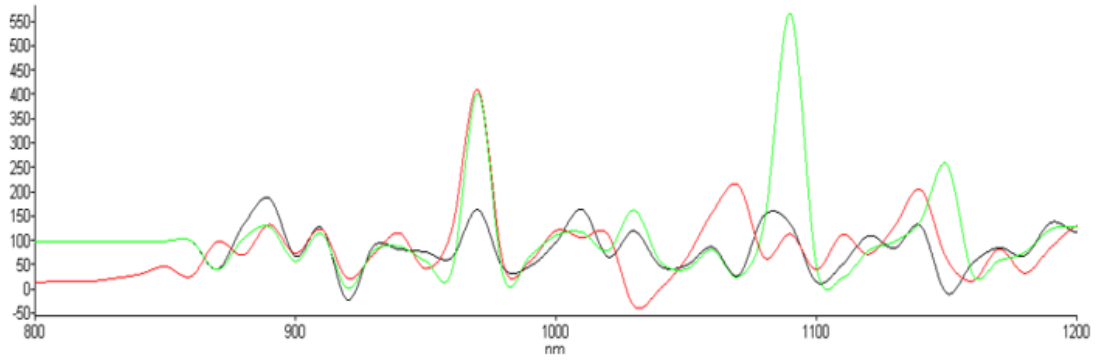
550
500
450
400
350
300
250
200
150
100
50
0
-50
800
900
1000
1100
1200
nm

b)

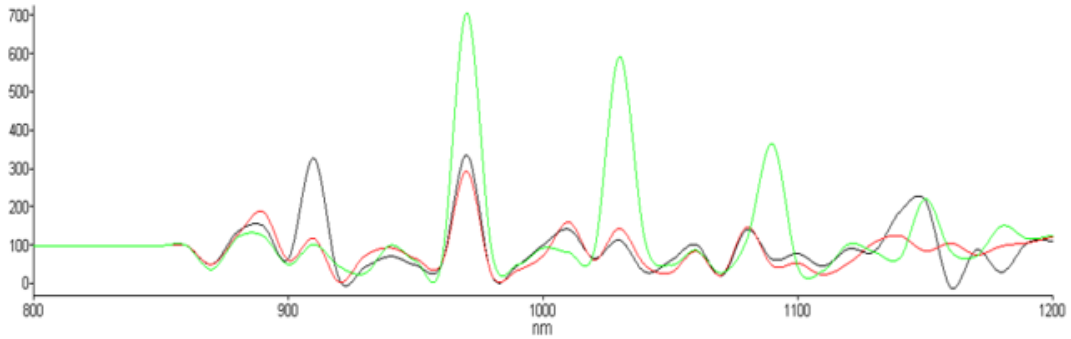
700
600
500
400
300
200
100
0
800
900
1000
1100
1200
nm

c)

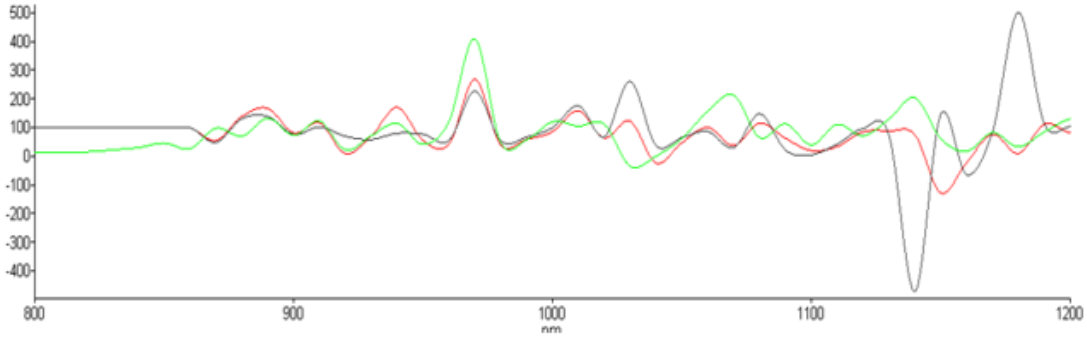
500
400
300
200
100
0
-100
-200
-300
-400
800
900
1000
1100
1200
nm

d)

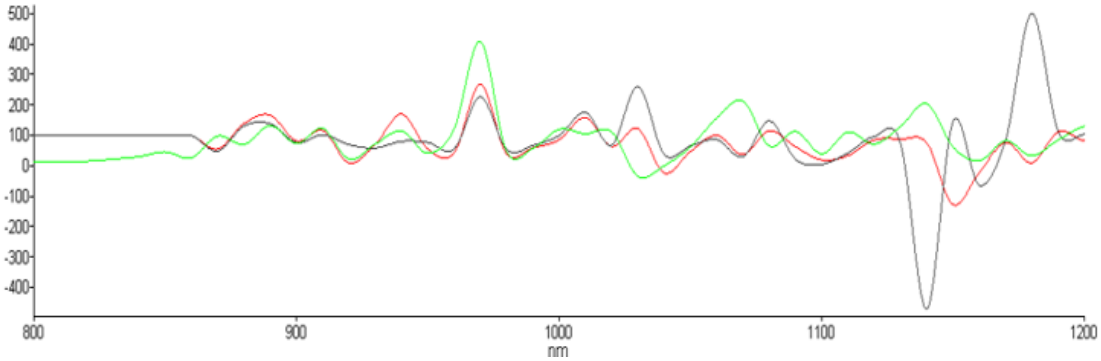
500
400
300
200
100
0
-100
-200
-300
-400
800
900
1000
1100
1200
nm

e)

Table 5. *Overlapped reflection curves for each of five color after snagging tests*

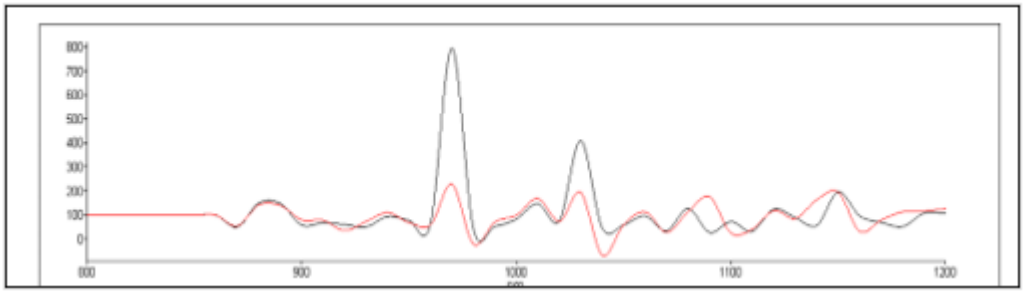

a) Beige-brown

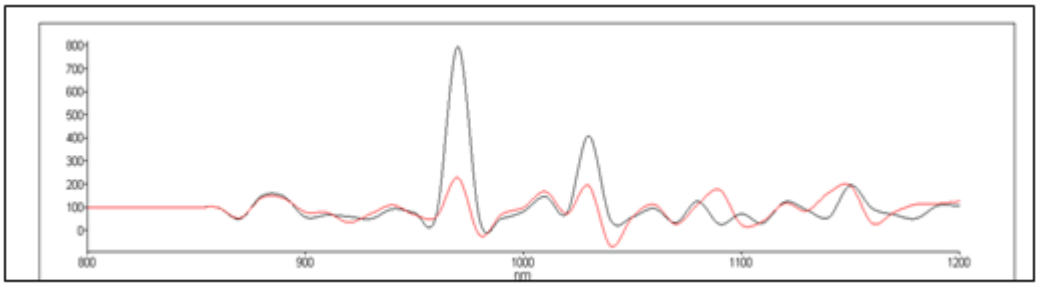

b) burgundy

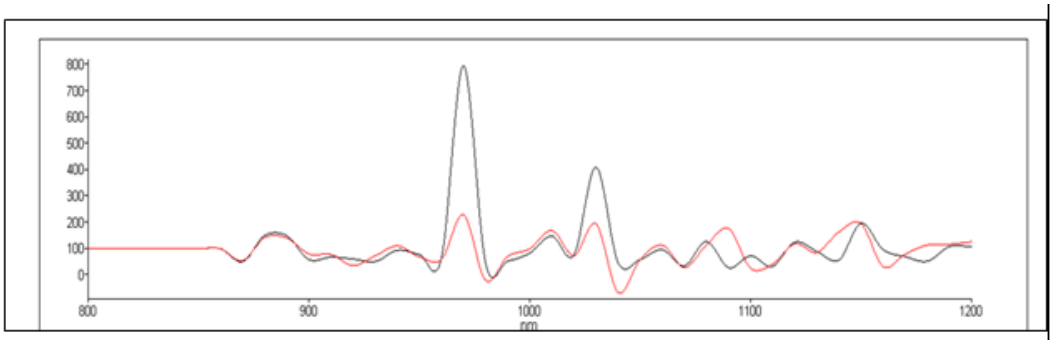

c) black

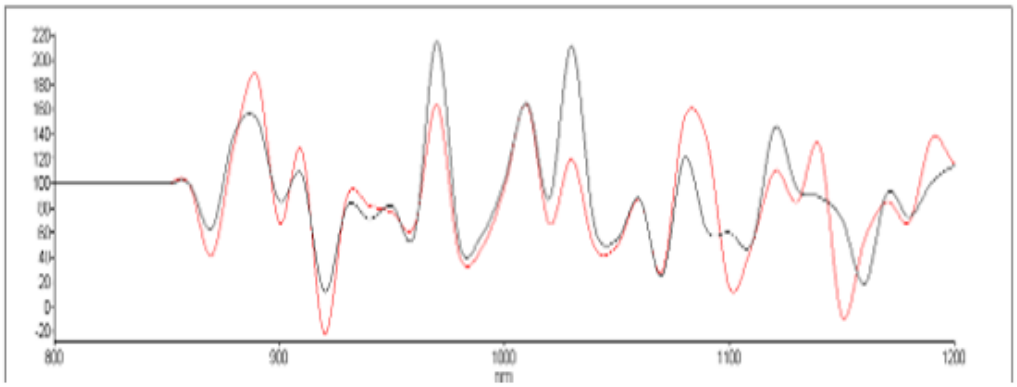

d) green

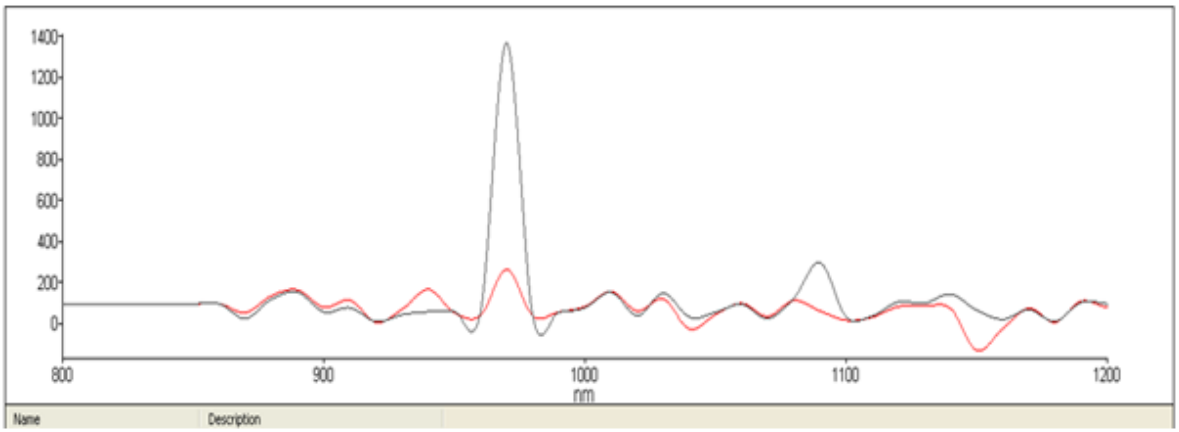

e) dark green

A comparison between the initial IR reflectance values and those obtained after 10,000 and 20,000 abrasion cycles, as well as after the snagging test, reveals the following:

Impact of Abrasion: for all five analysed colours, the IR reflectance index increased compared to the initial state, due to the fact that the mechanical abrasion process induces surface gloss (sheen) on the material. Increased gloss enhances reflectance in both the infrared and visible spectra, as polished surfaces promote specular reflection over diffuse reflection. Glossy materials are characterised by a smoothed surface profile that redirects radiation (including IR) at a precise angle, where the angle of reflection equals the angle of incidence. In contrast, matte (non-glossy) surfaces diffuse radiation in multiple directions, thereby reducing the intensity of the direct reflected signal.

Impact of Snagging: Following the snagging test, a decrease in the IR reflectance index was observed across all five colours compared to the initial samples. The snagging process (which introduces structural irregularities and pulls threads) reduces specular reflection while increasing diffuse reflection (scattering) of infrared radiation. The increased surface roughness caused by snagging forces incident IR rays to reflect in multiple directions (diffuse scattering) instead of a single, coherent direction (specular reflection), effectively reducing the detectable IR signature.

3.4. Reflectance Index Following Wash Tests

The wash fastness test was carried out in accordance with SR EN ISO 105-C06/2010 using the GIRO HW-Jams Heal washing machine, England, with the following operating parameters: temperature: 40°C; ECE phosphate-free detergent without optical brighteners: 4 g/L.Table 6 presents the reflectance index values obtained for each colour (IR) following the wash tests. Table 7 overlappes reflection curves for each of the five color afterat wash tests.

Table 6- *Results of the wasch tests*

No.	Sample Description	Color	Wavelength Range (nm)	Measured Reflectance (%)	
				Wash 5cycles	Wash 10cycles
	Camouflage	Beige-Brown		101,5	141.62
		Black		101,00	95.8

1. ***T***	material: abrasion and snagging	Bordeaux	860-1200	93.82	43.72
		Green		100.64	84.67
		Dark green		88.53	101.09

***Table** 7. Overlapped reflection curves for each of five color afterat wash tests*

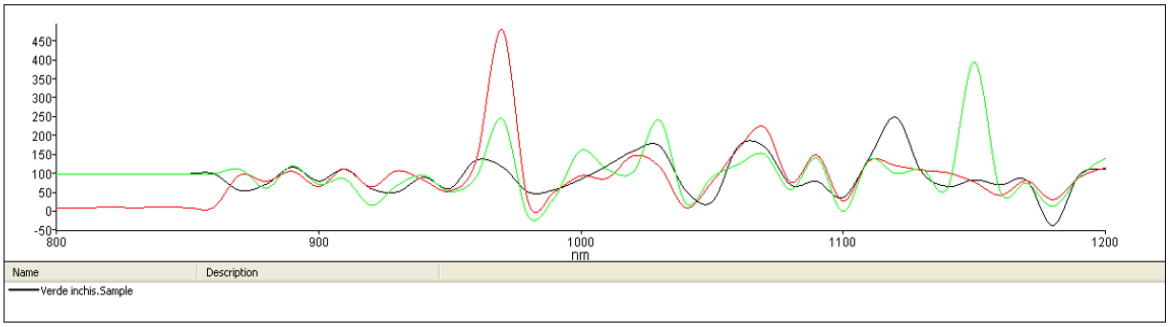

a)black

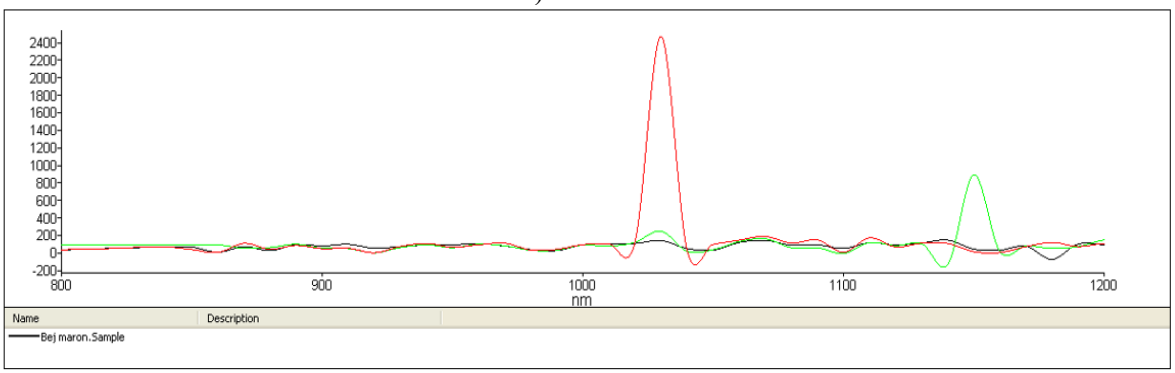

b)beige-brown

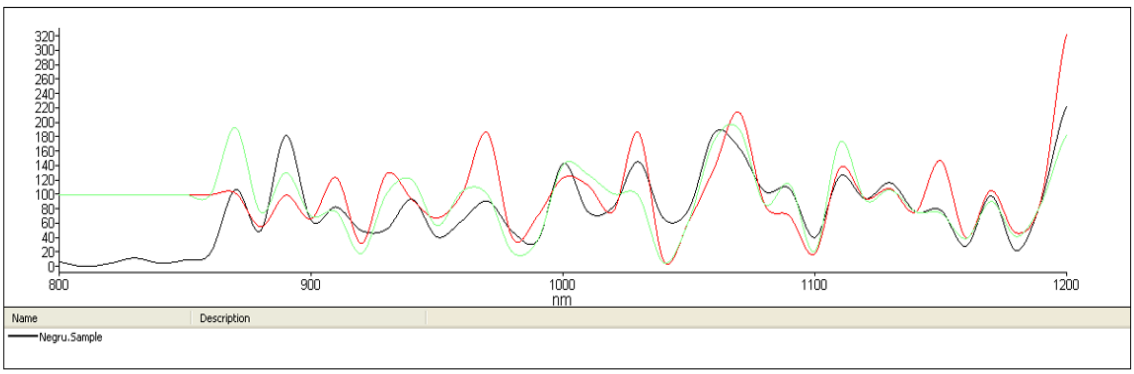

c) dark green

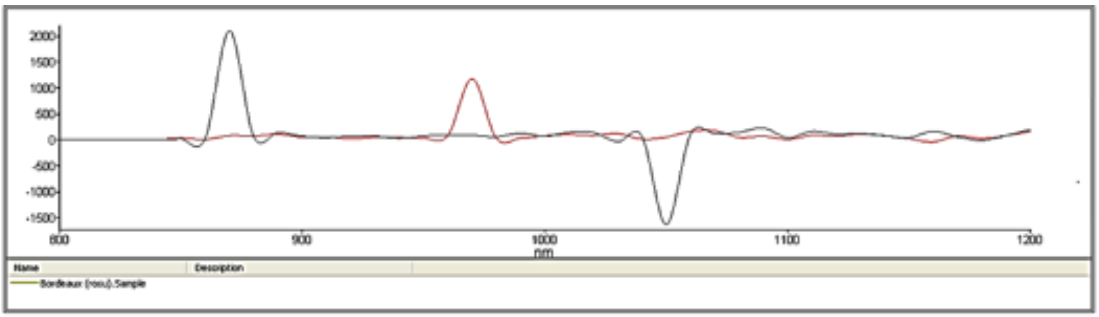

d)burgundy

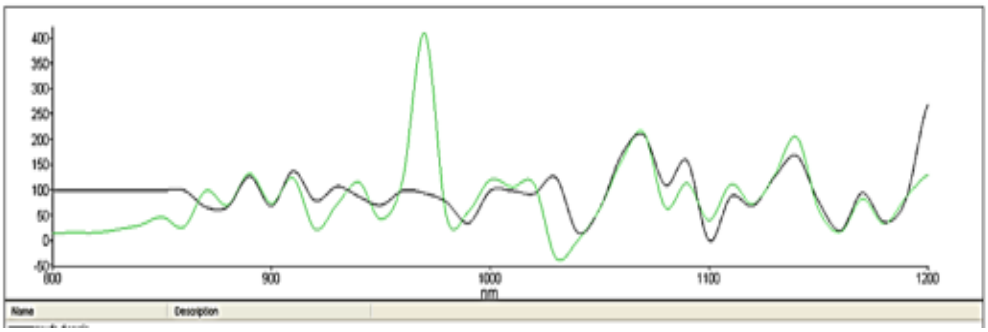

e)green

Neutral and dark colours (black, green) showed better stability after 5 washes, while warm and intense colours (beige, burgundy) showed large variations and a tendency to fade, which may suggest the need to adjust the printing formula or pigment fixation.

4. CONCLUSIONS

The reflectance index values for the initial sample printed with Grafco inks and Cromatex HD-10 pigments in the wavelength range of 680–1200 nm are good, ranging from 77.47% (black) to 97.56% (green).

Following mechanical stress, the IR reflectance index increased after rubbing, a phenomenon associated with the appearance of superficial gloss, respectively, with an increase in specular reflection. In contrast, after hanging tests, the IR decreased due to the increase in roughness and the transition to diffuse reflection, which leads to a reduction in the infrared signature.

After 5-10 washing cycles, dark and neutral colours (black, green) showed superior chromatic stability, while warm and intense shades (beige, burgundy) showed significant variations and a tendency to fade.

ACKNOWLEDGEMENTS

This work was carried out through the Core Programme within the National Research Development and Innovation Plan 2022-2027, project PN 23 26 01 02 - Echipament inteligent pentru asigurarea supraviețuirii combatanților în condiții operaționale (IRHEM).

REFERENCES

[1] Yahaya, R., et al., *Development and characterisation of near-infrared camouflage fabrics for military combat uniform*. Journal of Industrial Textiles, https://doi.org/10.1177/1528083725131, 2025.

[2] G.C. Holst, "Common Sense Approach to Thermal Imaging", SPIE Press, 2000.

[3] J. U. Duncombe, "Infrared navigation—Part I: An assessment of feasibility," IEEE Trans. Electron Devices, vol. ED-11, pp. 34–39, Jan. 1959. S. Menon, S., S. Tripathi, "Infrared Camouflage and Detection: Materials and Technologies", Defence Science Journal, 69(4), pp 367–379, 2019

[4] M. Vollmer, K.P. Möllmann, "Infrared Thermal Imaging: Fundamentals, Research and Applications", Wiley-VCH, 2010.

ANNALS OF THE UNIVERSITY OF ORADEA
FASCICLE OF TEXTILES, LEATHERWORK

SUSTAINABLE CELLULOSIC FIBROUS SUBSTRATE DYEING USING *CALENDULA OFFICINALIS* PETAL EXTRACT: COLORIMETRIC AND FASTNESS PROPERTIES EVALUATION

POPOVICI Lucia-Florina[1], COMAN Diana[2], OANCEA Simona[1], COMAN Andrei[3]

[1] "Lucian Blaga" University of Sibiu, Faculty of Agricultural Sciences, Food Industry and Environmental Protection, 550012, 7-9 Dr. I. Ratiu Street, Sibiu, Romania, E-Mail: luciaflorina.popovici@ulbsibiu.ro, simona.oancea@ulbsibiu.ro

[2] "Lucian Blaga" University of Sibiu, Romania, Faculty of Engineering, 550024, 10 Victoriei Blvd, Sibiu, Romania, Email: diana.coman@ulbsibiu.ro

[3] Medical Practice Comosan SRL, Sibiu, Romania, Email: dr.comanandrei@gmail.com

Corresponding author: Popovici Lucia-Florina, E-mail: luciaflorina.popovici@ulbsibiu.ro

Abstract: *Natural dyeing of cellulosic supports intended for hygienic and medical use is increasingly explored as a sustainable alternative to conventional coloration. In the present study, cotton samples were dyed with Calendula officinalis flower extract by two technological routes, exhaustion and ultrasonication, combined with two mordanting strategies: simultaneous mordanting and premordanting. Citric acid, tannic acid, oxalic acid, $CuSO_4$ + oxalic acid, and $FeSO_4$ + oxalic acid were applied at 10% owf. The chromatic response of the dyed fabrics was assessed through the CIELAB descriptors ΔL*, Δa*, Δb*, ΔC*, ΔH* and ΔE*, while durability was estimated through color fastness properties to acidic and alkaline perspiration and to dry and wet rubbing. The experimental matrix showed that most samples preserved a yellow to yellow-brown domain, whereas metal-assisted systems, especially $FeSO_4$ + oxalic acid, promoted greener or olive-like deviations together with the largest color differences. Premordanting generally intensified the chromatic modification relative to simultaneous mordanting, most markedly under exhaustion. Among the biomordants, citric acid maintained shades closest to the reference sample, while tannic acid offered a favorable balance between color enrichment and fastness. The best resistance values were recorded for $CuSO_4$ + oxalic acid and $FeSO_4$ + oxalic acid systems, whereas dry rubbing fastness was consistently superior to wet rubbing fastness, which still remains satisfactory. These results support the feasibility of Calendula-based eco-dyeing for cotton fabrics requiring moderate to good service performance and a reduced chemical footprint, such as those intended for disposable medical items.*

Key words: *natural dye, cotton fabrics, biomordants, ultrasonication, CIELAB, medical textiles*

1. INTRODUCTION

The replacement of synthetic dyes with plant-derived colorants has become a major direction in sustainable textile processing, because natural dyes are renewable, generally less hazardous, and compatible with circular-economy strategies when appropriate biomass resources are selected [1,2]. However, natural dyes still face important limitations related to shade reproducibility, fixation efficiency, and fastness, especially on cellulosic fibers such as cotton, where dye–fiber

affinity is often weaker than on protein substrates [2,3]. For this reason, mordanting remains a key step in natural dyeing, particularly when the target is to obtain deeper shades or improved resistance to use-related stresses.

Calendula officinalis L. (*C. officinalis)* is a valuable botanical resource due to its rich content in carotenoids, flavonoids and other bioactive constituents, which also account for its traditional medicinal and cosmetic uses [4]. Beyond pharmaceutical applications, *C. officinalis* flowers have attracted growing interest as a natural dye source capable of producing yellow to orange chromatic domains on natural fibres [4,5,6]. In addition, ultrasound-assisted textile processing has emerged as a promising route for reducing dyeing temperature, time, and chemical consumption while still promoting mass transfer and dye uptake [7].

The objective of the present study was to comparatively evaluate two *C. officinalis* dyeing routes applied to cellulosic textile supports, exhaustion and ultrasonication, combined with simultaneous mordanting or premordanting. The comparison was performed through CIELAB descriptors and color fastness properties to perspiration and rubbing, with the aim of identifying the most promising eco-dyeing conditions for cotton materials with possible medical or hygienic use.

2. MATERIALS AND METHODS

2.1. Preparation of Extract

Petals of *C. officinalis* were collected from a garden of Sibiu region, Romania. After collection, petals were dried at 50 °C, until moisture content reached 5%. Finely powdered *C. officinalis* petals, obtained using a Grindomix mill (Grindomix GM 200, Retsch, Germany), were subjected to extraction with 70% aqueous ethanol using a solid-to-solvent ratio of 1:15 (w/v). Extraction was carried out for 24 h at room temperature. Subsequently, the hydroethanolic extract was concentrated under vacuum at 50 °C to approximately 50% of its initial volume using a rotational vacuum concentrator (RVC 2-18 CDplus, Martin Christ, Germany).

2.2. Materials Used for Textile Dyeing

The textile material used as support was a 100% cotton fabric, with a basis weight of 145 g/m², a plain weave structure, and a threads fineness of 34/1Nm. All chemicals used in the dyeing experiments were of analytical grade, with purities higher than 98%.

Two application variants were investigated: simultaneous mordanting (Variant 1), in which the mordant was added directly to the dye bath together with the *C. officinalis* extract, and premordanting (Variant 2), in which the cotton samples were first treated with the mordanting solution and subsequently dyed. In both variants, dyeing was performed by two methods, conventional exhaustion and ultrasonic-assisted dyeing, and included unmordanted reference samples. The same mordanting formulations were used throughout the study: citric acid, tannic acid, oxalic acid, $CuSO_4$ + oxalic acid, and $FeSO_4$ + oxalic acid, each used at 10% relative to the mass of textile material. For the dyeing stage, the liquor ratio was 1:25. Exhaustion dyeing was carried out for 20 min at 80°C, whereas ultrasonication was performed for 15 min at 40°C. For the premordanting step, the liquor ratio was 1:20 before the subsequent application of the extract.

2.3. Fastness Properties to Perspiration and Rubbing

Color fastness to perspiration was evaluated according to Romanian standard in force SR EN ISO 105-E04:2013 (reconfirmed in 2023), using both acidic and alkaline artificial perspiration solutions. The composite specimens were impregnated at a liquor ratio of 50:1 for 30 min, squeezed, and placed under a nominal pressure of (12.5 ± 0.9) kPa between the plates of the testing device. The

samples were then maintained at 37 ± 2 °C for 4 h. After testing, the change in color and staining were assessed using the grey scale for color change/staining, with ratings from 1 to 5, where 5 indicates the highest fastness and 1 the lowest.

Rubbing fastness was evaluated under both dry and wet conditions according to ISO 105-X12:2016, using CrockMaster equipment (James Heal, UK) in order to assess the resistance of the dyed cotton samples to color transfer during mechanical action. The results were expressed on the grey scale from 1 to 5, where 5 corresponds to the best fastness.

2.4. Chromatic Characterization of Dyed Cotton in the CIELAB System

The chromatic data modifications of the dyed cotton samples was performed in the CIELAB color space by determining the parameters L* (lightness), a* (red-green coordinate), b* (yellow-blue coordinate), C* (chroma) and h* (hue angle), together with the total color difference (ΔE*) all expressed relative to the corresponding mordant-free dyed reference. Color measurements were carried out using a Datacolor 110 LAV reflection spectrophotometer (Datacolor International, Lawrenceville, USA) with Tools II Plus software, under D65/10° illuminant/observer conditions.

3. RESULTS AND DISCUSSIONS

3.1. Visual appearance and distribution of CIELAB coordinates

The photographed textile series (Fig. 1) confirmed that *C. officinalis* generated a predominantly pale yellow to yellow-brown palette, while the mordant type altered the warmth, depth and greenish tendency of the final shade. Citric and tannic acid generally preserved lighter yellow-beige tones, whereas the systems containing $FeSO_4$ + oxalic acid and, to a lesser extent, $CuSO_4$ + oxalic acid shifted some samples toward darker beige, olive or greenish-yellow appearances.

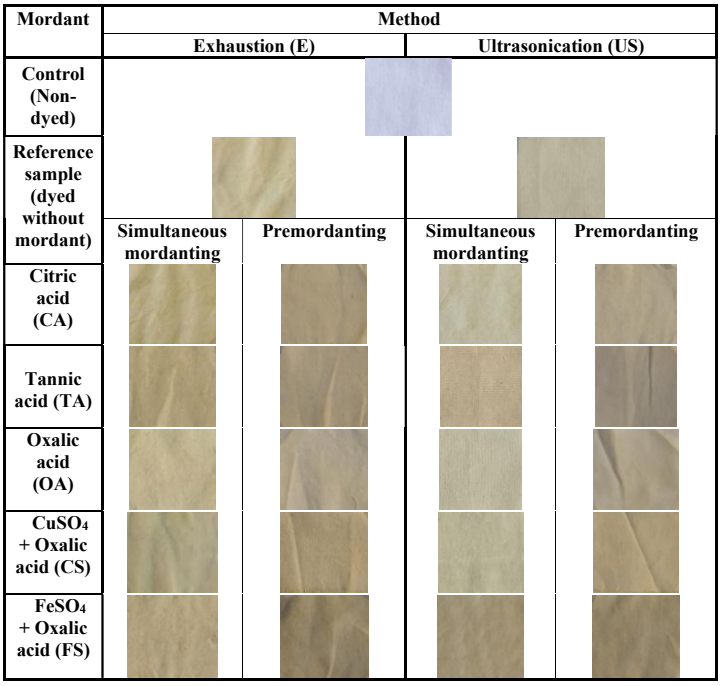

***Fig. 1**: Representative appearance of the Calendula-dyed cotton samples obtained by exhaustion and ultrasonication procedure, after simultaneous mordanting and premordanting*

The CIELAB coordinate distribution (Fig. 2) supports the visual interpretation. Most experimental points remained in the positive Δb* region, showing that yellowness remained the dominant chromatic component after dyeing. Under simultaneous mordanting by exhaustion, citric and tannic acid produced positive Δa* and positive Δb* values, which are consistent with warmer yellow-orange hues. By contrast, simultaneous exhaustion with $CuSO_4$ + oxalic acid moved the sample into the negative Δa* domain (Δa* = -2.46), indicating a greener deviation. The most pronounced green shift was observed for premordanting followed by ultrasonication with $FeSO_4$ + oxalic acid (Δa* = -5.24; Δb* = 4.16), corresponding to an olive-like chromatic tendency. This behavior agrees with the literature showing that *C. officinalis* and related marigold-based dye systems usually maintain a yellow family of shades, whereas transition-metal mordants can darken the color and move it toward olive, brown, or greenish coordinates because of metal–dye complex formation [2,5,6,8].

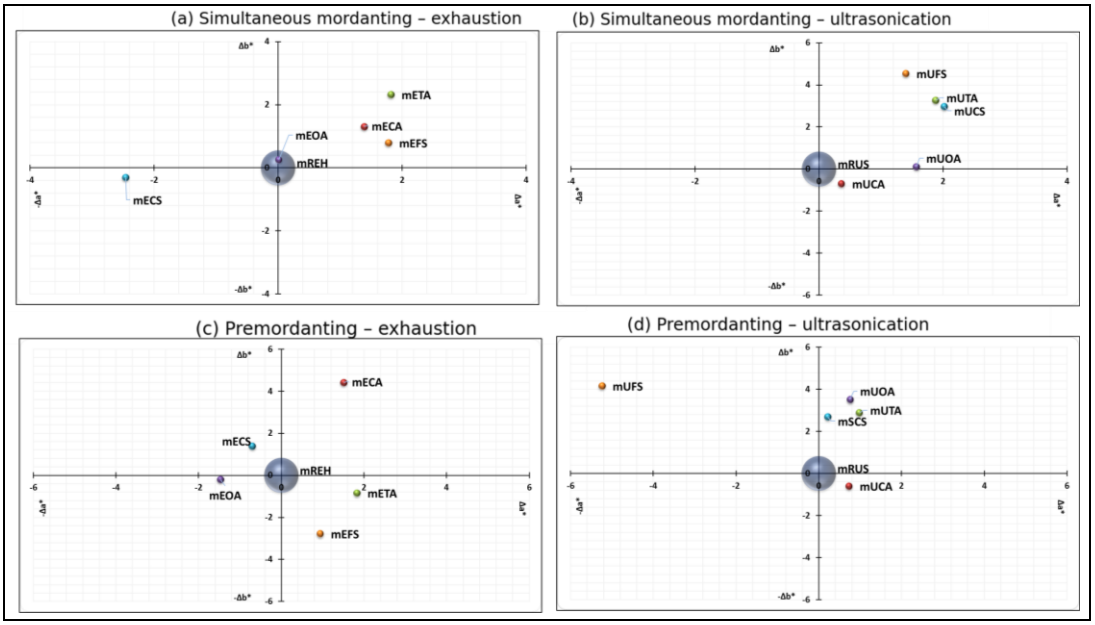

***Fig. 2**: Distribution of Δa* and Δb* coordinates for Calendula-dyed cotton samples: (a) simultaneous mordanting–exhaustion; (b) simultaneous mordanting–ultrasonication; (c) premordanting–exhaustion; (d) premordanting–ultrasonication*

3.2. Effect of mordanting route and dyeing procedure on total color difference

The data in Tables 1 and 2 show that the mordanting route strongly influenced the overall color change. For the same mordant, premordanting generally increased ΔE* compared to simultaneous mordanting, especially under exhaustion. This trend was particularly evident for $FeSO_4$ + oxalic acid, for which ΔE* increased from 3.04 in simultaneous exhaustion to 7.54 in premordanting exhaustion. The same mordant also produced large deviations under ultrasonication (ΔE* = 5.74 for simultaneous mordanting and 6.72 for premordanting).

Within the simultaneous mordanting series, the smallest color modifications were recorded for oxalic acid in exhaustion (ΔE* = 1.73) and for citric acid in ultrasonication (ΔE* = 0.80), indicating shades closest to the reference. Therefore, these treatments may be preferred when subtle color adjustment is desired. By comparison, tannic acid under simultaneous ultrasonication (ΔE* = 4.10) and $FeSO_4$ + oxalic acid under the same method (ΔE* = 5.74) caused substantially stronger chromatic departures.

Table 1: *Colorimetric parameters and fastness values for cotton samples dyed with Calendula extract by simultaneous mordanting process*

Sample[1]	Dyeing method/ Mordant	ΔL*	ΔC*	ΔH*	ΔE*	Acid persp.	Alkali persp.	Dry rub.	Wet rub.
	Exhaustion								
mREH	**Reference**	82.61	24.55	90.15	-	2-3	3	3	2
mECA	10% Citric Acid	-1.11	1.33	-1.36	2.20	4-5	4	3-4	3
mETA	10% Tannic Acid	-2.22	2.38	-1.74	3.69	4	4-5	4	3-4
mEOA	10% Oxalic Acid	-1.71	0.25	-0.01	1.73	3-4	3-4	4-5	3
mECS	10% $CuSO_4$ + 10% Oxalic acid	-0.96	-0.19	2.47	2.66	5	4-5	4	3-4
mEFS	10% $FeSO_4$ + 10% Oxalic acid	-2.33	0.86	-1.76	3.04	4-5	4-5	4-5	3-4
	Ultrasonication								
mRUS	**Reference**	86.18	18.48	94.57	-	2-3	3	2-3	2
mUCA	10% Citric Acid	-0.15	-0.73	-0.31	0.80	4-5	4	3-4	3
mUTA	10% Tannic Acid	-1.60	3.21	-1.98	4.10	5	4-5	4-5	4
mUOA	10% Oxalic Acid	-2.09	0.05	-1.57	2.61	3-4	3-4	4	3
mUCS	10% $CuSO_4$ + 10% Oxalic acid	-1.52	2.92	-2.09	3.90	4-5	3-4	4-5	3-4
mUFS	10% $FeSO_4$ + 10% Oxalic acid	-3.21	4.49	-1.58	5.74	4-5	4	4-5	4

Table 2: *Colorimetric parameters and fastness values for cotton samples dyed with Calendula extract after premordanting procedure*

Sample[1]	Dyeing method/ Mordant	ΔL*	ΔC*	ΔH*	ΔE*	Acid persp.	Alkali persp.	Dry rub.	Wet rub.
	Exhaustion								
pREH	Reference	82.61	24.55	90.15	-	3	2-3	3-4	3
pECA	10% Citric Acid	-1.74	4.43	-1.43	4.97	4	3-4	4	3-4
pETA	10% Tannic Acid	-4.43	0.78	1.86	4.87	4	4	4-5	4
pEOA	10% Oxalic Acid	2.74	-0.13	1.48	3.11	3-4	3-4	4	4
pECS	10% $CuSO_4$ + 10% Oxalic acid	-3.48	1.41	0.66	3.81	4	4-5	5	4
pEFS	10% $FeSO_4$ + 10% Oxalic acid	-6.94	-2.77	-0.97	7.54	4-5	4-5	4-5	4
	Ultrasonication								
pRUS	Reference	86.18	18.48	94.57	-	2-3	2-3	3	2-3
pUCA	10% Citric Acid	-1.98	-0.59	-0.73	2.19	4	3-4	4	3-4
pUTA	10% Tannic Acid	-1.24	2.84	-1.12	3.30	4	4-5	4	4
pUOA	10% Oxalic Acid	-0.74	3.46	-0.94	3.66	3-4	3-4	4	3-4
pUCS	10% $CuSO_4$ + 10% Oxalic acid	-2.75	2.67	-0.39	3.86	4-5	3-4	4-5	4
pUFS	10% $FeSO_4$ + 10% Oxalic acid	0.68	-4.40	5.04	6.72	4-5	5	4	3-4

[1] **Sample code explanation:** the first lowercase letter indicates the mordanting strategy (**m** = simultaneous mordanting; **p** = premordanting). The following letter(s) indicate the dyeing method (**E** = exhaustion; **U** = ultrasonication), while the final letter(s) indicate the mordant type (**R** = reference sample dyed without mordant; **CA** = citric acid; **TA** = tannic acid; **OA** = oxalic acid; **CS** = $CuSO_4$ + oxalic acid; **FS** = $FeSO_4$ + oxalic acid).

In the premordanting series, exhaustion clearly intensified the effect of the mordants. Besides the strong action of $FeSO_4$ + oxalic acid, citric acid ($\Delta E^* = 4.97$) and tannic acid ($\Delta E^* = 4.87$) also increased the difference from the control more than in the simultaneous route. This suggests that pre-establishing the mordant on the fiber before dyeing can favor more pronounced *Calendula* fixation or altered complexation on the cellulosic support. Mechanistically, this sequential route may allow the mordant to interact first with hydroxyl groups on the cellulose surface and then act as an intermediate binding site for plant-derived chromophores, thereby increasing dye retention and modifying light absorption. Overall, citric acid behaved as the most conservative biomordant, whereas $FeSO_4$ + oxalic acid acted as the most powerful shade-modifying system.

A similar process dependence was reported by Mijas et al. for hemp/cotton fabrics dyed with *Calendula*, where the timing of mordant application significantly influenced color intensity and fastness [5]. More broadly, previous work on cotton shows that mordant sequence is not a minor technical detail, but a decisive variable because it determines how many coordination sites become available before the dye molecules reach the cellulose surface [3,9]. The fact that ultrasonication still generated appreciable ΔE^* values at only 40 °C is also consistent with reviews showing that ultrasonication can improve diffusion and dye transfer under milder processing conditions [7,10,11]. Nevertheless, in the present dataset, exhaustion plus premordanting generally remained the strongest combination for maximizing color change.

3.3. Color fastness to perspiration and rubbing

The fastness results indicate that *Calendula* dyeing can achieve moderate to good performance, particularly when mordants capable of stronger coordination are applied. For acidic perspiration, the highest rating (5) was reached by $CuSO_4$ + oxalic acid under simultaneous exhaustion and by tannic acid under simultaneous ultrasonication. Alkaline perspiration values were generally between 3.5 and 4.5, with the best result obtained for premordanting followed by ultrasonication with $FeSO_4$ + oxalic acid (grade 5).

Dry rubbing fastness of the colored samples was consistently higher than wet rubbing fastness for all investigated combinations, which is advantageous for practical handling and daily use. The best dry rubbing behavior was recorded for premordanting by exhaustion with $CuSO_4$ + oxalic acid (grade 5), while several other treatments reached 4.5, including tannic acid and $FeSO_4$ + oxalic acid systems. Wet rubbing was lower, but still acceptable in the best-performing samples, usually reaching grade 4. These trends confirm that part of the *Calendula*-derived color remains more vulnerable under wet mechanical action than in dry contact. Such a difference between dry and wet rubbing is commonly reported for natural-dyed cotton because loosely adsorbed surface colorants become more mobile in the presence of water [5,8,9].

From an application perspective, tannic acid appears to be the most balanced biomordant because it combined moderate-to-high chromatic enrichment with good perspiration fastness and comparatively strong rubbing resistance. This observation is in line with recent reviews describing tannin-based biomordants as particularly effective for cellulosic substrate due to their ability to improve dye adhesion while remaining more compatible with green textile processing than many conventional metallic salts [4]. At the same time, the metallic combinations with oxalic acid produced the strongest shades and generally the best durability, but at the price of a more pronounced departure from the reference yellow hue, which agrees with the broader literature showing that Fe- and Cu-based mordants often increase fixation and darken the final color [8,9]. $FeSO_4$- and $CuSO_4$-based mordanting should not be excluded from dyeing strategies, since these systems may offer important functional benefits, particularly improved dye fixation, deeper and

more stable shades, and enhanced fastness performance. However, from a sustainability perspective, their use should be interpreted with an ecological caveat and rationally optimized for applications in which increased durability is required, while ensuring careful control of mordant concentration, fixation efficiency, and wastewater management. Therefore, the choice of mordant should be aligned with the desired end-use: subtle yellow shades with citric acid, balanced eco-performance with tannic acid, or darker olive-beige shades with enhanced fastness for $FeSO_4$/$CuSO_4$ systems.

4. CONCLUSIONS

The present study showed that *C. officinalis* petal extract can be successfully applied in the eco-dyeing of cotton fabrics through both exhaustion and ultrasonication. The dyed samples remained mainly in the yellow domain, but the final hue and intensity were strongly modulated by the mordant chemistry and by the application route.

Fastness properties to acidic and alkaline perspiration ranged from moderate to very good, and dry rubbing values were systematically superior to wet rubbing values. The best overall durability was obtained for $CuSO_4$ + oxalic acid and $FeSO_4$ + oxalic acid systems, while tannic acid emerged as a promising eco-friendlier alternative suitable for cotton products subjected to moderate use conditions.

The obtained results indicate that the appropriate selection of mordant type and dyeing route can significantly influence both chromatic expression and fastness performance. Biomordants such as citric and tannic acid maintained lighter yellow shades, while $FeSO_4$ and $CuSO_4$ combined with oxalic acid promoted darker olive-yellow tones and better fastness values, particularly under premordanting conditions. Overall, *C. officinalis* based dyeing offers a feasible route for developing aesthetically acceptable and functionally adequate cellulosic materials with potential hygienic or medical relevance. Further work should refine extract preparation, optimize fixation, and evaluate additional functional properties such as washing and light color stability, also possible antimicrobial activity.

REFERENCES

[1] P. Brudzyńska, A. Sionkowska, and M. Grisel, "*Plant-Derived Colorants for Food, Cosmetic and Textile Industries: A Review*" in Materials, vol. 14, no. 13, pp. 3484, 2021. https://doi.org/10.3390/ma14133484.

[2] B. Pizzicato, S. Pacifico, D. Cayuela, G. Mijas, and M. Riba-Moliner, "*Advancements in Sustainable Natural Dyes for Textile Applications: A Review*" in Molecules, vol. 28, no. 16, pp. 5954, 2023. https://doi.org/10.3390/molecules28165954.

[3] Y. Ding and H. S. Freeman, "*Mordant Dye Application on Cotton: Optimisation and Combination with Natural Dyes*" in Coloration Technology, vol. 133, no. 5, pp. 369–375, 2017. https://doi.org/10.1111/cote.12288.

[4] H. Benli, "*Bio-mordants: a review*" in Environmental Science and Pollution Research, vol. 31, pp. 20714–20771, 2024. https://doi.org/10.1007/s11356-024-32174-8.

[5] G. Mijas, M. Josa, D. Cayuela, and M. Riba-Moliner, "*Study of Dyeing Process of Hemp/Cotton Fabrics by Using Natural Dyes Obtained from Rubia tinctorum L. and Calendula officialis*" in Polymers, vol. 14, no. 21, p. 4508, 2022. https://doi.org/10.3390/polym14214508.

[6] M. Montazer and M. Parvinzadeh, "*Dyeing of Wool with Marigold and Its Properties*" in Fibers and Polymers, vol. 8, pp. 181–185, 2007. https://doi.org/10.1007/BF02875789.

[7] M. M. Hassan and K. Saifullah, "*Ultrasound-assisted sustainable and energy efficient pre-treatments, dyeing, and finishing of textiles – A comprehensive review*" in Sustainable Chemistry and Pharmacy, vol. 33, p. 101109, 2023. https://doi.org/10.1016/j.scp.2023.101109.

[8] M. R. Repon, M. T. Islam, and M. A. A. Mamun, "*Ecological risk assessment and health safety speculation during color fastness properties enhancement of natural dyed cotton through metallic mordants*" Fashion and Textiles, vol. 4, p. 24, 2017. https://doi.org/10.1186/s40691-017-0109-x.

[9] F. S. Ghaheh, M. K. Moghaddam, and M. Tehrani, "*Comparison of the effect of metal mordants and bio-mordants on the colorimetric and antibacterial properties of natural dyes on cotton fabric*" in Coloration Technology, vol. 137, pp. 689–698, 2021. https://doi.org/10.1111/cote.12569.

[10] M. Muruganandham, K. Sivasubramanian, P. Velmurugan, S. S. Kumar, N. Arumugam, A. I. Almansour, R. S. Kumar, S. Manickam, C. H. Pang, and S. Sivakumar, "*An eco-friendly ultrasound approach to extracting yellow dye from Cassia alata flower petals: Characterization, dyeing, and antibacterial properties*" in Ultrasonics Sonochemistry, vol. 98, p. 106519, 2023. https://doi.org/10.1016/j.ultsonch.2023.106519.

[11] M. D. Cocîrlea, A. Coman, L.-F. Popovici, S. Oancea, and D. Coman, "*Potential use of bio-dyes for green coloring of medical textiles*" in Annals of the University of Oradea. Fascicle of Textiles, Leatherwork vol. 25, no. 2, pp. 17-26, 2024. https://textile.webhost.uoradea.ro/Annals/Vol%2025%20no%202-2024/Art%20584%20pag%2017-26.pdf

ANNALS OF THE UNIVERSITY OF ORADEA
FASCICLE OF TEXTILES, LEATHERWORK

FLEXIBLE MICROSTRIP BANDPASS FILTER COATED ON TEXTILES FOR RESONANT SIGNAL TRANSMISSION

RADULESCU Ion Razvan[1], ENE Alexandra[2], VISILEANU Emilia[3], DINCA Laurentiu[4], PERDUM Elena[5], NEGROIU Rodica[6], BACIS Irina[7], IONESCU Ciprian[8], CIOBANU Luminita[9], TALPA Andreea[10]

[1-5] INCDTP - Bucharest, Str. L. Patrascanu 16, 030508, Bucharest, Romania, office@incdtp.ro

[6-8] National University of S&T Polytechnica Bucharest, Faculty of Electronics, CETTI, Bd. Iuliu Maniu 1-3, 061071, Bucharest, Romania, E-Mail: cetti@cetti.ro

[9-10] Technical University Iasi, Faculty DIMA, Center for R&I in textiles and fashion SMART-Tex-IS, Str. Dimitrie Mangeron 29, 700050, Iasi, Romania, luminita.ciobanu@academic.tuiasi.ro

Corresponding author: Radulescu, Ion Razvan, E-mail: razvan.radulescu@incdtp.ro

Abstract: *Textile structures for flexible microstrip transmission lines play a significant role in the development of wearable articles, as they connect the textile antenna with the wearable transceiver. Such articles are currently developed to monitor physiological parameters of humans with medical or sports applications. Our paper proposes two types of coated transmission lines on a textile substrate, with silver respectively with carbon paste, with two geometrical dimensions. Their designed functionality is to act as band pass filters at the resonant frequency of 900 MHz, (which is the GSM mobile phone frequency) in order to deliver maximum power at a wearable antenna. The four coated transmission lines were manufactured via screen printing on the dielectric substrate, while a conductive knitted fabric was sewn on the back side to act as ground plane. The manufactured transmission lines were characterized regarding their physical-mechanical, electrical and morphological properties. The reflection loss S11 of the transmission lines was measured via a Vector Network Analyser and the simulation data was subsequently updated with the parameters of the manufactured samples. Simulation results were validated with measurement results with a roughly agreement, mainly due to the differences between the electric conductivity of the microstrip ciruit in simulation and in manufacturing. These findings consolidate the continuation of the research work.*

Key words: *distributed elements, flexible microwave circuits, textile dielectric, transmission lines*

1. INTRODUCTION

Microwave transmission lines integrated into textile fabrics support smart garments wireless monitoring of physiological health parameters [1]. The advent of flexible textile antennas reaches back the early 2000, when a series of papers paved the first research results [2-7]. Their subsequent development was possible due to the progress of metallic yarns spinning and the miniaturization of electronic components [8-9]. A series of research contributions aim to reach a best possible integration of the electronic components into the garment's fabric structure, in order to ensure a reliable comfort, washability and electric functionality [9]. Applications focus on smart garments for monitoring of physiological parameters, especially for health and sport domains [10, 13-14].

Several scientific contributions dealt with the topic and brought both conceptual and technical developments. A scientific contribution related to five different textile materials for microstrip antennas and their electric and mechanic characterization was provided already 2004 in [1]. Another microstrip patch antenna with fewer risks for the humans than a wire antenna due to the groundplane close to the body was presented 2007 by [2]. Four types of patch antennas on different textile substrates, with simulation and measurement of reflection loss S11, Gain / Directivity and Far Field radiation pattern was achieved 2010 by [3].
Wearable antennas were developed for energy harvesting of EM radiation from the environment, in order to feed low-power devices attached to the smart garments [4]. Virtual prototyping (Lectra, Gerber, CLO3D) was used more recently to integrate wearable antennas into fashionable garments [5]. Slot antennas with circular shape were developed on two different textile substrates with simulation and measurement of reflection loss S11 in the ISM band of 5.8 GHz and 24 GHz (considered to be maximal frequency for wearable antennas) [6]. The bending properties and the simulation & measurement of a wearable microstrip patch antenna with and without high impedance surface structure was presented in [7].
Review papers [8,9] of the scientific domain related to wearable antennas tackle the various types adaptable to garments such as lens/array, reflector, horn, wire and patch antenna, the different manufacturing techniques as knitting, weaving, printing and embroidery and the main applications, such as cell phones, satellite communication, sports, military and telemedicine.
Microwave transmission lines enable communication at high frequencies (> 300 MHz) by connecting the textile antenna with the wearable transceiver [11], as an integrated system into the smart garment.

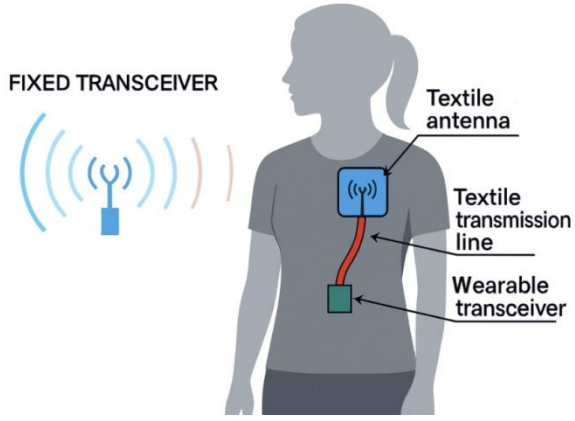

A resonant circuit is needed in order for the textile transmission line to deliver maximum power to the textile antenna at a certain frequency. Our scientific contribution presents several variants of textile microstrip transmission lines coated on a textile substrate, acting as band pass filters with destination GSM communication.

Fig. 1: *Graphical scheme for a wearable transmission line [11]*

The following research methodology was applied:

- a parametric study for modelling distributed microwave elements as bandpass filter at 900 MHz was developed;
- the bandpass filter circuit dimensional parameters were optimized (length, width), while considering given electrical (electric permittivity, electric losses) and dimensional parameters (thickness substrate, thickness coating) of the fabric and the coated circuit;
- the optimized microstrip circuit was coated by screen printing on the textile substrate, while a groundplane conductive fabric was sewed on the bottom side of the textile substrate;
- the Return Loss S11 of the resulting distributed circuit was measured via a VNA;
- modelled Return Loss S11 was updated according to physical textile parameters and validated with the VNA measurement.

2. MATERIALS AND METHODS

2.1 The dielectric substrate

The textile substrate was chosen for its suitable physical-mechanical and electrical properties and as well for its heat curing resistance: it is a woven fabric with 70% Kermel (Polyamide-Imide) and 30% Viscose fibres, having the following physical-mechanical and design parameters (table 1):

Table 1: *Physical-mechanical properties of the textile substrate*

No.	Physical mechanical property		UM	Values	Standard
1	Specific mass		g/m^2	268	SR EN 12127
2	Thickness		mm	0,59	SR EN ISO 5084:2001
3	Tensile strength	Warp	N	1389	SR EN ISO 13934-1
		Weft		905	
4	Elongation at break	Warp	%	24,6	
		Weft		14,0	
5	Tear resistance	Warp	N	66,0	SR EN ISO 13937-3
		Weft		70,2	
6	Dimensional change at washing	Warp	%	-1,72	SR EN ISO 6330
		Weft		-1,0	
7	Abrasion resistance		no. abrasion cycles	28.015	SR EN ISO 12947-2
8	Air permeability		l/m^2s (mm/s)	212	SR EN ISO 9237

2.2 Screen printing method

This woven fabric was screen printed with two types of conductive paste, namely silver paste from Sigma Aldrich (Ag60%+AgCl40%) and carbon paste from BareConductive. A knitted fabric with 10 Ωsq resistance was sewn on the back side of the dielectric woven fabric as ground plane, in order to achieve a micro strip textile structure. According to the simulation, two geometrical dimensions for the transmission lines were selected to be screen printed on the substrate with band pass filter functionality: 4 mm x 100 mm transmission line and 4 mm x 150 mm transmission line (figure 2).

Fig. 2: *Screen printing of the textile substrate with the two types of paste*

The four resulting samples were cured in oven at 80ºC for 30 minutes and the knitted fabric

was attached afterwards by sewing on the back side as ground plane (return path).

3. RESULTS

3.1. Electrical properties

A first task was to determine the electrical and geometrical parameters of the microstrip transmission line, in order to be able to complete the simulation. Several methods were applied in this regard (table 2).

Table 2: *Electrical properties of the flexible microstrip textile*

No.	Electrical property	UM	Values	Standard
1	Groundplane electric surface resistivity	Ω_{sq}	914	SR EN ISO 1149-1
2	Groundplane electric volume resistivity	Ω m	236	SR EN ISO 1149-2
3	Groundplane electric conductivity	S/m	$4.2*10^{-3}$	SR EN ISO 1149-2
4	Relative electric permittivity textile substrate (ε_r)	[1]	2.11 [at 1 GHz]	Measured according to [12]
5	Dielectric losses textile substrate (tanδ)	[1]	0.015 [at 1 GHz]	Measured according to [12]
6	Electric resistivity silver layer 10 cm / 15 cm	Ω m	$3.56*10^{-5}$ $1.06*10^{-5}$	Measured via multimeter
7	Electric conductivity silver layer 10 cm / 15 cm	S/m	28106 94193	Measured via multimeter
8	Electric resistivity carbon layer 10 cm / 15 cm	Ω m	$2.52*10^{-4}$ $2.83*10^{-4}$	Measured via multimeter
9	Electric conductivity carbon layer 10 cm / 15 cm	S/m	3975 3534	Measured via multimeter

The surface and volume electric resistance of the knitted fabric used as ground plane were computed with a PRS-801B Teraohmmeter of Prostat with PRF-911 concentric rings, according to the standard ISO 1149-1/2. The electric conductivity of this knitted fabric was computed of the volume electric resistivity. The relative electric permittivity and the losses of the dielectric textile substrate were measured via a specialized experimental setup in a previous scientific contribution [12]. Due to the fact that the thickness of the coating on the textile is not uniform, an average value for the thickness was computed. The electric resistivity and conductivity of the transmission lines were computed by measuring the linear resistance of the conductor with a multimeter and considering its geometrical dimensions (length, width, thickness).

3.2. SEM analysis of the coated layer thickness

The thickness of the silver and carbon layer applied onto the textile substrate was determined by SEM analysis. Images with magnification of 800x prove a good adhesion onto the textile substrate, however a less uniform thickness.

Fig. 3: *Measured thickness of the 100 mm Ag coating*

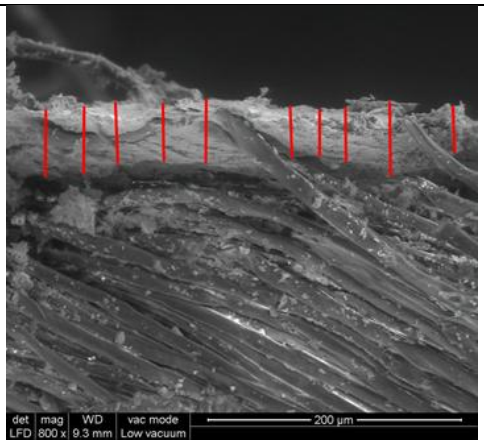

Fig. 4: *Measured thickness of the 150 mm Ag coating*

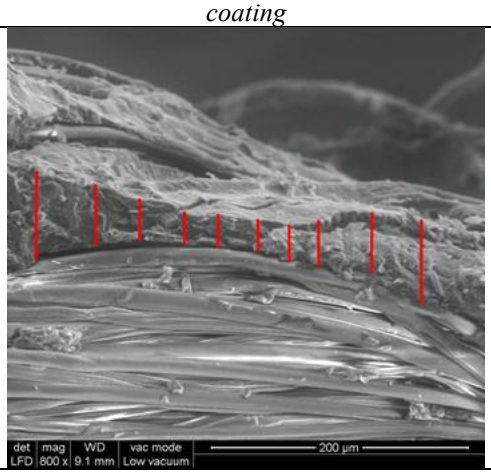

Fig. 5: *Measured thickness of the 100 mm Carbon coating*

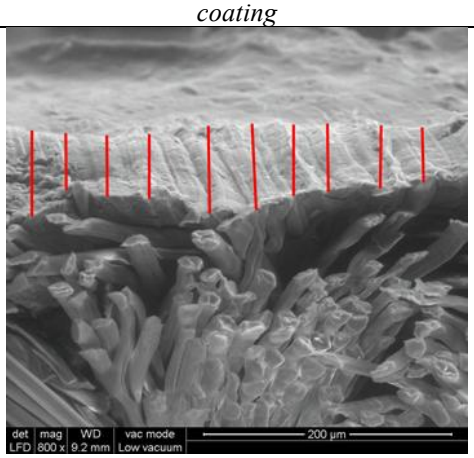

Fig. 6: *Measured thickness of the 150 mm Carbon coating*

Table 3 presents the average thickness computed of the SEM images.

Table 3. *Average thickness of the coated layers*

	100 mm transmission line	150 mm transmission line
Silver coating	15.2 µm (STDEV 6.5) 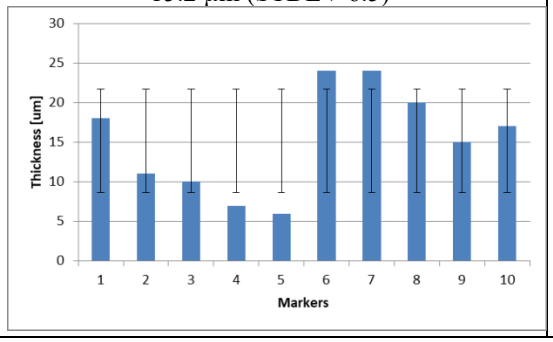	45.1 µm (STDEV 7.3) 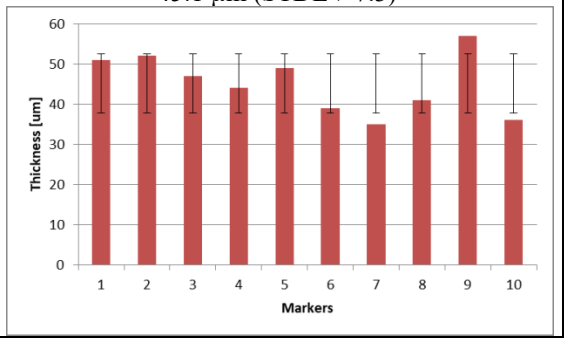

Carbon coating	38.6 µm (STDEV 16.4) 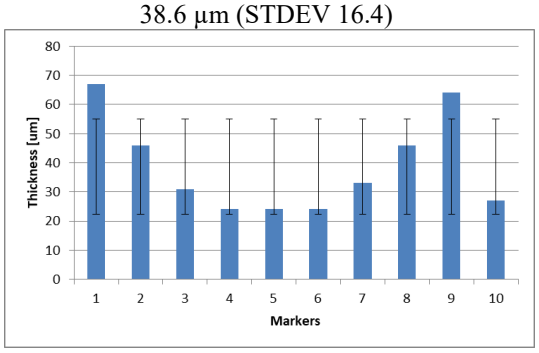	54 µm (STDEV 9.9) 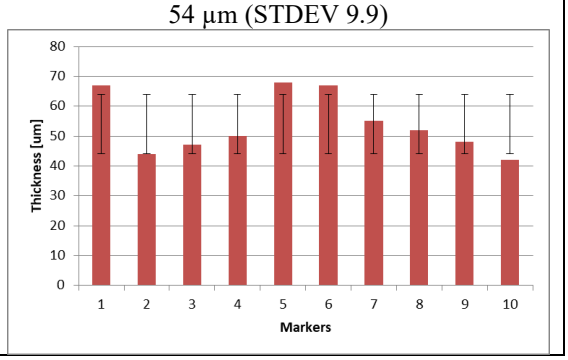

The values of the coated trace are quite scattered, but they ensure a continuous transmission of the electrical microwave signal.

3.3. Reflection loss simulation and measurement results

The S11 Reflection loss was simulated and measured for the four transmission lines. The simulation of the microstrip transmission lines was done in Sonnet Lite software, by introducing the electric parameters of the textile substrate and the geometric dimensions of the coated trace. The measurement was done via a Vector Network Analyzer, by connecting the electrodes to the 50 Ω input and output port, within the frequency range of 100-1000 MHz (Figure 7 and 8).

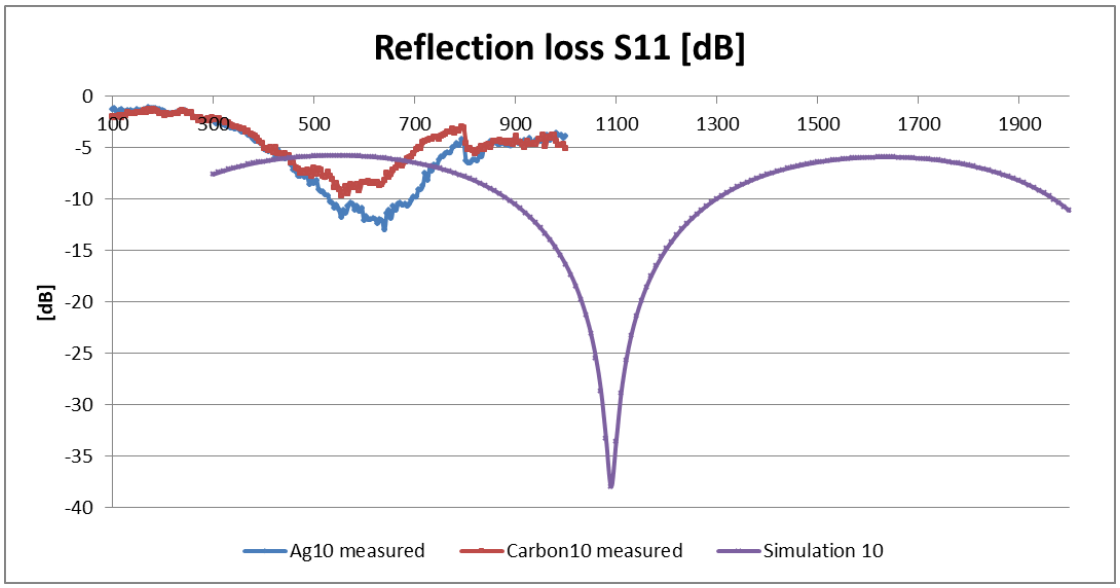

Fig. 7. *Simulated and measured results for the 100 mm transmission lines*

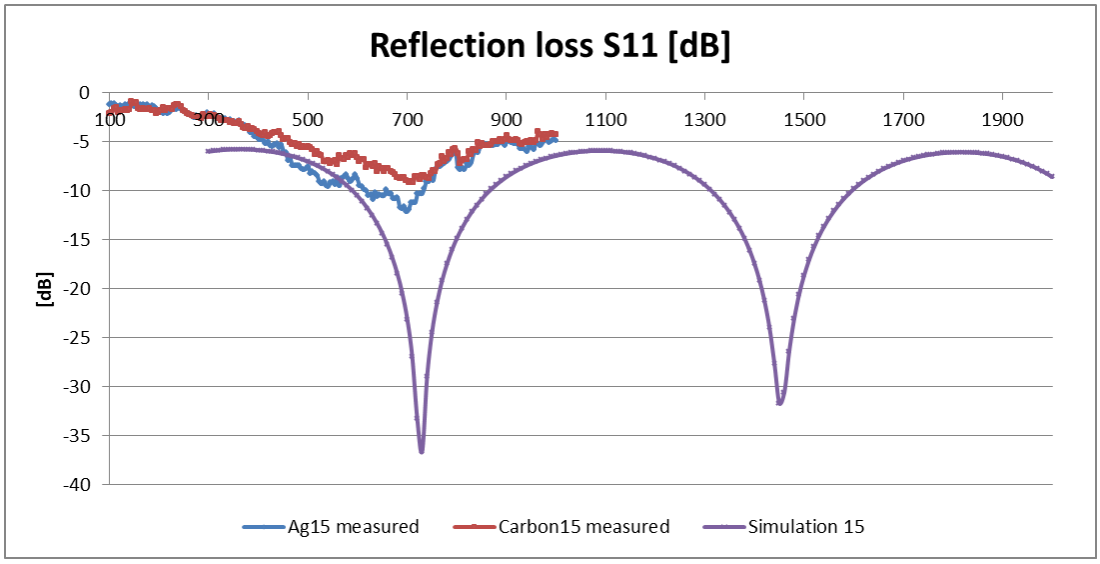

Fig. 8. *Simulated and measured results for the 150 mm transmission lines*

4. DISCUSSION

The measured results differ from the simulated results, especially for the case of the 100 mm transmission lines, mainly due to the different values of the coated trace electric conductivity. The simulation was performed with a conductivity of the traces of 10^7 S/m. Instead, the silver traces have a conductivity of 2.8-9.4*10^5 S/m, while the carbon traces have a conductivity of 3.5-3.9*10^3 S/m. Another deviation between the simulated and measured results may come due to the deviations in measurement of the dielectric parameters of the textile substrate (relative electric permittivity and loss tangent). It is known that such deviations have as result the displacement of the resonant frequency. On the other hand, the results for the 150 mm transmission line show a good agreement regarding the resonant frequency (700 MHz). Single the gain differs, with about -35 dB for the simulation (trace conductivity 10^7 S/m) when compared to the -12 dB for the measured silver coating (trace conductivity 94193 S/m) and the -8 dB for the carbon coating (trace conductivity 3534 S/m).

5. CONCLUSIONS

Aim of the research was to provide flexible microwave transmission lines to deliver maximum power to wearable antennas. The resonant frequency was initially designed for 900 MHz (GSM communication), however after updating the simulation with the current physical parameters of the coated transmission lines, the resonant S11 frequency of the 100 mm line shifted to 1100 MHz and the resonant S11 frequency of the 150 mm line shifted to 700 MHz. Moreover, due to significant differences of the electric conductivity of the traces (simulation = 10^7 S/m, measurement = 10^3-10^5 S/m), the gain in dB of the measured physical band pass filters is lower (simulation = -35 dB, measurement = - 8 dB and - 12 dB). Differences between the dielectric substrate parameters also play a role in the shift of the resonant frequency. Nevertheless, the proposed textile structure for the flexible microstrip transmission lines roughly meets its designed functionality. Future work envisages a better correlation of the design and simulation of the band pass filter in agreement with the physical and electrical parameters of the microstrip transmission lines.

ACKNOWLEDGEMENTS

This work was carried out through the Core Programme within the National R&D&I Plan 20222027, carried out with the support of MCID, project no. 6N/2023, PN 23 26 01 03, project 3DWearIoT.

REFERENCES

[1] P. Salonen, "*Effect of Textile Materials on Wearable Antenna Performance: A Case Study of GPS Antennas*", IEEE Xplore, 2004

[2] J. G. Santas, "*Textile antennas for on-body Communications: techniques and properties*", IEEE Xplore, Dec. 2007, DOI: 10.1049/ic.2007.1064

[3] S. Sankaralingam, B. Gupta, "*Development of textile antennas for body wearable applications and investigations on their performance under bent conditions*", Progress In Electromagnetics Research B, Vol. 22, pp. 53-71, 2010

[4] C. Loss et al., "*Developing sustainable communication interfaces through fashion design*", 5th STS Italia Conference a matter of design: Making society through science and technology, Milan, 2014

[5] E. Papachristou, H. T. Anastassiu, "*Application of 3D Virtual Prototyping Technology to the Integration of Wearable Antennas into Fashion Garments*", MDPI Technologies 2022, 10, 62. https://doi.org/10.3390/technologies10030062

[6] M. Cupal, Z. Raida, "*Slot Antennas Integrated into 3D Knitted Fabrics: 5.8 GHz and 24 GHz ISM Bands*", MDPI Sensors 2022, 22, 2707., https://doi.org/10.3390/s22072707

[7] M. M. Bait-Suwailam et al., "*Impedance Enhancement of Textile Grounded Loop Antenna Using High-Impedance Surface (HIS) for Healthcare Applications*", MDPI Sensors 2020, 20, 3809; doi:10.3390/s20143809

[8] R. Salvado et al., "Textile materials for the design of wearable antennas: A survey", MDPI Sensors 2012, 12, 15841-15857; doi:10.3390/s121115841.

[9] M. Rafiq, "*A review on the manufacturing techniques for textile based antennas*", Journal of Engineered Fibers and Fabrics, Volume 19: 1–18, s://doi.org/10.1177/15589250241226585

[10] Marterer et al. "*Wearable textile antennas: investigation on material variants, fabrication methods, design and application*", Fashion and Textiles (2024) 11:9, https://doi.org/10.1186/s40691-023-00369-1

[11] Ł. Januszkiewicz, I. Nowak, *"Knitted Microwave Transmission Line for Wearable Electronics",* Appl. Sci. 2024, 14(23), 10798; https://doi.org/10.3390/app142310798

[12] I.R. Radulescu, A. Ene, D. Toma eta al., "*Conductive textile transmission lines for microwave frequency filters*", ANNALS OF THE UNIVERSITY OF ORADEA FASCICLE OF TEXTILES, LEATHERWORK, Vol. 2, 2025

[13] R. V. Caramaliu, A. Vasile, I. Bacis, "*Wearable vital parameters monitoring system*", Proc. SPIE 9258, Advanced Topics in Optoelectronics, Microelectronics, and Nanotechnologies VII, 92580R (20 February 2015); https://doi.org/10.1117/12.2070041

[14] I.R. Rădulescu, L. Surdu, B. Mitu, C. Morari, C. Costea, N. Golovanov, "*Conductive textile structures and their contribution to electromagnetic shielding effectiveness*", Industria Textila, 2020, 71, 5, 432–437, http://doi.org/10.35530/IT.071.05.1783

ANNALS OF THE UNIVERSITY OF ORADEA
FASCICLE OF TEXTILES, LEATHERWORK

HYBRID WORKFLOW ACCESSIBILITY IN AFFINITY STUDIO

RAȚIU Georgiana Lavinia [1], ŞUTEU Marius Darius [2] ANDREESCU Nicoleta [2]

[1] Doctoral School of Engineering Sciences, University of Oradea, România.E-Mail: giaratiu@gmail.com

[2] Universitatea Oradea, Facultatea de Inginerie Energetică și Management Industrial, Departamentul Textile, Pielărie și Management Industrial, 410058, Oradea, România, E-Mail: suteu_marius@yahoo.com

Corresponding author: ŞUTEU Marius Darius, E-mail: suteu_marius@yahoo.com

Abstract: *In this paper, the authors propose to highlight the hybrid workflow within the Affinity Studio program. The hybrid workflow offered by Affinity involves the integration into one program of the 3 modules, the so-called "Studios": Vector, Pixel and Layout. The Vector module is meant as an equivalent of Adobe Illustrator, designed for vector graphics and design, allowing users to create scalable graphics, includes the pen tool, the pencil tool, the shape tool, the new tracing function, included in the 2026 Affinity Studio update, allows the tracing of raster images (pixels), such as PNG files, and their direct conversion into editable vector graphics. The Pixel Studio is the equivalent of Adobe Photoshop, a module dedicated to image processing and editing. Users can add pixel layers to paint or edit while keeping the original image data intact, another way of using it, the one presented in the paper, is to modify a text written in Vector mode and just by switching to Pixel mode, to stylize it with the image editing specific tools. Layout Studio is the equivalent of Adobe InDesign, it is designed for creating complex multi-page layouts, such as magazines, books and brochures, providing essential tools for typography, master pages and for print preparation.*

Key words: *Illustrator, Affinity Studio, Canva, Photoshop*

1. INTRODUCTION

Affinity Studio uses the "Personas" concept (renamed "Studios" in version 3.0), integrating vectors, raster editing, and pagination into a single unified interface [1]. The user can paint with pixel brushes over vector shapes or change the layout of a page without closing the document or changing the application [2]. This hybrid architecture allows a greater creative freedom. An illustrator or designer can draw the structure of a character in vectors for scalability, then switch to *Pixel Studio* to add organic shadows using charcoal or watercolor textured brushes, all on the same object and layer, without damaging the quality of the vector graphics [3].

Affinity evolved, under Canva's umbrella, into a high-performance and affordable alternative among freelancers, creative studios, and illustrators due to improved work speed and reduced cost.

As an established industry leader, *Adobe*'s fame precedes it. Known for its *Creative Cloud*, which includes ultra-popular apps like *Photoshop*, *InDesign*, *Illustrator*, and *Lightroom*. In addition to its 20 creative apps, *Adobe* also offers cloud storage, fonts, templates, services like *Adobe Portfolio* and *Behance*, and generative AI tools like *Adobe Firefly* [4].

Known as one of the alternatives to *Adobe Illustrator*, *Affinity Designer* has emerged as a new and fresh tool in the vector graphics space. Its development has focused more on modern

computer technology and user expectations, based on various surveys. It is modern and more advanced compared to other programs [4].

The software update, released on October 30, 2025, brought some radical changes to *Affinity*. First, the three-app suite, Designer, Photo, and Publisher, no longer exists. The three apps are now combined into a completely new app, in the form of separate studios: Vector, Pixel, and Layout, **Fig. 1.**

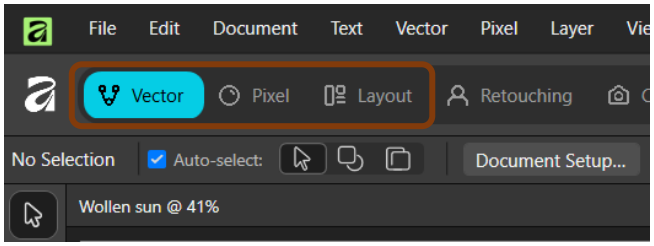

***Fig. 1**: Menu for switching between studios*

Vector Studio is meant as an equivalent of *Adobe Illustrator*, dedicated for vector graphics and design, allowing users to create scalable graphics, includes the pen tool, pencil tool, shape tools, the new trace function, included in the 2026 update, allows tracing of raster images (pixels), e.g. PNG files, and their direct conversion into editable vector graphics, **Fig. 2a** [3]. *Pixel Studio* is meant as an equivalent of *Adobe Photoshop*, a dedicated image editing module. Users can add pixel layers to paint or edit, keeping the original image quality intact, **Fig. 2b** [5].

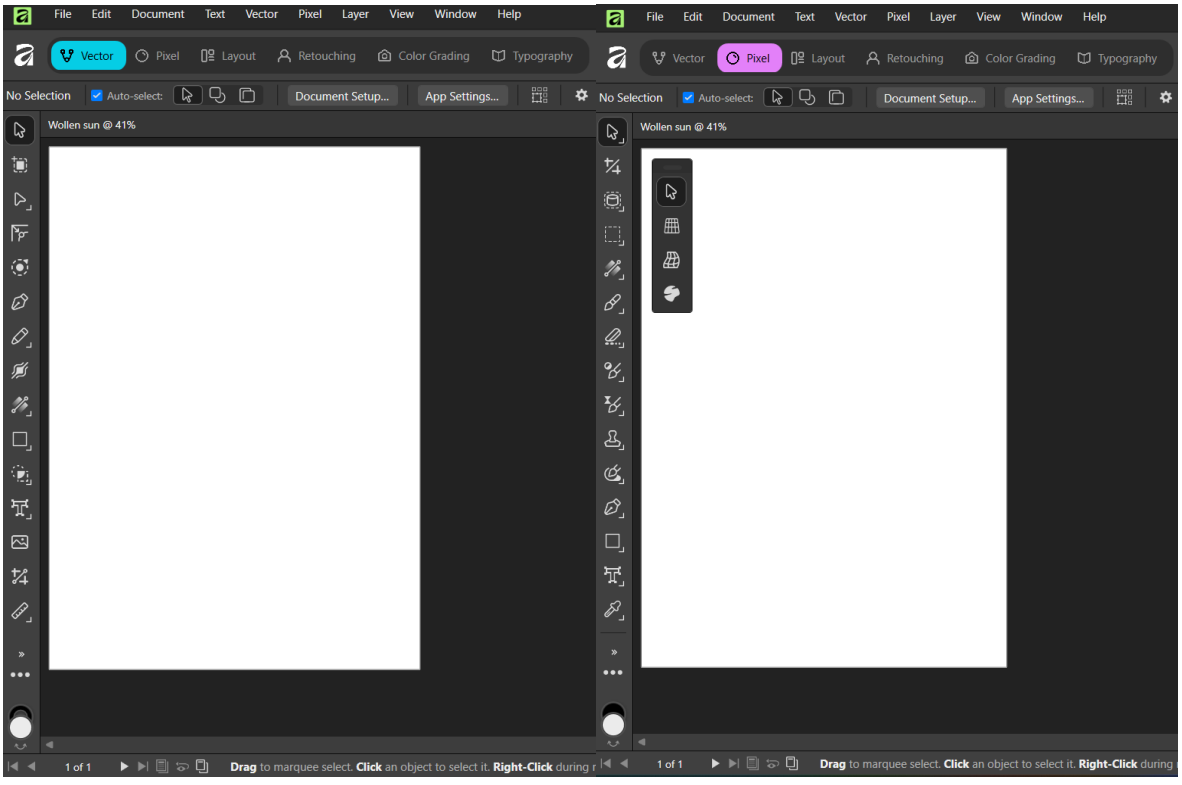

a) b)

***Fig. 2a,b**: Vector studio and Pixel studio*

Layout Studio is meant as the equivalent of *Adobe InDesign*, designed for creating complex multi-page layouts such as magazines, books, and brochures, providing essential tools for typography, master pages, and prepress settings, **Fig. 2c** [6].

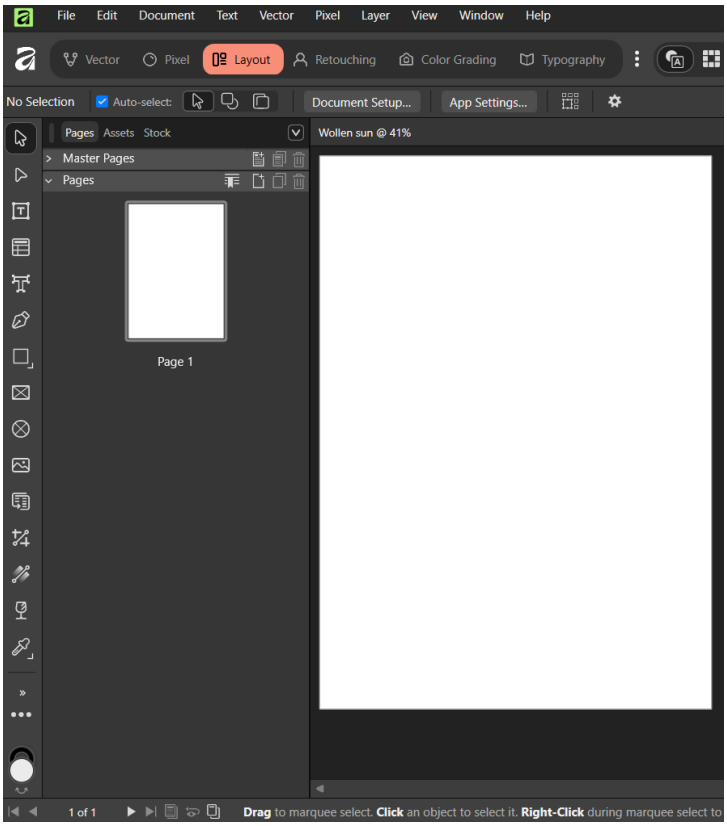

c)

Fig. 2*c: Layout studio*

Custom boards are also fully shareable, promoting the collaboration between users. Integration with *Canva Pro* offers a fourth studio, *Canva AI*, which includes features like fill, background removal and image and vector generation [2].

2. ACCESSIBILITY OF USING THE BLUR BRUSH TOOL IN AFFINTY VERSUS THE BLUR TOOL IN PHOTOSHOP AND ILLUSTRATOR

This part of the paper highlights the positive influence of *Affinity Studio* on work speed and how a vector graphic can be transfered from the *Vector Studio* in which it was created to the *Pixel Studio* just by switching between the studios. The chosen example is: creating a text in *Vector Studio*, editing it with the 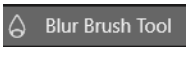

Blur Brush Tool, proper for the *Pixel Studio* and with 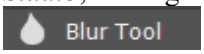

Blur Tool, proper for *Photoshop* and transfering the edited text to *Vector Studio* for further desired changes.

2.1 Affinity Designer

In the *Vector Studio*, we start by drawing a circle, for this we select from the toolbar, the shape tool, as shown in **Fig. 3a** and by holding the shift key we draw a circle **Fig. 3b**, which serves as a pattern for the text, which will follow the shape of the circle, **Fig. 3c**.

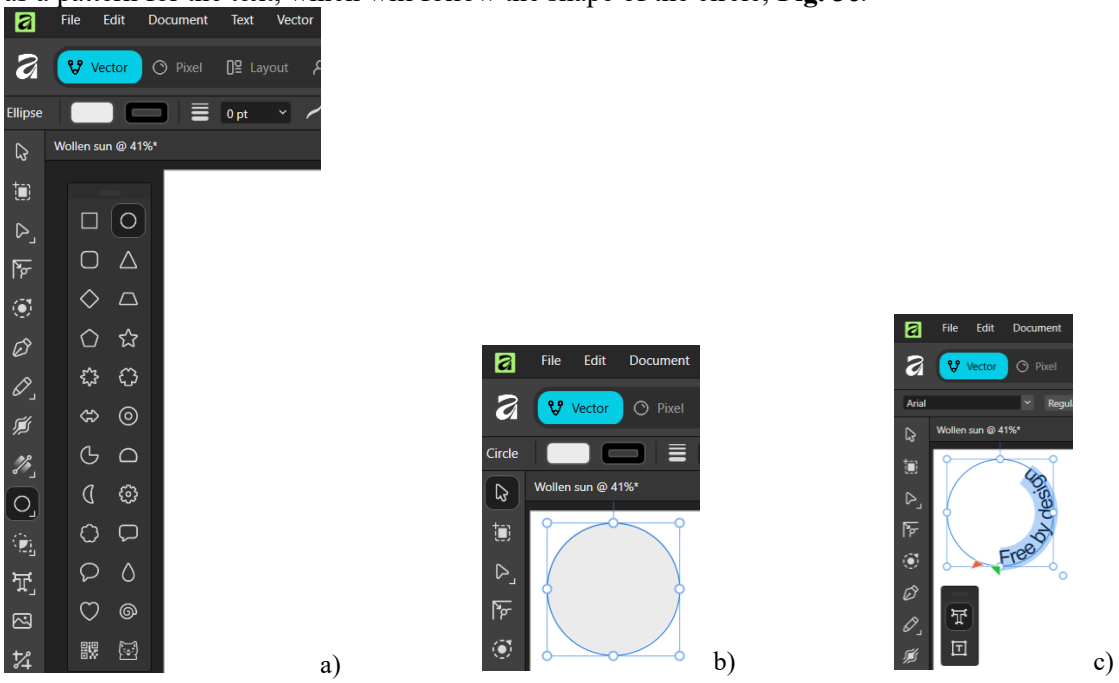

a) b) c)

***Fig. 3, a,b,c**: Drawing the circle and writing the desired text in Affinity*

We switch to *Pixel Studio*, as shown in **Fig. 4a** and from the menu bar we select the Blur Brush Tool 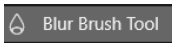

and we go over the text with the brush to give the text the desired blurry look, **Fig. 4b**. Thus, the text can be integrated into a graphic by simply switching and continuing in *Vector Studio*.

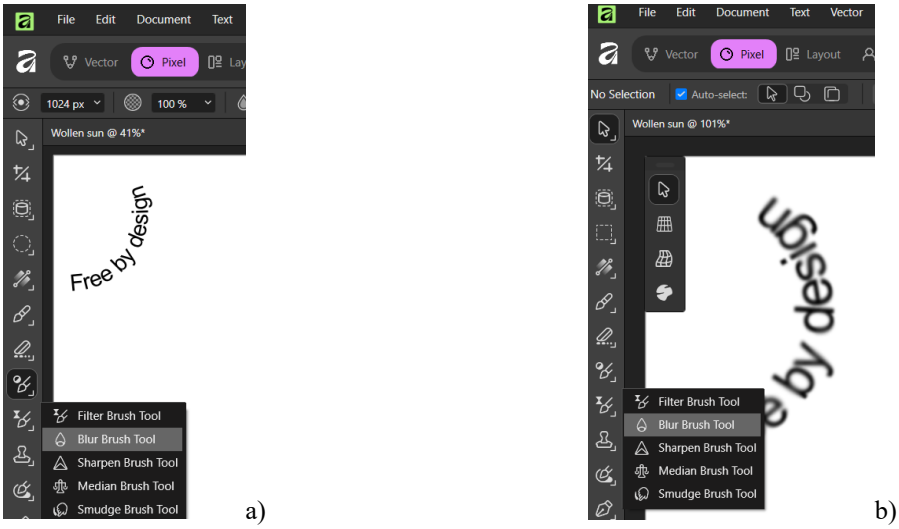

a) b)

***Fig. 4 a,b**: Switching to Pixel Studio and using the Blur Brush Tool*

2.2. Adobe Illustrator

In *Adobe Illustrator*, we also start by drawing a circle, for this we select the shape tool from the toolbar as shown in **Fig. 5a, b,** select the text tool, we choose the Type on path tool and we type the desired text following the shape of the circle, **Fig. 5c**.

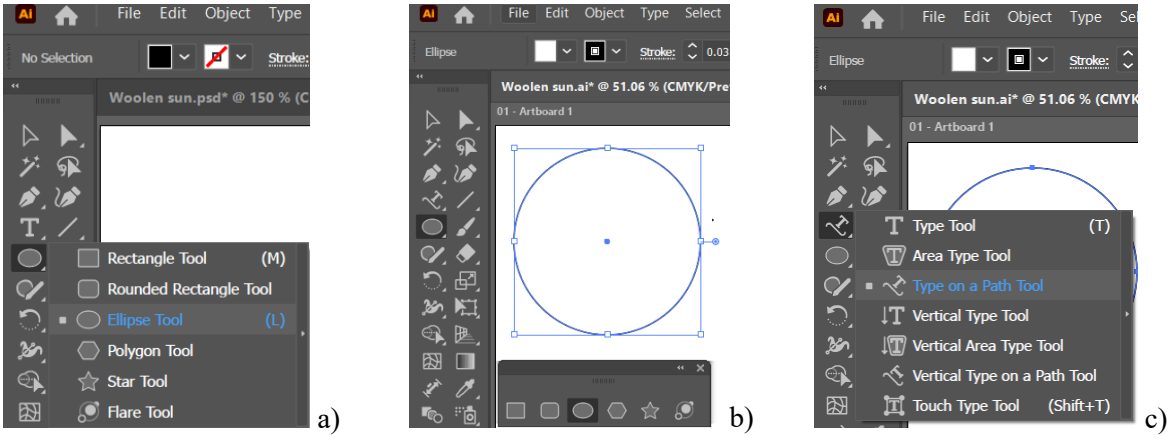

***Fig. 5a,b,c**: Drawing a circle and writing text in Adobe Illustrator*

To continue with the editing steps of the text, the *Illustrator* file must be imported or opened with *Adobe Photoshop*, so the user requires access to both apps *Illustrator* and *Photoshop*. [7], [8], [9] Once the file is open in *Photoshop* as shown in **Fig. 6a**, from the menu bar we select the Blur Tool 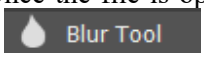

and we go over the text to give the text the desired blurry look as shown in **Fig. 6b**, the steps required to integrate the edited text into a vector graphic, in this case can be continued in *Illustrator*, **Fig. 6c**.

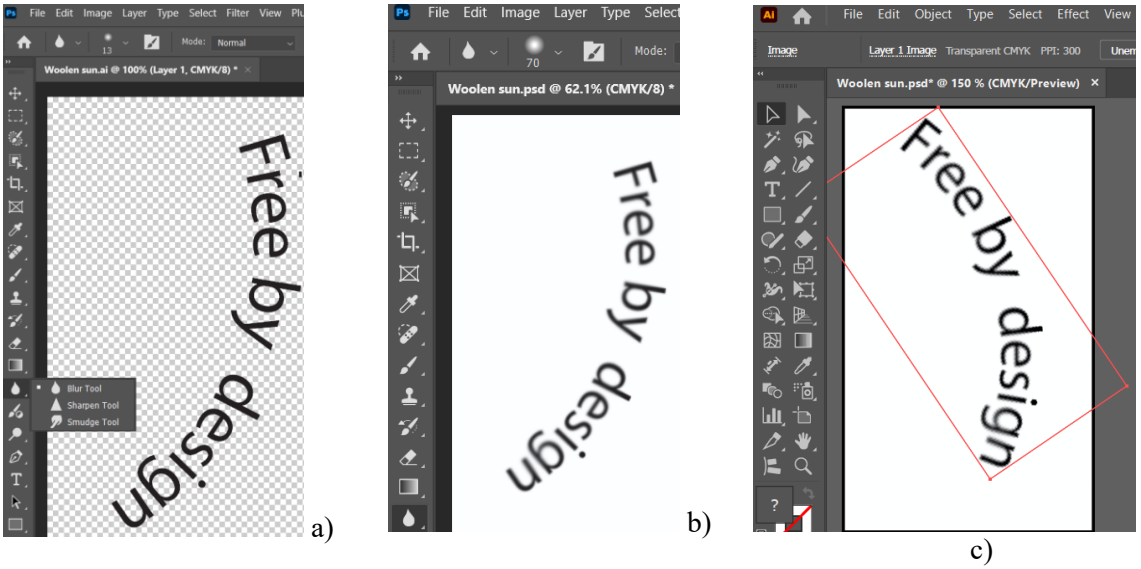

***Fig. 6, a,b,c**: Opening the text in Photoshop, editing, reopening the file in Illustrator*

3. CONCLUSIONS

The most important aspect that was highlighted in this paper is the hybrid workflow that allows the user to say goodbye to the window switching function, known as Alt+Tab for Windows and Command+Tab for Apple or requiring access to separate applications but completing their work in a single application, thus *Affinity Designer* is growing in popularity among freelancers, creative studios and illustrators due to improved work speed and reduced cost.

However, Adobe Illustrator remains the industry's standard, most companies, publishing houses and production studios (such as animation studios that use After Effects) depend on native Adobe formats, this is where the experience and longevity in the market of over 30 years comes into play.

The choice between *Illustrator, Photoshop, Indesign* and *Affinity Designer* for vector graphics, photo editing and creating layouts for magazines or books should no longer be seen as a dispute between master and amateur, but the choice should be based on the working style and available resources.

BIBLIOGRAFIE

[1] "Canva Relaunches Affinity as Free App," *MacRumors*, Oct. 31, 2025. [Online]. Available: https://www.macrumors.com/2025/10/31/canva-relaunches-affinity-free-app/. Accessed: Apr. 10, 2026.

[2] "Affinity Download," *Affinity Studio*. [Online]. Available: https://www.affinity.studio/download. Accessed: Apr. 10, 2026.

[3] "Affinity Designer: How to Use the Pixel Persona," *DesignHost*. [Online]. Available: https://designhost.gr/topic/10036-affinity-designer-how-to-use-the-pixel-persona/. Accessed: Apr. 20, 2026.

[4] "Adobe vs Affinity: 2025 Update," *Jump Design Print*. [Online]. Available: https://www.jumpdp.com/latest-news/adobe-vs-affinity-2025-update. Accessed: Apr. 4, 2026.

[5] "Affinity vs Adobe," *XP-PEN Blog*. [Online]. Available: https://www.xp-pen.com/blog/affinity-vs-adobe.html. Accessed: Apr. 10, 2026.

[6] "Graphic & Vector Design Software | Creative Freedom | Affinity," *Affinity*. [Online]. Available: https://affinity.serif.com/. Accessed: Apr. 4, 2026.

[7] M. D. Șuteu, G. L. Rațiu, and N. A. Andreescu, "Using the golden ratio principle to create a continuous print by means of the graphic program Adobe Illustrator®," *Annals of the University of Oradea, Fascicle of Textiles, Leatherwork*, vol. 23, no. 1, pp. 51–64, 2022.

[8] M. D. Șuteu, G. L. Rațiu, and N. A. Andreescu, "Applicability of Adobe Illustrator® program in accomplishing technical-graphic drawings in the textile industry," *Annals of the University of Oradea, Fascicle of Textiles, Leatherwork*, vol. 21, no. 2, pp. 81–86, 2020.

[9] M. D. Șuteu, G. L. Rațiu, and L. Doble, "The interconnection of the programs Adobe Illustrator® and Adobe Photoshop® and their applicability in the textile industry," *Annals of the University of Oradea, Fascicle of Textiles, Leatherwork*, vol. 19, no. 1, pp. 101–104, 2018

ANNALS OF THE UNIVERSITY OF ORADEA
FASCICLE OF TEXTILES, LEATHERWORK

CIRCULAR BUSINESS MODELS AS A MODERNISATION STRATEGY FOR THE FASHION INDUSTRY IN THE REPUBLIC OF MOLDOVA

SCRIPCENCO Angela

Technical University of Moldova, Faculty of Design, Department of Design and Textile Technology, MD 2004, bd. Stefan cel Mare, 168, Chisinau, Republic of Moldova, E-Mail: angela.scripcenco@dtt.utm.md

Corresponding author: Scripcenco, Angela, E-mail: angela.scripcenco@dtt.utm.md

Abstract: *This article examines the relevance of circular business models for the fashion industry in the Republic of Moldova, with particular attention to the structural advantages of a small market and the practical implications for local firms. It proceeds from the premise that circular business models can reduce dependence on the continuous production of new garments by extending product life, retaining material value, and generating revenue through repeated use. The analysis focuses on the suitability of such models within the Moldovan context, where geographic proximity, shorter logistics loops, the persistence of tailoring and repair skills, and the operational flexibility of small and medium-sized enterprises create favourable conditions for gradual circular transition. While the article remains primarily conceptual, it is supplemented by illustrative observations from local apparel practice, which help to ground the discussion of repair, remaking, take-back, and controlled resale in the context of a small economy. The article argues that the most feasible entry points for local companies are repair services, the remaking of deadstock materials, brand-led take-back schemes, and controlled resale formats. By contrast, rental models are considered more appropriate for narrowly defined segments characterised by occasional use or rapid product turnover. In this sense, circular business models are presented not only as an environmental response, but also as a practical pathway for market modernisation and improved resource efficiency.*

Keywords: *circular economy; circular business models; fashion industry; repair; remaking; resale; small market.*

1. INTRODUCTION

The fashion industry is increasingly confronted with the need to reconcile economic performance with environmental responsibility. For several decades, the dominant model of growth in the sector has been based on high volumes, rapid turnover, and short product lifecycles. This linear logic of production and consumption has generated significant environmental pressures, including resource depletion, textile waste, and the loss of value embedded in garments after relatively limited use. In response, circular economy thinking has gained prominence as a framework through which the fashion sector may reduce waste, extend product lifespans, and generate value through more efficient systems of use, recovery, repair, and redistribution.

Within this broader context, the Republic of Moldova presents a particularly relevant case. The Moldovan fashion market is currently at a point of transition, positioned between a strong industrial legacy and the growing need to adapt to contemporary sustainability imperatives. Although

the domestic market is relatively small, it remains dynamic and structurally complex. Its current configuration is marked by a pronounced duality: on the one hand, local brands, including those promoted under the DININIMA umbrella, have succeeded in drawing upon local identity, domestic production, and cultural authenticity; on the other hand, international fast-fashion retailers continue to dominate sales volumes through aggressive pricing strategies and wide product accessibility.

At the same time, the structure of the market remains highly fragmented. A clear contrast exists between official distributors operating in modern retail environments and the extensive network of small independent traders supplying a more informal and often weakly regulated segment of the market. In this setting, consumer behaviour in Moldova reflects a persistent contradiction. Limited purchasing power constrains access to premium products, yet there is also a strong aspiration to align with global fashion trends. This combination reinforces dependence on a linear consumption model characterised by frequent purchase, short-term use, and disposal.

These conditions generate several pressing challenges, including the accumulation of unsold stock and the inadequate management of textile waste, both of which place increasing pressure on local infrastructure. However, the Republic of Moldova also possesses two strategic advantages that deserve closer consideration. The first is proximity. Owing to the country's small geographical scale, activities such as collection, sorting, repair, and redistribution may be organised more quickly and at lower cost than in larger markets, where reverse logistics are usually more complex and resource-intensive. The second is cultural capital. Moldova retains a living culture of repair, supported by a dense network of tailoring and alteration workshops and by longstanding practices of mending and reconditioning garments. Rather than being regarded as residual features of the past, these capabilities may serve as an operational foundation for the development of circular business models.

From this perspective, the transition to circularity should not be understood solely as an environmental obligation. In the Moldovan context, it may also be interpreted as a practical strategy for improving resource efficiency, strengthening local competitiveness, and modernising a market that already possesses important human and organisational preconditions for more extended and intelligent forms of product use.

Against this background, the present article examines the relevance of circular business models for the fashion industry in the Republic of Moldova. It proceeds from the premise that such models can reduce dependence on the continuous production of new garments by keeping products and materials in use at their highest possible value. Particular attention is given to the advantages associated with a small market, the barriers that may constrain implementation, and the most realistic entry points for local companies. The article argues that repair services, remaking based on deadstock, brand-led take-back schemes, and controlled resale formats are especially promising for the Moldovan context, whereas rental models appear more suitable for narrowly defined categories characterised by occasional use or rapid turnover. Although the analysis is conceptual rather than empirical, it proposes a structured framework for understanding how circular business models may contribute to the modernisation of the local fashion sector.

Methodologically, the article combines conceptual analysis of circular business models with brief illustrative observations from local apparel practice in the Republic of Moldova. These observations are not presented as a full empirical dataset, but as grounded examples intended to test the practical plausibility of repair, remaking, take-back, and resale strategies in a small-market context.

2. CONCEPTUAL FRAMEWORK OF CIRCULAR BUSINESS MODELS

In a circular economy, economic value is preserved by keeping products and materials in use for as long as possible and at the highest feasible level of utility. Circular business models decouple

revenue streams from the continuous production of new goods and from the intensive consumption of virgin resources. Their logic is not merely to sell more units, but to generate value through repeated use, prolonged use, repair, redistribution, and transformation [1], [6].

For the fashion sector, four models are especially important. Resale transfers a product to a new user after its first phase of ownership. Rental provides temporary access instead of permanent ownership. Repair extends the useful life of a product already in circulation. Remaking creates new products or product components from existing garments or materials. These models are best understood not as marginal add-ons, but as alternative ways of organising revenue around the same material base [1]. The economic potential is substantial. According to the Ellen MacArthur Foundation, resale, rental, repair, and remaking represented a market of approximately USD 73 billion in 2019 and, under favourable conditions, could grow to nearly USD 700 billion by 2030 [1]. Their environmental relevance is also considerable. If these models reached 23% of the global fashion market by 2030, they could contribute to an overall reduction of up to 16% in fashion-sector CO2e emissions, which would amount to roughly one third of the abatement required for a 1.5 degrees Celsius pathway [1], [3]. In a small-market context such as Moldova, these general advantages may be reinforced by shorter logistics loops, closer customer contact, and the continued presence of repair-oriented skills.

The benefits of circular models are not automatic. The Ellen MacArthur Foundation warns that models such as resale and rental may fail to reduce pressure on resources when they remain only superficial extensions of a core linear business that continues to incentivise the sale of new garments at high volume [1]. Three conditions are therefore decisive. First, performance indicators must reward longer use, customer retention, recovery rates, and value recapture rather than simple sales volume. Second, products must be designed for multiple use cycles, which means physical durability, emotional durability, reparability, and the ability to be remade or recycled at the end of use. Third, companies need service and logistics networks able to support collection, inspection, cleaning, repair, redistribution, and data tracking [1], [4], [5].

3. THE RELEVANCE OF CIRCULAR BUSINESS MODELS TO A SMALL MARKET

For small economies, the strongest argument in favour of circular business models is *proximity and shorter logistics loops*. Shorter geographical distances can reduce the cost and complexity of collection, sorting, cleaning, repair, and redistribution. In practical terms, this means that the time between return, refurbishment, and re-entry into the market may be shorter, whilst inventory that would otherwise remain idle can be recirculated more efficiently. What is logistically difficult in a large territory may be commercially manageable in a compact one.

A second advantage concerns *skills and operational flexibility* already present in the local economy. Repair, alteration, and the transformation of garments are not entirely new activities in Moldova. The continued existence of tailoring workshops, small sewing businesses, and alteration services means that at least part of the practical infrastructure for repair and remaking is already available. Circularity, in this sense, does not begin from zero; it formalises and scales practices that are already familiar to both firms and customers. A third advantage is the *flexibility* of small and medium-sized enterprises. SMEs can usually test new services more quickly than large mass-market chains. They can adjust collections, collaborate with local partners, and refine pilot programmes on the basis of customer feedback without redesigning an entire global supply system. For a market such as Moldova, this capacity for limited experimentation is highly relevant, because circularity is more

likely to succeed when introduced through staged pilots than through large, capital-intensive transformation from the outset.

Customer knowledge and closer market feedback is another advantage. Small markets also allow firms to stay closer to their customers. Circular models rely on understanding why products are returned, which defects occur most often, how frequently repairs are requested, and what levels of quality, style, and hygiene customers expect. In a compact market, these signals can be collected and translated into product and service decisions more rapidly. This creates favourable conditions for iterative business model development.

4. PRIORITY CIRCULAR MODELS FOR LOCAL COMPANIES

For Moldovan companies, *repair and remaking* appear to be the most realistic entry points. They require less behavioural change from the customer than rental and less brand repositioning than large-scale resale platforms. A firm can begin with after-sales repair, paid alterations, warranty-linked mending, or the transformation of slow-moving and deadstock items into limited capsule products [7]. Actually, such small workshops present in Malls. These activities extend product life, recover value from unsold materials, and strengthen customer trust in product quality. Remaking is especially relevant where deadstock fabrics, unsold garments, or returned products accumulate in storage. Instead of writing these items off entirely, firms can redesign them into accessories, revised garments, or small experimental collections. This is not merely an environmental measure; it is also a margin-protection strategy for businesses operating with limited financial buffers.

A second promising direction is the development of *take-back schemes* linked to controlled resale. In this model, the brand retains greater control over product condition, hygiene, presentation, pricing, and customer experience than it would have in the informal second-hand market. The *resale* offer can therefore be presented not as a low-status residual channel, but as a curated and quality-assured extension of the brand. In the Moldovan context, however, such schemes should be designed carefully. If customer incentives are structured only as discounts on new products, the programme may stimulate additional new consumption rather than genuine displacement of virgin production. A better approach is to link take-back to retention and loyalty, to offer controlled store credit, and to use recovered products selectively where inspection, repair, and cleaning can be performed to a reliable standard [1].

***Table 1**: Recommended directions for integrating circular models*

Model	Why it is suitable for Moldova	Recommended first step
Repair	Local workshops would reduce loss of value after sale.	Launch of after-sales service with repairs.
Remaking	Dead stock would turn into new products.	Small capsules made from deadstock
Resale	Take advantage of brand proximity.	Own buy-back program
Rental	Occasional and high price categories.	For ceremonial attire or children's clothing.

Rental should be approached more cautiously. The model can be effective where garments are used only occasionally but carry a relatively high purchase price, such as occasion wear, formalwear, or selected childrenswear categories (for example wedding clothes, children carnaval clothes). In such segments, the number of wears per item can increase substantially, making the model more viable both economically and environmentally [1]. By contrast, rental is less suitable as an immediate mass-

market strategy where garments are not designed for repeated cleaning and repeated handling, or where customers are reluctant to share everyday clothing. For local firms with constrained resources, a narrow rental is more prudent.

5. MAIN BARRIERS AND RISKS

One barrier remains cultural because of *consumer perceptions and the stigma of second-hand use*. Although attitudes are changing, some consumers still associate reused garments with lower status, lower quality, or hygiene concerns. This means that circular offers must be framed carefully. Language such as 'pre-owned', 'archive', or 'restored' may be commercially more effective than labels associated with low-value informal trade.

A second barrier is *weak infrastructure and limited policy incentives*. Moldova does not yet have a mature textile collection, sorting, and recirculation system at national scale. As a result, much of the organisational burden falls directly on the company. In addition, fiscal and regulatory incentives for repair and textile recovery remain limited, even though European policy is increasingly moving in the direction of circularity and product longevity [4], [5].

A third barrier is strategic *as a risk of poorly designed incentives*. A circular initiative can fail if it is measured by the wrong indicators. When firms reward take-back primarily through discounts on new products, or when they count success only in terms of gross sales, the programme may reinforce rather than reduce the linear flow of production and disposal. This risk is particularly important in small markets, where margins are already narrow and poorly designed promotions can quickly erode profitability [1].

6. RECOMMENDATIONS FOR LOCAL COMPANIES

Start with small pilots and measurable targets. Local firms should begin with limited pilots rather than with a full-scale transformation. A pilot repair service, a deadstock capsule, or a small take-back scheme provides operational evidence at relatively low risk. Each pilot should be linked to measurable indicators, such as repair rate, resale conversion, recovery rate, average number of uses, margin per recovered item, and customer retention.

Formalise partnerships with local workshops. Where internal repair capacity is limited, brands should build structured partnerships with local tailoring workshops. Such partnerships can lower logistics costs, shorten service times, and preserve quality through clear specifications and simple service-level agreements. In a small market, these local service networks may become a core competitive asset.

Use take-back as a retention tool, not as a discount engine. Take-back schemes should not be designed simply to accelerate the sale of new items. They should be used to retain customers, recover products fit for recirculation, and create data about product durability and customer behaviour. Store credit may still be appropriate, but its role should be to support recirculation and loyalty rather than indiscriminate volume growth.

Introduce simple digital product tracking. Even modest digital tools can improve circular operations. QR codes, basic product passports, or internal item histories can record collection date, repair actions, material composition, and care requirements. This is particularly useful for resale and rental, where trust depends on traceability and condition management.

Align circularity with brand positioning. Circularity should not be presented as a detached ethical add-on. For local firms, it is more effective when linked to quality, craftsmanship, durability,

and smart value. This is especially relevant in Moldova, where customers may respond better to arguments about quality and economy than to abstract environmental claims alone.

Build cross-sector collaborations. Where direct recirculation is no longer possible, firms should seek cross-sector uses for textile remnants and unusable returns. Partnerships with design studios, interior applications, educational workshops, or social enterprises may create secondary outlets for material that would otherwise become waste. Such collaboration will not solve the whole problem, but it can reduce losses and stimulate local circular ecosystems.

7. CONCLUSIONS

In the case of the Republic of Moldova, circular business models represent a practical route towards greater resilience, improved stock management, stronger customer retention, and closer alignment with the broader European transition towards circularity. At the same time, the revised analysis suggests that their relevance is not only conceptual. Illustrative observations from local apparel practice indicate that repair, alteration, limited-batch remaking, and direct customer relationships already provide part of the operational basis from which gradual circular experimentation may develop. Small markets require specific analysis, since their scale, logistics, retail structure, and consumer behaviour shape the feasibility of circular strategies in distinctive ways. The Moldovan case suggests that such markets may also possess underexplored advantages. Geographic proximity can reduce the cost and complexity of collection, repair, redistribution, and other reverse-logistics activities, while the continued presence of tailoring and alteration skills provides a strong basis for product-life-extension models. More broadly, the example of the Republic of Moldova may be relevant for other small markets with similar structural features. However, such applicability depends on careful contextual analysis rather than direct replication. For this reason, the transition to circularity should remain gradual, evidence-based, and commercially disciplined. When combined with stronger service design, clearer performance indicators, and modest digital support, circular business models can become not only an environmental objective, but also a viable strategy for market adaptation and modernisation.

REFERENCES

[1] Ellen MacArthur Foundation, Circular Business Models: Redefining Growth for a Thriving Fashion Industry, 2021.

[2] Ellen MacArthur Foundation, A New Textiles Economy: Redesigning Fashion's Future, 2017.

[3] McKinsey & Company and Global Fashion Agenda, Fashion on Climate: How the Fashion Industry Can Urgently Act to Reduce Its Greenhouse Gas Emissions, 2020.

[4] European Commission, A New Circular Economy Action Plan: For a Cleaner and More Competitive Europe, COM(2020) 98 final, Brussels, 2020.

[5] European Commission, EU Strategy for Sustainable and Circular Textiles, COM (2022) 141 final, Brussels, 2022.

[6] N. M. P. Bocken, I. de Pauw, C. Bakker and B. van der Grinten, "Product design and business model strategies for a circular economy," Journal of Industrial and Production Engineering, vol. 33, no. 5, pp. 308–320, 2016.

[7] Studii de caz: Afaceri circulare în industria textilelor și a îmbrăcămintei, 2026, [Online]. Available: https://e-circular.org/resurse/afaceri-circulare-in-industria-textilelor-si-a-imbracamintei/

ANNALS OF THE UNIVERSITY OF ORADEA
FASCICLE OF TEXTILES, LEATHERWORK

CREATION CLOTHING PRODUCTS PATTERNS WITH THE HELP OF A MANNEQUIN FOR CLOTHING DESIGN

ȘIMON Andreea Anca[1], ALBU Adina-Victoria[2]

[1, 2] University of Oradea, Faculty of Energy Engeenering and Industrial Management, Department of Textiles, Leather and Industrial Management, Universitatii Street no 1, 410087, Oradea, Romania

Corresponding author: Șimon, Andreea Anca, E-mail: anca.simon@yahoo.com

Abstract: *These The industrial manufacturing of clothing products involves obtaining, with great flexibility and speed, the patterns necessary to make the products. Now, nowadays, it is possible to draw them with the help of computing techniques, through software dedicated to this design process. Considering these aspects, what is wanted in this paper is to carry out, with the help of a dimensionally adjustable mannequin and with the help of a high-performance apparatus for taking and processing photographed images, a study through which the mannequin is obtained virtual. In this way, as many anthropometric measurements as possible were used on people with different shapes and sizes, so that the creation of mannequins for fashion design and then the construction of patterns for the various clothing products could ensure consumer demand. This virtual mannequin was created starting from the knowledge about the anatomical structure of the human body and especially its external shape, and after researching the possibilities of geometric modeling of curves and surfaces, it was possible to obtain the complex shapes of the human body. The work aims to create a virtual mannequin for clothing design, whose shapes and sizes can change depending on the dimensional typology of the population. In the end, it was passed to the computerized obtaining of the patterns for the clothing products.*

Key words: *virtual, 3D shapes, mannequin, pattern, clothing, AutoCad*

1. INTRODUCTION

In the conventional technology of obtaining clothing products, they are made from a different number of pieces, cut from flat materials and assembled by different processes. The fundamental problem of clothing construction is the adaptation of flat textile structures to the irregular shape of the human body and solving this problem conditions the correct position of the product on the body and its functionality. Patterns represent the unfolded planes of the landmarks of the clothing products, whose shape and dimensions must be correlated with the shape and dimensions of the human body.

The classical method of pattern construction, still widely used, is the geometric method, the method that is the basis of pattern construction and modern methods, based on the calculation technique. In the geometric method, the construction of patterns is performed based on information about the dimensions of the human body and the size of the additions corresponding to the type of product being designed. In construction, one starts from a limited number of main dimensions of the type of body, and the other secondary dimensions are calculated based on some relationships, mostly proportional, relationships that differ according to the authors of the different variants of the method,

which is a disadvantage. Another disadvantage, from the point of view of calculations, is the gradation of the patterns, obtaining the patterns for the entire dimensional range in which a clothing product is made [1].

2. METHODS OF CREATING PATTERNS WITH AN ADJUSTABLE MANNEQUIN ASSOCIATED WITH THE COMPUTER

A faster and easier way to make patterns for clothing products is to use the InSpeck Halfbody machine together with the software attached to this machine and with the parallel use of the AutoCad software. To better understand how the InSpeck Halfbody device works, a brief description of this device and its operating principle will be made in the following.[2]

Carrying out the actual investigation, i.e. taking images for the purpose of 3D reconstruction of the surface of interest, requires a special space, which fulfills a series of conditions regarding the dimensions, shape, lighting characteristics, as well as facilities regarding the electricity supply.

The InSpeck system, in various configurations (1 to 4 cameras) is intended for 3D digitization. The 3D digitization technique allows obtaining a three-dimensional copy of a certain physical surface. In the optical digitization process, each camera takes an image consisting of a set of level surfaces, from different angles. The separate images are connected at predetermined points so that a total field angle of 360 degrees is ensured by soft processing. The retrieved images partially overlap so that they contain the preset connection points. The InSpeck technique allows not only the reconstruction of the shape, but also the rendering of the color and texture of the target surfaces.

***Fig. 1**: 3D Mega Capturer II camera*

The content and location of the InSpeck Halfbody device is presented in the following:

- 3 rooms. The cameras used are of the 3D Mega Capturer II type with support, as in the image in **Fig.1**, they are composed, and in addition to the camera itself, it also includes a vertical support with a guide for translational movement and a camera locking mechanism in the position established to satisfy the condition of optical alignment, as well as a support - sole for supporting and fixing the other elements;
- a PC for data retrieval and access processing (**Fig. 2**).
- a closed enclosure with professional lighting for placing the cameras in a position established by the manufacturer, and this placement is done as in the image in **Fig.3**.

***Fig. 2**: PC for data acquisition and processing*

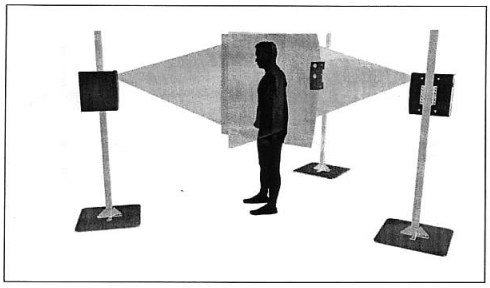

***Fig. 3**: Premises for the location of the rooms*

The operating method of the InSpeck Halfbody device uses the imaging investigation technique together with specific software applications: FAPS (Fringe Acquisition and Processing Software) and EM (Editing and Merging). Their installation follows the installation of the drivers for the three digital cameras. The FAPS program identifies the three cameras that it will recognize during all subsequent uses based on the serial numbers written by the manufacturer on the camera housing. To determine such images with digitized physical surfaces, considering that the image acquisition is done optically, it is very important to calibrate the acquisition system, an operation that generates residual information throughout the use of FAPS and EM [3].

3. CALIBRATION OF DATA ACQUISITION EQUIPMENT

Calibration represents a procedure of relating, on a given domain, between the coordinates measured by a device and the coordinates accepted in a standard reference system.

In the case of the InSpeck acquisition system, the cameras take one image from the real space from three conical perspectives with concurrent axes, and the coordinates of these perspectives must be transformed into coordinates related to a Euclidean system. This operation ensures the virtual reconstruction of the real surface at a level of similarity that satisfies a submillimeter precision condition.

For calibration, in principle, any shape can be used, provided that its characteristic points have known coordinates. The InSpeck supplier delivers with the equipment a panel with holes placed at calibrated distances (**Fig. 4**).

For the acquisition of the images, it is necessary that the ambient lighting be sufficiently uniform so as not to introduce stray shadows.

***Fig. 4**: Panel with holes placed at calibrated distances*

4. MANNEQUIN IMAGE PROCESSING

With the help of FAPS, the images are acquired by the three cameras in the system and separate files related to each image are generated.

The study is carried out on the adjustable mannequin, whose three main perimeters can be dimensioned: Pb (bust perimeter), Pt (waist perimeter) and Pş (hip perimeter), according to anthropometric standards and according to the dimensional range in which we want to make a clothing product.

The preparation of the mannequin for this study consists in fixing some adhesive tapes on its surface, so that the tapes follow the main contour lines of the body, necessary for making the patterns.

Thus, the following were followed: the line of symmetry of the face, the line of the cut of the neck to the front, the line of the cut of the sleeve to the front, the line of symmetry of the back, the line of the cut of the neck to the back, the line of the cut of the sleeve to the back, the assembly line of the face to the back, as well as the main width sizing lines of the patterns (bust line, waist line and hip line).

After fixing the strips, the anthropometric points specific to the construction of the patterns are positioned, as well as the control points necessary for taking and processing the images [4].

The following figures (**Fig. 5**; **Fig. 6**; **Fig. 7**) show the images of the mannequin, as they are to be used for the 3D reconstruction in a single image.

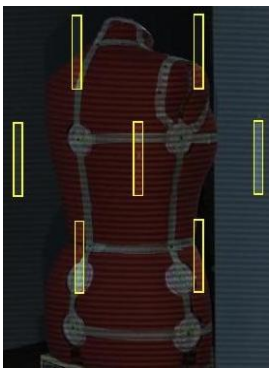

***Fig. 5:** Mannequin image provided by camera 1*

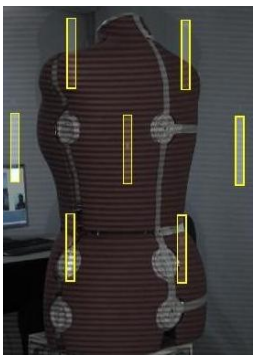

***Fig. 6**: Mannequin image provided by camera 2*

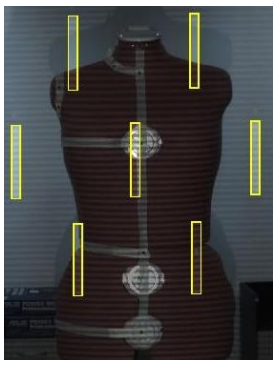

***Fig. 7**: Mannequin image provided by camera 3*

5. EDITING AND PROCESSING OF PURCHASED IMAGES

In addition to the acquisition of images, the FAPS program also offers the possibility of editing and processing them.

Several ways of editing and processing the acquired images to obtain the 3D model in EM are explained in the following observations.

1. After the images have been purchased, proceed to their processing by cutting out the area of interest, i.e. the mannequin. Cutting out the area of interest is done with the help of some tools of the FAPS program menu, this is done according to the following algorithm:

- select the cropping tool of the image of interest from the menu, then enlarge the image to achieve the best possible cropping.
- after choosing the area of interest, proceed to the actual cutting, which looks like the figures in the following images (**Fig.8, Fig.9, Fig.10**).

***Fig. 8**: Image 1 of the mannequin, provided by camera 1 and processed*

***Fig. 9**: Image 2 of the mannequin, provided by camera 2 and processed*

***Fig. 10**: Image 3 of the mannequin, provided by camera 3 and processed*

2. After cutting out the area of interest, proceed to a new stage of image processing. This consists in the appearance of a parallax image in which only the area of interest appears with the calibration points where an X is located, and if this X does not appear, it means that the marked area has an error that must be repaired. This error may be due to improper cropping. To solve this problem, the manufacturer and the staff who use this equipment suggest in this case a move of the points, which appear on the outline of the img3 mannequin, to another defining position (**Fig.11**).

3. The following images represent the area of interest, the area that will be exported in EM to make the 3D model [5].

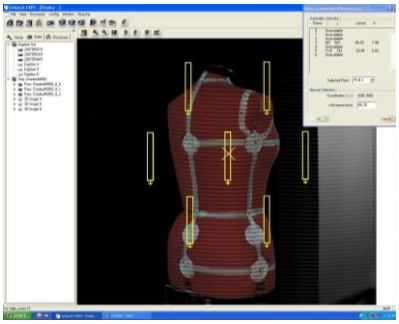

***Fig. 11**: Image with the area where the X is must be an area on the mannequin*

After the images have been processed in FAPS, the aim is to create the model in EM (**Fig. 12**). As in FAPS and EM, there are a series of stages that must be completed to reach the 3D model from which the data will be taken to make the patterns of the clothing products.

The EM processing program presents the following facilities:

- opening and viewing 3D models
- correcting model defects (closing gaps, cutting overlaps)
- selection of some polygonal shapes
- editing models
- scaling
- creating symmetrical models
- interpolations
- measuring distances

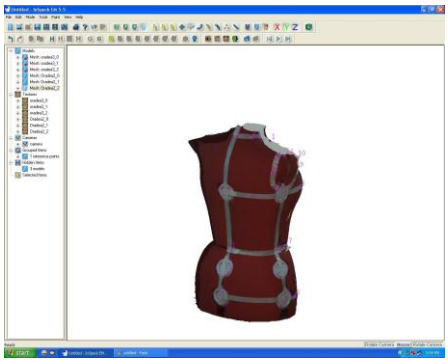

***Fig. 12**: Image of the graphical interface of the EM program*

6. EXPERIMENTAL RESULTS

In EM, after creating the 3D model, with the help of the 3 images processed in FAPS and by calibrating them in EM with the help of a calibration matrix, the next step is to mark the points of interest on the mannequin and through this marking I get the coordinates of the points on the mannequin, coordinates that will be saved in files created in EM that can be exported to various other software, which allow more complex numerical determinations, but easy to perform.

In this case, saving is done in "txt" format, a format that looks like the image in **Fig.13**.

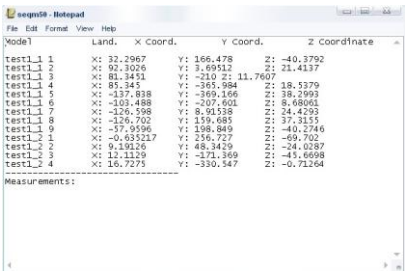

Model	Land.	X Coord.	Y Coord.	Z Coordinate
test1_1 1		X: 32.2967	Y: 166.478	Z: -40.3792
test1_1 2		X: 92.3026	Y: 3.69512	Z: 21.4137
test1_1 3		X: 81.3451	Y: -210 Z: 11.7607	
test1_1 4		X: 85.345	Y: -365.984	Z: 18.5379
test1_1 5		X: -137.838	Y: -369.166	Z: 38.2993
test1_1 6		X: -103.488	Y: -207.601	Z: 8.68061
test1_1 7		X: -126.598	Y: 8.91538	Z: 24.4293
test1_1 8		X: -126.702	Y: 159.685	Z: 37.3155
test1_1 9		X: -57.9596	Y: 198.849	Z: -40.2746
test1_2 1		X: -0.635217	Y: 256.727	Z: -69.702
test1_2 2		X: 9.19126	Y: 48.3429	Z: -24.0287
test1_2 3		X: 12.1129	Y: -171.369	Z: -45.6698
test1_2 4		X: 16.7275	Y: -330.547	Z: -0.71264

Measurements:

***Fig. 13**: Image of the "txt" file with the coordinates of the points extracted from EM*

A special procedure is required to perform this rescue, following certain steps, namely:

- after opening the marking tool within the EM program and selecting the points of interest, a save is made by the name of the file with the ending "txt".

- after finishing this procedure, open the "txt" file from the folder where it was saved and proceed to the next step, namely entering the coordinates in AutoCad.

The AutoCad program is a 2D or 3D design software that has a series of tools for making different drawings, and in this case, as it is about patterns for clothing products, they will be made with the help of the program. In AutoCad, the coordinates of each point are manually entered in the command line and a series of points in a 2D space is obtained, based on the coordinates entered in the command line.

After entering the points in AutoCad, select the "line" from the tools menu and join the points with it. In order for the pattern to be complete and usable, the points are joined together with lines, thus obtaining patterns for the front and back respectively of the clothing product, and with the help of the AutoCad program, its scale can be increased or decreased (**Fig. 14**).

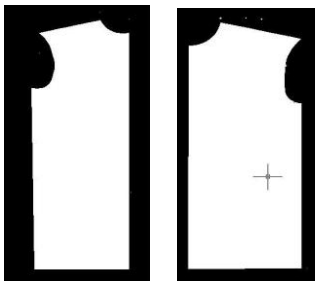

***Fig. 14**: The images of the back and front patterns, processed in AutoCad*

Another possibility that the AutoCad program offers for obtaining the best possible pattern is to fill the area of the template with a solid shape and thus be able to plot the template, and the result obtained being a template that can be used immediately [6-7].

Both the front of the template and the back were made in AutoCad at a scale of 1:5, a scale that could not be maintained in word format, but by directly plotting the template in AutoCad the desired size is obtained. Following the processing of the patterns and the corrections made to the characteristic points on their outline, the images in **Fig.15** will be obtained.

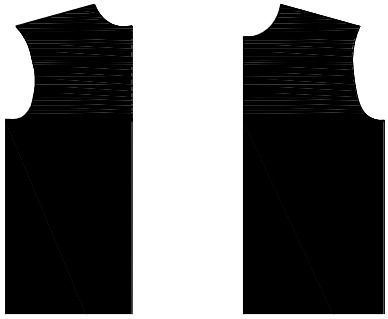

***Fig. 15**: The images with back and front patterns, processed in AutoCad, made on a scale of 1:5*

7. CONCLUSIONS

This paper aims to use up to 3 different sizes during the mannequin measurement operation. Each size taken requires a new sizing of the mannequin, which being adjustable makes this easy. The steps to get all the patterns involve the same methods shown previously.

To make the models of the clothing products, the front and back marks are completed by introducing lightness additions, necessary for freedom of movement and breathing, or additions dictated by fashion, depending on the silhouette of the product and the desired model.

This new method of creating models for clothing products, in a wide range of sizes, with the help of the adjustable mannequin, requires some improvements, which, once achieved, will considerably facilitate the construction of the models and will represent a real advance for the textile industry.

REFERENCES

[1] A. Albu, T. Caciora, Z. Berdenov, D. C. Ilieș, B. Sturzu, D. Sopota, G. V. Herman, A. Ilieș, G. Olah, "Digitalization of garment in the context of circular economy," Industria Textila, vol. 72, no. 1, pp. 102–107, 2021. DOI: 10.35530/IT.072.01.1824.

[2] D. C. Ilieș, C. Lite, L. Indrie, C. Moș, A. Ilieș, M. Ropa, B. Sturzu, A. Sambou, A. Axinte, A. Albu, P. Szabo-Alexi, M. Costea, G. V. Herman, "Researches for the conservation of cultural heritage in the context of the circular economy," Industria Textila, vol. 72, no. 1, pp. 50–54, 2021. DOI: 10.35530/IT.072.01.1807.

[3] E. Codău, Inginerie generală în textile – pielărie: îndrumar de laborator. Iași: Editura Performantica, 2019, pp. 68–82.

[4] Capture 3D. [Online]. Available: https://www.capture3d.com/

[5] iStock, "Half body illustrations." [Online]. Available: https://www.istockphoto.com/ro/ilustra%C8%9Bii/half-body

[6] Autodesk, "3D CAD Software." [Online]. Available: https://www.autodesk.com/solutions/3d-cad-software

[7] E. Pintilie, G. Ciubotaru, and M. Avadanei, Proiectarea confecţiilor textile asistată de calculator. Iași: Editura Performantica, 2006, pp. 82–93.

[8] E. Filipescu, Construcția și modelarea îmbrăcămintei – Îndrumar de laborator. Iași: Editura Performantica, 2013, pp. 36–93.

[9] E. Filipescu, Structura şi proiectarea confecţiilor textile. Iași: Editura Performantica, 2013, pp. 65–87.

ANNALS OF THE UNIVERSITY OF ORADEA
FASCICLE OF TEXTILES, LEATHERWORK

RECENT DEVELOPMENTS IN EMI SHIELDING BASED ON TEXTILE AND FLEXIBLE MATERIALS

TABĂRĂ Octavian-Adrian

National Institute for Research and Development for Textiles and Leather
16 Lucretiu Patrascanu Street, Sector 3, 030506, Bucharest, Romania, office@incdtp.ro

Corresponding author: Tabără Octavian-Adrian, E-mail: octavian.tabara@incdtp.ro

Abstract: *In today's interconnected, world we use many electronic devices. In order to provide dependable and functional devices, electromagnetic shielding devices are crucial. Electromagnetic interference (EMI) has become a major issue, leading to circuit issues caused by signal noise, data loss, malfunctions, and even potential health dangers. The current advancements in electromagnetic shielding devices are the main topic of this essay, with an emphasis on new solutions. An overview of EMI shielding screens with an emphasis on domain development is given in this paper. The creation of bending EMI shielding is one way that textile materials affect the EMI properties.*

Key words: *screens, interference, efficiency, fabrics, coefficients*

1. INTRODUCTION

With the rapid development of wireless communication technology and the continuous development of smart exchange products, it has been found that the increase in electromagnetic waves can reach up to 10% in limited frequencies and spaces. The health effects are numerous including high blood pressure, heart disease, pregnancy complications, increased risk of immune deficiencies, headaches, physiological disorders and other health problems. Electromagnetic radiation is an important perturbation factor. It is known that electromagnetic waves propagate from the radiation source, the electric and magnetic fields interconnecting perpendicular in space, creating waves of particles coupled for propagation. Protection against electromagnetic radiation can be addressed through shielding, remote protection and control of the radiation source.

Shielding instruments and people against electromagnetic interference (EMI) has become increasingly important in recent decades, due to the growing number of electric cars and devices that radiate electromagnetic waves. Textile fabrics as a general category, can have these properties, combined with potentially good mechanical properties, depending on the textile structure and the material chosen. On the other hand, the necessary electrical properties, especially conductivity and magnetic properties, cannot be taken for granted in ordinary textile fabrics.

Electromagnetic interference (EMI) shielding materials are known to be able to protect people, instruments, etc. from electromagnetic radiation (EM) by absorbing or reflecting radiation, often combining both. EM shielding is used to minimize exposure to electromagnetic radiation.

EMI shielding must be distinct from magnetic shielding. Magnetic shielding refers to low frequencies (50 or 60 Hz). Radio waves and microwaves emitted by electronic devices operate in radio

and mobile wave frequencies. Since today there are many electronic devices that interfere, the research of EMI shielding materials has increased greatly in recent times [1].

2. GENERAL INFORMATION

By either absorbing or reflecting radiation—often a combination of both—electromagnetic interference (EMI) shielding materials are known to be able to protect people, equipment, etc. from electromagnetic (EM) radiation shielding

The investigation of electromagnetic interference shielding, EMI, for different materials is done according to Figure 1: open field methods, coaxial transmission line methods (according to the ASTM D4935 standard, can be applied in different frequency ranges and require different amounts of time and equipment), armored box methods and armored camera methods.

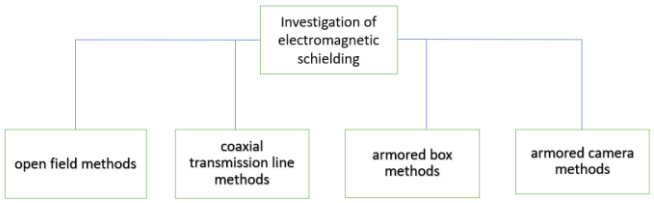

Figure 1. Methods for investigating electromagnetic schielding

By measuring the radiated emissions which emanates from a final product, the open-field or free-space approach assesses the practical efficacy of shielding a whole electronic assembly. Due to changes in how each finished product is assembled, the test is highly variable and does not assess the performance of any particular material.

Another method used is the shielded box method. This method is comparative and is used in measurement on different shielding materials. The test essentially consists of a metal case and an electrically sealed joint. The joint has a receiving antenna placed on the outside of the box that is used to measure the strength of the received signals, both through the open hole and through a sample mounted over the hole.

The disadvantage of this method is that it is difficult to achieve adequate electrical contact between the test samples and the shielded box. The other problem is the limited frequency range of about 500 MHz. Currently, the results obtained experimentally with this method show a weak correlation. The method of the coaxial chamber is similar from an ideal/principled point of view to the shielding box method. The coaxial transmission line method for measuring shielding effectiveness is a preferred method to be used nowadays, being more efficient than the previous two. The main advantage of this technique is that the results obtained in different laboratories are comparable. In addition, the coaxial transmission line can also be used to break down data into reflected, absorbed and transmitted components.

In particular, coaxial transmission line methods can be applied in different frequency ranges and require different amounts of time and equipment. A more detailed discussion of the effect of these physical properties on EMI protection and measurements can be found in [2].

EMI protection is one of the deeply investigated topics in the field of smart textiles. The necessary physical properties, such as electrical and/or magnetic conductivity, can be added to common textile fabrics through layers with conductive polymers, carbon-based or metal-based layers. As it results from the review of the papers published in the article, it is found that several approaches

can be used to achieve a high efficiency of EMI shielding, measured both in the X-band, technologically relevant and in other frequency ranges.

The calculation of the electromagnetic efficiency of screens is based in the above article on Skelkunoff's theory [3]. Textiles, as low-cost substrates, are known to offer advantages such as cutability, comfort, breathability and ease of processing, making them suitable for flexible wearable electromagnetic protection. In the progress of research on textile-based electromagnetic protective materials is analyzed, providing references for their application.

Electromagnetic waves are known to propagate from the radiation source, with electric and magnetic fields interconnecting perpendicularly in space, creating waves of particles coupled for propagation. Electromagnetic shielding mechanisms can be divided into electromagnetic field shielding, magnetic field shielding, and electrostatic field shielding. In practice, electromagnetic shielding mainly refers to shielding the electromagnetic field.

Metallic or non-metallic materials with electromagnetic protection properties generally have a high initial modulus and stiffness, which makes them difficult to use in this field. By converting these materials into fibers and mixing them with conventional textile fibers, it is possible to meet the efficiency requirements of the electromagnetic screen while improving textile substrates. The conductive network formed by the mutual conduction of the electromagnetic protection fibers inside the fabric improves its shielding performance.

The efficiency of shielding increases with the content of stainless-steel fibers per unit area up to a certain point, beyond which it decreases. Two theories — small pore coupling and pore transmission — try to explain this, but no consensus has been reached. Some researchers conclude that when the fiber content of stainless steel is between 20% and 30%, the blended material achieves a protective efficacy of 30-40 dB, balancing the protection and the fabric [4].

Today, the commercialization of electromagnetic protective fabrics made of stainless-steel fibers has had some success, with positive feedback in the market. In [5] shielding effectiveness is defined as the ratio of impact to energy to residual energy. When an electromagnetic wave passes through a screen, absorption and reflection occurs. The residual energy is part of the remaining energy, which is neither reflected nor absorbed by the shield, but is removed from the shield. All electromagnetic waves are made up of two essential components, a magnetic field (H) and an electric field (E) as shown in Figure 4. These two fields are perpendicular to each other, and the direction of propagation of the wave is perpendicular to the plane containing the two components.

The efficiency of shielding is defined using the terms before and after attenuation is given in equations (1) and (2), with transversal and incident/longitudinal components.

$$SE = 20 \lg\left(\frac{E_t}{E_i}\right) \quad (1)$$

$$SE = 20 \lg\left(\frac{H_t}{H_i}\right) \quad (2)$$

The paper [6] also presents a literature study on EMI shielding on graphite fibers, thermoplastics, intrinsically conductive polymers, etc. The paper concludes that polymers based on polyaniline, polypyrol are important candidates for shielding electromagnetic interference due to their lightweight, non-corrosive nature and commercial viability.

The attenuation of an electromagnetic wave is achieved by: Absorption (A), Reflection (R), Multiple reflections (B) and the shielding effectiveness is calculated with equation (3):

$$SE = \frac{1}{4}A + \frac{3}{4}R + \frac{3}{4}B \quad (3)$$

where SE – shielding efficiency
A – absorption coefficient
R – coefficient of reflection
B – coefficient of multiple reflections

Several materials used for electromagnetic screens are reviewed. Carbon-based shielding materials suffer from limited mechanical flexibility. Metal-based shielding materials face high weight, corrosion, and difficulties in adjusting shielding efficiency. Therefore, the organic polymers represent the most attractive candidates for EMI shielding due to their ease, non-corrosive nature, and commercial viability.

3. DEVELOPMENTS IN EMI SHIELDING

In [7], the shielding of the electromagnetic field is done to protect human health and ensure the immunity of electronic equipment, in the context of the accelerated development of telecommunications. The shielding solutions offered by textile materials were studied, in order to support economic agents in the production of competitive products. A mathematical model was used to predict the electromagnetic attenuation of an enclosure covered in fabric, which is characterized according to its geometric and electrical parameters. Thus, according to the principles of electromagnetic compatibility (EMC), radiation shielding is one of the solutions for ensuring the health of living beings and the immunity of electronic equipment. Adolf Schwab concludes that conductive textiles can be used as protective curtains, screens, tents and other construction elements, to shield electromagnetic radiation and ensure the maintenance of human health along with ensuring the electromagnetic compatibility of the operation of electronic equipment.

Using a shielding efficiency approximation relationship proposed by Heinreich Kaiden [8], it has been processed according to the circuit method to describe the shielding produced by conductive lattice structures, and is therefore applicable to structures woven with conductive wires. It represents a "mechanical" mathematical model, unlike previous research carried out with phenomenological mathematical models. In order to obtain the desired shielding properties for textile fabrics, conductive wires made of ferromagnetic (stainless steel – Fe) and diamagnetic (Ag) materials were introduced into the weft system of the fabrics.

The shielding effectiveness of a housing for the near-field electromagnetic spectrum is studied [9]. An analytical relationship for the effectiveness of shielding, taking into account both the geometric and electrical aspects in which the parameters of the conductive fabric were simplified by the authors was proposed, and a validation study was also carried out. Calculations based on the proposed simplified relationship are possible to obtain an optimization between the fabric processing capacity, costs and targeted shielding effectiveness. The frequency range proposed for testing is limited by the near electromagnetic field conditions, on the one hand, and by the resonance conditions specified by the IEEE 299.1 standard, at 1 MHz - 20 MHz. The experimental results show lower values for shielding effectiveness than the analytical values, which depends on: because the electrical continuity at the edges of the cube is only partially ensured, and the analytical relationship represents an ideal model, very difficult to reproduce with physical equipment. The experimental arrangement and the applied procedure are useful primarily to compare the characteristics of different fabrics. The simplified analytical relationship provides a good approximation for the analytical relationship in the literature for the specified frequency range and supports the calculation of the distance between the conductive wires in relation to the targeted shielding effectiveness. Thus, an important question

regarding the necessary distance between the conductive grid for textile fabrics and its raw material could be answered. A parametric study for the distance between conductive weft wires shows that the denser the conductive wires, the better the shielding effectiveness of the near electromagnetic field. Calculations based on the proposed simplified relationship are possible, in order to achieve an optimization between the fabric processing capacity, costs and the targeted shielding effectiveness.
Conductive polymers are a solution for textiles to shield against electromagnetic interference. Such compounds may have metallic conductivity or can be semiconductors.

In [10] textiles for electromagnetic shielding (EMI) made with conductive polymers are treated. These materials are important for the protection of humans and electronic devices against electromagnetic radiation. It is known that most textiles should have protective properties, properties of reflecting incident electromagnetic radiation (EMR), without being able to absorb it. Normally, natural fibers do not have shielding properties against electromagnetic radiation. To allow the shielding of the electromagnetic field, textiles must have conductive properties. This can be implemented if the textiles have electroconductive properties and are achieved by: surface changes of the fibers or textiles made of such fibers and by changes in the volume of the fibers themselves (in the case of artificial fibers) in their formation stage (spinning).

As the development of miniature electronics is constantly expanding, there is also a need for transparent and flexible materials that provide EMI protection, especially for: windows, touch screens, displays, aerospace and military applications. In [11] 4 major classes of materials are analyzed: thin films (oxides, metals, metal-dielectric structures) with example of TiO_2-Ag, nanocarbon-based materials with example of graphene multilayer structures, conductive polymers with example of polyaniline and metallic nanowires with example of nanowire networks deposited on metallic structures. The paper concludes that most current solutions rely on increased conductivity, which leads to reflection shielding. In the current context, a major challenge remains the balance between transparency, flexibility and shielding efficiency.

The increase in the use of wireless technologies (including 4G, more recently 5G) has led to an increase in electromagnetic radiation, which can affect both the operation of electronic equipment and human health. Textiles are investigated as lightweight, flexible and cost-effective solutions for EMI (Electromagnetic Interference) protection.

Like electromagnetic shielding mechanisms there are three main mechanisms: loss by reflection – waves are reflected due to the conductivity of the material; dielectric loss – electromagnetic energy is transformed into heat by polarization processes; Magnetic loss – magnetic materials absorb wave energy through magnetic resonances. Schelkunoff's theory, used to characterize shielding efficiency, is also discussed [12].

3. CONCLUSIONS

EMI-protected fabrics need a certain set of characteristics. These are required in many scientific domains as well as in the defense sector. The intended shielding in a variety of applications will result from new advancements and ongoing research in this area. In order to promote the development of the area, this study provides a thorough but non-exhaustive survey of materials for EMI shielding. Due to the need for wearable devices and 4G/5G, textiles for EMI shielding are changing quickly. Therefore, the main trends are enhanced production processes, hybrid materials, and nanocomposites. Long-term durability, washing stability, and environmental impact are still unknowns. Multifunctional fabrics that can combine EMI shielding with additional features (thermoregulation, sensors, energy capture) are anticipated to be the way of the future. The coupling of signals from one system to another is known as electromagnetic interference (EMI). It is an issue for the majority of electronics because it

can lower circuit performance or even lead to circuit failure. Specific shielding efficiency (SSE), which is defined as shielding efficacy per unit weight/thickness, is becoming the focus of modern materials. The electronics could malfunction due to interference. Shielding materials for radiation sources and electronics are becoming more and more necessary as radio and microwave wave devices proliferate. As a result, during the past 20 years, research into the creation of EMI shielding materials has grown significantly.

ACKNOWLEDGEMENT

This work was carried out through the Core Programme within the National Research Development and Innovation Plan 2022-2027, carried out with the support of MCID, project no. 6N/2023, PN 23 26 01 03, project title "Electroconductive materials based on multilayer metallization for thermoelectric systems, electromagnetic shielding and biomedical sensors integrated in IoT systems (3D-WearIoT)".

REFERENCES

[1] Fatemeh Saeedi, Reza Ansari, Saeid Sahmani, "*Recent advances and comprehensive review of electromagnetic interference shielding materials and technologies*", Materials Today Physics, Volume 59, 2025. Available: https://www.sciencedirect.com/science/article/abs/pii/S2542529325002731

[2] Blachowicz, T.; Hütten, A.; Ehrmann, A. "*Electromagnetic Interference Shielding with Electrospun Nanofiber Mats— Review of Production, Physical Properties and Performance*" *Fibers* 2022, *10*, 47, pp. 1-16.

[3] Mengyue Peng et al., "Clarification of Basic Concepts for Electromagnetic Interference Shielding Effectiveness," *Journal of Applied Physics*, vol. 130, no. 22, p. 225108, 2021.

[4] Lixue Zhao et al. – *"Research Progress on Electromagnetic Shielding Mechanisms and Textile-Based Protective Materials",* TEXTILE & LEATHER REVIEW No. 7, 2024, pp. 1417-1436.

[5] S. Geeth et al., "*EMI Shielding: Methods and Materials—A Review*", Journal of AppliedPolymer Science, Vol. 112, No. 4, 2009, pp. 2073-2086.

[6] Bigg D.M. *"The effect of chemical exposure on the EMI shielding of conductive plastics*" ,", Polymer Composites Volume 8, No. 1, 1987, pp. 1-7.

[7] Ion Razvan Radulescu et al., "*Ecranarea campului electromagnetic apropiat prin structuri textile tesute*" , Buletinul AGIR nr. 3, 2018, pp. 46-50.

[8] H. Kaden. "*Wirbelströme und Schirmung in der Nachrichtentechnik*", Springer-Verlag, 1959.

[9] Ion Razvan Radulescu et al., "*Modelling and testing the electromagnetic near field shielding effectiveness achieved by woven fabrics with conductive yarns*", Industria Textila, Vol. 69 No. 3, 2018, pp. 169-176.

[10] Tomasz Rybicki, Iwona Karbownik, "*Chapter 17 - EMI shielding textile materials based on conducting polymers*" , Materials for Potential EMI Shielding Applications,, Processing, Properties and Current Trends, 2020, pp. 267-285.

[11] Bishakha Ray et al., "*Flexible and Transparent EMI Shielding Materials*", Advanced Materials for Electromagnetic Shielding: Fundamentals, Properties, and Applications, 2018, pp. 167-175.

[12] Lixue Zhao et al., "*Research Progress on Electromagnetic Shielding Mechanisms and Textile-Based Protective Materials*", Textile and leather review, Vol. 7, 2024, pp. 1417-1436.

ANNALS OF THE UNIVERSITY OF ORADEA
FASCICLE OF TEXTILES, LEATHERWORK

CONTENTS

			Management, 410058, Oradea, România,	
4	**SUSTAINABLE REDUCTION OF GRAPHENE OXIDE ON POLYESTER SPUNBOND NONWOVEN FABRIC USING RED ONION PEEL EXTRACT**	**DEMİREL GÜLTEKİN Nergis[1], SERT Zişangül[1], AKSOY Şevval[1]**	[1] Marmara University, Faculty of Technology, Department of Textile Engineering, 34854, İstanbul, Türkiye	**21**
5	**INVESTIGATION OF THE PHYSICAL AND MECHANICAL PROPERTIES OF COTTON FABRICS WITH DIFFERENT WEAVE STRUCTURES**	**DJORDJEVIC Suzana[1], STOJANOVIC Sandra[2], KODRIC Marija[3], DJORDJEVIC Dragan[4]**	[1,2]Academy of Applied Studies Southern Serbia, Department of Technology and Art Studies Leskovac, Leskovac, Serbia, E-Mail: szn871@yahoo.com [3,4]University of Nis, Faculty of Technology, Bulevar oslobodjenja 124, 16000 Leskovac, Serbia	**27**
6	**NON-DESTRUCTIVE ULTRASONIC EVALUATION OF TECHNICAL TEXTILES AND COMPOSITE FABRICS: A GRADIENT OPTIMIZATION OF FRAMEWORK FOR DEFECT DETECTION**	**FLOCA Alina Mihaela[1], POP Daniel Nicolae[2], VRINCEANU Narcisa[1*]**	[1] „Lucian Blaga" University of Sibiu, Faculty of Engineering, Department of Industrial Machines and Equipments, 4 Emil Cioran, Sibiu, Romania [2] Lucian Blaga" University of Sibiu, Faculty of Engineering, Department of Electric Engineering and Computers, 4 Emil Cioran, Sibiu, Romania	**37**
7	**INTEGRATION OF DIGITAL LIBRARIES IN CONTEMPORARY FASHION DESIGN**	**FLOREA-BURDUJA Elena[1], CANGAŞ Svetlana[2], OVCEARENCO Cristina[3]**	[1, 2, 3] Technical University of Moldova, Faculty of Design, 4 Sergiu Radautan Street,	**43**

			Romania [2] "Lucian Blaga" University of Sibiu, Romania, Faculty of Engineering, 550024, 10 Victoriei Blvd, Sibiu, Romania, [3] Medical Practice Comosan SRL, Sibiu, Romania	
16	**FLEXIBLE MICROSTRIP BANDPASS FILTER COATED ON TEXTILES FOR RESONANT SIGNAL TRANSMISSION**	**RADULESCU Ion Razvan[1], ENE Alexandra[2], VISILEANU Emilia[3], DINCA Laurentiu[4], PERDUM Elena[5], NEGROIU Rodica[6], BACIS Irina[7], IONESCU Ciprian[8], CIOBANU Luminita[9], TALPA Andreea[10]**	[1-5] INCDTP - Bucharest, Str. L. Patrascanu 16, 030508, Bucharest, Romania [6-8] National University of S&T Polytechnica Bucharest, Faculty of Electronics, CETTI, Bd. Iuliu Maniu 1-3, 061071, Bucharest, Romania [9-10] Technical University Iasi, Faculty DIMA, Center for R&I in textiles and fashion SMART-Tex-IS, Str. Dimitrie Mangeron 29, 700050, Iasi, Romania	**119**
17	**HYBRID WORKFLOW ACCESSIBILITY IN AFFINITY STUDIO**	**RAȚIU Georgiana Lavinia[1], ȘUTEU Marius Darius [2] ANDREESCU Nicoleta[2]**	[1] Doctoral School of Engineering Sciences, University of Oradea, România [2] Universitatea Oradea, Facultatea de Inginerie Energetică și Management Industrial,	**127**

The editors take no responsibility of the results, opinions and conclusion expressed in the published papers.